AD NUMBER: AD0142349

LIMITATION CHANGES

TO:

Approved for public release; distribution is unlimited.

FROM:

Distribution authorized to U.S. Gov't. agencies and their contractors; Administrative/Operational Use; Jan 1958. Other requests shall be referred to Wright Air Development Center, Wright-Patterson AFB, OH 45433.

AUTHORITY

AFAL ltr dtd 27 Dec 1979

THE ESTABLISHMENT OF VIBRATION AND SHOCK TESTS FOR AIRBORNE ELE

EDWARD J. LUNNEY
CHARLES E. CREDE

BARRY CONTROLS INCORPORATED
WATERTOWN 72, MASSACHUSETTS

JANUARY 1958

WRIGHT AIR DEVELOPMENT CENTER

NOTICES

When Government drawings, specifications, or other data are used for any purpose other than in connection with a definitely related Government procurement operation, the United States Government thereby incurs no responsibility nor any obligation whatsoever; and the fact that the Government may have formulated, furnished, or in any way supplied the said drawings, specifications, or other data, is not to be regarded by implication or otherwise as in any manner licensing the holder or any other person or corporation, or conveying any rights or permission to manufacture, use, or sell any patented invention that may in any way be related thereto.

- - - - -

Qualified requesters may obtain copies of this report from the ASTIA Document Service Center, Arlington Hall Station, Arlington 12, Virginia

- - - - -

Copies of WADC Technical Reports and Technical Notes should not be returned to the Wright Air Development Center unless return is required by security considerations, contractual obligations, or notice on a specific document.

WADC TECHNICAL REPORT 57-75
ASTIA DOCUMENT No. 142349

THE ESTABLISHMENT OF VIBRATION AND SHOCK TESTS FOR AIRBORNE ELECTRONICS

EDWARD J. LUNNEY
CHARLES E. CREDE

BARRY CONTROLS INCORPORATED

JANUARY 1958

ELECTRONIC COMPONENTS LABORATORY
CONTRACT NO. AF 33(038)-22704
PROJECT NO. 4157

WRIGHT AIR DEVELOPMENT CENTER
AIR RESEARCH AND DEVELOPMENT COMMAND
UNITED STATES AIR FORCE
WRIGHT-PATTERSON AIR FORCE BASE, OHIO

Carpenter Litho & Ptg. Co., Springfield, O.
200 — June 1958

FOREWORD

This report was prepared by Edward J. Lunney and Charles E. Crede of Barry Controls Incorporated, Watertown Massachusetts, and summarizes the results obtained from October 1951 to April 1957 on Air Force Contract No. AF 33(038)-22704, under Project No. 4157, Task No. 41572 (formerly R-112-143-A) "Vibration and Shock Design Criteria for Electronic Equipment". Messrs. Maurice Gertel and Richard D. Cavanaugh were active in the initial stages of the investigation which resulted in the publication of WADC Technical Report 54-272 and subsequent progress reports.

The work was administered under the direction of the Electronic Components Laboratory, Wright Air Development Center, with Mr. Carl A. Golueke initially in charge of the project. He was later succeeded by Mr. Norman P. Kempton and more recently by Mr. R. W. Sevy.

ABSTRACT

The results of an analysis of the vibration and shock environment in piloted aircraft are presented. The objectives of the study were to define such environment and to devise appropriate laboratory tests for certifying the suitability of electronic and accessory equipment for use in aircraft service. The analysis used in the study is based on the thesis that the vibration and shock as measured in aircraft are relatively unimportant, but that the response of equipment to such vibration and shock is of paramount importance. This follows from the fact that the stress experienced by structures of the equipment is directly related to the response of such structures to the applied vibration and shock.

PUBLICATION REVIEW

The publication of this report does not constitute approval by the Air Force of the findings or the conclusions contained therein. It is published only for the exchange and stimulation of ideas.

FOR THE COMMANDER:

C. C. Eckert

for GEORGE F. WATKINS
Lt. Colonel, USAF
Chief, Electronic Components Laboratory
Directorate of Laboratories

TABLE OF CONTENTS

TABLE OF CONTENTS (Cont'd)

LIST OF TABLES

LIST OF ILLUSTRATIONS

LIST OF ILLUSTRATIONS (Cont'd)

SYMBOLS

a = length dimension, inches

b = a coefficient, integer or fraction also width dimension, inches

c/c_c = percent critical damping at resonance

D = number of landings in life of equipment also, number of drops in repeated drop tests

D' = number of applications of shock in shock test.

E = Young's modulus,

f = forcing frequency, cps.

f_n = natural frequency, cps.

F = force, lbs.

g = acceleration due to gravity, 386 in./sec^2

h = rate of change of test frequency, cycles/sec./sec.

I = moment of inertia - beam section, inches^4

J = experimentally determined constant

k = stiffness of equipment element, lb./in.

K = Miner's constant

K_c = cross sectional shape factor

K_m = material factor

K_s = longitudinal stress distribution factor

L = total length of member, in.

m = mass of equipment element, lb.sec.^{2}/in.

M_m = maximum bending moment, in lbs.

n = experimentally determined constant

n = number of cycles of stress of a designated magnitude for one application of environmental shock

n' = number of cycles of stress of a designated magnitude for one application of laboratory shock

n_t = total number of cycles = Dn

n_t' = total number of cycles = $D'n'$

N = cycles to failure in fatigue test at constant stress amplitude

Q = value of transmissibility at resonance in steady-state vibration

r = number of cycles of free vibration, also, radius of cross section of beam, in.

R = a particular value of r, number of cycles

R' = a constant

S = stress, psi, also maximum stress in fatigue test, psi

S_a = stress at any point a, psi

S_m = maximum stress, psi

$S_{E.L.}$ = endurance limit stress, psi

S_{ULT} = ultimate stress, psi

t = thickness dimension from neutral axis, inches or time in seconds

t_o = maximum thickness from neutral axis, inches

x = vibration amplitude of support or airplane structure, half peak-to-peak, in.

x_o = maximum vibration amplitude of support, or airplane structure, half peak-to-peak, in.

$\dot{x}_o$ = maximum velocity of support or airplane structure vibration, inches/second

$\ddot{x}_o$ = maximum acceleration of support or airplane structure vibration, g

$\ddot{x}_{EL}$ = support acceleration which produces endurance limit stress in equipment element during resonant vibration, g

$\ddot{x}_{ULT}$ = support acceleration which produces ultimate stress in equipment element during resonant vibration, g

Y = response vibration amplitude of equipment element, half peak-to-peak, in.

Y_o = maximum value of y, inches

$\dot{Y}_o$ = maximum response velocity of equipment element, inches/second

$\ddot{Y}_o$ = maximum response acceleration of equipment element, g

δ = maximum deflection of beam, in.

γ = density of beam, pounds/in^3

θ = polar coordinate for circular cross section

Ω = natural frequency, rad./sec.

ω = forcing frequency, rad./sec.

ω_n = natural frequency, radians/sec.

SECTION I

INTRODUCTION

This technical report is essentially a revision to Wright Air Development Center Technical Report No. 54-272 of the same title which presents revisions to that report in light of further progress and extensions in the scope of the work. The principle objective of this study is to establish laboratory testing procedures which will simulate the destructive effects of the vibration and shock environments which electronic equipment and components experience during service in aircraft. The earlier report presented recommended test procedures for components to withstand the vibration and shock environment of reciprocating engined aircraft. In this report test procedures are devised for the jet engined aircraft environment, a further evaluation of the landing shock testing environment, and the design modifications have been developed for existing shock testing machines necessary to provide a test more representative of the service shock environment.

Equipment mounted in aircraft is subjected to vibration and shock of various degrees. It is important to the designers of such equipment that techniques be available for proving the suitability of the equipment for use in these shock and vibration environments. In many fields not related to aircraft, such answers are obtained by a direct approach. Automobile designs are proved, for example, by operating the automobile under actual but severe conditions for a period corresponding to its maximum expected life. Washing machines are tested in a somewhat similar manner in the laboratory, and internal combustion engines are proved by operating them at maximum load for a period corresponding to the life of the engine. These techniques are not feasible for electronic and accessory equipment installed in aircraft for reasons which may be summarized as follows:

(a) Equipment of a given design usually is installed in many different types of aircraft. These aircraft encounter many different operating conditions, and it becomes impractical to test a given equipment in environments representing all possible operating conditions in all types of aircraft.

(b) Electronic and accessory equipment, in general, is not designed or manufactured by the airframe manufacturer. The equipment must be received ready for installation in the airframe with assurance that it will render satisfactory performance during all conditions of flight.

This report analyzes some of the problems introduced by the above circumstances, and suggests a rational procedure for establishment of laboratory tests. The objective of such tests is to qualify equipment for operation under actual aircraft operating conditions.

Manuscript released by the author 19 August 1957 for publication as a WADC Technical Report.

If the procedure referred to above for testing automobiles were to be used for qualifying electronic equipment intended for airborne service, it would be necessary to first measure all conditions of shock and vibration encountered in all aircraft in which the equipment is to be installed. The next step would be to determine the desired life of the equipment in hours. One equipment would then be subjected to each measured condition of shock and vibration for a period equal to the desired life of the equipment. This would require that a new equipment be made available for each test condition, because damage from vibration and shock tends to be cumulative and the results would not be significant if some of the tests were conducted on equipment previously subjected to environmental tests. It is well known that failure caused by repeated application of stress tends to be erratic. Consequently, many samples would have to be tested under identical conditions so that the results could be examined statistically. The quantity of equipment and the testing time required for such a program would be exorbitant.

One method of resolving the question of an unreasonably long testing procedure is to adopt a concept of accelerated testing. It is generally assumed that equipment tends to sustain the same damage as a result of mild vibration or shock for a long period of time as it would sustain as a result of severe vibration or shock for a short period of time. This philosophy appears to underlie many of the vibration and shock tests now required by military specifications. In most cases, the tests appear to have been established arbitrarily and without a rational study of the effect of increased severity. To the best knowledge of the authors, the concept of accelerated testing exists only qualitatively, and no critical analysis of the problem has been made to establish a quantitative basis of accelerated testing. An attempt is made in this report to fill this deficiency by examining critically and quantitatively the problem involved in establishing vibration and shock test specifications based on accelerated testing.

A detailed consideration of the subject of accelerated testing reveals many diverse and complex problems, some of which may be outlined as follows:

(a) A criterion of failure must be established. It is common experience, borne out by recent studies, (see reference 90) that certain types of equipment tend to deteriorate gradually during use and in the absence of significant shock and vibration. Depending on its nature, this normal deterioration may or may not be accelerated in the same manner as damage resulting from shock and vibration. If the deterioration is not accelerated by shock and vibration tests, such tests tend to be unconservative, because greater damage would occur if the tests were continued for a longer period.

(b) Questions of both operation and strength become involved in any consideration of accelerated testing. Equipment should be required to operate only at the maximum severity of vibration and shock expected to be encountered in actual operating conditions. The increased severity associated with accelerated tests should be applied only to investigations of the strength of the equipment from a mechanical or structural viewpoint. There should be no requirement that the equipment continue to operate properly under these severe conditions.

(c) Many types of failure occur in equipment subjected to shock and vibration. These are difficult to categorize in general. A review of damage reports indicates that failure of brackets and other structural members as a result of repeated stressing is common. Another group includes somewhat similar failure of wires, tube elements, and other electrical components. A third group includes loosening of fasteners, crumbling of ceramic and mica insulators, and similar failures that may or may not have any relation to the magnitude of the stress existing in the element.

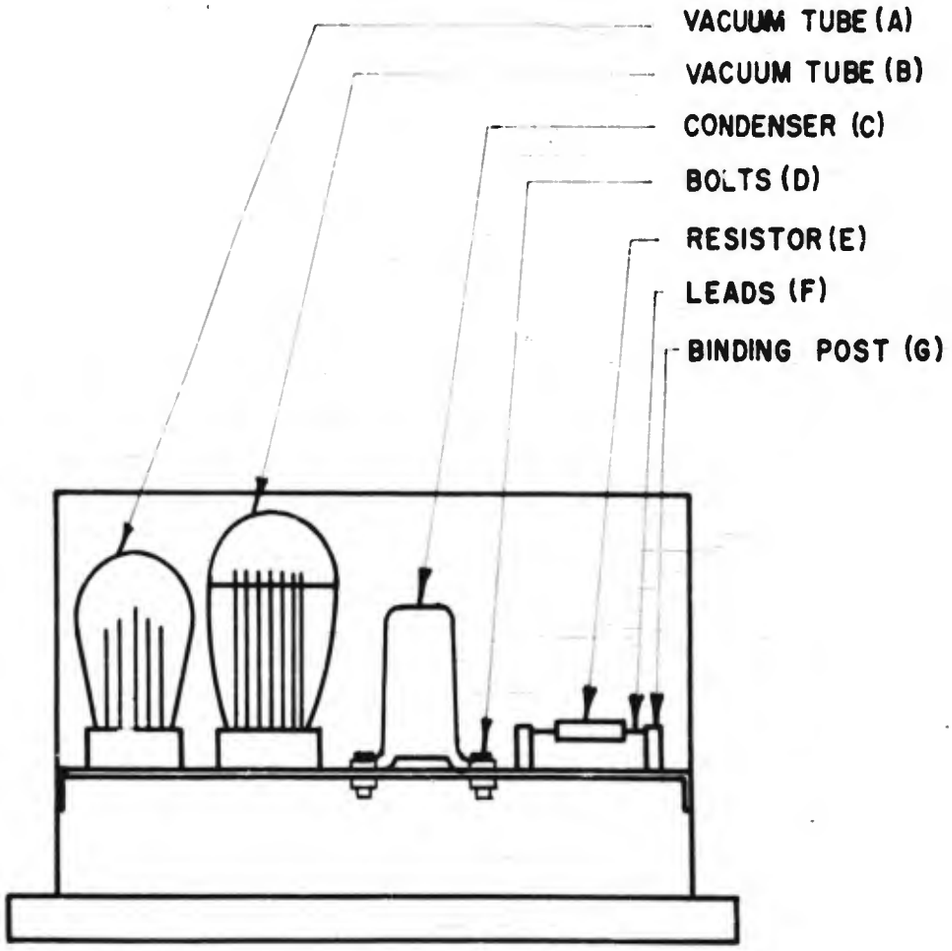

FIG. 1 SCHEMATIC DRAWING OF HYPOTHETICAL EQUIMENT HAVING TYPICAL COMPONENTS

SECTION II

IDEALIZATION OF EQUIPMENT

The problems involved in analyzing the various types of failures may be considered by creating a hypothetical equipment having components of the types known to involve failure. It may then be possible to study the manner in which the various parameters affect the likelihood of failure. The hypothetical equipment to be discussed is illustrated schematically in Figure 1. This equipment includes a housing having a horizontal panel on which several components are mounted. The components include vacuum tubes A and B, a condenser C secured to the panel by the bolts D, and a resistor E fastened by its electrical leads F to binding posts G mounted upon the panel. Failure of the equipment may occur as a result of various effects discussed in the following paragraphs.

If failure of the panel occurs, it is probable that the failure is the result of excessive stress in the panel. It may be assumed that the stress in the panel is proportional to the vibration amplitude of the panel relative to the housing. Probability of failure thus tends to increase as the vibration amplitude of the panel increases.

Vacuum tube A is of a type in which the internal elements are supported entirely from the base structure. It may be assumed that failure tends to occur when these elements deflect excessively with respect to the base. The maximum deflection of the elements is proportional to the maximum acceleration of the panel, multiplied by a dynamic factor which takes the frequency relation into account. Except for this frequency relation and others to be considered below, the damaging potential applied to tube A tends to be proportional to the vibration amplitude of the panel on which the tube is mounted.

Tube B is somewhat similar to tube A, but includes the additional feature of a mica spacer adjacent to the upper ends of the internal elements to maintain such elements in properly spaced relation to each other and to the envelope of the tube. The forces applied to the spacer are a function of the tendencies of the elements within the tube to deflect. Such tendencies are related to the vibration amplitude of the panel as discussed previously with reference to tube A. The damaging potential on the mica spacer is therefore related, but in a somewhat less definite way, to the vibration amplitude of the panel which supports the tube.

Components mounted to the panel by brackets, such as the condenser C tend to fail as a result of excessively high stress in the mounting brackets. The sole function of such brackets is to mount the condenser to the panel of the equipment, and the stress in the brackets tends to be directly

proportional to the inertia forces involved in causing the condenser to move in the same manner as the panel upon which it is mounted. The damaging potential on these brackets thus tends to be directly proportional to the maximum vibration amplitude of the panel.

Failures may occur as a result of loosening of bolts D. In spite of many investigations and considerable analysis, the laws governing the loosening of bolts are not well established. One possible explanation is that the bolt stretches somewhat under the influence of dynamic forces, with a consequent momentary release of the friction force between the face of the nut and the bolted surface. This momentary release of friction encourages the nut to back off the bolt. It may thus be assumed that the loosening tendency increases as the vibration amplitude of the panel increases.

The problem of the resistor E is somewhat similar to that of the condenser C except that the mounting wires have the additional function of providing an electrical circuit to the resistor. These wires also constitute the mechanical support for the resistor. The maximum stress in the wire tends to increase as the vibration amplitude of the panel increases, for the reasons discussed with reference to the brackets which support the condenser C.

Although subject to many qualifications, it may be stated that, to a first approximation, the likelihood of damage to the hypothetical equipment illustrated in Figure 1 tends to increase as the vibration amplitude of the mounting panel increases. This simplified approach to a complicated problem thus suggests the designation of the vibration amplitude of this panel as the single parameter that may serve as an index of likelihood of failure of the electronic equipment when subjected to vibration and shock. Problems involved in determining this amplitude are considered below in great detail for the various kinds of motion embodied in vibration and shock environments.

SECTION III

VIBRATION ENVIRONMENT

The words "shock and vibration" are commonly used together to describe certain aspects of the environmental conditions which exist on aircraft. The use of the two discrete words implies a distinction between two classes of phenomena. The meaning of the word "vibration" is much better established in a technical or engineering sense. In general, it refers to a periodically varying force or motion which may be either steady-state or transient in nature. Vibration is defined here as a vibratory motion of the aircraft structure which is steady-state in nature and may consist of one or more frequencies with the motion at each frequency being harmonic. Steady-state vibration may be completely defined by designating the frequency or frequencies, together with the amplitude at each frequency. The amplitude is commonly defined in terms of displacement, velocity or acceleration.

The meaning of the word "shock" tends to be vague and indefinite. It carries with it a connotation of suddenness, and perhaps also of significant over-all motion. In impact of rigid bodies, the velocities of the bodies change instantaneously, and a condition of shock clearly exists. Shock in aircraft may, and often does, originate from suddenly applied forces. These forces result from gun fire, landing, aerodynamic buffeting, and similar conditions. The structures of aircraft are generally light and non-rigid, and therefore incapable of transmitting suddenly applied forces. The impact forces, instead, tend to excite transient vibration of the aircraft structure. This transient vibration often is of substantial amplitude and occurs at many frequencies which are generally dictated by (1) the natural frequencies of the aircraft structures and (2) the frequency components in the applied impact force. In this report, an oscillating motion will be referred to as vibration if it is sufficiently regular that it can be defined by a frequency or frequencies together with the steady-state amplitude at each frequency. If it does not meet these requirements, it must be considered transient in nature, and will be referred to as a shock motion. It is not possible to define a shock motion by assigning numerical values to established parameters. A shock motion can be defined adequately only by describing the time history of a physically significant parameter, such as acceleration, velocity or displacement.

Although shock or transient vibration can be described only by an oscillogram setting forth the time history of acceleration, displacement or velocity, such oscillograms are not included in reference 65 which nominally is the basis for the present study. It has been necessary to go beyond the initially intended scope of this investigation and to obtain oscillograms of vibration

and shock conditions suitable for analysis leading toward the establishment of laboratory testing procedures. A number of oscillograms giving acceleration as a function of time have been made available to the Contractor by the Aircraft Laboratory, Wright Air Development Center, Wright-Patterson Air Force Base and the Carrier Suitability Group at the Naval Air Test Center, Patuxent River, Maryland. From this group of records, selections were made for analysis. All of the records analyzed were the results of measurements made at the center-of-gravity of the respective aircraft during a landing. Insofar as could be determined prior to analysis, the records were selected on the criterion that they be the most severe of the group, and represent a diversity of characteristics so that the results would be representative of a range of shock conditions. The selected oscillograms are set forth as insets to the several sheets comprising Appendix III, wherein the particular aircraft are identified. The details of the analysis carried out on these records are discussed in a subsequent section of this report.

A somewhat cursory examination of the several conditions and variables which define the vibration and shock environment that airborne electronic equipment experiences in service use is considered worthwhile to illustrate the difficulties experienced in attempting to define such an environment. Factors and conditions which control the environment are itemized below:

(a) Aircraft Environment - The nature of the environment experienced in aircraft is directly related to the physical characteristics of the aircraft, its service mission and means of propulsion. According to present structural design criteria requirements, as implemented by the Services, the mission of the aircraft, that is, its classification as a fighter, bomber, cargo, trainer or helicopter type of aircraft, dictates the required structural strength for satisfactory accomplishment of the mission. There is a significant difference between the design strength of the different aircraft types as related to their missions and the aircraft types differ in relative flexibility and consequent response to external excitation. Internal or self-contained vibratory excitation arises from the power plants which may be of the reciprocating engined type, the turbo jet or turbo prop types. The use of assisted take-off rocket power provides another internal source of excitation.

(b) Operational Conditions - Vibration and shock exciting forces are generated on the ground during the engine run-up period where rough engine operation may give rise to severe vibratory excitation. The taxiing run prior to take-off will subject aircraft and associated equipment to vibratory inputs resulting from runway roughness and transient excitation due to brake application.

During the take-off with power plants operating near maximum power, perhaps the most severe power-plant-excited vibration may be experienced with the exception of rough engine operation on the ground. Some variation in vibration levels may be expected as a result of the power and rpm settings of the power plant required to maintain various altitudes and air speeds. Fighter aircraft are subjected to sustained maneuver accelerations which may result in an inadvertent approach to stalling speed and give rise to vibrations excited by flow separation or buffeting. A major source of in-flight transient vibration excitation arises from the aircraft response to continuous turbulence or to discrete gusts. Although little published information appears to be available on aircraft excitation in the transonic flight area it would appear that this operational condition could provide severe inputs from aerodynamic considerations. An important source of transient excitation arises from gun firing from either fixed guns or turret type installations. The transient disturbance generated by multiple gun installations either in the fuselage or wing can and has resulted in severe damage to equipment and to aircraft structure. Because of the relatively close approach to the aircraft stalling speed on the landing approach, and due to the aerodynamic effect of extended flaps on flow over the tail surfaces, a buffeting phenomenon is experienced which affords severe excitation of these components and equipment mounted in the aft fuselage section. The landing impact is perhaps the most severe shock condition that the aircraft and equipment experience. Definition of this shock is not clear cut and its magnitude and duration are influenced by a multitude of variables.

(c) Surface Transportation and Handling - Although the electronic component is intended for airborne use primarily, some part of its useful life will be spent in transportation by rail, truck and sea going vessels which may be designated as surface transportation media. In addition to being exposed to the shock and vibration associated with surface transportation, the component will be subjected to trans-shipment or handling shock.

Aside from the considerations which govern the physical response of items installed in the aircraft, in the evaluation of

vibration and shock data reported, two major categories must be considered. These are the location on the aircraft where the measurement was made and the direction of measurement. Realizing that the aircraft is a flexible structure with several natural modes of vibration and with a complex mass distribution in its many structural components, it is readily apparent that some locations for equipment installation are preferable to others. A wide range of vibration amplitudes may be measured depending upon the location selected on the aircraft structural component. Some thought has been given in the past to breaking down the aircraft environment according to nose, center section, and aft compartment locations in the fuselage and similarly, considering the inner and outer panels of the wings and an area adjacent to the engine location as different environmental areas. Within recent years, especially on fighter aircraft, the addition of external stores which may carry electronic equipment has generated a new and perhaps severe environmental area. This concept of environmental areas appears attractive provided enough statistically significant information to permit this type of definition is collected and evaluated. The necessity for consideration of the direction of measurement that is, as conventionally expressed, vertical, longitudinal, and lateral direction, is obvious.

It should be realized that consideration of all of the above factors and conditions in defining a vibration and shock environment must be predicated on a statistically significant amount of data for each and all of the conditions. Naturally, such a wealth of data does not exist at this time, and as a result several expedients are resorted to in the establishment of a shock and vibration environment which may be considered reasonable under the circumstances. For some of the operational conditions, little or no data may be found as indicated earlier.

Vibration in aircraft has been measured by many agencies. These agencies used a wide variety of instrumentation and adopted various methods of reporting the data. All such data available several years ago were examined and correlated during a project initiated by Curtiss-Wright Corporation and completed by North American Aviation, Inc. The results of this analysis are set forth in reference 65, a voluminous report containing a great mass of data. The usefulness of these data is subject to many qualifications as follows:

(a) The data are reported without regard to probable occurrence in actual service conditions. In the reference, the repeated recurrence of similar data may indicate only that trouble was being encountered under certain conditions, and that repeated measurements became necessary. Other conditions more likely to occur in service may be represented in the reference by relatively few data if there were no circumstances requiring repeated measurements. For these reasons,

large concentrations of data, as reported in the reference, should not be accepted as evidence that the conditions described thereby predominate in actual service.

(b) Some of the data included in the reference represent unrealistic operating conditions, such as stalls and maneuvers that occurred during flights made to investigate air-worthiness of the aircraft. It is questionable whether such data should be included in the present study. If it is included, it is desirable to accord such data less significance than similar data recorded under standard operating conditions.

(c) Some of the data were taken on experimental planes, as indicated by the prefix X on the model number of the plane. In general, not more than a few such planes exist, and the conditions measured thereon are not necessarily typical of those that may be expected to be encountered by aircraft equipment in general.

(d) The reference includes a number of measurements made at locations on the airframe not suitable for mounting electronic and other accessory equipment. Inasmuch as the purpose of this study is to establish testing procedures for such equipment, it would appear evident that measurements made at such locations should be deleted from consideration in this analysis.

(e) The reference describes all vibration and shock environments in terms of numerically defined amplitudes and frequencies. There is no apparent distinction between transient and steady-state conditions. It thus becomes necessary to apply careful discrimination to the interpretation of the data to insure, if possible, that transient data are not being treated as steady-state data.

For the several reasons set forth above, it has been considered necessary to reconsider the environmental data set forth in reference 65. These data are expressed in terms of double amplitude as a function of frequency. By screening the tabulated data in reference 65, the plot shown in Figure 2 was obtained. This figure includes data taken only from measurements on primary airframe structure of fuselage nose and center sections. Data obtained from measurements on equipments, experimental type planes, and obsolete planes have been excluded. An effort was made in the plotting of Figure 2 to include only the substantially steady-state vibration resulting from normal tactical flight. It is hoped that this figure excludes, to a substantial extent,

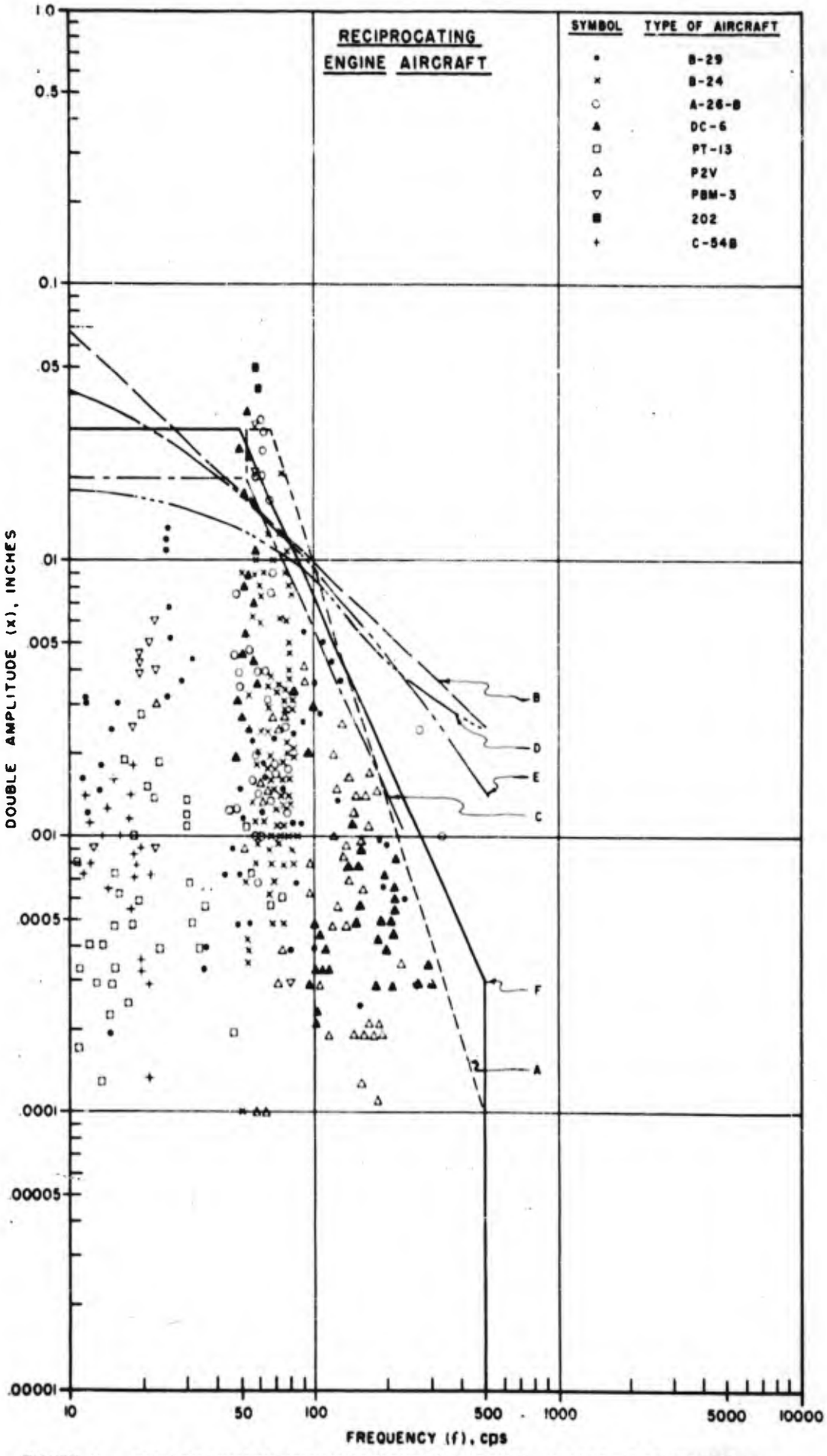

FIGURE 2. STEADY STATE VIBRATION DURING NORMAL FLIGHT - RECIPROCATING ENGINE AIRCRAFT - FUSELAGE LOCATIONS - VERTICAL, LATERAL, AND LONGITUDINAL DIRECTIONS COMBINED

data representing transients resulting from landing, gunfire, and unusual flight conditions. This cannot be guaranteed, however, because in many cases the actual flight conditions are not known.

An envelope indicated by line A in Figure 2 has been drawn around the spectrum of experimentally obtained vibration data. These data represent measurements made only on aircraft powered by reciprocating engines. Reference 65 includes relatively few measurements on airframe structures of jet-powered aircraft during conditions of normal tactical flight which would qualify for presentation in Figure 2. In order to assemble data on jet engined aircraft environment, it was necessary to solicit directly various Service agencies and airframe manufacturers. These data have been analyzed and accorded a treatment similar to that given the data presented in Figure 2. Enough significant differences in the envelope characteristics for the jet engined aircraft vibration data exists so that these data are discussed and evaluated in later paragraphs.

The data reported in reference 65 describing the environment in various types of aircraft powered by reciprocating engines have been examined statistically. The results of this statistical analysis are set forth in reference 80. This analysis reveals the trend of a median line which establishes the relation between frequency and amplitude. It also establishes a line parallel with the trend line below which 95% of all data lie. The inference to be drawn from the analysis is that the 95% line constitutes a reasonable expectancy limit for use in formulating specification requirements. It is set forth on Figure 2 as envelope B.

Existing data on steady-state vibration in Naval aircraft have been examined independently by personnel of the Bureau of Aeronautics of the Navy Department. As a result of this analysis, an envelope representing maximum severity of expected vibration has been formulated. This envelope is shown by line C in Figure 2. At the lower frequency part of the spectrum, the envelope has two branches. The lower of these branches is considered representative of the fuselage center section, while the upper is considered representative of the fuselage tail section and wing outer panels.

It is interesting to compare the envelope derived from a refinement of reference 65 with similar data compiled in England. The latter are available in Specification G.100 of the Royal Aircraft Establishment. Data are given in this specification for several regions of aircraft. An envelope for the central region is indicated by line D in Figure 2, and a corresponding envelope for outer region of aircraft is given by line E in Figure 2. Central regions are defined as the main fuselage and inboard wing sections, while outer regions are described as constituting the tail and outboard wing sections. A comparison of the British data with that obtained from a

refinement of reference 65 shows that the vibration amplitudes embodied in the British data are lower at low frequency vibration and higher at high frequency vibration. This leads to the suggestion that some of the low frequency data set forth in reference 65 may represent transient conditions. If this is true, such data should be deleted from the summary of steady-state conditions. It is unfortunate that the original data from which reference 65 was prepared are not readily available for review.

The assignment of numerical values to the envelope of maximum vibration conditions is important. This envelope defines a region whose coordinates are amplitude and frequency, and in which all steady-state aircraft vibration is likely to occur. The significance of the envelope is that airborne equipment must be capable of withstanding for an indefinite period any combination of amplitude and frequency represented by a point on or below the envelope. Difficulties of interpretation arise because most of the data are the abstracted data set forth in reference 65, and the original data from which such abstract was drawn are not readily available. Several of the envelopes devised by other agencies and included in Figure 2 are subjected to the same limitations because they are based upon the same abstracted data. Taking such data at its face value, envelope A is indicated. Based upon limited information on the nature of available records, the authors of this report have some reservations regarding the validity of the envelope. These reservations are based upon the suspicion that certain of the environmental data have been recorded as steady-state, whereas they are in fact transient. It is hoped to have the opportunity to analyze certain basic flight data at a future time and thereby either confirm the established envelope or modify it to agree with measured environmental conditions.

Considering the vibration data reported in reference 65, for reciprocating engined aircraft, the qualifications that apply thereto, and the interpretations of these and other data that have been made independently by other agencies, a composite envelope of maximum expected vibration has been drawn as follows:

> A displacement amplitude of 0.030 inch peak-to-peak at all frequencies between 10 and 50 cycles per second, and an acceleration amplitude of 4g at all frequencies between 50 and 500 cycles per second. This composite envelope is indicated by line F in Figure 2. It is evident that this envelope is a good fit to test data and that it is consistent with other interpretations of the appropriate vibration envelope. Any apparent deviation of envelope F from experimental data is easily justified by the fact that the envelope may be expressed simply as a maximum displacement amplitude at low frequencies and a maximum acceleration amplitude at high

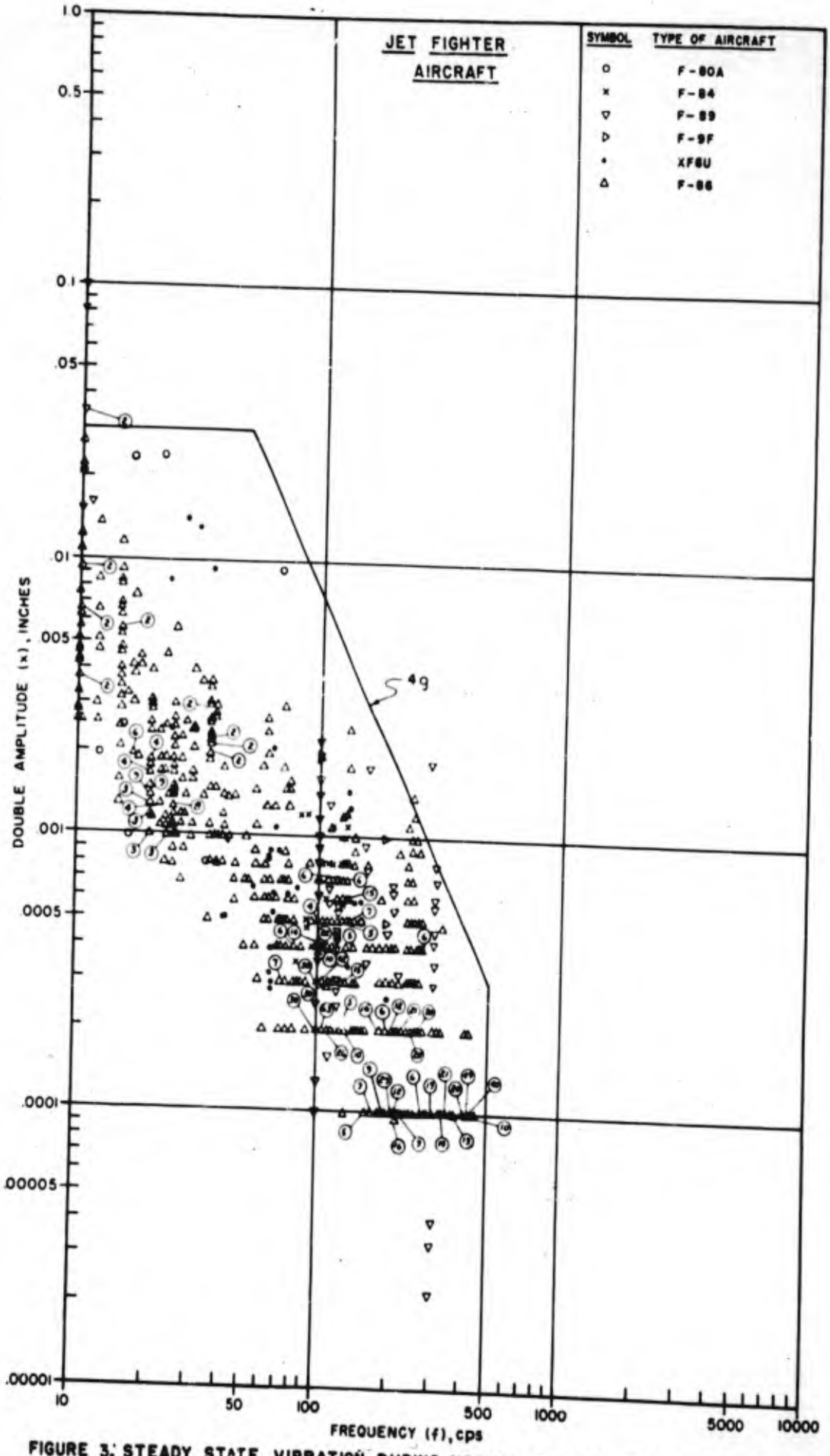

FIGURE 3. STEADY STATE VIBRATION DURING NORMAL FLIGHT - JET FIGHTER AIRCRAFT - FUSELAGE LOCATIONS - VERTICAL, LATERAL, AND LONGITUDINAL DIRECTIONS COMBINED

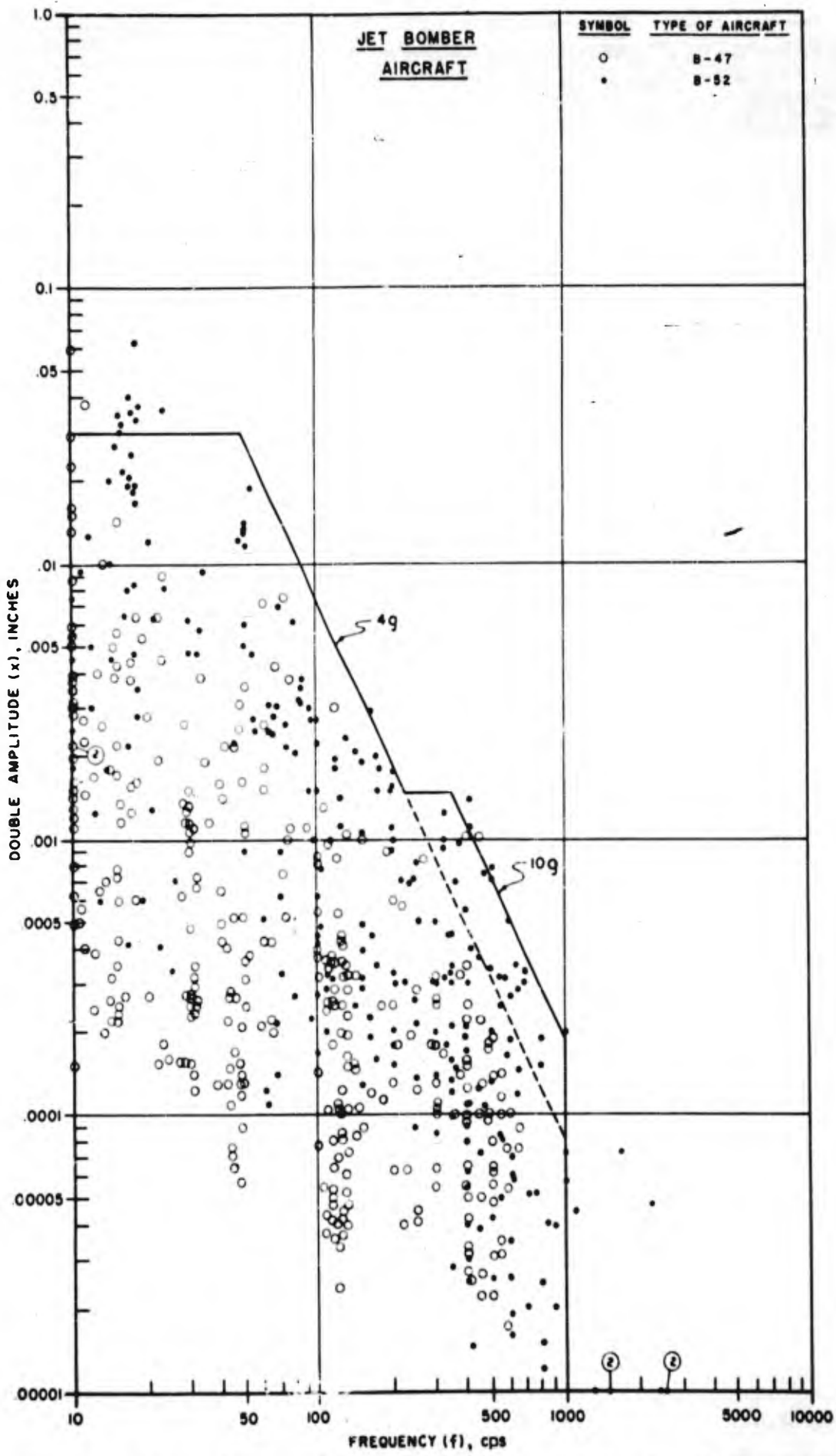

FIGURE 4. STEADY STATE VIBRATION DURING NORMAL FLIGHT - JET BOMBER AIRCRAFT - FUSELAGE LOCATIONS - VERTICAL, LATERAL, AND LONGITUDINAL DIRECTIONS COMBINED

frequencies. The envelope extends to approximately 500 cps, although few experimental points lie above 200 cps. This lack of data at high frequency may be the result of limited response of instruments or to deletions in the interpretation of the data.

The data obtained for jet engined aircraft is restricted to turbo-jet types. Some steady-state vibration data were obtained from Reference 65, but the majority of the information was obtained directly from reports published by aircraft manufacturers. Figure 3 presents a plot of vibratory double amplitude versus frequency for jet fighter aircraft. In Figure 4 similar flight vibration data are plotted for the bomber jet aircraft. The data presented in both of these figures are for fuselage locations only, and the data were accorded the same evaluation treatment as that given the data of Figure 2, in that insofar as possible, transient vibration information was deleted. These data for both types of aircraft were originally plotted for each primary direction of vibratory motion; that is, vertical, lateral, and longitudinal. However, it was readily apparent that not enough statistically significant information would be provided with this method of plotting and as the data did not indicate significant differences between the magnitudes indicated as a function of direction, both the fighter jet and bomber jet vibration data have been plotted for combined directions.

Referring to Figure 3, the jet fighter aircraft envelope plot, it is apparent that an envelope identical to that derived for the reciprocating engined aircraft will readily fit these data. A comparison of the data that defines the jet fighter aircraft envelope diagram with that for the reciprocating engined aircraft indicates that for both figures, the data density appears to be relatively heavy in the 90 to 150 cps frequency band. However, in the data plot for the jet fighter aircraft, the data density in the 200 to 500 cps frequency band is considerably greater than that shown for the reciprocating engined aircraft.

The double amplitude versus frequency data plot for the jet bomber aircraft is somewhat surprising. It should be realized that this is based upon the measurements made on but two jet bomber aircraft, but in both cases a great amount of data was obtained and constitutes the most recent acquisition of vibration environmental data. For information purposes, a constant 4 "g" line has been drawn on the plot basically to indicate the number of significant points that lie outside the 4"g" lines. A constant "g" envelope line that envelopes all but a few points between 350 and 1000 cps would of necessity be a 10 "g" line.

The selected envelope shown would then consist of a constant amplitude section of .030" double amplitude from to 10 to 50 cps, from 50 cycles to 225 cps the envelope is a constant 4"g" line, and from 225 to 1000 cps a constant 10"g" line. This steady-state

vibration environmental envelope expressed in terms of acceleration amplitude is shown graphically in Figure 5.

In attempting to account for the more severe vibration environment found in the jet bomber aircraft it may be of significance to note that the structural design criteria stipulated by the Air Force are such that bomber aircraft are designed for lower load factors for several design conditions and consequently are less rigid inherently than fighter aircraft. If data on reciprocating engined aircraft of a gross weight comparable to the B-47 and B-52 were available for analysis, it would be interesting to speculate on a comparison of their environments with the jet bomber environmental envelope.

The selected envelopes of Figures 2,3 and 4 have been plotted in terms of acceleration amplitude in Figure 5.

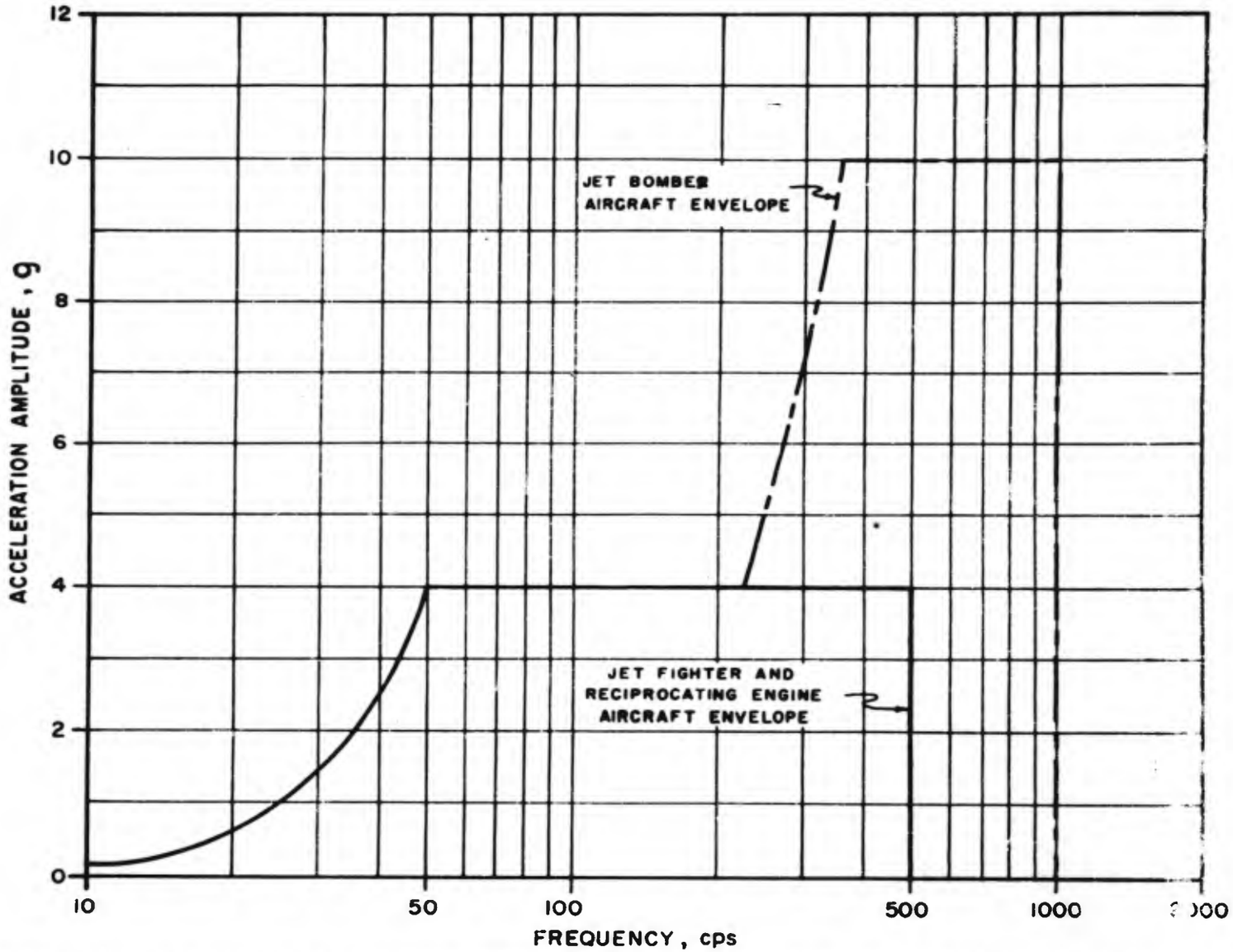

FIGURE 5. STEADY STATE ENVIRONMENT ENVELOPES FOR RECIPROCATING ENGINE, JET FIGHTER, AND JET BOMBER AIRCRAFT EXPRESSED IN TERMS OF ACCELERATION AMPLITUDE

SECTION IV

RESPONSE OF ELASTIC SYSTEMS TO STEADY-STATE VIBRATION

A vibration test embodying an exaggerated test amplitude intended to cause failure of the equipment after a relatively short time duration will be referred to here as an accelerated vibration test. An hypothesis of accelerated testing may be formulated by referring to the single-degree-of-freedom system shown in Figure 6. This system consists of a massless, linear spring k supporting a rigid mass m constrained by vertical guides to move only along a vertical line. The motion y of the supported mass is induced by the steady, simple harmonic motion x of the base. The motion of the base may be described by the following expression:

$$X = X_0 \text{ SIN } \omega t \qquad (1)$$

where x is the displacement amplitude of the vibration of the base in the vertical direction and ω is the vibration frequency expressed in radians per second.

A complete solution of the differential equation describing the motion of this system includes terms representing the transient motion of the mass at the natural frequency of the mass-spring system. (See reference 3). The natural frequency is expressed in units of radians per second by

$$\Omega = \sqrt{k/m}$$

and in units of cycles per second by

$$f_n = \sqrt{K/m}\,/2\pi$$

In any practical system, the spring will embody some damping, and these transient vibrations will be damped out ultimately. The motion of the mass may then be assumed to be simple harmonic at the same frequency as the motion of the base, but with a different amplitude. The relation between the motion of the mounted mass and the motion of the base is illustrated in Figure 7. The vertical scale is the ratio of displacement amplitudes, or since both x and y occur at the same frequency, the vertical scale also represents the ratio of acceleration amplitudes. The horizontal scale is the ratio of the forcing frequency ω to the natural frequency Ω of the mass spring system. For an undamped system, the curve theoretically reaches infinity at a frequency ratio of unity. This is a condition of resonance. All practical systems have some damping, and the amplitude at resonance is a finite value, as shown in Figure 7.

If the spring in the system of Figure 6 is linear and if

the mass is infinitely rigid, the relation between the acceleration of the mass and the deflection of the spring is given by the following equation:

$$m\ddot{y} = k(x - y) \tag{2}$$

Inasmuch as the stress in the spring is proportional to the deflection (x-y) of the spring, the stress is also directly proportional to the acceleration of the mass.

This relation may now be extended by analogy to the hypothetical equipment illustrated in Figure 1. The parameter x may be considered to represent the motion of the airframe while the parameter y represents the motion of the center of the panel. The maximum expected motion of the airframe is defined by the acceleration-frequency plot shown in Figure 5 while the ratio of the maximum acceleration of the panel to the maximum acceleration of the airframe is given by Figure 7. Consequently, the maximum expected acceleration of the panel is the product of the ratio given in Figure 7 and the maximum acceleration of the airframe given in Figure 5. Repeated stressing of the panel thus occurs because its central part is being loaded with an inertia force proportional to the maximum acceleration of the center of the panel. Furthermore, components mounted upon the panel are also subjected to repeated stressing because the forces applied thereto increase as the vibration of the panel increases. This involves consideration of the strength of structural members which are subjected to repeated stresses.

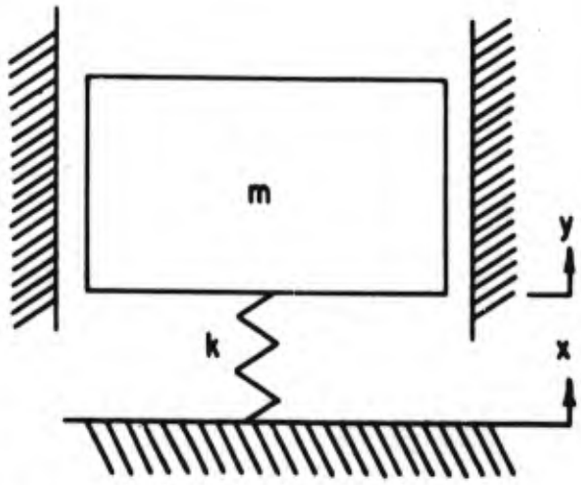

FIG. 6. IDEALIZED SYSTEM REFERRED TO IN DEVELOPMENT OF HYPOTHESIS OF ACCELERATED VIBRATION TESTING.

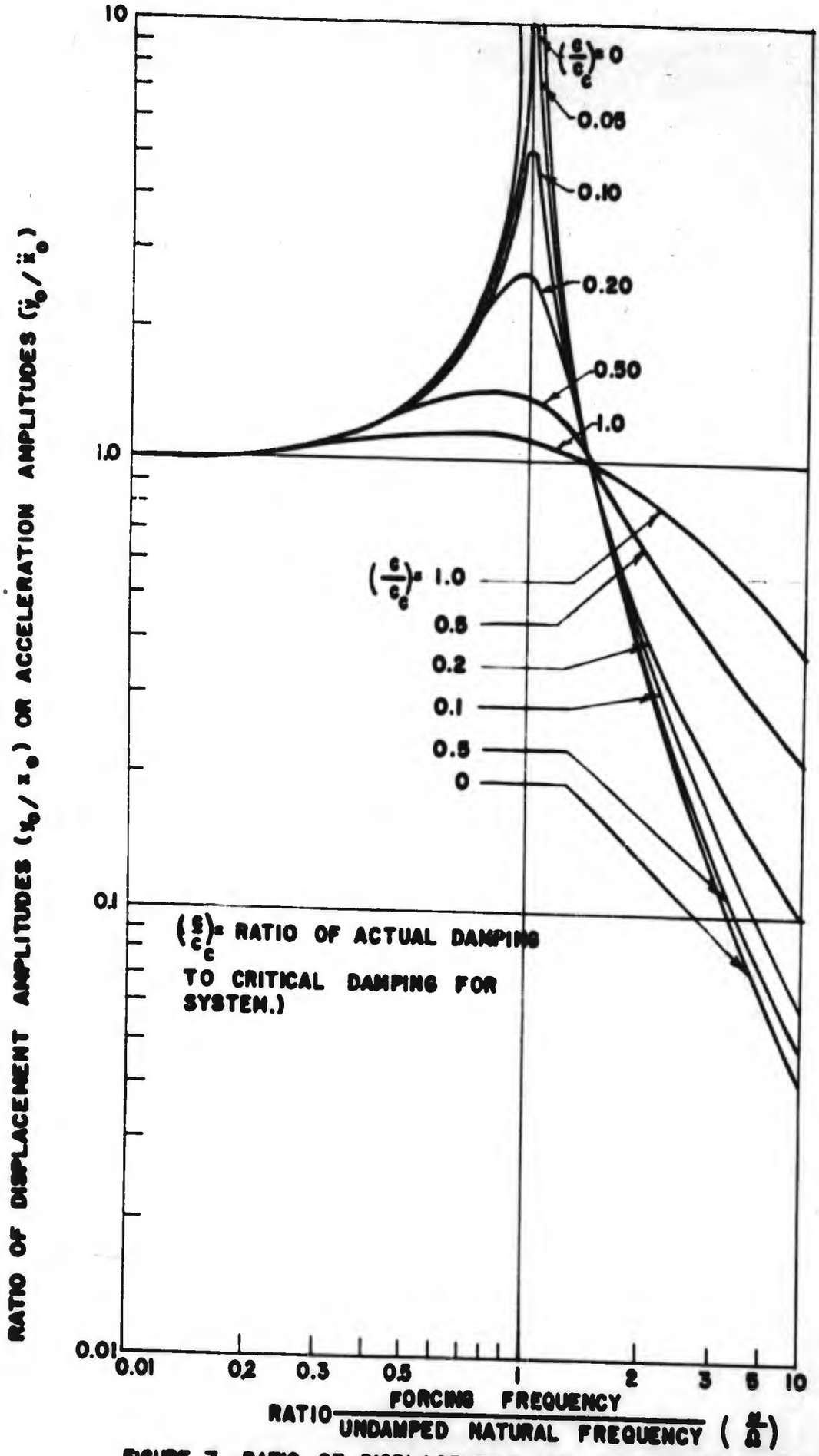

FIGURE 7. RATIO OF DISPLACEMENT AND ACCELERATION AMPLITUDES DESCRIBING MOTION OF SYSTEM IN FIGURE 6 IN STEADY-STATE VIBRATION.

SECTION V

CONCEPT OF THE FAILURE SURFACE

The properties of metals when subjected to repeated stressing have been well investigated, and much data exist in the technical literature describing the results of such investigations. The tests are usually conducted by manufacturing a number of test specimens which are as nearly identical to each other as possible. These specimens are used in testing machines that are arranged to impart alternating cycles of tensile and compressive stress to the specimen, or to impart bending stresses alternating in opposite directions. Tests are then run under similar conditions for each specimen, except that a different value of maximum stress is selected for each specimen in the test. Repeated applications of stress according to the selected stress pattern are then applied until the specimen fails. It is usually found that a specimen with a lower maximum stress will endure a greater number of cycles of stress reversal than a specimen with a higher maximum stress. The results are commonly reported as shown by the typical curve in Figure 8. This curve is commonly referred to as the S-N curve, where S represents the maximum stress and N represents the number of cycles to failure. The exact shape of the curve differs somewhat from metal to metal. The curves for many metals have a well-pronounced knee, and the curve extends in a substantially horizontal direction rightwardly from the knee for an infinite number of cycles. This means that if the maximum stress is below the level represented by this horizontal part of the line, the specimen will endure an infinitely large number of cycles without experiencing failure. This stress level is referred to as the endurance limit for the material.

It was pointed out that the maximum stress in the spring k in Figure 6 tends to be proportional to the maximum acceleration $\ddot{y}_o$ of the mounted mass m. Consequently, the parameter of the ordinate scale in Figure 8 may be changed from maximum stress to maximum acceleration of the mass m if the endurance properties of the spring k are to be investigated. Since the maximum acceleration $\ddot{y}_o$ of the mass m and the maximum acceleration $\ddot{x}_o$ of the support are related as shown in Figure 7, the maximum acceleration $\ddot{y}_o$ of the mass and the maximum acceleration $\ddot{x}_o$ of the support are directly proportional for any given forcing frequency. This makes it possible to draw the family of $\ddot{x}$ - N curves illustrated in Figure 9 by converting S in Figure 8 to the appropriate value of $\ddot{y}_o$, and then multiplying by the applicable ratio obtained from Figure 7. The vertical scale $\ddot{x}_o$ is the maximum acceleration of the support, the horizontal scale N is the number of cycles to failure, and each of the curves corresponds to a particular forcing frequency. Now just as each specimen has a characteristic S-N curve as shown in Figure 8, each system may be considered to have a characteristic $\ddot{x}$ - N - f relation as shown in Figure 9,

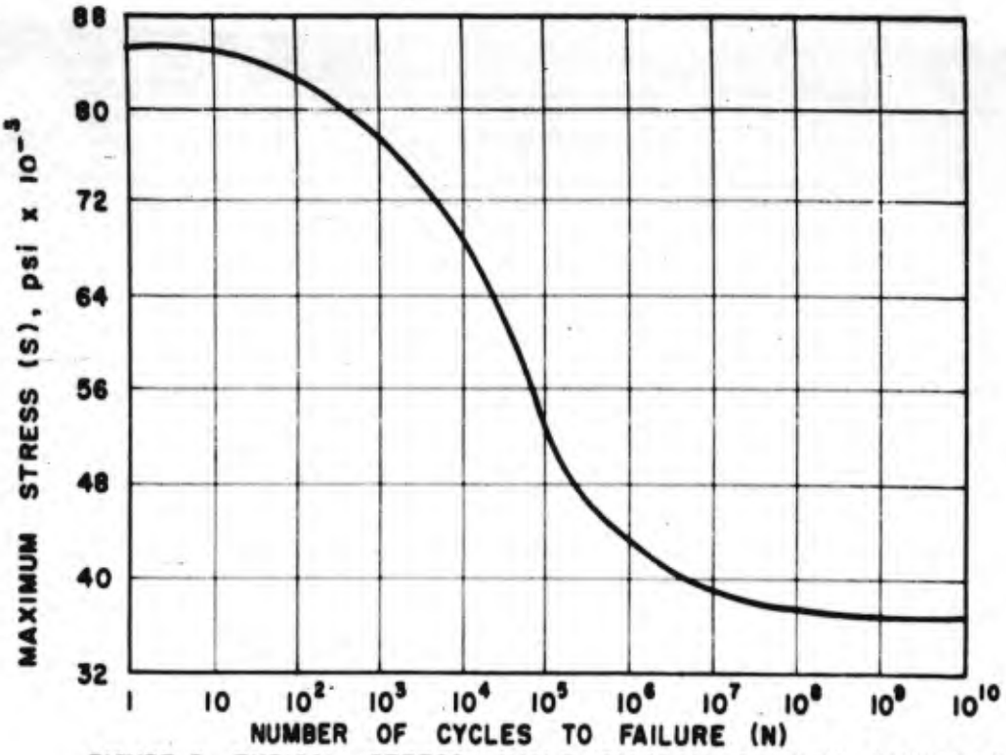

FIGURE 8. TYPICAL STRESS- CYCLE DIAGRAM SHOWING PROPERTIES OF STEEL WHEN SUBJECTED TO REPEATED STRESSING

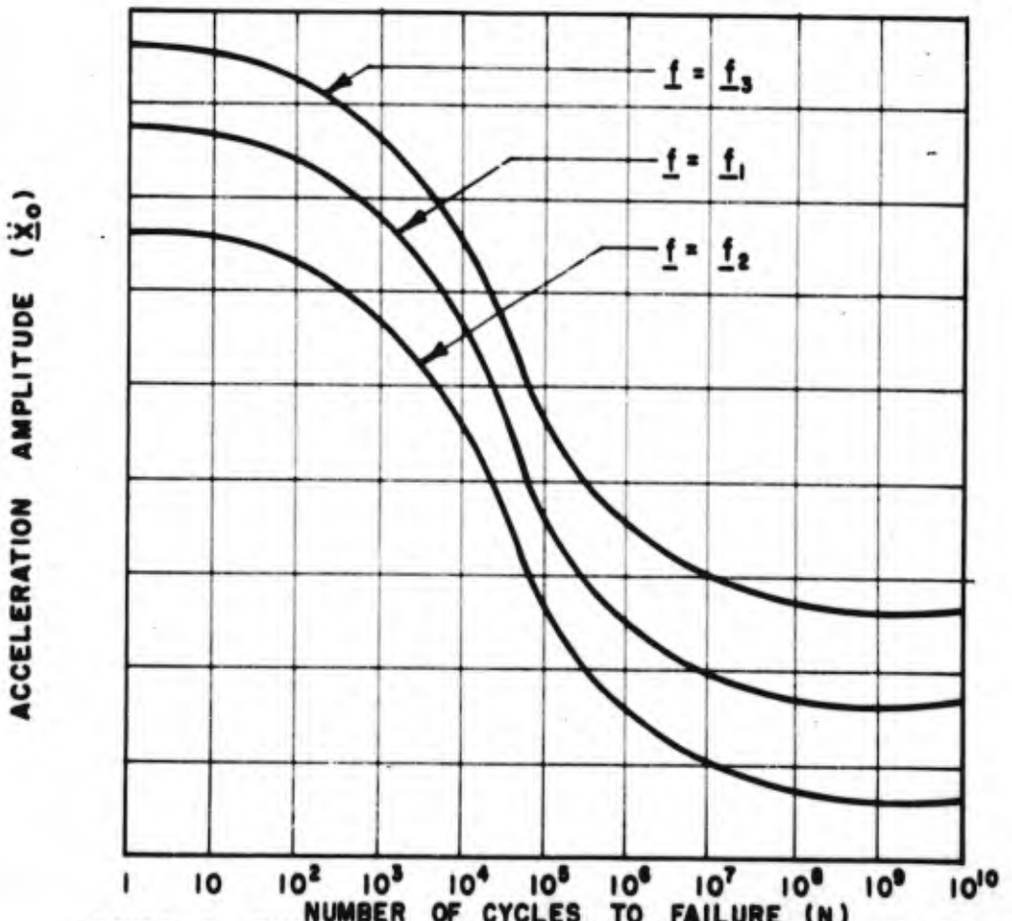

FIGURE 9. TYPICAL CURVE SHOWING ENDURANCE PROPERTIES OF SYSTEM ILLUSTRATED IN FIGURE 6 FOR A GIVEN NATURAL FREQUENCY AND KNOWN RELATION BETWEEN y_o AND S.

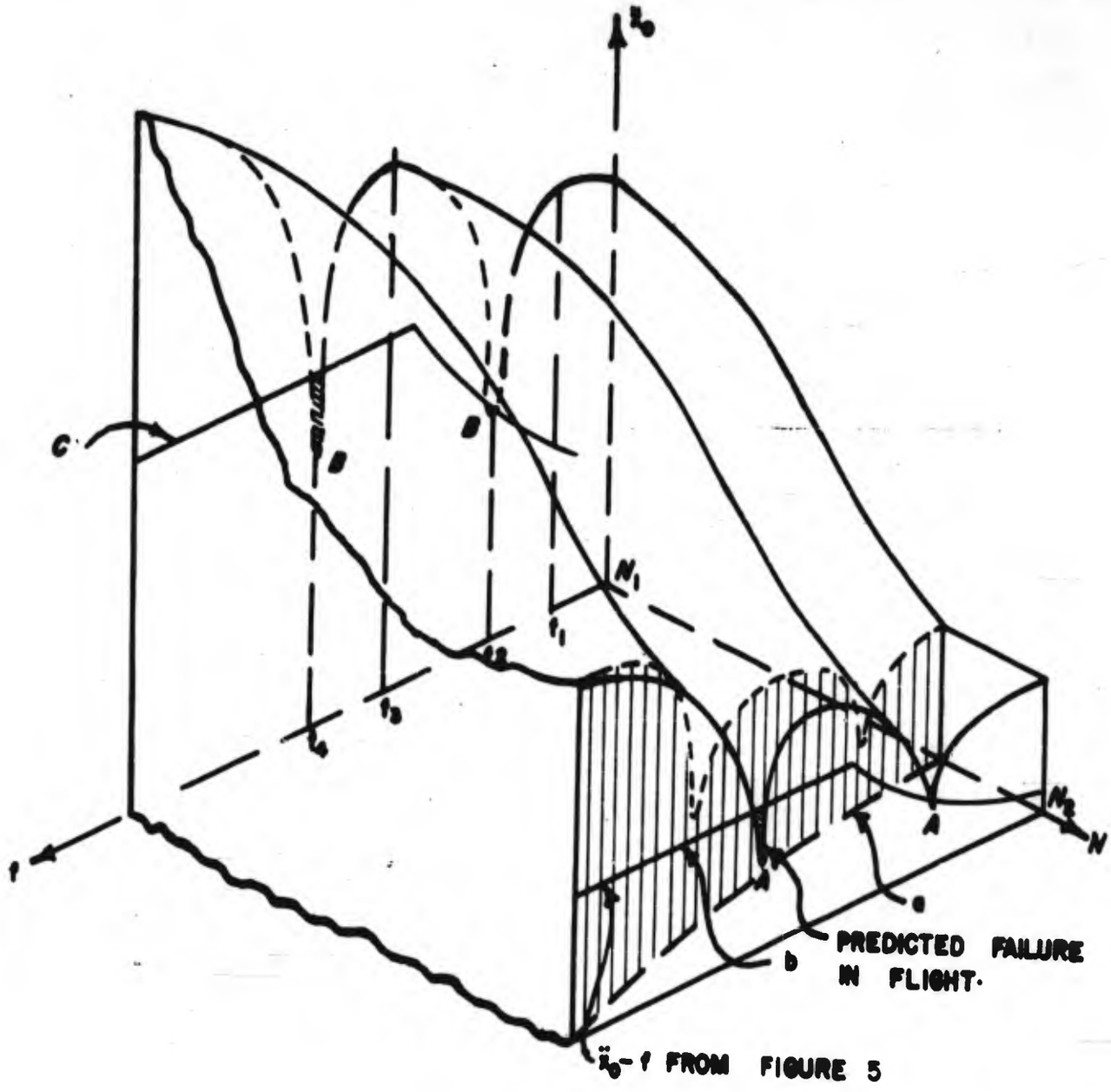

FIGURE 10. FAILURE SURFACE FOR EQUIPMENT HAVING COMPONENTS WITH NATURAL FREQUENCIES f_2 AND f_4, AND SUPERIMPOSED ENVELOPES SHOWING ENVIRONMENTAL AND LABORATORY CONDITIONS.

where it is presumed that the natural frequency of the system and the relation between S and $\ddot{Y}_o$ are known.

The conditions defined by the family of curves in Figure 9 can be expressed more conveniently in three dimensions as the surface shown in Figure 10. This surface will be referred to as a failure surface. Each equipment has a failure surface that is typical of that equipment, and the surface fully defines the combination of parameters that will produce failure of the equipment. The parameter of the vertical coordinate axis is the maximum acceleration embodied in the vibration of the support in Figure 6, the left-hand axis is the test frequency in cycles per second, and the right-hand axis represents the number of cycles to failure.

The surface illustrated in Figure 10 is for a hypothetical equipment having resonant frequencies f_2 and f_4. Resonant frequencies are indicated by valleys in the surface, because a lower value of applied acceleration $\ddot{X}_o$ is required to cause failure if the test frequency coincides with one of the natural frequencies of the equipment. These valleys extend generally parallel to the $\ddot{X}_o$ - N plane so that any plane through the surface parallel to the $\ddot{X}_o$ - f plane shows depressions at the characteristic resonant frequencies. The failure surface for a single-degree-of-freedom system would show only a single valley, because such a system has only one natural frequency. The failure surface for a complex equipment would show many valleys, depending on the number of frequencies at which damaging resonances occur within the equipment. The valleys in a particular failure surface may be of different depths if the resonances that the valleys represent apply to structures with different degrees of damping.

Assuming that the failure surface is in existence for the equipment being considered, a specification for an accelerated test may now be formulated. A time in hours is first selected which represents the duration of the actual service in flight which the equipment is required to endure. A line a is then drawn on the f - N plane to represent the number of cycles at each frequency that would be required to reach the selected flight time. Theoretically, line a would be curved as shown in Figure 10 because the number of cycles in a given period increases with an increase in frequency. Practically, a plane may be used because the failure surface is parallel with the N axis for large values of N. A curved surface is then generated by a vertically extending line moving along the path a drawn on the f - N plane. The envelope $\ddot{X}_o$ - f representing the maximum severity of vibration conditions expected in flight, as set forth on Figure 5, is then transcribed onto the curved surface which was generated by moving a straight line along the path a in Figure 10. This envelope $\ddot{X}_o$ - f is designated by b in Figure 10.

If the intersection of the failure surface with the surface generated along line a falls below the envelope b of maximum vibration conditions, failure of the equipment may be expected during flight if the vibration environment in the particular aircraft is at the [illegible] level. The condition of predicted failure is indicated by the crosshatched area in Figure 10. For this particular equipment, it is thus indicated that the component having a resonant frequency f_4 may fail before the equipment receives N_2 cycles of vibration. The probability of the equipment failing is equal to the probability that the vibration level in the particular airplane reaches the maximum expected level.

Inasmuch as Figure 10 predicts possible failure of the component with a natural frequency f_4 during flight conditions, the accelerated testing procedure for laboratory use should cause failure of the same component. The accelerated testing procedure is established by selecting a relatively small value for the number of cycles to failure, as designated by N_1 in Figure 10. In this instance, N_1 is made small enough to be feasible for laboratory testing. It is now necessary to construct a new surface whose coordinates are $\ddot{x}$ and f, intersecting the N axis at the value N_1. This newly selected surface may be a plane as shown in Figure 10. If the selected test procedure applies the same number of cycles of vibration at each test frequency; i.e., a shorter testing time at the higher frequencies, the surface $N - N_1$ will be a plane. If it is desired to conduct a test for equal periods at each testing frequency, the surface in the region of the Number N_1 will be a curved surface generated by a vertical line following a curved path in the $f - N$ plane. This corresponds to the procedure used to establish the surface representing flight conditions except that the number of cycles is small to correspond to laboratory conditions.

The laboratory test conditions, as represented by line c, are now inscribed upon the surface recently constructed in the region of the value N_1. If the laboratory test is to be valid, the line c defining the laboratory testing procedure must intersect the failure surface at the frequency f_4 but avoid intersection at the frequency f_2. This indicates that the component having a natural frequency f_4 will fail during laboratory testing. The validity of the laboratory test thus tends to be established, because it predicts the same type of failure predicted for service of the equipment in actual flight.

The hypothesis embodying the failure surface is difficult

to apply in formulating an accelerated testing procedure, primarily because the failure surface is not known to exist for any particular equipment. A tremendous amount of testing would be required to establish a single surface. If sufficient tests were conducted, it would undoubtedly be found that failure conditions would be described by a blanket of appreciable thickness rather than by a surface of zero thickness. This is expected because the scatter of results in endurance testing is relatively great, and scatter would tend to produce a blanket rather than a surface. In the hope that significant data exists from which a failure surface could be plotted, Contractor solicited test data from more than 300 potential sources of such information. The results obtained from these inquiries indicate that the data probably do not exist. It thus becomes necessary, in order to apply this hypothesis using a failure surface, to make certain assumptions as follows:

(a) It must be assumed first that the shape of the $\ddot{x}_o$ - N curve is similar to the shape of the S - N curves obtained by subjecting specimens of material to repeated stresses under closely controlled conditions. This assumption may be valid for certain conditions in which the failure occurs as a result of repetition of excessive stress in the equipment being tested. In other circumstances, the failure may have little relation to stress, and the assumption of an analogy between the $\ddot{x}_o$ - N and S - N curves may be unwarranted. Assuming the analogy to be valid, because no other assumption appears indicated, it may be assumed that the $\ddot{x}_o$ - N curve is flat for values of N greater than five million, and has an established slope for values of N less than five million and greater than one thousand.

(b) It may be further assumed that all equipment installed in aircraft will be required to endure more than five million cycles of vibration. A scale of values may then be assigned to the $\ddot{x}_o$ axis in such a way that the flat part of the $\ddot{x}_o$ - N curve ($N > 5 \times 10^6$) is sufficiently far above the measured values of acceleration in aircraft service that the valleys of the failure surface do not fall below the environmental line (b in Figure 10) when large values of N are assumed.

(c) It may be assumed that the depth of each valley is proportional to the height of the surface in the region of the valley. This is equivalent to assuming that the damping associated with each resonant element is equal and does not vary with amplitude of vibration. It is with some misgiving that this assumption is made because damping is neither uniform nor linear in many instances.

SECTION VI

CORRELATION OF VIBRATION AND FATIGUE

The technical literature on fatigue or endurance testing has been very carefully surveyed in an attempt to establish the validity of assumption (a) in the previous section. The principal source of data has been reference 7 . This survey has established the following numerical values which are assumed for purposes of this analysis to be representative of the properties of metals subjected to repeated stressing:

(a) The curve of maximum stress in steel as a function of number of cycles to failure is substantially flat for cycles greater than five million. In other words, if a test specimen made of steel has not failed after having been subjected to five million stress reversals, it is probable that failure will not occur if the test is continued indefinitely.

(b) The maximum stress at which infinite life of the test specimen is obtained is on a general average 38 per cent of the ultimate strength of the material. In other words, the maximum stress for which five million stress reversals may be obtained without failure is 38 per cent of the stress at which failure will occur upon one application of load. Some substantiation for the above assumption is indicated in Figure 11, which has been obtained from reference number 1 . The straight line delineating the ratio of endurance limit stress to ultimate stress equal to 0.38 has been added to the original figure. Further generalizing on the basis of the typical S-N curve shown in Figure 8, the maximum stress at 10^3 cycles to failure is assumed equal to the maximum stress at one cycle to failure.

The endurance or stress-cycle curve taken from the above generalization is shown by line I in Figure 12. Point A in Figure 12 corresponds with points A on the failure surface in Figure 10. The acceleration amplitude scales $\ddot{x}_o$ are brought into correspondence by establishing a scale on Figure 12 so that the acceleration amplitude $\ddot{x}_o$ at point A on Figure 12 equals the acceleration amplitude $\ddot{x}_o$ at the bottom of a depression in Figure 10 that is representative of the particular element considered vulnerable. This assumes that $N_2 = 5 \times 10^6$ in Figure 10.

A question naturally arises concerning the validity of endurance tests of materials as a basis for establishing

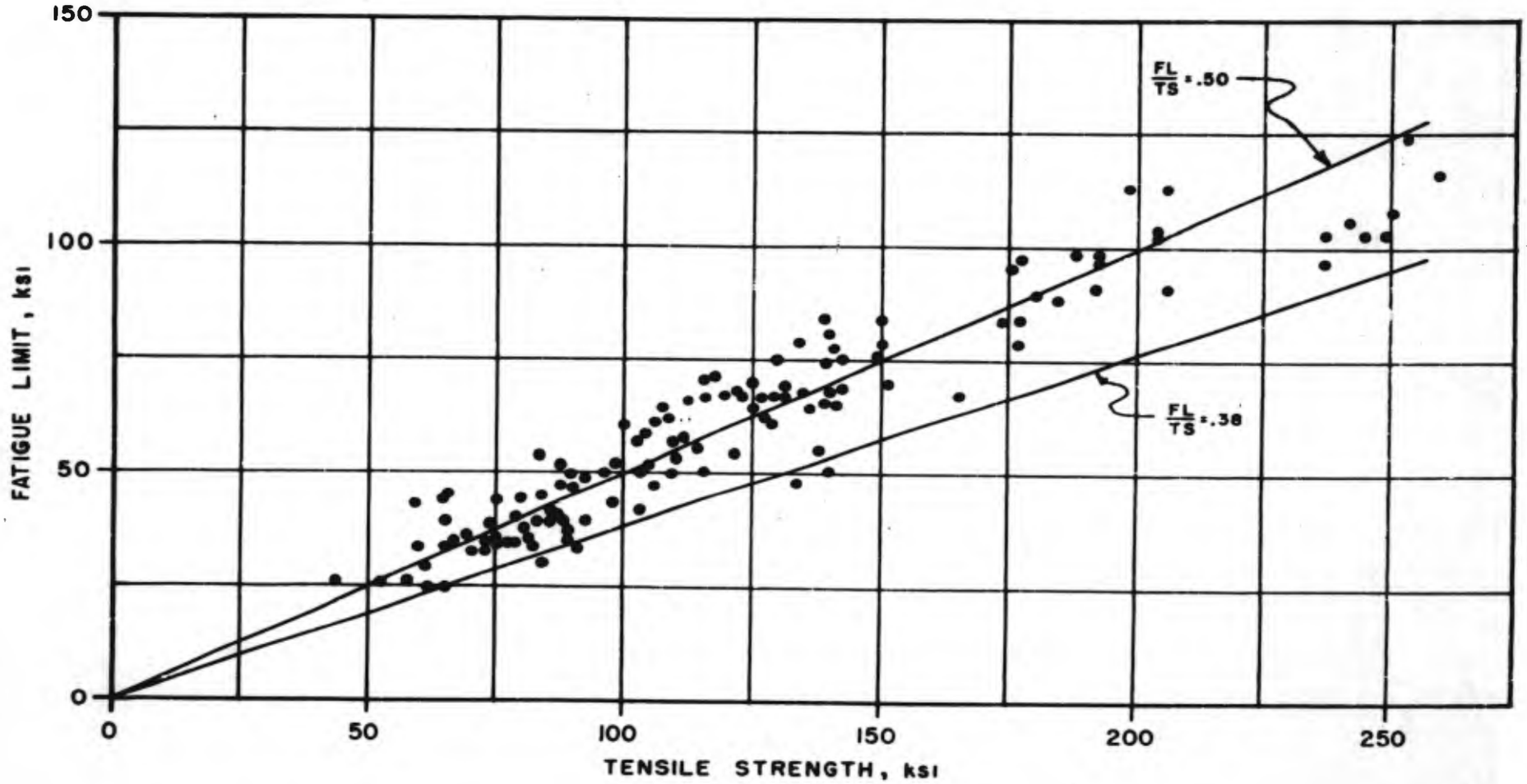

FIGURE 11. ROTATING-BENDING FATIGUE LIMITS OF CAST AND WROUGHT STEELS

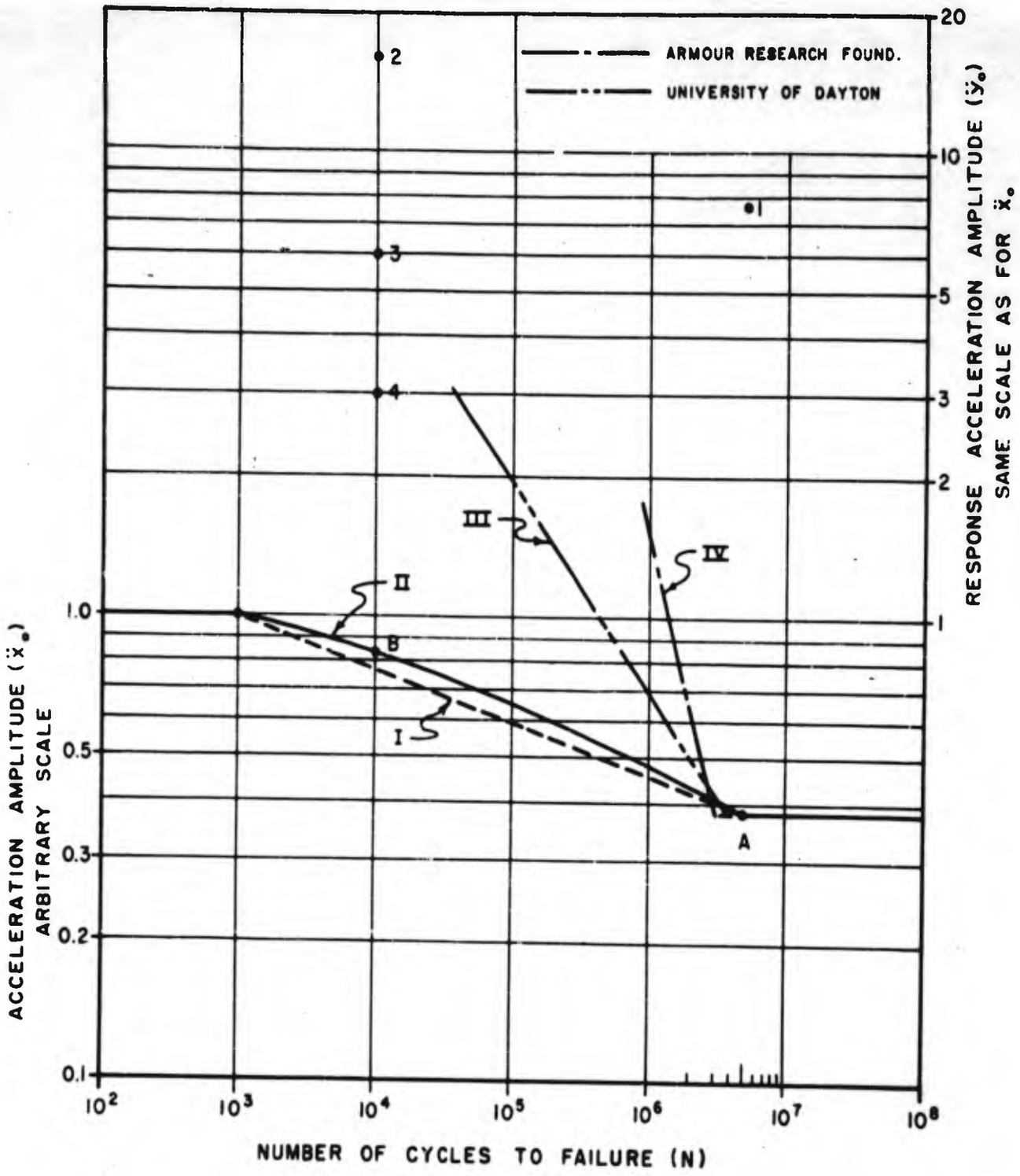

FIGURE 12. IDEALIZED ENDURANCE CURVE WITH SUPERIMPOSED DATA SHOWING RESULTS OF VIBRATION ENDURANCE TESTS

vibration test specifications. All known vibration test data bearing on this relationship have been studied. Useful data are extremely scarce, but the fragmentary information that is available tends to lend validity to the assumption:

(a) The Calidyne Company, under Contract #DA-36-039 SC-5545 with the U. S. Army Signal Corps Engineering Laboratories, conducted an investigation of fasteners for mounting electronic components. In the course of this work, extensive vibration tests were conducted on complete equipments and on typical components. The components tested were not identical and it is, therefore, impossible to establish an endurance curve. The number of cycles of vibration necessary to cause failure of the various components has been analyzed, however, and the results are shown in Figure 13. It is evident that substantially all failures occurred at fewer than five million cycles of vibration, and that failure did not occur if the component withstood 3.4 million cycles. This tends to confirm the previous conclusion that a curve of acceleration amplitude vs. cycles to failure becomes horizontal for cycles greater than five million.

(b) Vibration tests to failure were conducted by Contractor, using a number of identical resistors. The resistors were supported by attaching the leads at opposite ends to spaced binding posts. Several resistors were grouped on a common panel and each group was subjected to vibration at a different level of maximum acceleration. Although the tests were not conducted at a resonant frequency of the resistors, the results are useful to establish the relation between acceleration amplitude and cycles of failure. Failure occurred generally by rupture of the electrical leads. The test results show considerable scatter, but the median is indicated by line II in Figure 12 in which the acceleration amplitude is adjusted to attain coincidence of lines I and II at $\underline{N}=5\times10^{6}$. A comparison of lines I and II in Figure 12 suggests agreement between the results of repeated stressing of metals and continued vibration tests of resistors. Insofar as the authors are aware, this is the best information available tending to establish a relation between vibration amplitude and number of cycles to failure.

Although the data discussed in the above paragraph tend to establish laws of mechanical failure, it is evident that electrical failure of the equipment is equally important. Data to establish the relation between severity of vibration and electrical failures are also scarce. Data on failure of

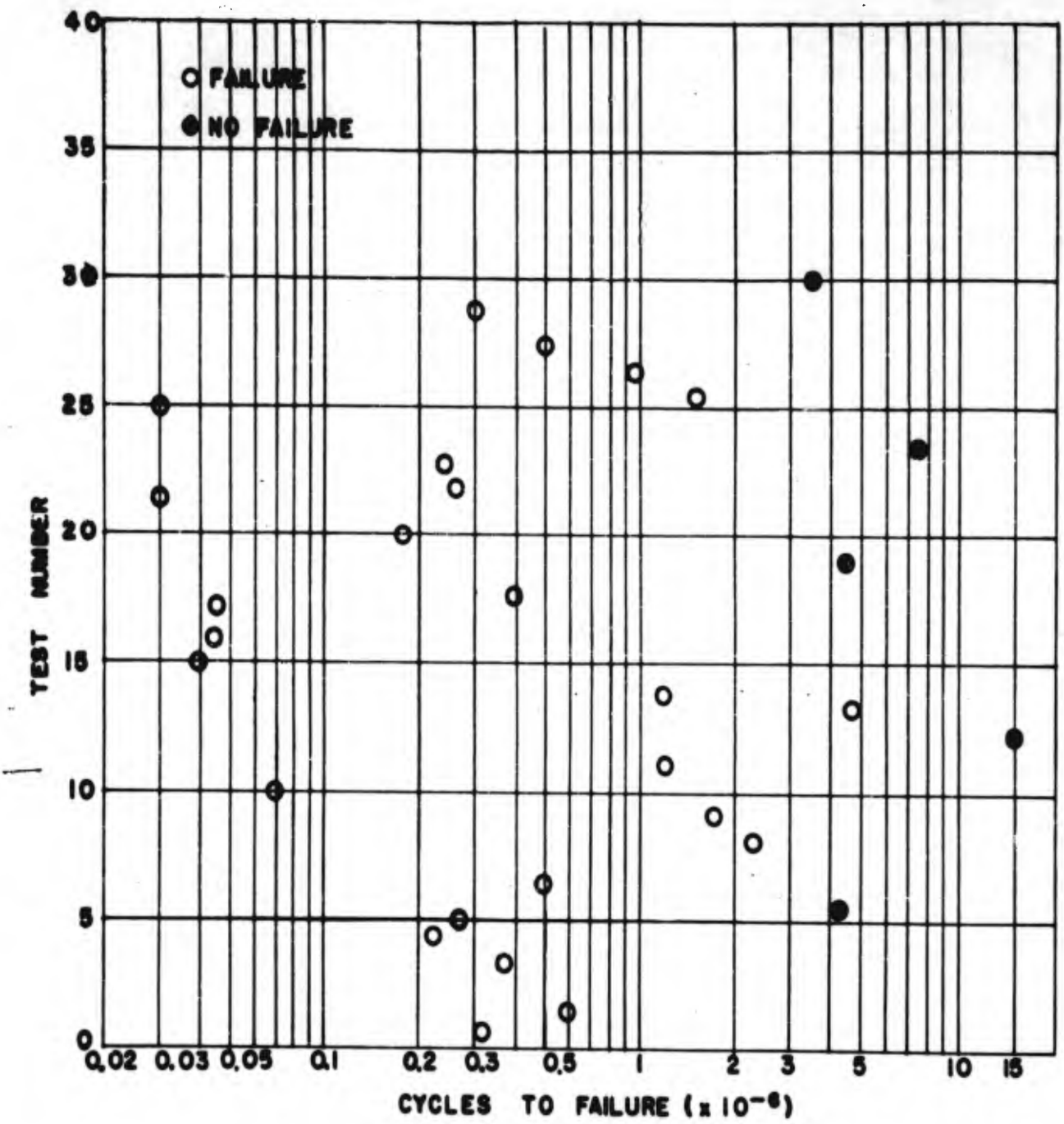

FIGURE 13. NUMBER OF CYCLES TO FAILURE IN VIBRATION TESTS CONDUCTED BY THE CALIDYNE CO.

vacuum tubes as a result of vibration, based upon tests conducted by the University of Dayton and by the Armour Research Foundation, have been obtained. Although the severity of these tests cannot be successfully correlated because resonance effects are not known, some indications of relative strength may be obtained. The test results are shown by lines III and IV in Figure 12 assuming the acceleration amplitude to be adjusted to obtain coincidence with lines I and II at $\ddot{x}$=0.38. The drastically different slope of lines III and IV indicates a complete lack of agreement between electrical and mechanical failure. This tends to cast some doubt on the validity of the previous assumptions. The theory based upon mechanical failure should not be ruled out, however, until additional significant data on electrical failures are available.

However the extent to which this analogy may be justified can be determined, at least in a qualitative sense, by comparing resonant vibration failures of electronic components with resonant fatigue data for metals. Such a comparison will be made in the following several pages.

Considerable data on the fatigue properties of metals exist in the technical literature. For example, Figure 14, summarizes bending fatigue data for a variety of high strength steel specimens, with and without stress concentrations, and with ultimate tensile strengths ranging between 100,000 and 200,000 psi. This fatigue information is drawn from Reference 47. Figure 15 is a fatigue life curve estimated for cold drawn copper from information in Reference 31. The results in Figures 14 and 15 were obtained from rotating beam fatigue tests at non-resonant frequencies. Recent investigations of the damping properties of materials provide a basis for reinterpreting these non-resonant fatigue data so as to include the effect of resonant conditions.

Under resonant conditions, the only forces acting to constrain the amplitude of response motion in a structure are the internal damping or internal energy dissipation properties of the structural material. The internal damping properties of metals are in general quite small and amplification factors at resonance extending to as high as 300 for high strength steels and aluminum are not uncommon. The amplification factor referred to here may be defined as the ratio of the excited (or response) motion or force, to the applied motion or force. Once the resonant amplification factor or Q of a structure is known, the resonant strength of the structure may be readily determined in terms of the forces or motions which are applied. Since environmental data for aircraft are by convention expressed in terms of vibration amplitude or acceleration as a function of frequency, it is convenient for purposes of the present work to evaluate

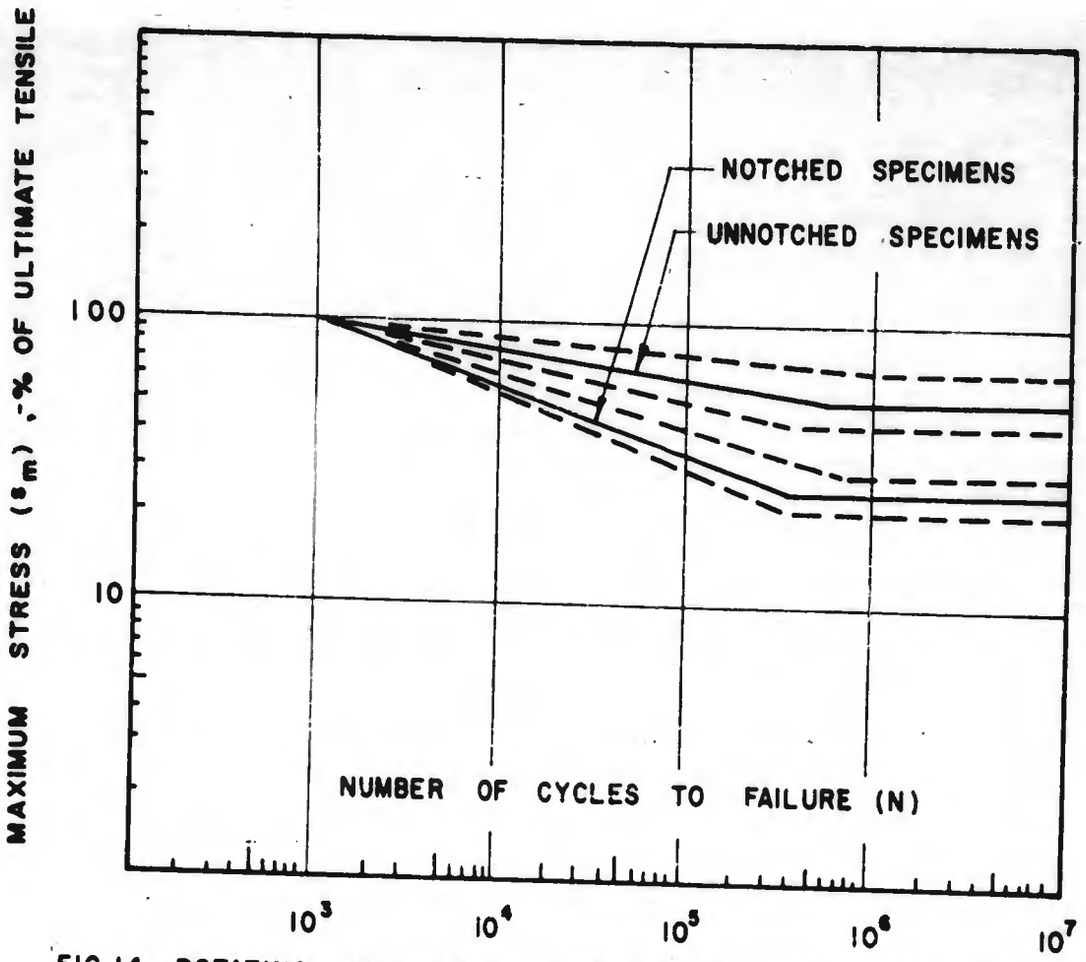

FIG. 14. ROTATING BEAM FATIGUE DATA FOR HIGH STRENGTH STEELS

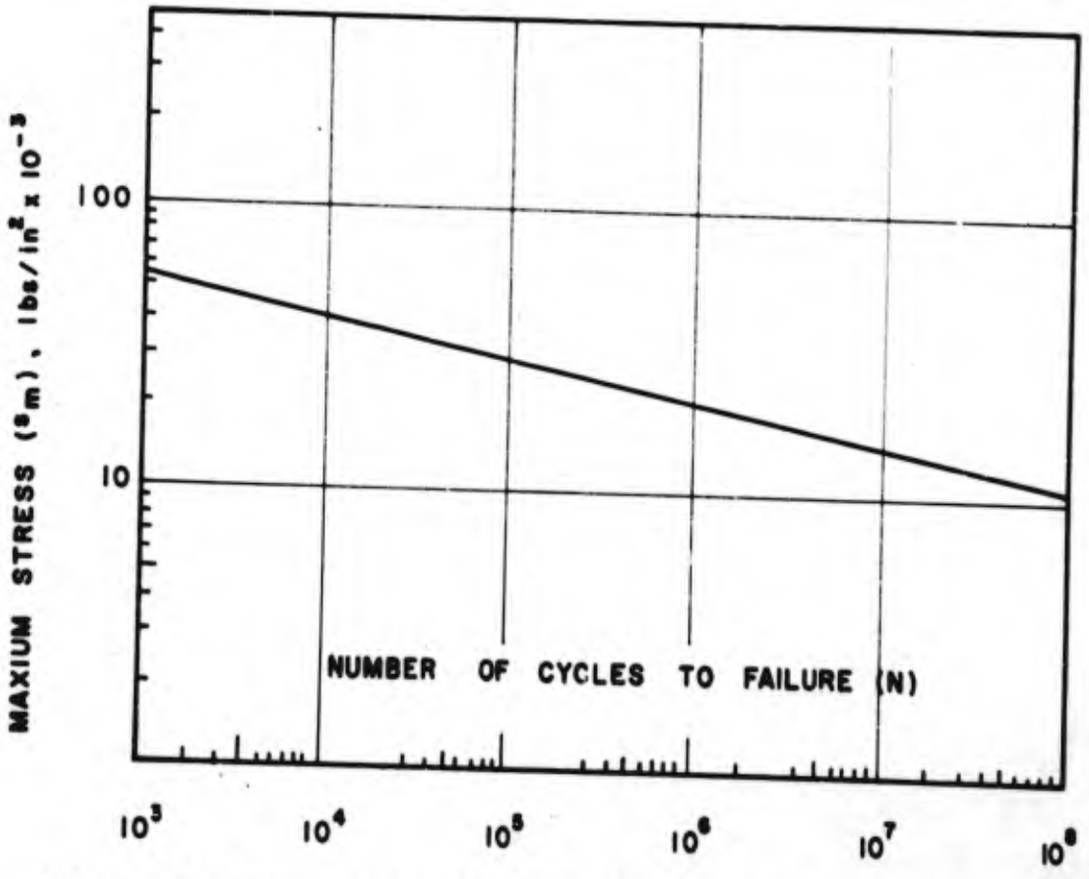

FIG. 15. ROTATING BEAM FATIGUE DATA FOR COLD DRAWN COPPER

the resonant fatigue strength of a typical or idealized structure in terms of an allowable acceleration which may be applied to the base of the structure.

Consider the equipment which is idealized in Figure 16 as a number of cantilever beams with distributed mass and with different natural frequencies. At resonance, the following relation exists between the motion x_o of the base and the response y_o at the tip of the beam:

$$y_o = Qx_o \tag{3}$$

Similarly $$\dot{y}_o = Q\dot{x}_o \tag{4}$$

and $$\ddot{y}_o = Q\ddot{x}_o \tag{5}$$

where the single and double dot notation are used to indicate the first and second derivitives with respect to time; i.e. velocity and acceleration.

B. J. Lazan has shown in Reference 22 that the resonant amplification factor Q for a material may be considered to be the product of three basic factors as follows:

$$Q = K_m \cdot K_s \cdot K_c \tag{6}$$

where K_m = Material factor

K_s = Longitudinal stress distribution factor

K_c = Cross sectional shape factor

General expressions for the above factors are given as follows:

$$K_m = \frac{\pi}{EJS_m^{n-2}} \tag{7}$$

$$K_s = \frac{\int_o^L (S_a/S_m)^2 da}{\int_o^L (S_a/S_m)^n da} \tag{8}$$

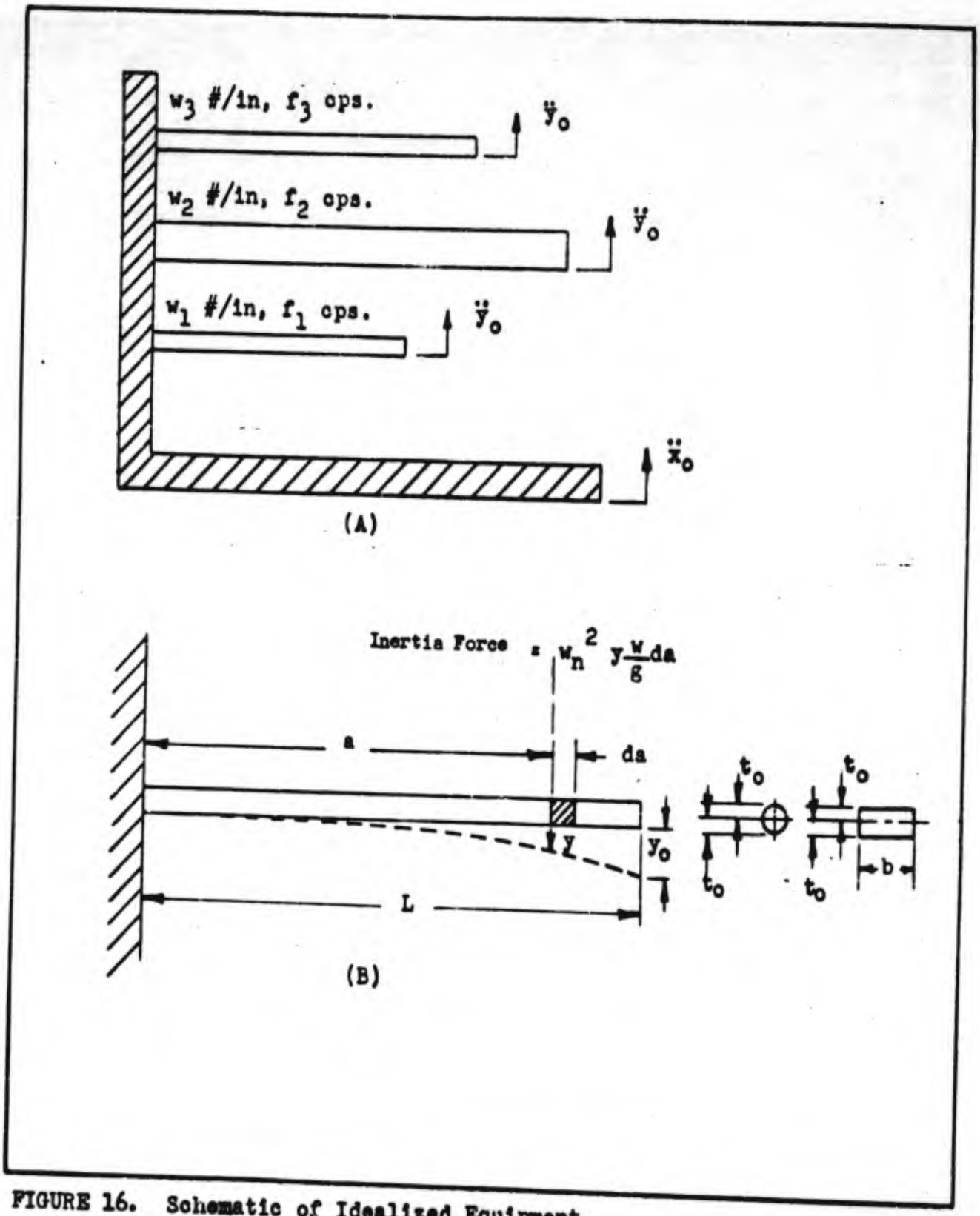

FIGURE 16. Schematic of Idealized Equipment

(A) Equipment comprised of Cantilever Beams with Distributed Mass and Various Natural Frequencies.

(B) Inertia Load of Beam Increment during Vibration at Resonance.

$$K_c = \frac{I t_o^{n-2}}{\int_{-t_o}^{t_o} t^n b\,dt} \qquad (9)$$

$$K_c = \frac{I\, t_o^{n-2}}{4\int_0^{t_o}\int_0^{\pi/2} t^{n+1}\sin^n\theta\, d\theta\, dt} \qquad (10)$$

(Equation 9 is applicable for rectangular cross sections and Equation 10 is for circular cross sections).

where

E = Young's Modulus, psi

J, n = Experimentally determined constants

S_m = Maximum stress, psi

S_a = Stress at any point a, psi

a = Length dimension, inches

L = Total length of member, inches

b = Breadth dimension, inches

t = Thickness dimension from neutral axis, inches

t_o = Maximum thickness from neutral axis, inches

I = Moment of inertia with respect to neutral axis for cross section, inches^4

θ = Polar coordinate for circular cross section, radians

The material constant K_m includes two parameters J and n which are determined experimentally from resonant vibration tests of materials. Reference 22 reports values obtained from resonant tests of a variety of plastics and metals. It is noted that exponent n = 3 is a representative value for these commonly used engineering materials. More recent observations indicate that while n = 3 is a reasonably good approximation for stress conditions up to approximately the endurance limit stress, the value of n increases markedly (to approximately 8) beyond this value. Expressions similar to Equations 7 to 10 can be written which would take the variation of n into account, however, solution by graphical integration means would be necessitated. For purposes of the present discussion, it will be assumed that n = 3 throughout

the stress range, as this permits derivation of simple expressions for the resonant strength of a vibrating member. The expressions which are derived on this basis will be conservative in that they will predict a lower resonant strength than would actually exist. Equations 8 to 10 are solved for some typical situations in Appendix I.

With the relationships provided by Lazan above, it is possible to derive a variety of expressions for the resonant strengths of simple structures. This will now be done for the simple equipment idealized in Figure 16. The maximum bending moment M_m due to inertia loading for a cantilever beam vibrating at resonance is as follows:

$$M_m = \int_o^L \omega_n^2 \, y \frac{w}{g} \, a \, da \qquad (11)$$

where ω_n = Natural frequency, radians/second

w = Weight per unit length of beam, lbs./inch

g = Acceleration of gravity, 386 in/sec^2

The deflection y at any dimension a along the length of the beam may be defined approximately as:

$$y = y_o \left(1 - \cos \frac{\pi a}{2L}\right) \qquad (12)$$

then

$$M_m = \frac{\omega_n^2 \, y_o \, w}{g} \int_o^L a\left(1 - \cos \frac{\pi a}{2L}\right) da \qquad (13)$$

which reduces to

$$M_m = 0.27 \left(\frac{w}{g}\right) L^2 \omega_n^2 \, y_o \qquad (14)$$

Noting that $\ddot{y}_o = \omega_n^2 y_o$, the maximum stress in the beam, as a function of the acceleration at the support of the beam, may be written from Equations (5), (6) and $S = MC/I$ as follows:

$$S_m = \frac{0.27 \, w L^2 t_o}{Ig} K_m K_s K_c \ddot{x}_o \qquad (15)$$

In order to further simplify Equation 15, it will be assumed that the systems idealized in Figure 16 have circular cross-sections as this is representative for many electronic components; for example, the support rods or wires in a vacuum tube, resistor leads, etc. Substituting Equation 7 for K_m and the values of $K_s = 3\pi/8$ and $K_c = 1.47$ as derived in Appendix I, the

equation follows for the motion of the support as a function of the maximum stress in the system:

$$\ddot{x}_o = \frac{J S_m^2}{0.15\pi^2 t_o} \cdot \frac{E I g}{wL^2} \qquad (16)$$

Equation 16 may be more conveniently expressed as a function of natural frequency rather than physical dimensions by substituting the expression $f_n = (3.52/2\pi)\sqrt{EIg/wL^4}$ for the natural frequency of a cantilever with distributed mass as follows:

$$\ddot{x}_o = 11.9\, J\, S_m^2 f_n \sqrt{E/\gamma} \qquad (17)$$

where γ = density of beam, pounds/in^3

Equation 17 provides the desired relationship for interpreting the stress in non-resonant fatigue data, into an equivalent resonant acceleration which can be applied to the support of the system to produce the same stress. Equation 17 is plotted for high strength steel and cold drawn copper as a family of constant stress lines versus frequency in Figures 17 and 18 respectively. A value of $J = 0.043 \times 10^{-12}$ for steel was obtained from Reference 35, and an estimated value of $J = 0.2 \times 10^{-12}$ was used for the cold drawn copper.

It is now possible to establish $\ddot{x}_o$ - N (acceleration versus cycles-to-failure) curves for resonant systems with different natural frequencies by combining the information in Figures 14, 15, 17 and 18. For example Figure 19 shows three such curves for steel systems with natural frequencies of 100, 200, and 300 cps respectively. For purposes of illustration, the "ultimate accelerations", plotted at $N = 10^3$, correspond with an ultimate tensile strength of 200,000 psi; and the "endurance limit accelerations", plotted at $N = 4 \times 10^5$, correspond with a stress which is 26% of the ultimate stress. These are based on the fatigue data in Figure 14 for bending specimens with stress concentrations present. The life curve representative of conditions with stress concentrations was selected for illustrative purposes here, since in practice, it almost is impossible to avoid such conditions. It is of interest to note from Figures 17, 18 and 19, that systems with higher natural frequencies exhibit greater resonant strengths. This observation may be considered to apply only when comparing systems where all the factors contributing to the stress in the system are maintained equal as in the present analysis. Namely, in the present analysis, base excited distributed mass systems have been studied. These results are not directly comparable with systems containing a concentrated mass.

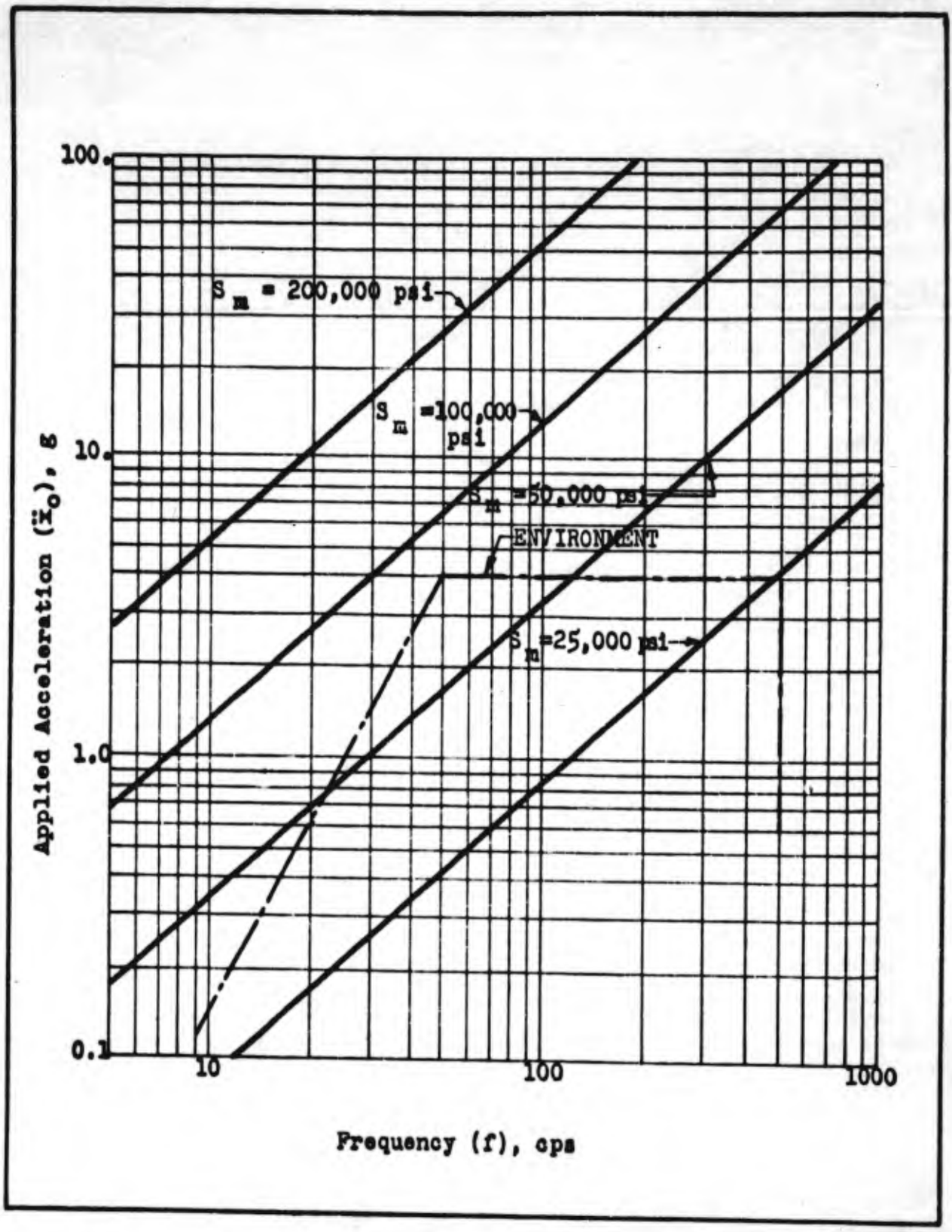

FIGURE 17. RESONANT STRENGTH OF HIGH STRENGTH STEEL CANTILEVER BEAMS

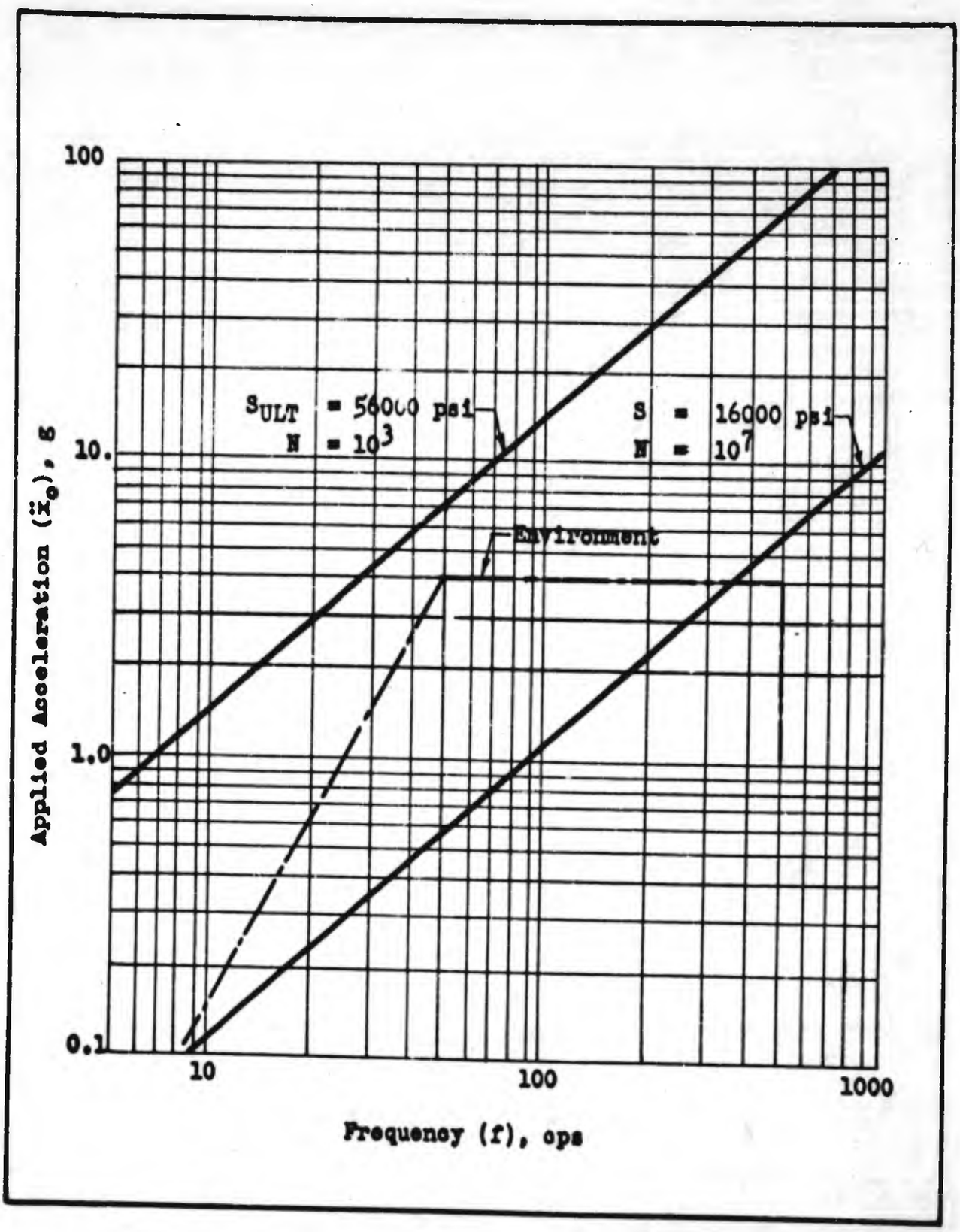

FIGURE 18. RESONANT STRENGTH OF COLD DRAWN COPPER CANTILEVER BEAMS

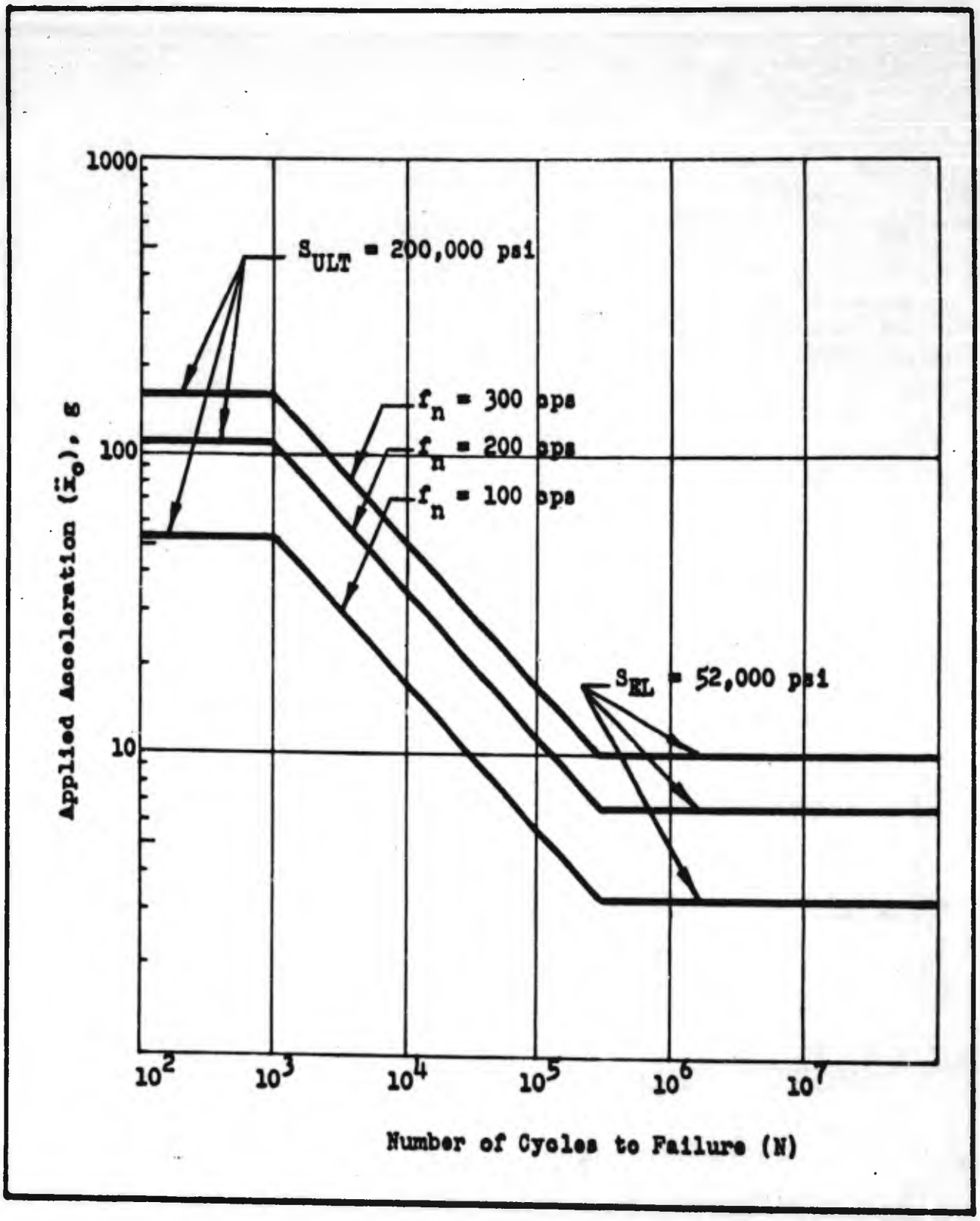

FIGURE 19. THEORETICAL RESONANT FATIGUE CURVES FOR 200,000 PSI ULTIMATE TENSILE STRENGTH STEEL CANTILEVER BEAMS.

For purposes of reference, the envelope Figure 5 representative of the maximum vibration environment in reciprocating engined aircraft, is reproduced in Figures 17 and 18. Since maximum life of components is a design objective, it should be considered that, from a design point of view, this envelope defines the endurance limit acceleration and stress at each frequency. For example, consider that the internal construction of a particular vacuum tube is comprised essentially of a number of alloy steel wires cantilevered at the base of the tube. The ultimate tensile strength of the wires is assumed to be 200,000 psi as in the previous example. Accordingly, from Figure 14, we may estimate, as before, that the endurance limit stress of the material will be 0.26 x 200,000 or 52,000psi and $\underline{N} = 4 \times 10^5$ cycles or greater. Again referring to Figure 17 we see that the constant stress line for $\underline{S} = 52{,}000$ psi, intersects the environment envelope between approximately 25 and 120 cps. This immediately indicates that structural failure can be anticipated in less than the endurance life of 4×10^5 cycles at the maximum environment, if the elements of the tube should be resonant between 25 and 120 cps. It is evident that one of the principal design objectives in the example cited, should be a natural frequency greater than 120 cps.

The foregoing discussion and observations must be considered as qualitative to a very great extent, in view of the numerous simplifying assumptions which have been made as follows:

1. The effect of stress concentrations on resonant amplification have not been considered. Stress concentrations in effect lower the maximum allowable working stress in a member. This reduces the damping energy in the member and will increase resonant amplification.

2. The effect of a concentrated mass located on the beam has not been considered. The addition of concentrated mass will lower the natural frequency and alter the longitudinal stress distribution of the cantilever. As may be observed in Equation 17 decreasing the natural frequency will also lower the resonant base acceleration which can be applied.

3. The idealization of electronic components as cantilever beams is perhaps not a good approximation for all equipments.

A study was made of all the recently published vibration failure information on electronic components. In the course of this study, it became apparent that a criterion for failure must be established. It is necessary to differentiate between

permanent failures and malfunctions of the equipment. For example, Reference 62 reports the results of a comprehensive study of the effects of vibration on a variety of relays, during vibration at various frequencies and levels of acceleration. During these tests certain types of relays malfunctioned by opening or chattering contacts and thus disrupting the continuity of the circuits in which they were installed. Similarly, Reference 63 reports vibration tests on vacuum tubes which exhibited a microphonic output too great to be tolerated. In the majority of these cases, when the vibration was stopped, the malfunction disappeared and the equipment again operated satisfactorily. Certainly these are serious defects to contend with, but must be ruled out as a consideration of failure in life or endurance testing of equipment. It is believed malfunctions must be treated separately; that is, by operational proof tests at the level of the vibration environment anticipated in service. If malfunctions occur during such operational proof tests, the offending components should be replaced by components of higher quality. In the event that no higher quality component exists, this will indicate that modification of either the component or the environment is necessary.

Figures 20 to 22 summarize the results of recently published data on the failure of vacuum tubes, and lead-supported resistors and capacitors at various levels of resonant vibration. In each case, the failure noted is of a permanent nature. In the case of the lead-supported resistors and capacitors, the failure generally occurred as broken leads; for the vacuum tubes, the failure point was based upon specification MIL-E-1B limit values for plate current. The data plotted in Figures 20 to 22 were obtained from References 63, 64, 98 and 115. A minimum anticipated $\ddot{x}_o$ - N or life curve has been drawn in each figure with dotted lines to envelope the failure data plotted for the various components. Also superimposed in each of these figures are calculated $\ddot{x}_o$ - N curves. These curves, indicated by solid lines, are based on the following:

1. The resonant fatigue strength considerations set forth in the previous section.

2. The average natural frequency of the tested components.

3. In the case of the vacuum tube data, it is presumed that the critical elements are alloy steel. The endurance limit accelerations indicated by the "knees" of the calculated curves are estimated.

4. In the case of the lead mounted capacitors, the fatigue data, in Figure 15 for cold drawn copper, applies.

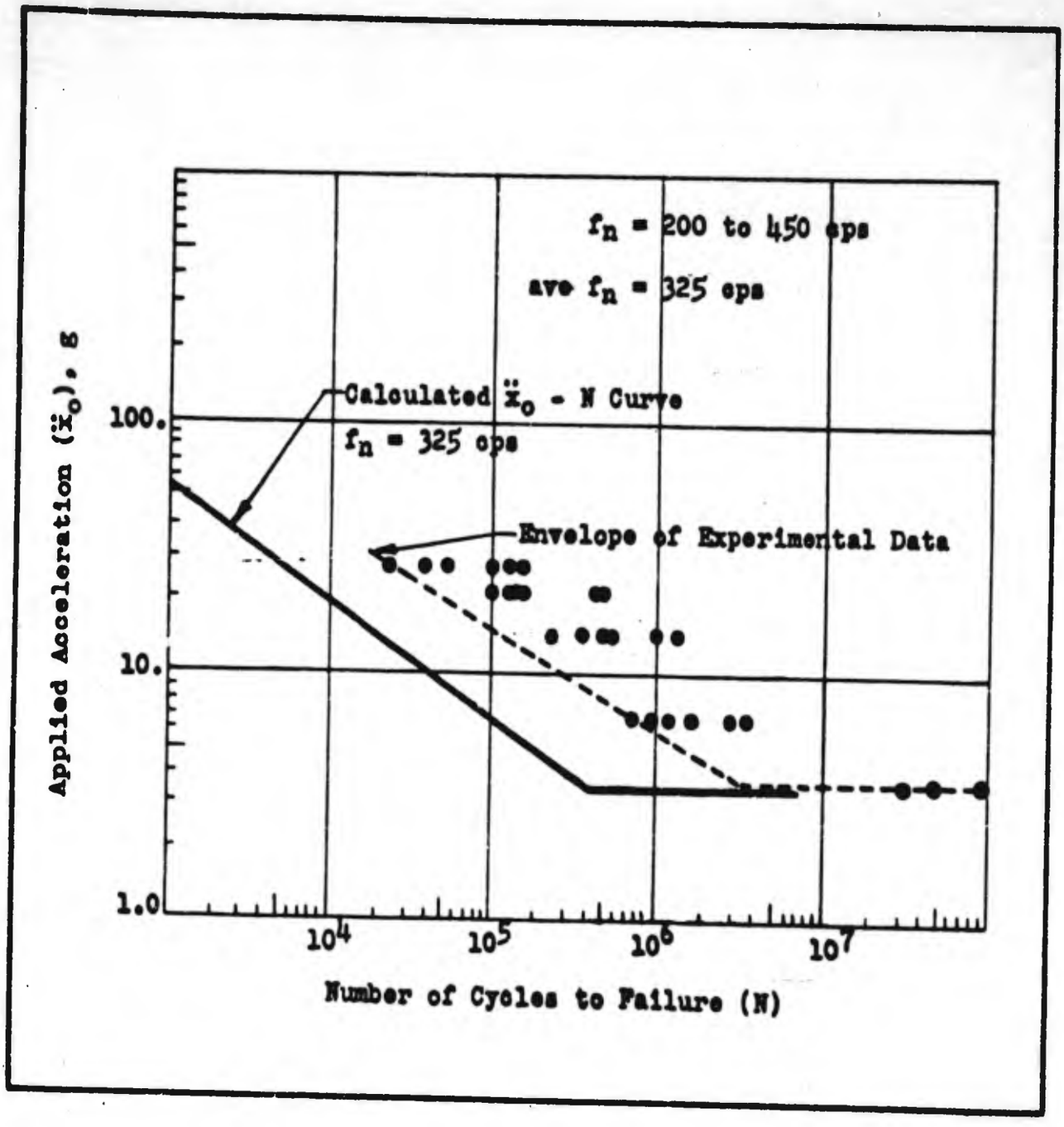

FIGURE 20. RESONANT FATIGUE TESTS OF 6AR6 TUBES (UNIVERSITY OF DAYTON)

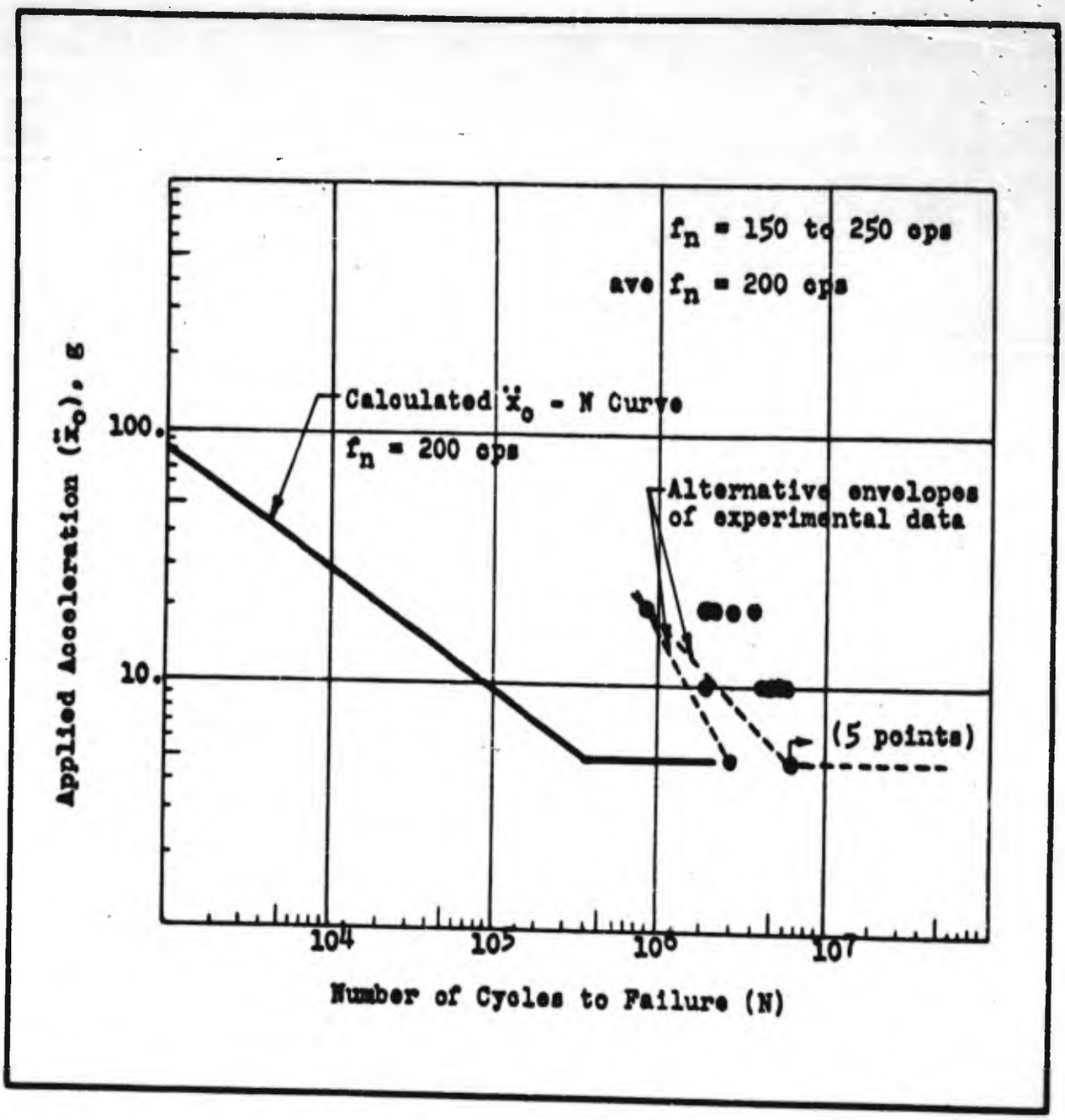

FIGURE 21. RESONANT FATIGUE TESTS OF 6J5 WGT TUBES(ARMOUR)

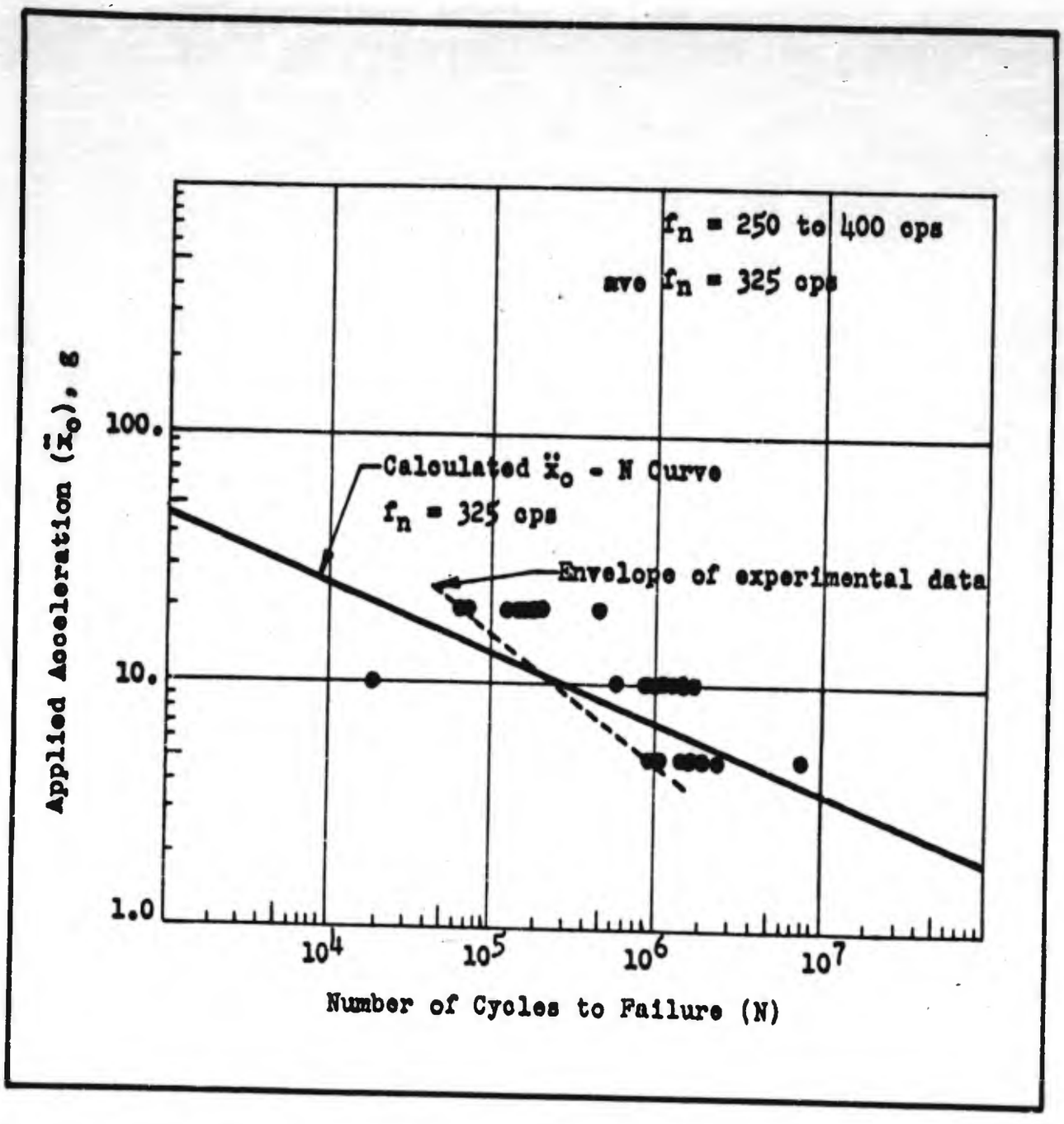

FIGURE 22. RESONANT FATIGUE TESTS OF LEAD SUPPORTED CAPACITORS (ARMOUR)

It is difficult to draw any definite conclusions from a broad comparison of the calculated and experimental $\ddot{x}_o$ - N curves in Figures 20, 21, and 22. It is encouraging to note in these Figures that there is a reasonable degree of correlation in the slopes of the calculated and experimental $\ddot{x}_o$ - N curves. This indicates that the analogy between the failure of electronic equipment and the fatigue of metals, which was assumed in WADC Technical Report 54-272 is at least a good first approximation.

In general it may be said, from observation of the calculated and experimental data in Figures 20 to 22, the calculated resonant strengths underestimate the actual strengths. This result was anticipated in the previous section when it was pointed out that a constant exponential n = 3 relationship was assumed throughout the stress range, for purposes of simplying Lazan's material constant in Equation 7. Evidence appears to exist that still closer correlation could be obtained between calculated and experimental $\ddot{x}_o$ - N curves by minimizing the simplifying assumptions pointed out in the previous section.

As pointed out above, it may be considered that study reported herein justifies the analogy assumed earlier between the failure of electronic equipment and the fatigue of metals. It should be noted however that in earlier pages and Figure 12 a direct relationship between the ratios of endurance limit stress and acceleration to ultimate stress and acceleration was assumed as follows:

$$\frac{S_{E.L.}}{S_{ULT.}} = \frac{\ddot{x}_{E.L.}}{\ddot{x}_{ULT.}} \qquad (18)$$

The analysis immediately preceding indicates that a more accurate approximation of the ratio of endurance limit to ultimate acceleration involves a squared stress relationship as follows:

$$\left(\frac{S_{E.L.}}{S_{ULT.}}\right)^2 = \frac{\ddot{x}_{E.L.}}{\ddot{x}_{ULT.}} \qquad (19)$$

The application of this approximation will have a significant effect on the determination of the magnitude of an "exaggerated" or "accelerated" acceleration factor for application to testing procedures. This subject will be treated in the following Section.

SECTION VII

CYCLING VS. DISCRETE TEST FREQUENCIES IN STEADY-STATE VIBRATION

If equipment fails during vibration tests, it is probable that failure occurs as a result of a resonant structure. The vulnerability of a structure in this respect is a function of the internal damping of the structure. If the damping is small, amplification at resonance is great and damage is more likely. Vibration tests are more difficult to conduct if the damping is small because the most damaging conditions may not be obtained unless the test frequency is carefully monitored. The following analysis is based upon an assumed internal damping equal to 2.5% of critical damping ($c/c_c = 0.025$). This degree of damping gives an amplification at resonance of 20 by classical vibration theory. This is sometimes referred to as a system having a Q of 20. If the internal damping of the structure is greater than 2½%, the following analysis tends to be conservative as will become evident with reference to Figure 7. It is considered unlikely that the damping in any practical structure will be less than 2½% for the relatively large displacement amplitudes being considered here.

It is generally conceded that the frequencies embodied in a vibration test should extend from the lowest to the highest found to be significant from a study of environmental conditions. One type of vibration test involves a continuous sweep of test frequency from the minimum to the maximum and back to the minimum. Another type of test involves vibration at a constant frequency for a predetermined period, followed by a period of vibration at a slightly different frequency, and followed by periods of vibration at other discrete frequencies until the entire range of frequencies is covered. The relative merits of these two types of tests will now be discussed.

As pointed out previously, Figure 12 represents a plane parallel to the plane of acceleration amplitude $\ddot{x}_o$ vs. cycles to failure N, taken through one of the valleys of the failure surface illustrated in Figure 10. This would be a critical test for a component having a natural frequency f_2 if the vibration environment were at the upper limit for such environment as established by the line b. Such a component would be expected to withstand five million cycles of vibration, as indicated by point A in Figure 12. Similarly, if $N_1 = 10^4$, it would be expected to barely withstand ten thousand cycles at a slightly higher value of acceleration amplitude, as indicated by point B in Figure 12. Points A and B in Figure 12 correspond to points A and B, respectively, in Figure 10.

In Figure 10, the values along the $\ddot{x}_o$ axis represent values of maximum acceleration embodied in the vibration environment. These correspond to acceleration associated with the parameter x in Figure 6. These values of acceleration, when multiplied by the

ratio $\ddot{y}_o/\ddot{x}_o$ set forth in Figure 7, give values of maximum acceleration $\ddot{y}_o$ associated with the motion of the mass m in Figure 6. As explained previously with reference to equation 2 , the stress in the spring k is directly proportional to the acceleration $\ddot{y}$ of the mass m.

The relation between $\ddot{x}_o$ and $\ddot{y}_o$ is indicated in Figure 12 wherein the point A corresponds to the point A in Figure 10 and the response acceleration amplitude $\ddot{y}_o$ is indicated by point 1. The coordinate scale for $\ddot{x}_o$ is at the left side of Figure 12, while the scale for $\ddot{y}_o$ is at the right side. The scale for the response acceleration amplitude is for a component having 2½ percent of critical damping. To be suitable for aircraft service the component must withstand the response acceleration amplitude $\ddot{y}_o$ indicated by point 1 for an indefinitely long duration; i.e., for a minimum of five million cycles.

Since it is not feasible to conduct a laboratory vibration test for five million cycles, it becomes necessary to select a smaller number of cycles and an increased test amplitude. Selecting ten thousand cycles ($N = 10^4$), as a reasonable test period, the acceleration amplitude $\ddot{x}_o$ of the vibration test is indicated by point B in Figure 12 and the response acceleration amplitude $\ddot{y}_o$ of the component is indicated by point 2. This applies only if the test frequency has been adjusted to exactly coincide with the natural frequency f_2. If the difference between test and natural frequencies is one (1) percent the response acceleration amplitude $\ddot{x}_o$ of the component is indicated by point 3. It is important to note that point 3 represents a lower response than point 1. Consequently, failure of the component may not be expected even though the test is continued indefinitely. If the mismatch of test and natural frequencies is two (2) percent, the corresponding response acceleration amplitude $\ddot{y}_o$ is indicated by point 4. Under these circumstances, it is still less likely that failure of the component will occur during the test period. This appears to indicate that it is not practical to conduct vibration tests at discrete frequency intervals because an excessively large number of increments will be involved and because it becomes necessary to adjust the test frequency with unreasonable accuracy.

The alternative to a test at discrete frequencies is one in which the test frequency is continuously varied between limits. This may be illustrated by reference to Figure 23. A hypothetical equipment under consideration is assumed to include two elements whose natural frequencies are f_2 and f_4. The test frequency then is assumed to vary continuously from a minimum of f_0 to a maximum f_3. The environment is indicated by line 1 in Figure 23, corresponding to a portion of the environment line b in Figure 10.

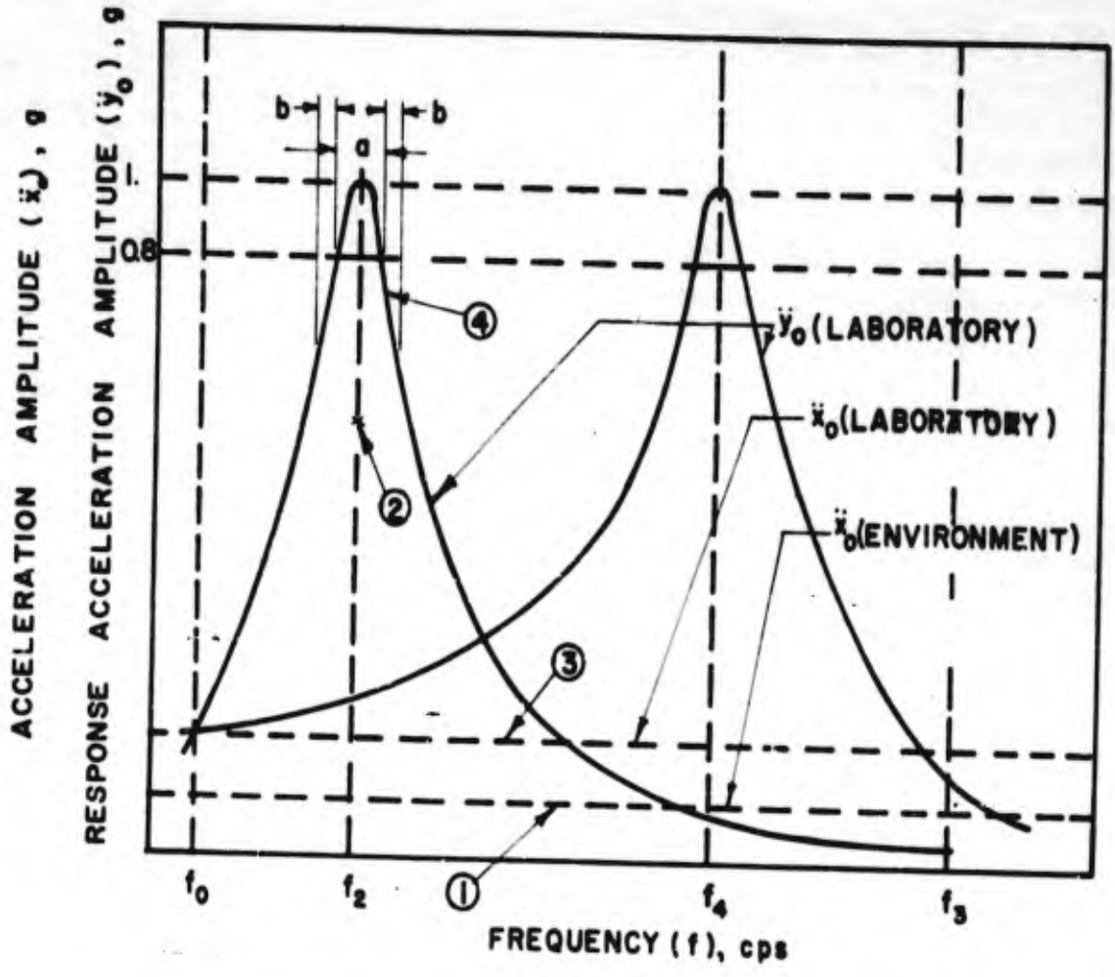

FIGURE 23. RELATION BETWEEN ACCELERATION AMPLITUDE $\ddot{x}_0$ AND RESPONSE ACCELERATION AMPLITUDE $\ddot{y}_0$ FOR CONDITION OF CONTINUOUSLY VARYING TEST FREQUENCY.

Inasmuch as the laboratory test will be conducted for relatively few cycles, the acceleration amplitude $\ddot{Y}_o$ for the test is increased with respect to the acceleration amplitude $\ddot{X}_o$ of the environment, as indicated by line 3 in Figure 23. If the environment includes vibration at a frequency f_2 and at an acceleration amplitude $\ddot{X}_o$ corresponding to the maximum expected amplitude represented by line 1, the element whose natural frequency is f_2 will have a response acceleration amplitude $\ddot{Y}_o$ at resonance indicated by point 2 in Figure 23. During the laboratory test with increased acceleration amplitude, the element whose natural frequency is f_2 will exhibit the response acceleration amplitude $\ddot{Y}_o$ outlined by line 4 as the test frequency continuously changes from f_o to f_3. The value of $\ddot{Y}_o$ at the frequency f_2 can be determined from $\ddot{X}_o$ and Figure 7 if the rate of change of the test frequency is very slow. If the rate of change is not slow, $\ddot{Y}_o$ may have a lower value because the resonant condition endures only momentarily. Furthermore, the element will experience a very small number of cycles at maximum response acceleration amplitude. It does, however, experience a greater number of cycles at somewhat reduced amplitudes on either side of resonance and certain of these lower cycles may contribute to damage of the element. As compensation, it may be assumed that all of the cycles in region a, of Figure 23 which are 80% or more of the resonant response, experience maximum response to compensate for neglecting the damage contributed by the lower responses in adjacent regions b.

The pattern by which a continuously varying test frequency varies is important. If the test frequency varies too fast, the response amplitude of equipment being tested does not build up as high as predicted by steady-state vibration theory. If the rate of variation of the test frequency is low, the response amplitude builds up approximately to that obtained during steady-state vibration and it is possible to obtain an appreciable number of cycles of vibration at a response close to the maximum. This suggests that care should be exercised in selecting a rate of variation of the test frequency.

This problem has been studied in detail in Reference 25 and the results are summarized in Figure 24. This figure illustrates the ratio $\ddot{Y}_o/\ddot{X}_o$ for a damped, single-degree-of-freedom system (Q = 20) at various rates of change of the test frequency as a function of the dimensionless time r/R. The relation between f_n, h and R is:

$$h = f_n^2/R \qquad (20)$$

Where:

f_n = The natural frequency of the vibrating system in cycles per second.

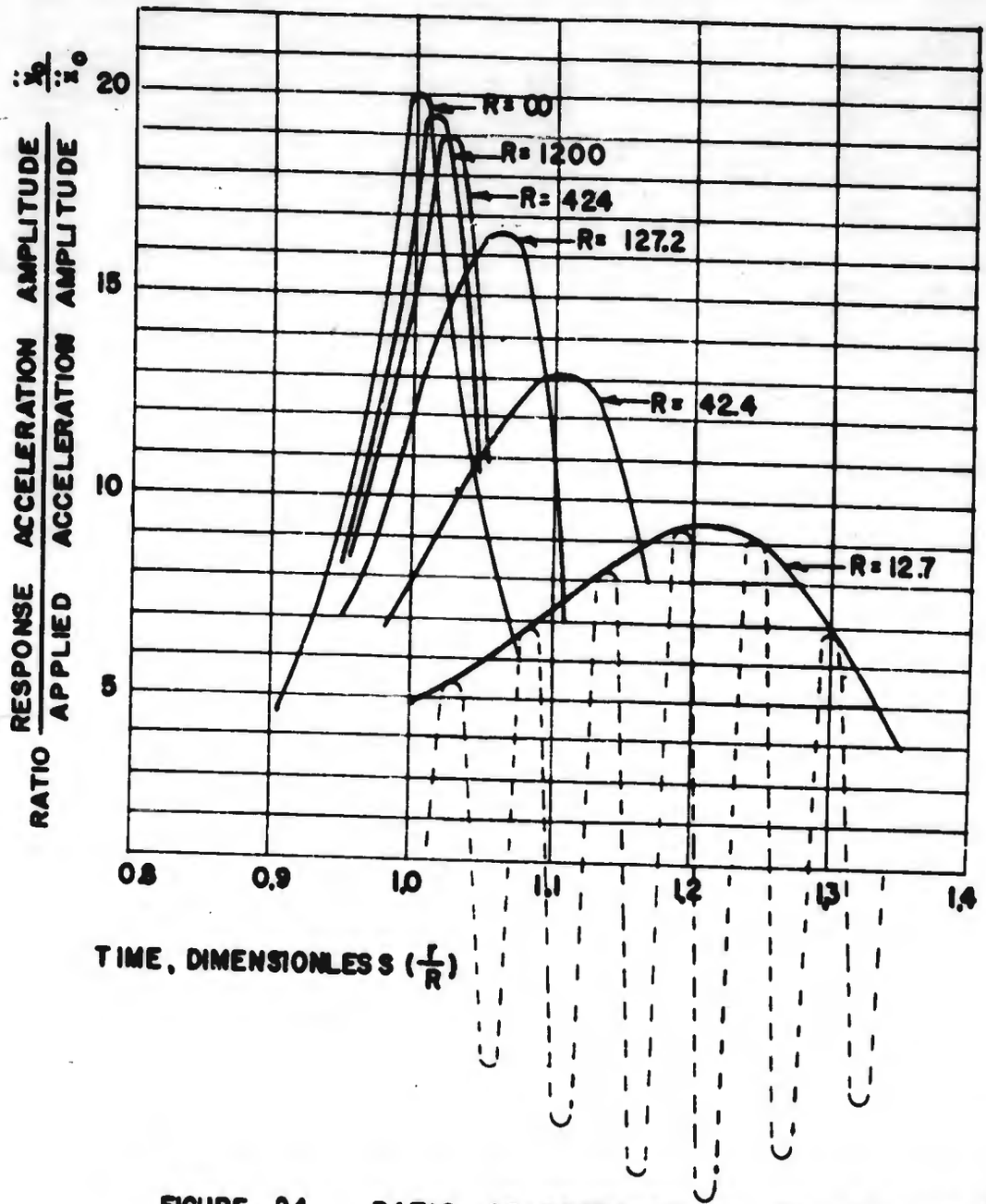

FIGURE 24. RATIO OF RESPONSE TO APPLIED ACCELERATION AMPLITUDES FOR SYSTEM WITH $Q = 20$ WHEN TEST FREQUENCY VARIES CONTINUOUSLY.

h = The rate of change of the test frequency in cycles per second per second.

r = The total number of free vibrations of the system starting at zero time.

R = The value of r at which the instantaneous forcing frequency equals the natural frequency of the system. A large value of R therefore, indicates a slow rate of change of the test frequency.

As pointed out previously, significantly great stress cycles occur only at test frequencies approximating the natural frequencies of vulnerable elements. It is desirable that each element of the equipment experience the same number of significant stress cycles during vibration tests independently of the natural frequency of the element. Consequently, the rate of change of the test frequency should increase as the test frequency increases. Referring to Figure 24, this indicates that the dimensionless ratio r/R should be maintained constant.

It is possible to write an expression as follows for any instantaneous test frequency f_1 in terms of the minimum test frequency f_o and the time t_1 required to change the test frequency from its minimum value f_o to frequency f_1:

$$f_1 = f_o + \int_o^{t_1} h\,dt \qquad (21)$$

This equation may be evaluated numerically by assuming a value for the parameter R. It is evident from the relation set forth in Figure 24 that the parameter R should be maintained relatively large to permit the response amplitude to build up to a significantly high value. A value 1200 is assumed for the parameter R. By reference to Figure 24, it is observed that the stress in an element at resonance is above 80 percent of the maximum value when $0.990 < r/R < 1.038$. Since $R = 1200$, $1188 < r < 1245.6$ and the stress is above 80 percent of the maximum value for 57.6 cycles of vibration during each sweep of the test frequency. Inasmuch as the dimensionless ratio r/R is a constant, the stress will exceed 80 percent of the maximum for any element, independent of its natural frequency, provided the rate of change of test frequency defined by equation 21 is maintained.

The results of a numerical evaluation of equation (21) are given in Table I. At the rate of change of the test frequency indicated by a value $R = 1200$, a period of approximately 180 seconds is required to increase the test frequency from 5 to 50 cycles per second, and approximately 18 seconds is required to increase the test frequency from 50 to 500 cycles per second. These periods are noted separately here, and will be maintained separate throughout

TABLE I

NUMERICAL EVALUATION OF SWEEP TIME FOR 5 TO 500 CPS

R = 1200 ; Number of significant cycles per sweep = 1200 (1.038 - .990) = 57.6

$$f = f + \int_0^{t_1} h \, dt$$

$$\Delta f = \int_0^{t_1} \frac{1}{2} \left(\frac{f_1^2}{R} + \frac{f_0^2}{R} \right) dt$$

$$\Delta t = t_1 - t_0 = \frac{\Delta f}{\left(\frac{f_1^2 + f_0^2}{2R} \right)}$$

f_1 cps	f_0 cps	$h_{ave.} = \frac{f_1^2 + f_0^2}{2R}$ cyc/sec^2	$\Delta t = \frac{\Delta f}{h_{ave.}}$ sec.	t sec.
10	5	.052	96.2	
20	10	.208	48.	
30	20	.541	18.5	
40	30	1.04	9.6	
50	40	1.70	5.9	178.2
100	50	5.20	9.62	
200	100	20.8	4.8	
300	200	54.1	1.85	
400	300	104.	.96	
500	400	170.	.59	17.8

the discussion because different testing machines probably are required for testing in these two frequency intervals. As the test frequency is increased from 5 to 500 cycles per second according to this pattern, each element with a natural frequency within this range will experience a stress of 80 percent or more of the maximum for 57.6 cycles.

The testing procedure being discussed here contemplates an equal number of stress reversals throughout the frequency range, independent of the test frequency. It is thus necessary that the rate of change of test frequency, $\underline{h}$ increase as the frequency increases. The necessary rate of change of test frequency is obtained from equation (20) by setting the natural frequency equal to the test frequency. For a selected value of $\underline{R}$, the instantaneous rate of change of test frequency $\underline{h}$ is proportional to test frequency squared ($\underline{f}^2$). This type of sweep is sometimes referred to as a "log-log" sweep as depicted in Figure 25. Figure 26 summarizes the results of calculations similar to Table I for various values of $\underline{R}$, and also the number of cycles of significant stress; i.e., greater than 80% of maximum response. It can be seen that both the number of significant cycles and the sweep time increase in direct proportion to $\underline{R}$. Accordingly, it can be concluded that the total time required for a test, with an equal number of stress reversals throughout the frequency range, is independent of $\underline{R}$. The parameter $\underline{R}$ will govern the number of sweeps required to complete the test.

To determine the relation between (1) the number of sweeps between minimum and maximum test frequencies and (2) the applicable test amplitude, it is necessary to define the characteristics of the idealized endurance curve shown in Figure 27a and its alternate form as shown in Figure 27b. Figure 27 provides a comparison of the two proposed forms of the idealized endurance curves. The actual numerical values which apply to the ordinate scale on Figures 27a and 27b are not important because these curves are employed only to determine the ratios of acceleration amplitudes which correspond to certain ratios of cycles to failure. Curve 27a is assumed to have a relative amplitude of unity at $N = 10^3$ cycles to failure and a relative acceleration amplitude of 0.38 at $N = 5 \times 10^6$ cycles to failure. Based upon a linear relation between these two extreme points when plotted on log-log paper, the equation defining Curve 27a in Figure 27 in the interval $10^3 < N < 5 \times 10^6$ is:

$$\ddot{X} = \left(\frac{N}{10^3}\right)^{-.114} \qquad (18)$$

In equation (22), N is any value of cycles to failure between 1000 and 5,000,000 while $\ddot{x}_o$ is the ordinate value corresponding to the selected value of N, based upon a relative ordinate of unity at 1000 cycles and 0.38 at 5,000,000 cycles.

In a similar manner the equation for Curve 27b is derived. Curve 27b is based on the relation

$$\left(\frac{S_{E.L.}}{S_{ULT.}}\right)^2 = \frac{\ddot{X}_{E.L.}}{\ddot{X}_{ULT.}} \qquad (19)$$

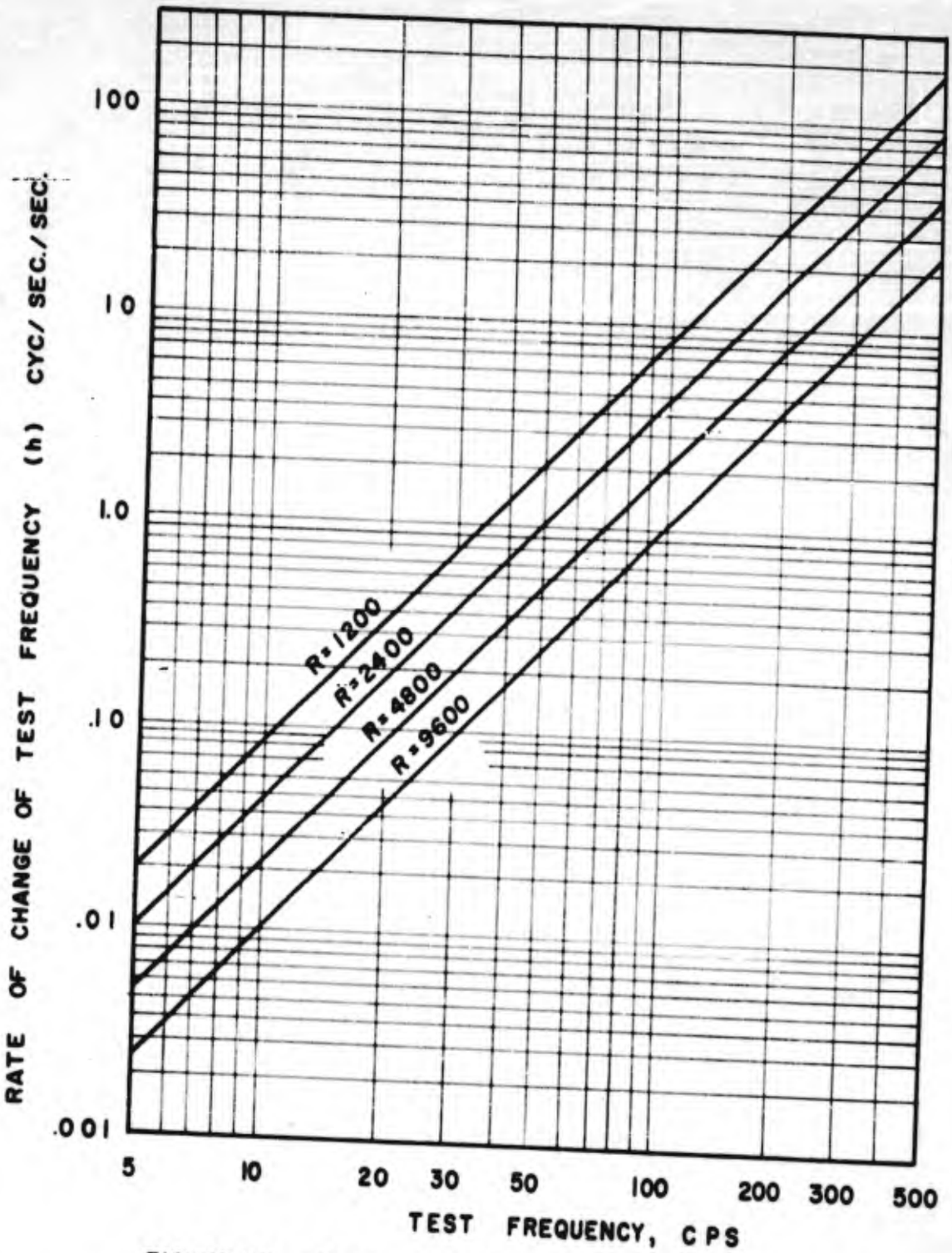

FIGURE 25. RATE OF CHANGE OF TEST FREQUENCY FOR STEADY - STATE TEST FOR VARIOUS VALUES OF THE PARAMETER R.

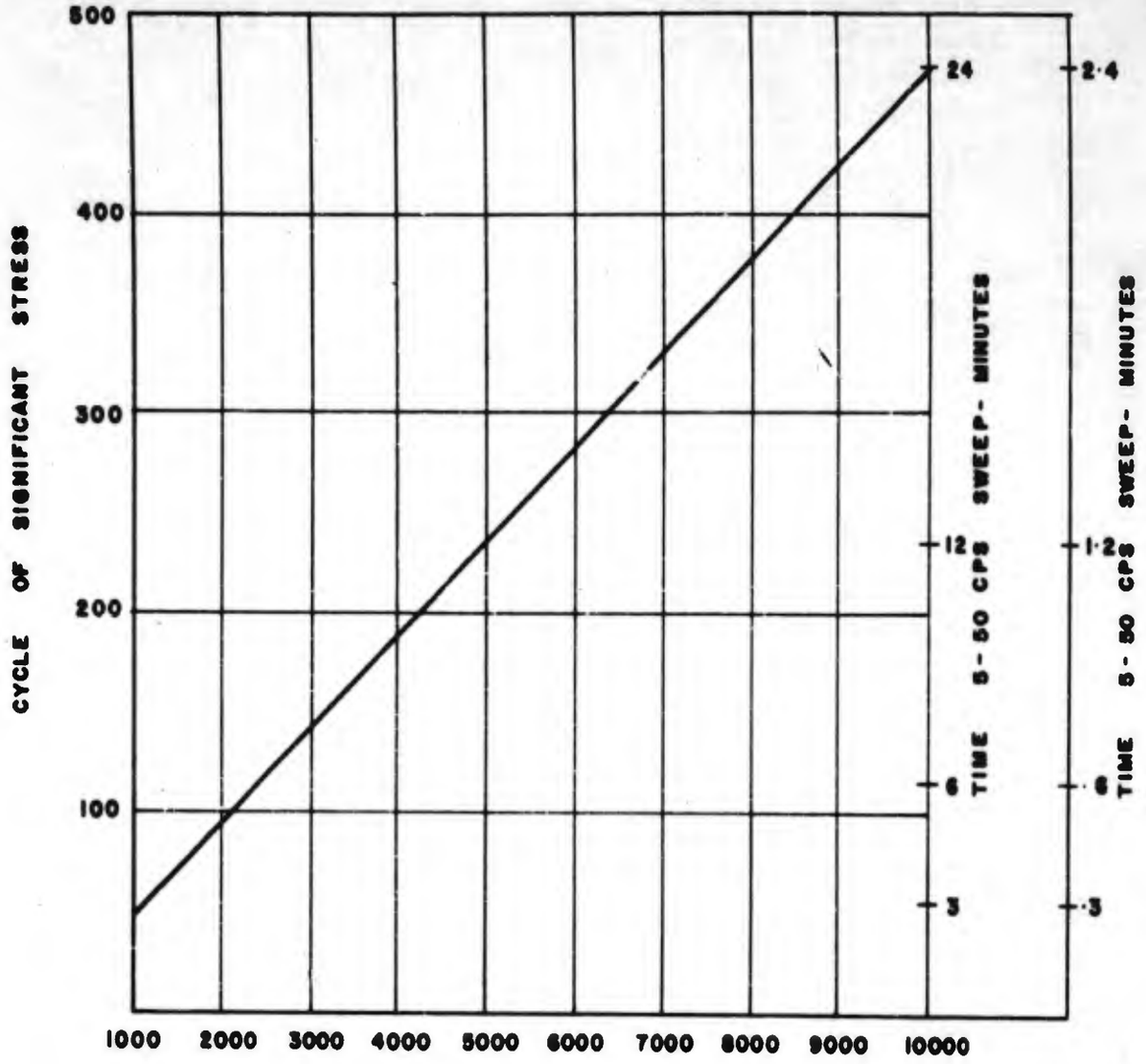

FIGURE 26. SWEEP TIME AND CYCLES OF SIGNIFICANT STRESS AS A FUNCTION OF THE PARAMETER "n".

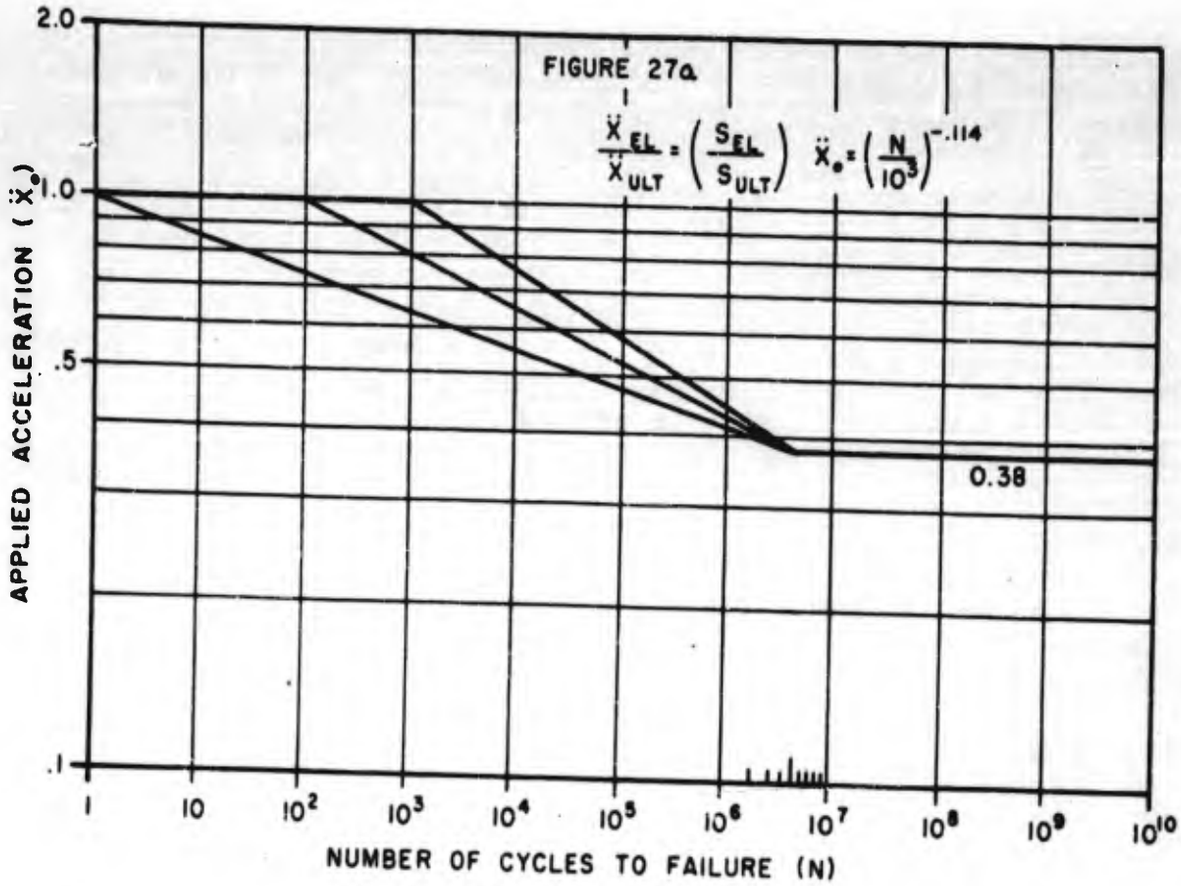

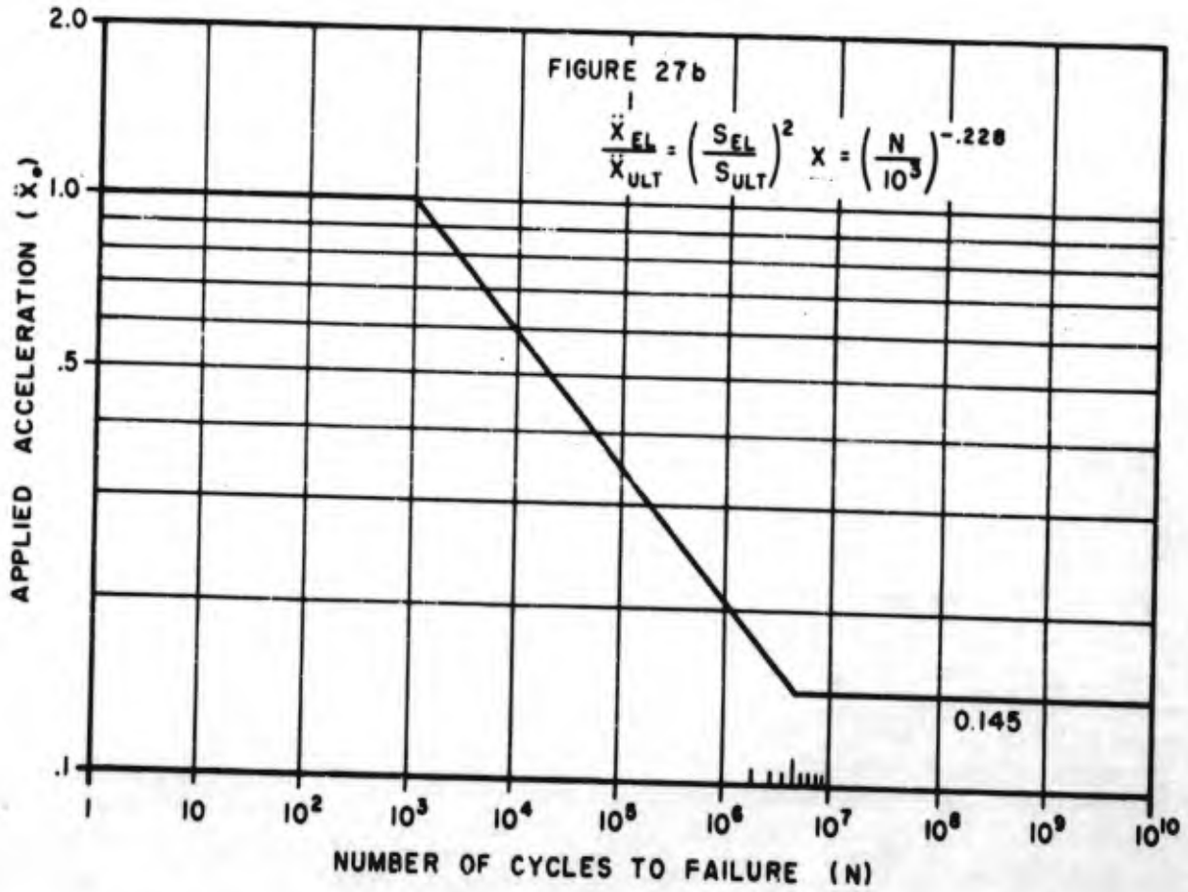

FIGURE 27. RELATION BETWEEN STRESS, ACCELERATION, AND CYCLES TO FAILURE

rather than the linear relation assumed for Curve 27a. Consequently, Curve 27b will have a relative amplitude of unity for $\ddot{X}_o$ at N = 10^3, but at N = 5 x 10^6 the relative amplitude will be $(0.38)^2$ or 0.145. The equation for Curve 27b when plotted on log-log paper is then:

$$\ddot{X}_o = \left(\frac{N}{10^3}\right)^{-.228} \qquad (23)$$

Although infinite life is a practical objective, analysis predicts failure after 5 x 10^6 cycles of vibration at a relative amplitude of 0.38 of Curve 27a or .145 of Curve 27b. An amplitude exaggeration factor will now be determined in Table II for the reciprocating engined and jet fighter environment of Figure 5 to find the relative amplitude necessary to cause similar failure in a substantially fewer number of cycles. Assuming several representative values for N, corresponding values of $\ddot{X}_o$ are calculated from equations 23 and 24 and are setforth in the second and third columns of Table II. The ratio of these values of $\ddot{x}_o$ to the value 0.38 and the value 0.145 which apply to N = 5 x 10^6 are setforth in columns 4 and 5 of Table II. These ratios in columns 4 and 5 are, in effect, exaggeration factors by which the test amplitude must be increased to cause failure in N number of cycles.

As indicated above, the tests being considered here contemplate a sweep frequency procedure which causes the number of cycles of significant stress per sweep indicated in Figure 26 for various values of the parameter R. To attain the total number of cycles set forth in the first column of Table II, it is necessary to employ a number of sweeps equal to the ratio N divided by significant cycles from Figure 26. This ratio (for a value of R = 1200) is then multiplied by 178 and 17.8 seconds, respectively, to obtain the times set forth in columns 6 and 7. The total testing time is the sum of the times set forth in columns 6 and 7, and is given in column 8.

A laboratory test for the reciprocating engined and jet fighter aircraft environment is now established by selecting an appropriate line in Table II. An examination of the exaggeration factors as determined from Curve 27a and Curve 27b as shown in columns 4 and 5 of Table II, indicates that the exaggeration factors as derived from Curve 27b are considerably greater for a given value of N than those derived from Curve 27a. At this point in the analysis, a selection of one or the other of these exaggeration factor curves must be made. Basically because of the assumption that was necessary in the derivation of Curve 27b which is predicated on an assumed value of n = 3 as discussed on page 41, it is felt that the exaggeration factor curve of 27b although analytically a

TABLE II

EVALUATION OF TOTAL VIBRATION TEST TIME FOR VARIOUS EXAGGERATION FACTORS - RECIPROCATING ENGINED AND JET FIGHTER ENVIRONMENT OF FIG. 5

$$\text{EXAGGERATION FACTOR} = \frac{\ddot{x}_{o_{n = N}}}{\ddot{x}_{o_{n = 5 \times 10^6}}}$$

N cycles	$\ddot{x}_o$ CURVE Fig.27a	$\ddot{x}_o$ CURVE Fig.27b	EXAGGERATION FACTOR Fig. 27a	EXAGGERATION FACTOR Fig. 27b	TIME FOR 5-50 cps TEST minutes	TIME FOR 50-500 cps TEST minutes	TOTAL TIME hours and minutes
10^3	1.00	1.00	2.63	6.95	51.6	5.16	0 - 56.8 min
2×10^3	.925	0.855	2.44	5.94	103.2	10.32	1 - 53.5
$*4 \times 10^3$	.855	0.730	2.25	5.07	206.4	20.64	3 - 47.0
10^4	.770	0.592	2.03	4.11	516.0	51.6	9 - 27.6
4×10^4	.658	0.431	1.73	2.99	2064.0	206.4	37 - 50.4
10^5	.592	0.350	1.56	2.43	5160.0	516.0	94 - 36.0

refinement of Curve 27a is still based upon enough tenuous assumptions to make its validity questionable. From a practical standpoint, the exaggeration factors of Curve 27b when applied to the previously defined environments would mean that acceleration amplitudes of the order of 50g would be applied at low frequencies. This level of severity may result in vibratory amplitudes in the non-linear range for most components, or amplitudes that would very closely approach the non-linear range. It is believed, however, that the theoretical direction taken which has resulted in Curve 27b should be further explored, and attempts made to develop this approach on a firmer basis. The several assumptions made should be validated by either application of experimental techniques or by further theoretical refinements. Consequently, in the succeeding paragraphs and in the process of specifying a vibration test, the exaggeration factor based on Curve 27a will be used.

Various considerations must be kept in mind in making this selection of an exaggeration factor. It is desirable that the exaggeration factor be maintained as small as possible for the response amplitude of the equipment under test may be affected by non-linearities introduced by high amplitude testing. On the other hand, it is generally desirable to maintain the total testing time small. The best compromise between these opposing considerations from the alternatives setforth in Table II, appears to embody a test in which each element receives 4000 cycles of stress reversal ($N = 4 \times 10^3$). This gives a testing procedure involving approximately four (4) hours of vibration testing in which the testing frequency is varied continuously between 5 and 50 cycles per second in a period of 178 seconds and between 50 and 500 cps during a period of 17.8 seconds. A number of sweeps of test frequency variation between 5 and 500 cps is selected as indicated in Figure 28 for various values of the parameter R. This involves an exaggeration factor of 2.25. The environmental condition for the reciprocating engined aircraft and the jet fighter aircraft which embodies a displacement amplitude of .030 inches is then exaggerated to a displacement amplitude of .068 inches for laboratory testing in the frequency range of 5 to 50 cps. In a similar manner, the environmental condition of 4g acceleration amplitude is exaggerated to an acceleration amplitude of 9.0g for laboratory testing and in the frequency range from 50 to 500 cps.

The significant differences pointed out earlier between the environmental envelope indicated for the reciprocating engined aircraft and jet fighter aircraft when compared to the jet bomber aircraft will require, because of the shape of the envelope as defined in Figure 4, a similar analysis of testing time and the determination of an exaggeration factor.

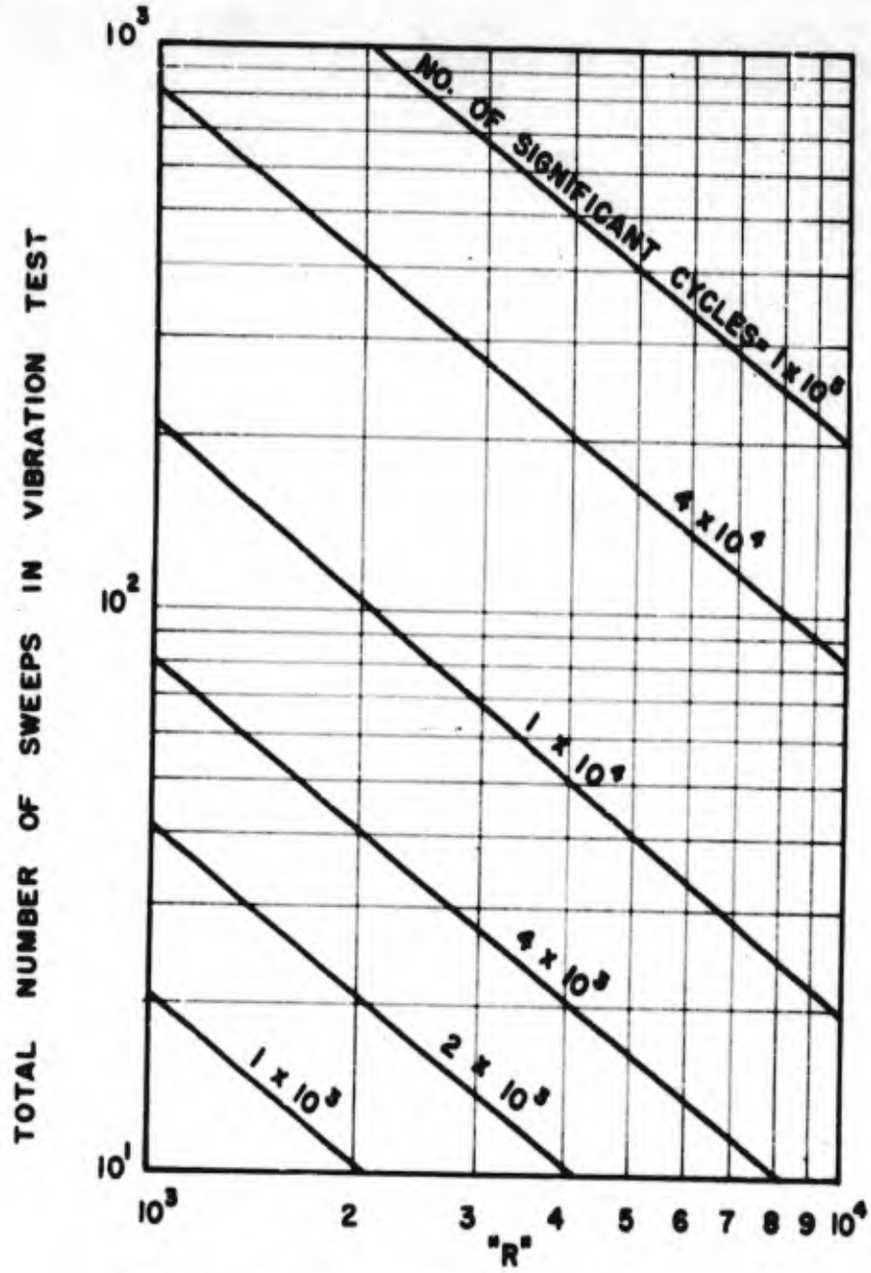

FIGURE 28. TOTAL NUMBER OF SWEEPS IN VIBRATION TEST FOR VARIOUS VALUES OF PARAMETER R AND SIGNIFICANT CYCLES.

Following a similar procedure, the numerical evaluation of the sweep time for the environmental envelope for the jet bomber aircraft as shown in Figure 5 is presented in tabular form in Table III. Table IV presents the evaluation of the total vibration test time for the various exaggeration factors for the jet bomber environment of Figure 5. Referring to Table IV, it will be noted that a comparison of the comparable values of N and the total of testing times differ very slightly when computed for the environment of Figure 5. Consequently, the same reasoning regarding a selection of an exaggeration factor and total testing time will apply to the jet bomber environmental vibration test. This test procedure then would provide that each element receives 4000 cycles of stress reversal and would result in a procedure involving approximately four (4) hours of vibration testing.

The testing frequency is varied continuously between 5 and 50 cycles per second for a period of 178 seconds and between 50 and 225 cycles per second for a period of 14.6 seconds and between 225 and 350 cps for a period of 1.73 seconds and between 500 and 1000 cps for a period of 2.15 seconds. The total number of sweeps of test frequency variation between 5 and 1000 cycles per second may be selected from Figure 28 depending upon the value of the parameter R selected. The exaggeration factor involved is 2.37. For this envelope the exaggerated amplitude and "g's" are tabulated below:

FREQUENCY RANGE	ENVELOPE VALUE	EXAGGERATED AMPLITUDE, IN.	EXAGGERATED ACCELERATION, "g"
5 - 50 cps	.030"	.068"	---
50 - 225 cps	4g	---	9.0
225 - 350 cps	.0015"	.0034"	---
350 - 1000 cps	10g	---	22.5g

TABLE III

NUMERICAL EVALUATION OF SWEEP TIME
FOR 5-1000 CPS TEST OF FIGURE 5 (JET BOMBER ENVIRONMENT)

For R = 1200:

Number of significant cycles per sweep = 1200(1.038 - .990)

= 57.6

f_1	f_o	$h_{ave} = \frac{f_1^2 + f_o^2}{2R}$	$\Delta t = \frac{\Delta f}{h_{ave}}$	t
cps	cps	cps/sec	sec	sec
10	5	0.052	96.2	0
20	10	0.208	48.0	
30	20	0.541	18.5	
40	30	1.04	9.6	
50	40	1.70	5.9	178.3
100	50	5.20	9.62	
225	100	25.1	4.98	14.54
350	225	72.0	1.73	1.73
500	350	155.0	0.97	
600	500	254.0	0.393	
700	600	354.0	0.283	
800	700	471.0	0.212	
900	800	605.0	0.16	
1000	900	755.0	0.132	2.16

TABLE IV

EVALUATION OF TOTAL VIBRATION TEST TIME FOR VARIOUS EXAGGERATION FACTORS - JET BOMBER ENVIRONMENT OF FIGURE 5

N	EXAGGERATION FACTOR	TIME FOR 5-50 cps TEST	TIME FOR 50-225 cps TEST	TIME FOR 225-350 cps TEST	TIME FOR 350-1000 cps TEST	TOTAL TIME	TOTAL TIME
cycles	(Fig.27a)	minutes	minutes	minutes	minutes	minutes	hours and minutes
10^3	2.63	51.6	4.23	0.502	0.622	56.95	0 - 57.0
2×10^3	2.44	103.2	8.46	1.004	1.244	113.91	1 - 53.9
*4×10^3	2.25	206.4	16.92	2.008	2.488	227.82	3 - 47.8
10^4	2.03	516.0	42.3	5.02	6.22	569.54	9 - 29.5
4×10^4	1.73	2064.0	169.2	20.08	24.88	2278.16	37 - 58.2
10^5	1.56	5160.0	423.0	50.2	62.2	5695.4	94 - 55.4

SECTION VIII

VIBRATION TEST SPECIFICATION

The preceding analysis presumes failure of the equipment as a result of repeated stressing of structural members. The test embodies an amplitude greater than that encountered in the environment for the purpose of causing structural failure in a relatively short period of time. Under the assumed conditions, vibration of this magnitude never occurs in service. Consequently, it should not be required that the equipment under test be functionally operative during this exaggerated test condition. The preceding endurance test should be supplemented by a scanning test at an environment level corresponding to that actually experienced in service, and the equipment should be functionally operative under such conditions.

In summary, the recommended vibration tests for reciprocating engined and jet fighter aircraft components are as follows:

(a) A scanning test at a displacement amplitude of 0.030" peak-to-peak throughout a frequency range of 5 to 50 cycles per second, and at an acceleration amplitude of 4g throughout a frequency range of 50 to 500 cycles per second. This test is intended not to investigate the structural integrity of the equipment but only to determine that it operates satisfactorily. This vibration test is considered to simulate the expected maximum environment.

(b) Vibration at a displacement amplitude of .068" peak-to-peak throughout a frequency range of 5 to 50 cycles per second for an elapsed time of 210 minutes. This is a sweep frequency test in which the test frequency is continuously varied at any of the rates set forth in Figure 25. In addition, vibration at an acceleration amplitude of 9.0g throughout the frequency range of 50 to 500 cycles per second for an elapsed time of 21 minutes. This is also a sweep frequency test with any of the rates of change of test frequency set forth in Figure 25. This is a test to investigate structural strength. The equipment should not be required to function during the test but should remain undamaged and fully operative at the conclusion of the test.

The recommended vibration tests for jet bomber aircraft components are as follows:

(a) A scanning test at a displacement amplitude of .030" peak-to-peak throughout a frequency range of 5 to 50 cps for a period of 210. minutes, and an acceleration amplitude of 4g throughout the frequency range of 50 to 225 cps for a period of 16.9 minutes, a vibration amplitude of .0015" throughout the frequency range from 225 to 350 cps for a period of 2.0 minutes, and a constant 10g acceleration amplitude from 350 to 1000 cps for a period of 2.50 minutes. This is a sweep frequency test in which the test frequency is continuously varied with any of the rates set forth in Figure 25. This test is intended not to investigate the structural integrity of the equipment but only to determine that it operates satisfactorily. This vibration test is considered to simulate the expected maximum environment.

(b) Vibration at a displacement amplitude of .068" peak-to-peak throughout a frequency range of 5 to 50 cps for an elapsed time of 210 minutes, vibration at an acceleration amplitude of 9.0g throughout the frequency range of 50 to 225 cps for an elapsed time of 16.9 minutes, vibration at a displacement amplitude of .0034" peak-to-peak throughout a frequency range of 225 to 350 cps for a period of 2.0 minutes, vibration at an acceleration amplitude of 22.5g throughout the frequency range of 350 to 1000 cps for a period of 2.49 minutes. This is a sweep frequency test and any of the rates of change of test frequency as set forth in Figure 25 may be applied. This test is to investigate structural strength. Equipment should not be required to function during this test but should remain undamaged and fully operative at the conclusion of the test.

The data defining the vibration environment in aircraft make but few distinctions with regard to direction of motion. The directions must be assumed to be completely random with the result that the environment defined in Figure 5 is considered applicable to each of three coordinate axis independently. In many equipments, there is coupling between two or more directions of motion. In other words, vibration that is applied along one axis may cause certain structures to vibrate in the direction of one or more other axes. For this reason, vibration of one equipment in each of three directions for a period of three hours each may subject certain structures to more than four hours of vibration. It is recommended, therefore, that the vibration test

sequence apply equally to vibration along each of three coordinate axes and that separate or rebuilt equipments be used for each direction.

As described in complete detail on the preceding pages, the procedure followed in arriving at a laboratory test involving steady-state vibration consists of three discrete steps. These may be summarized as follows:

(a) The limits of the probable maximum severity of the environment in terms of steady-state vibration must be defined.

(b) The principles governing the relation between failure after a relatively long period of mild vibration and failure after a relatively short period of severe vibration must be established.

(c) Using the environment established in (a), the principles established in (b) may be applied by selecting an exaggerated test condition which will cause a representative type of failure within a reasonable testing period.

The testing routine set forth above for conditions of steady-state vibration is the result of applying this procedure to data defining the environment in the establishment of a laboratory test. The validity of the routine is dependent upon the authenticity of the data which defines the environment. Further comments regarding data are set forth in the section of this report entitled "Conclusions". Data defining vibration environments make few distinctions with regard to simultaneous environments of humidity, sand and dust, extreme temperatures or other environments. In general these latter environments must be considered as additive to vibration or shock environments and should be tested simultaneously.

SECTION IX

CONCEPTS OF DAMAGE AS A RESULT OF SHOCK

This section of the report discusses the analysis of records of acceleration as a function of time used to define conditions of shock or transient vibration. These records are the oscillograms mentioned earlier in the report. In analyzing the effect of vibration upon mechanical systems, there is a fundamental distinction between procedures for considering transient and steady-state vibration. In steady-state vibration, it is assumed that all transient effects occur at the natural frequency of the system and are ultimately damped out. The motion of the system then takes place entirely at the frequency of the disturbing vibration. This frequency is referred to as the forcing frequency.

In shock or transient vibration, the equipment which is subjected to the vibration is caused to vibrate in a mode that includes both forced and natural frequencies. In the foregoing analysis of an equipment subjected to steady-state vibration, it was assumed that damage results primarily from a resonant condition at the forcing frequency. In a sense, the same consideration applies to transient vibration except that the forcing frequency is not as well defined as in steady-state vibration. Consequently, there are no established standards of frequency to use in setting up a laboratory test. An entirely different approach is thus needed in adopting a criterion of damage.

As pointed out previously in connection with steady-state vibration, a primary cause of certain types of failure is excessive stress in structural members. This stress tends to be proportional to the acceleration experienced by such members. From a hypothetical standpoint, it is possible to predict the stresses in the structural members by attaching an accelerometer to each element of the equipment being tested and multiplying the measured acceleration by the mass to obtain the force acting upon the member. If the strength of each such element were known, it would then be possible to predict from the acceleration measurements whether the elements were close to failure as a result of the test. Although such a procedure is possible in a hypothetical sense, it is not practically feasible because the vulnerable elements tend to be small and inaccessible whereas applicable accelerometers tend to be relatively large.

Even though this suggested procedure is impractical, the theory suggests an approach to evaluating the severity of shock or transient vibration in terms of possible damage to an equipment. Assume now that each equipment is comprised of many

structural elements having characteristic natural frequencies assumed to fall within a certain frequency range. A single equipment cannot include elements of all natural frequencies. If many equipments are taken as a group, however, it is probable that at least one element of each discrete natural frequency within the accepted frequency range will be found in one of the equipments in the group.

To a first approximation, the maximum acceleration experienced by a structural element of an equipment is a function of only the natural frequency of the element. Consequently, a simulated equipment may be constructed in any convenient form, such as the base equipped with cantilever beams illustrated in Figure 29. Each of the cantilever beams of this simulated equipment has a different natural frequency, and the range of natural frequencies to be studied may be changed at will by varying the lengths of the cantilever beams. If it is desired to determine the required strength of the elements of an equipment which must withstand a certain shock, the simulated equipment illustrated in Figure 29 may be subjected to the shock and the maximum deflection of each beam noted. The maximum acceleration of each beam is then calculated from the recorded maximum deflection. The values of maximum acceleration determined in this manner are used in conjunction with the masses of elements of the actual equipment having corresponding natural frequencies as the cantilever beams to determine the dynamic forces acting on each element as a result of the shock. Theoretically, this simulated equipment may be subjected to all possible occurrences of shock or transient vibration and the maximum acceleration of each cantilever beam noted. With this information for each natural frequency, the designer may design the actual equipment so that each element has at least the strength indicated by the maximum acceleration of the cantilever beam having the same natural frequency.

The use of a mechanical instrument to obtain the information outlined in the above paragraph tends to be cumbersome. Equivalent results can be obtained by electrical analogy. Electrical circuits can be assembled in such a way that they respond to an output voltage in the same manner as a mechanical structure responds to an applied shock or transient vibration. The details of a suitable analog computer, together with a specially constructed function generator, are described in Appendix II. With this analog computer, the natural frequencies and damping coefficients of the systems under investigation can be varied readily by adjusting the constants of the electrical circuits. It is then possible to obtain electrical responses which, by analogy, can be converted to values of maximum acceleration experienced by mechanical structures having known characteristics. Each shock or transient vibration is then defined in terms of maximum response acceleration. This may be expressed as a curve

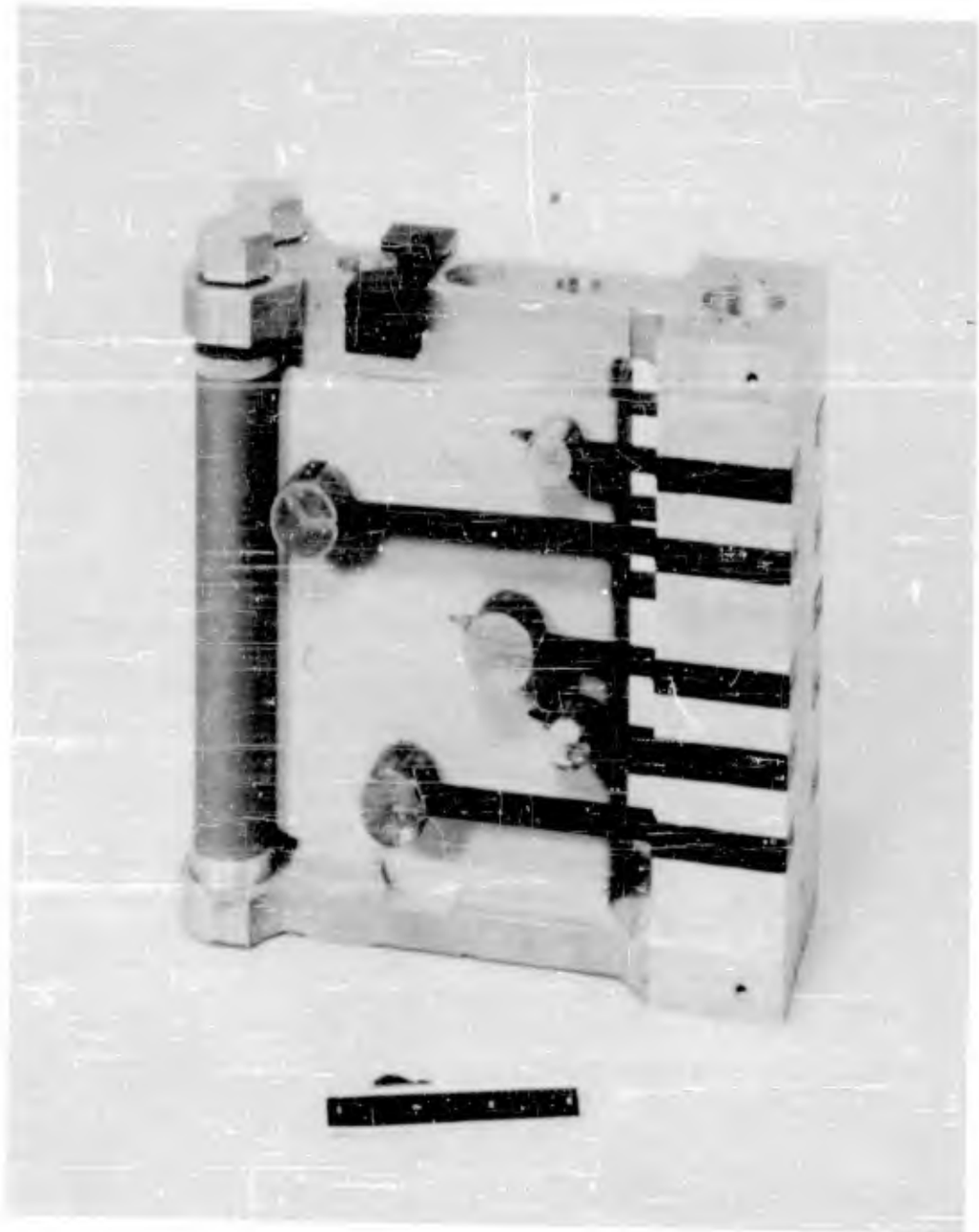

Courtesy of The David Taylor Model Basin, USN
Photo No. NP21-48384.

Figure 29. Simulated equipment, consisting of base and several cantilever beam systems of different natural frequencies.

showing maximum response acceleration as a function of natural frequency of element for a single shock motion; for a group of shock motions, an envelope may be drawn to encompass the curves for the individual shock motions.

This concept of severity, together with the method of expressing equivalents of shock motions, is soundly endorsed in the technical literature. References 29, 39, and 110 in the Bibliography, Appendix V, are significant with respect to this concept. This approach is satisfactory where the response embodies a relatively high value of acceleration for a single cycle and where the remainder of the response embodies relatively small values of acceleration. Under these conditions, only the maximum acceleration tends to be significant. The present analysis, however, is concerned with shock and transient vibration occurring in aircraft as a result of landing, gun fire, air buffeting and other disturbances having many repetitions. As a consequence, it may not be possible to express the results in terms of a single cycle or a few cycles of stress reversal.

As an example of the different types of responses that may be obtained, a record of acceleration as a function of time resulting from the landing of a type AT-11 airplane and several typical responses thereto are shown in Figure 30. The acceleration as measured on the airplane is the lower trace in each of the four oscillograms, the differences in calibration factors accounting for the different appearances. This trace, suitably expressed in terms of voltage as a function of time was fed into the analog computer, and the responses of several systems of different natural frequencies were obtained. These responses are reproduced as the upper traces of the several oscillograms in Figure 30.

The response set forth in Figure 30 (A) is for a system having a natural frequency of 10 cycles per second. This low frequency system fails to respond to the high frequency components in the input, and the response is an irregular record having predominantly low frequency components. At the other extreme of the frequency spectrum, the responses of systems having natural frequencies of 110 and 200 cycles per second are shown in Figures 30 (C) and (D), respectively. The general shapes of these responses are similar to the shape of the input but have superimposed thereon transient vibration at the natural frequencies of 110 and 200 cycles per second. The amplitude of this superimposed vibration is relatively small. In Figure 30 (B), the upper trace is the response of a system having a natural frequency of 33 cycles per second.

In the response of Figure 30 (B), the shape of the input is almost obscured, and the predominant characteristic

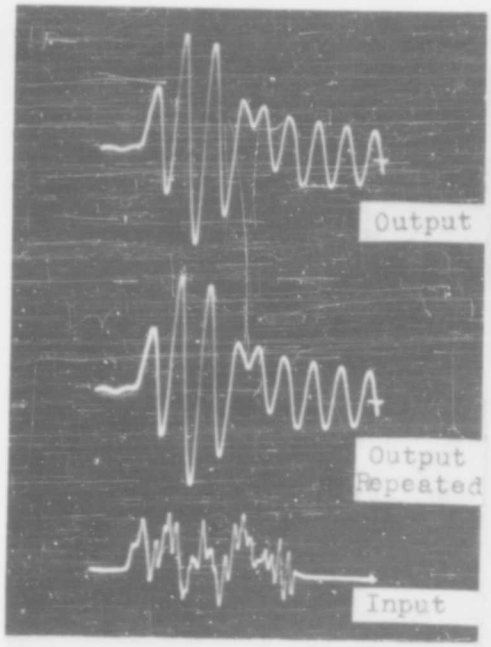

(A) f_n = 10 cps., Q = 50

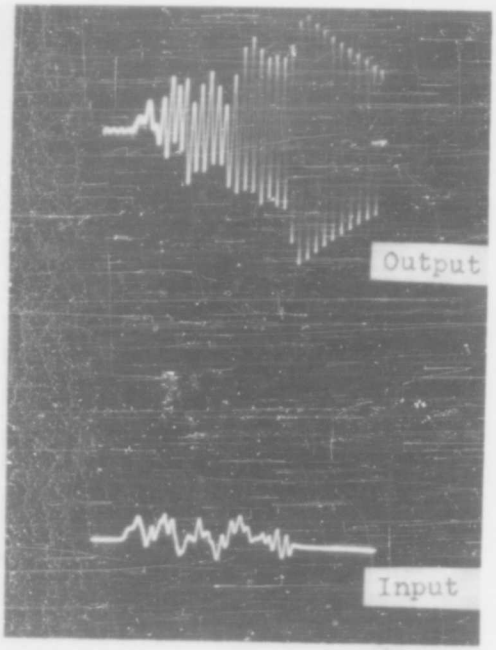

(B) f_n = 33 cps., Q = 50

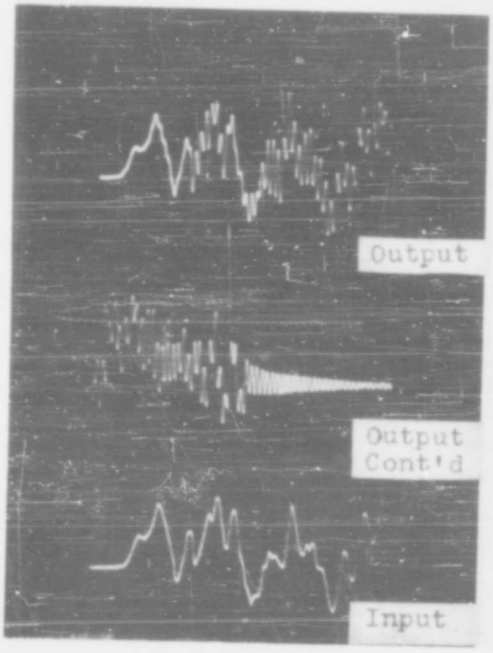

(C) f_n = 110 cps., Q = 50

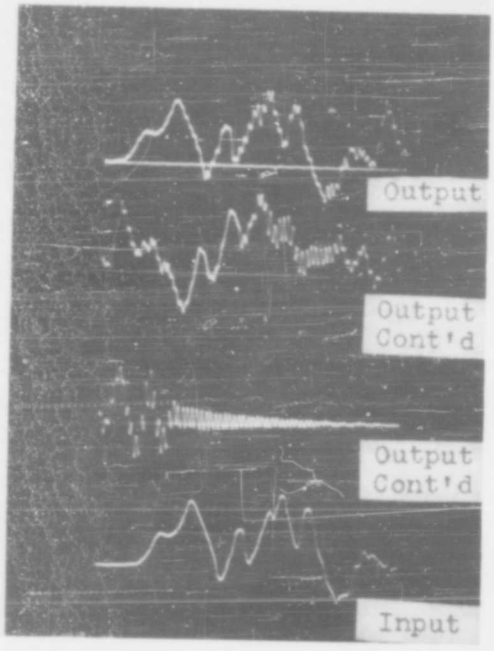

(D) f_n = 200 cps., Q = 50

Figure 30. Response acceleration as a function of time for systems having natural frequencies of 10, 33, 110, and 200 cps. when subjected to landing shock measured on Type AT-11 airplane.

of the response is a transient vibration having a natural frequency of 33 cycles per second and a relatively great amplitude. This frequency is the natural frequency of the system and represents a sort of resonance. This resonance occurs because the input vibration has a prominent component at a frequency of approximately 33 cycles per second, even though this component of the input is not steady-state in nature. The response of the system whose natural frequency is 33 cycles per second illustrates the type of response in which many cycles of acceleration of appreciable amplitude may be more significant than the acceleration of maximum amplitude. In general, the acceleration measured on aircraft will be found to be irregular with certain predominant frequencies. The responses of systems covering a range of frequencies will be similar generally to the several responses illustrated in Figure 30.

It is necessary in describing the characteristics of an elastic system to define not only the natural frequency but also the damping. The response of an elastic system to steady-state or transient vibration is greatly influenced by the damping of the system. In the preceding analysis of steady-state conditions, the environment is defined in terms of measured parameters and is not a function of the properties of systems subjected to the environment. In the analysis of transient conditions, the environment is defined in terms of the response of elastic systems to the measured parameters. The environment can be defined completely only by setting forth the responses of elastic systems having natural frequencies and degrees of damping encompassing the range expected to be encountered in equipments.

In classical mechanics, damping is defined as a percentage of the damping in a critically damped system. If the damping is small, the transmissibility at resonance is numerically equal to one-half of the reciprocal of the damping ratio. This concept has come into common use, and the symbol Q is applied to the maximum transmissibility at resonance during steady-state vibration. In the analysis of transient conditions discussed here, systems having values for Q of 10, 20, and 50 are considered. The selection of an appropriate value for Q is difficult. The damping in structural members tends to increase with an increase in strain. If the vibration amplitude is small, it may be expected that large values of Q will be encountered, and the maximum value of 50 used here may seem too low. For the relatively large deflections embodied in the transient conditions being studied here, however, strains tend to be large, and it is believed that a range of 10 to 50 for the parameter Q is representative of these conditions.

SECTION X

CUMULATIVE DAMAGE IN FATIGUE

In the establishment of laboratory tests to simulate the environmental conditions encountered in the operation of aircraft, cognizance must be taken of the fact that an aircraft experiences many landings in its lifetime. As indicated in Figure 30, elastic structures carried in such aircraft experience several stress reversals per landing. It may be deduced intuitively that the cumulative effect of these several cycles of stress reversal may be of great importance if the stress magnitude at each cycle is approximately the same. On the other hand, if the response exhibits one cycle of stress of relatively great magnitude, the cumulative effect of other cycles may be neglible if the magnitudes of these other cycles are substantially less than the magnitude of the maximum stress. It cannot be determined by an inspection of the response patterns whether the cumulative effect of the cycles of lower stress is important. Consequently, two types of analysis have been carried out concurrently, and the results thereof compared. The first part of the analysis is devoted to a consideration of the cumulative effect of cycles of stress having a magnitude somewhat less than the maximum. This is then compared with the corresponding results obtained by considering only the maximum stress encountered during a single landing.

The technical literature includes numerous papers setting forth the fatigue or endurance properties of materials. The tests generally are conducted under such circumstances that the maximum stress is constant at each cycle of stress reversal. The responses illustrated in Figure 30 do not meet these requirements for two principal reasons as follows:

(a) A different maximum stress is encountered at each succeeding cycle of stress reversal. An analysis of endurance strength under conditions involving a stress pattern having something in common with this was carried out initially by M. A. Miner who reported the results of his analysis in Reference 30. The problem considered by Miner involved the application of many cycles of stress having the same maximum value at each cycle, followed by many cycles at a different maximum stress, etc. Although the hypothesis formulated by Miner does not contemplate the present situation in which the maximum stress is different at each succeeding cycle of stress reversal, it appears quite general. The assumption is made here that the hypothesis may be extended to the type of stress pattern found here, even though the paper by Miner does not establish the validity of this assumption.

(b) In the oscillograms set forth in Figure 30, the mean value of response acceleration is generally different than zero. In the conventional rotating bending type of test for endurance strength, a tensile stress is followed one half cycle later by a compressive stress of equal magnitude. There is considerable information in the technical literature on fatigue tests in which the value of one of these stresses exceeds the other, thereby introducing a mean stress not equal to zero. It is possible to make a correction to a condition of zero mean stress, a correction which has become known as the Goodman correction. The validity of the Goodman correction has been established only for conditions of a regular stress pattern, and has not been demonstrated to apply to the type of stress pattern investigated by Miner. It is possible, however, by making several assumptions to apply the Goodman correction to an hypothesis of the transient problem based upon the approach proposed by Miner. A few sample calculations revealed that the results are not modified appreciably by introducing the Goodman correction for mean stress. Consequently, all of the ensuing calculations are based upon the assumption that only the maximum stress is significant, and that the problem should be handled as if the mean stress were zero.

Reference is now made to the conventional fatigue or endurance curve initially illustrated in Figure 8 and essentially reproduced in Figure 31 to serve as a basis for discussion of Miner's hypothesis. This curve shows a typical relation between maximum stress S and number of cycles N to failure, when the test is conducted under such conditions that the maximum stress at each cycle is constant. The hypothesis formulated by Miner is concerned with the degree of damage caused when a specimen is subjected to n_1 cycles of stress reversal at a maximum stress S_1, n_2 cycles of stress reversal at a maximum stress S_2, and n_3 cycles of stress reversal at a maximum stress S_3. Referring to Figure 31, Miner's hypothesis states that failure of the specimen should not occur by fatigue if

$$\frac{n_1}{N_1} + \frac{n_2}{N_2} + \frac{n_3}{N_3} + \cdots < 1 \qquad (24)$$

On the other hand, if

$$\frac{n'_1}{N'_1} + \frac{n'_2}{N'_2} + \frac{n'_3}{N'_3} + \cdots > 1 \qquad (25)$$

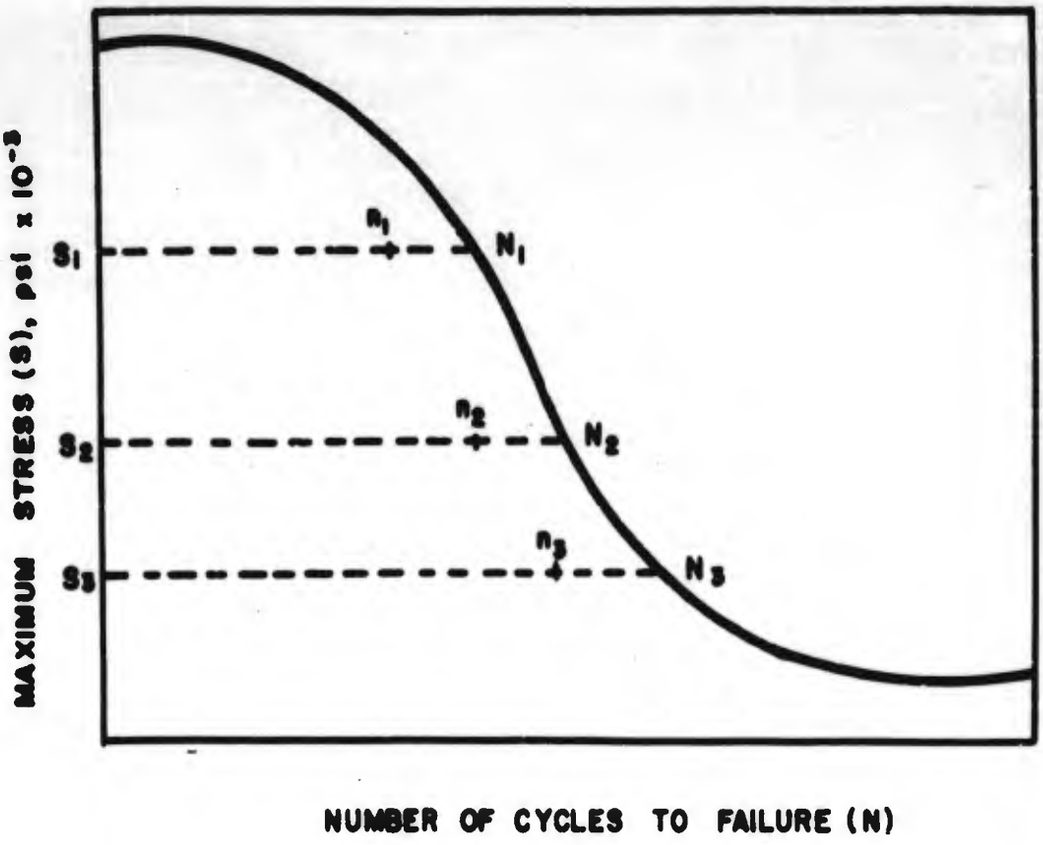

FIGURE 31. TYPICAL STRESS-CYCLE DIAGRAM SHOWING RELATION OF PARAMETERS IN HYPOTHESIS OF CUMULATIVE DAMAGE IN FATIGUE FORMULATED BY M.A. MINER

failure of the specimen may be expected to occur.

In his original hypothesis of accumulative damage, Miner has suggested that the constant shown on the right hand side of the inequality in equations (24) and (25) above might have a value of unity, but later investigators have shown that the value of this constant may be substantially less or substantially greater than unity, depending upon the pattern in which the stress is varied from one sequence of cycles to another. The stress pattern experienced by a structure subjected to shock varies in a random-like manner, and does not fall strictly within the scope of the investigations of either Miner or other investigators working in this field.

Inasmuch as the technical literature contains no information known to be strictly applicable to the shock problem, investigation described in the following paragraphs was undertaken to supply a basis for the establishment of laboratory shock test.

In order to apply the reasoning formulated by Miner it is necessary to know (1) the endurance properties of the material under investigation when subjected to repeated cycles of stress, and (2) the history of stress cycles experienced by the material as a result of the applied shock. When a structure is subjected to shock, the history of the stress cycles is a function not only of the shock, but also of the natural frequency of the structure and its damping capacity. For purposes of carrying out this investigation, a number of substantially identical cantilever beams were constructed as shown in Figure 32. These beams were constructed from SAE-4130 steel in a normalized condition, and were in the form of rods whose diameter was .218 inches. Each beam carried a weight of 0.211 pound at its free end, and the length was approximately 10.5 inches. The exact length was determined by the requirement that the natural frequencies of the beams be identical. Using a series of such beams, vibration tests were conducted to determine the damping capacity of the beams, which was used subsequently in determining the maximum stress for use with the theory of cumulative damage in fatigue.

The relation between the stress in the beam and the maximum deflection was established by first conducting a static force-deflection curve by applying static loads to the free end of the beam. The resulting force-deflection curve is shown in Figure 33. The stress in the beam is a maximum at the fixed end, and may be calculated as follows:

$$S = \frac{Mc}{I} \qquad (26)$$

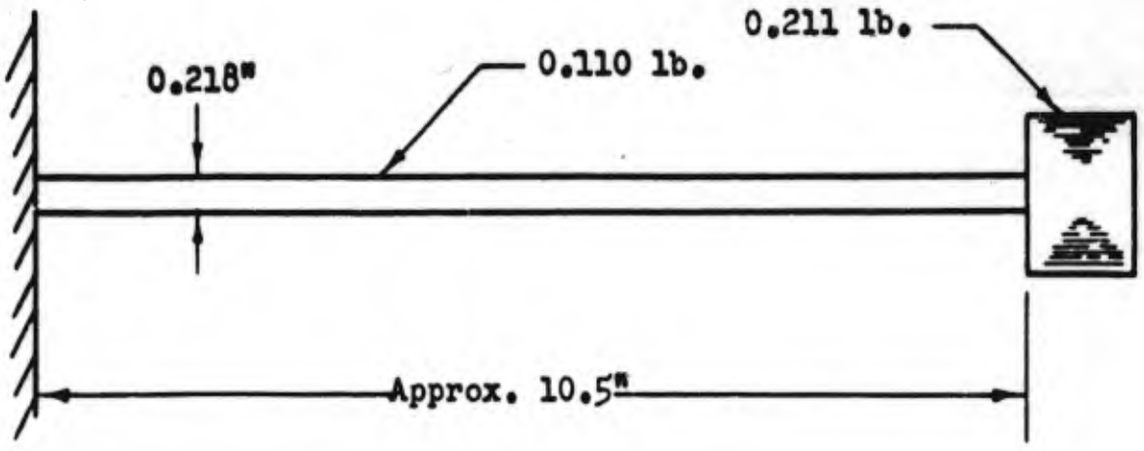

FIGURE 32. BEAM USED FOR TEST PURPOSES
(material - SAE 4130 steel, normalized)

For a beam of circular cross section,

$$S = \frac{FLr}{\pi r^4/4} = \frac{4FL}{\pi r^3} \qquad (27)$$

where F is the force applied to the free end, L is the length of the beam, and r is the radius of the cross section. Substituting a length L = 10.5 inches and a radius r = 0.109 inch, the following expression is derived giving the maximum stress as a function of the load on the free end of the beam:

$$S = 10{,}200\ F \qquad (28)$$

The force-deflection curve included as Figure 33 indicates a deflection of approximately 0.125 inch resulting from a force of one pound. Making this substitution for F in equation (28), the following expression setting forth the relation between deflection and maximum stress is obtained:

$$S = \frac{10{,}200\delta}{0.125} = 81{,}500\delta \qquad (29)$$

The relation defined by equation (29) will be used below to estimate the maximum stress in the beam when the deflection at the free end has been measured.

The dynamic characteristics of the beam illustrated in Figure 32 were determined by attaching several beams to a mechanical vibration machine, and operating the machine at the resonant frequency of the beams. The displacement amplitude of the vibration table, designated here as the input vibration, was varied in discrete steps and the displacement of the mass at the end of the beam was noted. The displacement of this mass is designated here as the response displacement. The response displacement divided by the input displacement gives a value for transmissibility at resonance which is designated here by the symbol Q. The numerical values for transmissibility, as determined in this manner and set forth in Table V, are shown graphically in Figure 34. Inasmuch as the transmissibility is large compared with unity, and because the mass tends to vibrate 90° out of phase with the input vibration at resonance, the maximum stress in the beam may be determined from equation (29)

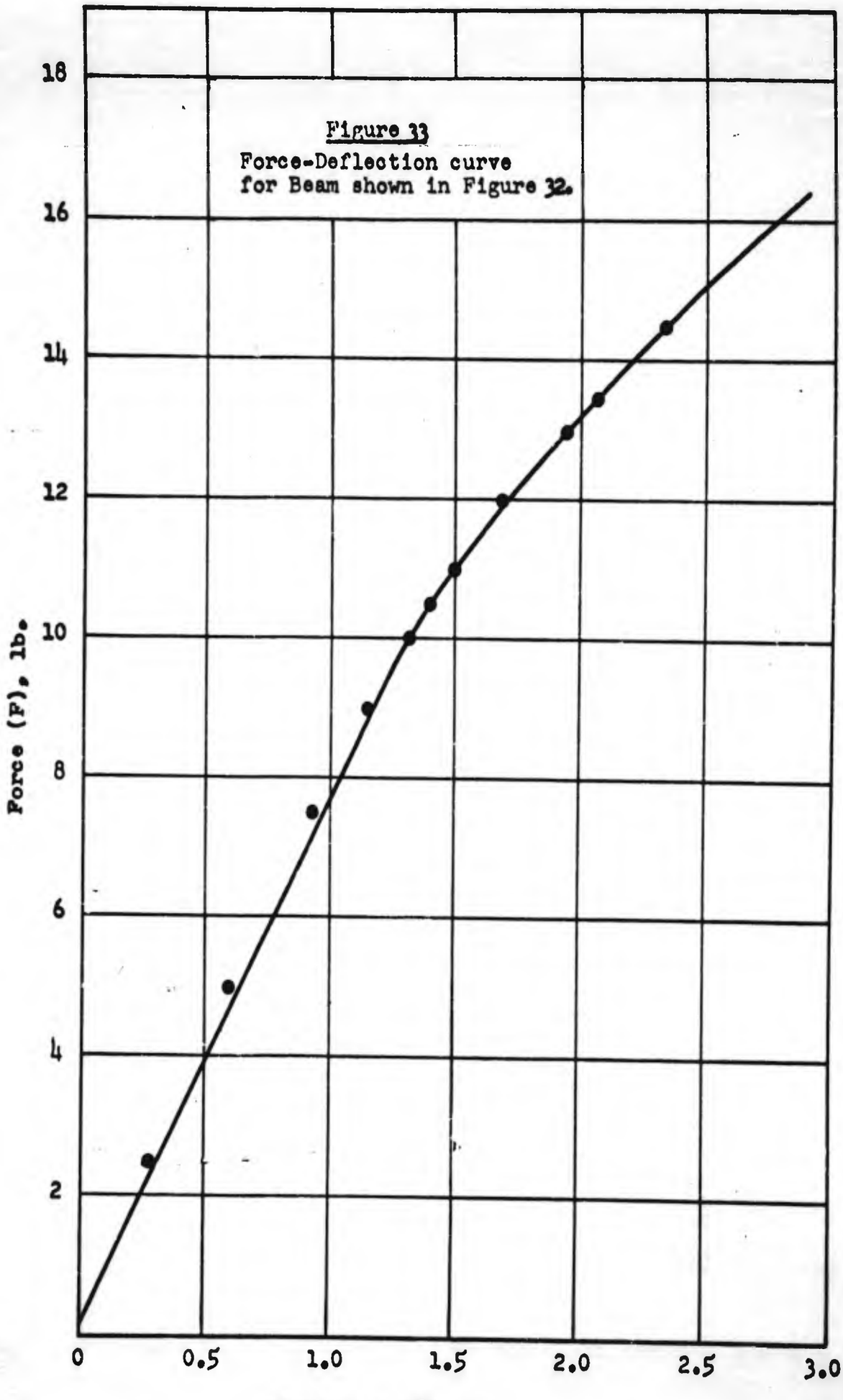

Figure 33
Force-Deflection curve
for Beam shown in Figure 32.

TABLE V

Maximum Transmissibility and Maximum Stress for Specimens of Beams Shown in Figure 34.

Test Freq., cps.	Double Displacement Amplitude, Inches		Trans.	Max. Stress, p.s.i.
	Input	Response		
18.5	0.020	1.188	59.4	48,500
18	0.025	1.375	55.0	56,000
18	0.040	1.690	42.2	68,600
17.8	0.050	1.940	38.8	79,200
17.8	0.060	2.188	36.5	89,000
17.5	0.075	2.250	30.0	92,000
17.5	0.085	2.500	29.4	102,000
17.5	0.100	2.562	25.6	105,000
17.3	0.110	2.625	23.9	107,500

Figure 34
Maximum Transmissibility and Maximum stress in Beam as a Function of Vibration Input

by converting the response amplitude given as double displacement in Table V to single displacement. This gives the values of maximum stress set forth in the last column of Table V and shown graphically in Figure 34.

To determine the endurance properties of the beam structure, several identical beams having equal natural frequencies were attached to the vibration machine. The beams were then excited at resonance, and the test continued until all beams had failed. The number of stress cycles required to cause failure in each beam was noted. The test was then repeated for three additional groups of beams, each being vibrated with a different vibration input, and the results recorded in Table VI. The maximum stress, as included in Table VI, was calculated from equation (29) using the response amplitude noted during the vibration test. The number of cycles necessary to cause failure at each stress level was averaged, and the resultant average is plotted in Figure 35, to provide the conventional type of stress-cycles to failure curve. This curve does not exhibit the usual straight line when plotted to semi-logarithmic co-ordinates, but it cannot be determined at this time whether the shape of the curve is the result of unusual characteristics of the cantilever beam structure or whether it reflects the relatively small quantity of data. A curve with this shape tends to result from a specimen having pronounced stress concentration, and it is believed that this factor may contribute to the shape of the curve.

The strength of the beam when subjected to repeated impact was investigated using the machine illustrated in Figure 36. This machine is comprised of a table which is constrained by guides and rollers to move only in translation along a vertical axis. Vertical motion is imparted by a pair of cams arranged to gradually lift the table to a desired height and then to suddenly drop the table upon a suitable arresting means. If the arresting means is elastic, the table tends to rebound several times with the consequent result that a series of impulses of decreasing severity is imparted to a structure attached to the table. The investigation was carried out by mounting to the table a number of identical beams as shown in Figure 32 and having the same natural frequency. The machine was then operated continuously until all of the beams had failed. Two series of tests were run, one in which the table was dropped from a height of 5 inches and the other in which the table was dropped from a height of 10 inches. The number of drops required to cause failure of each beam was noted, and the results are recorded in Tables VII and VIII for the 5 inch and 10 inch drops, respectively.

TABLE VI

Cycles to Failure for Specimens of Beams Shown in Figure 32.

Spec. No.	Length Inches	Double Displacement Amplitude, Inches Input	Response	Trans.	Maximum Stress p.s.i.	Time of Test Min.	Cycles to Failure	Average Cycles to Failure
1	10.5	0.125"	2.250"	18	92,000	22	21,800	
2	—	—	—	—	—	—	—	
3	10.5	0.125"	2.250"	18	92,000	20	19,800	
4	10.5	0.125"	2.250"	18	92,000	24	23,800	21,200
5	10.5	0.125"	2.250"	18	92,000	21	20,800	
6	10.5	0.125"	2.250"	18	92,000	20	19,800	
7	10.5	0.100"	1.875"	18.75	76,400	27	26,800	
8	10.6	0.100"	1.875"	18.75	76,400	27	26,800	28,250
9	10.5	0.100"	1.875"	18.75	76,400	25	24,800	
10	10.5	0.100"	1.875"	18.75	76,400	35	34,600	
11	10.6	0.100"	2.0"	20	81,500	23	22,800	22,800
12	—	—	—	—	—	—	—	—
13	10.5	0.050"	1.75"	35	71,200	53	57,300	
14	10.5	0.050"	1.75"	35	71,200	57	61,500	61,200
15	—	—	—	—	—	—	—	—
16	10.5	0.050"	1.75"	35	71,200	60	64,900	
17	10.565	.040"	1.625"	40	66,000	150	162,000*	
18	10.565	.040"	1.625"	40	66,000	150	162,000*	162,000*
19	10.565	.040"	1.625"	40	66,000	150	162,000*	
20	10.565	.040"	1.625"	40	66,000	150	162,000*	

*Failure did not occur.

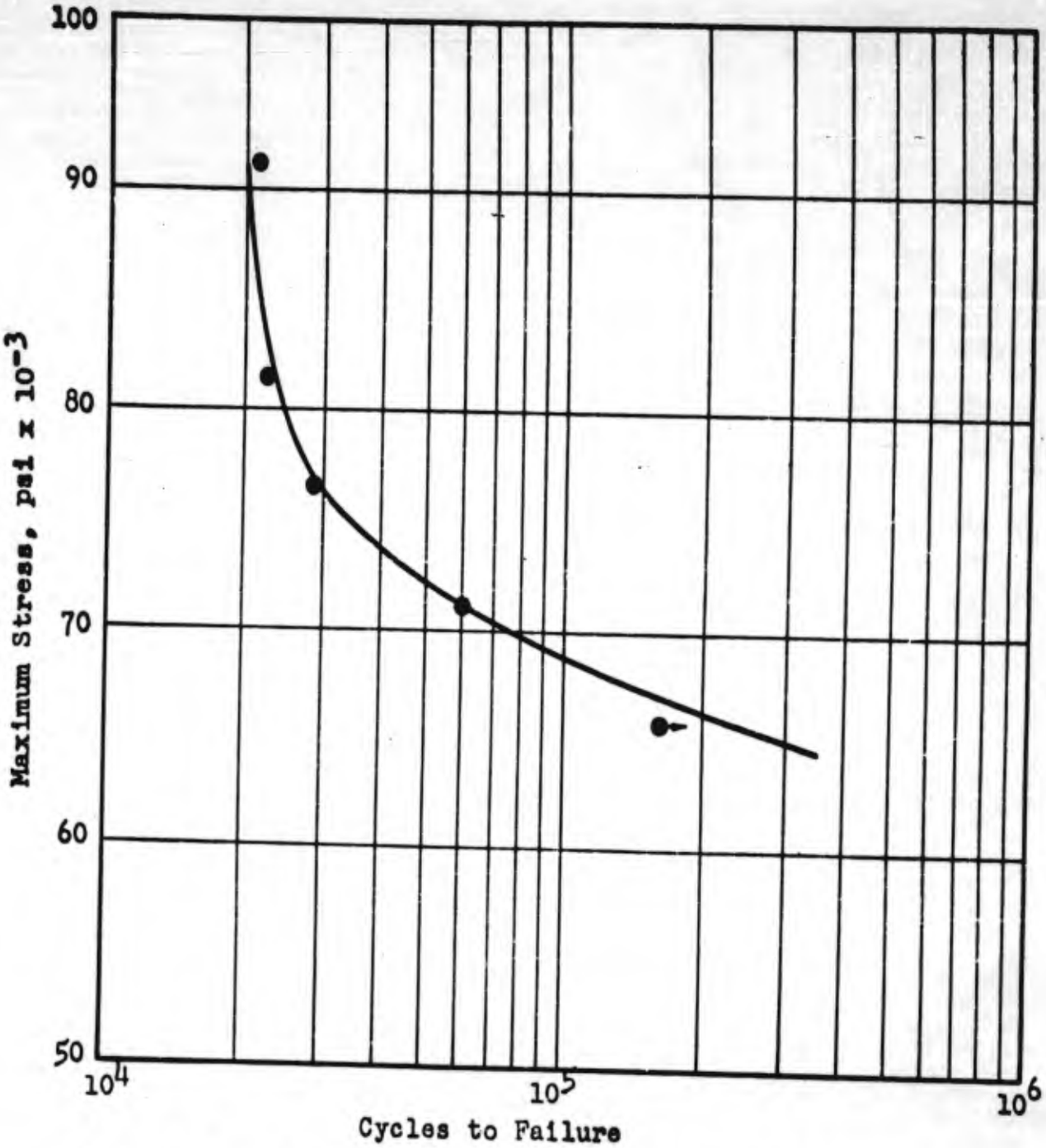

Figure 35- Maximum stress vs. Cycles to Failure for Beam shown in Figure 32.

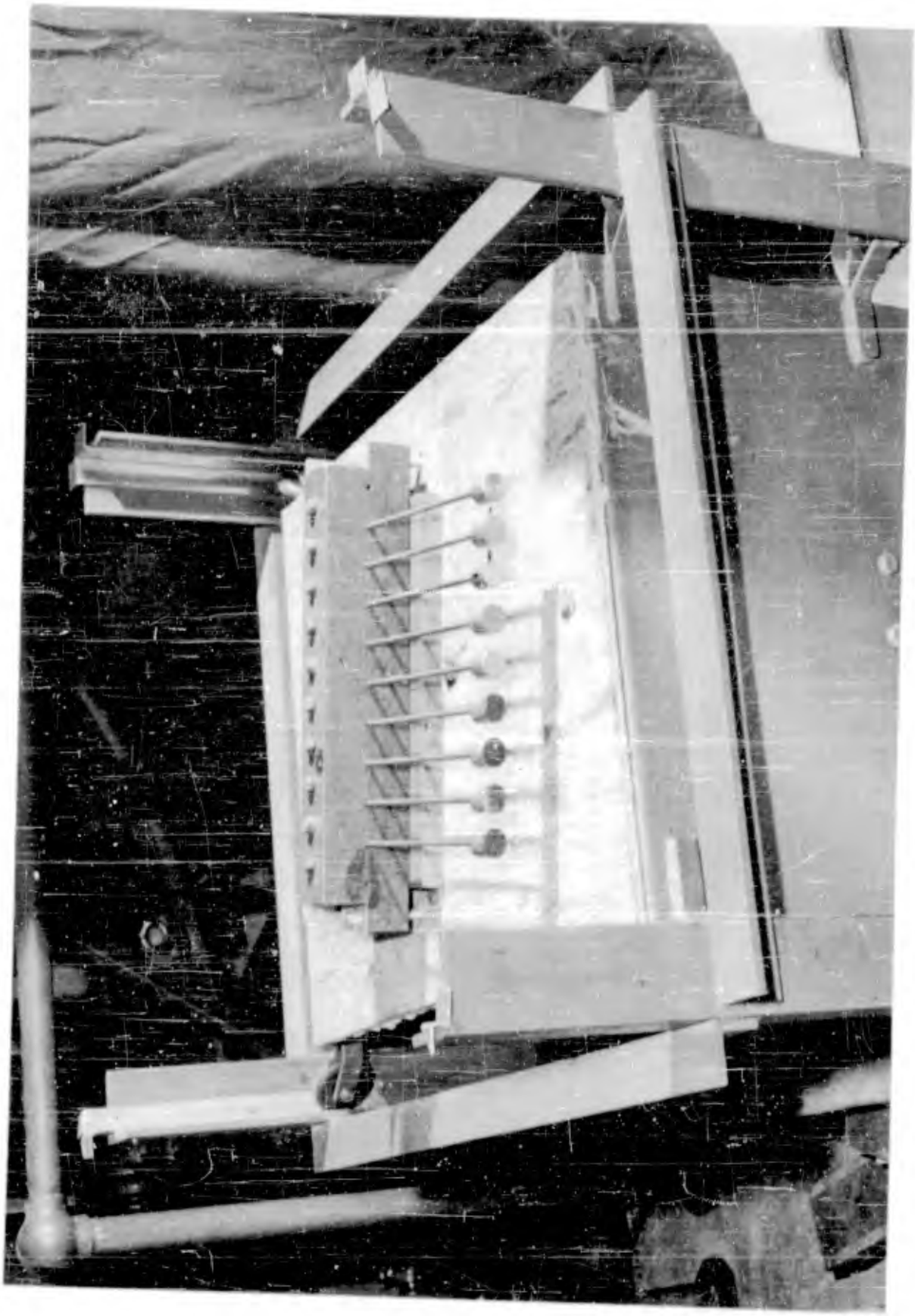

Figure 36. Repeated Drop Test Machine

TABLE VII

Repeated Drops Sustained by Beams Prior to Failure - 5 Inch Drop.

Spec. No.	Length of Beam, In.	No. of Drops
21	10.75	3660
22	10.66	3240
23	10.69	—
24	10.72	2940
25	10.59	—
26	10.72	4440
27	10.63	3900
28	10.72	3960
29	10.66	4500
	Average -	3806

TABLE VIII

Repeated Drops Sustained by Beams Prior to Failure - 10 Inch Drop

Spec. No.	Length of Beam, In.	No. of Drops
30	10.625	2808
31	"	2060
32	"	--
33	"	--
34	"	2568
35	"	--
36	"	2898
37	"	2118
38	"	--

Average - 2490

The motion experienced by the table as it rebounds from the arresting means is illustrated by the acceleration-time traces shown in the oscillograms in Figure 37. The time scale in these oscillograms reads from right to left. The lower trace in Figure 37a shows the acceleration experienced by the table when subjected to a 5 inch drop whereas the lower trace in Figure 37b is the corresponding record for the 10 inch drop. The record for the 5 inch drop is shown with a compressed time scale by the upper trace in Figure 37(c), wherein the peaks decreasing in height from right to left indicate the relative severity of succeeding pulses as the table rebounds repeatedly from the arresting means. The pulses of the type shown in Figure 37 were recorded on magnetic tape, and the signal was subsequently used as the input to an electrical analog of the cantilever beam illustrated in Figure 32. Inasmuch as each beam had a natural frequency of approximately 18 cps, the analog was maintained with this natural frequency. As indicated in Figure 34, the damping in the beam is a function of the maximum stress. For this reason, two values of damping were selected in analyzing the response of the analog to the input represented by the acceleration of the table. Typical traces of response acceleration of the beam as a function of time are reproduced in Figure 38 for drop heights of 5 inches and 10 inches and for values of $Q = 20$ and $Q = 40$.

The number of stress reversals at each stress level was taken from the oscillograms reproduced in Figure 38. The amplitude was first measured in terms of acceleration as noted in Tables IX and X. The conversion from maximum acceleration to maximum stress is made by substituting in equation (29) the value $\delta = 0.03$, the static deflection of a system whose natural frequency is 18 cps. The relation given by equation (29) is then expressed in terms of maximum stress per unit of gravitational acceleration as follows:

$$S = 81{,}500 \times 0.03 = 2440 \text{ psi/g} \qquad (30)$$

Values of maximum acceleration set forth in Tables IX and X are now converted to values of maximum stress by applying the relation of equation (30). Entering Figure 35 with the values of maximum stress set forth in Tables IX and X, the corresponding number of cycles to failure may be determined at each value of maximum stress, as set forth in Table XI. Stress levels below the curve of Figure 35 are omitted because they apparently contribute nothing to the damage. For purposes of subsequent computation, the reciprocals of

Figure 37

Acceleration - Time Pulse Produced by Repeated Drop Machine

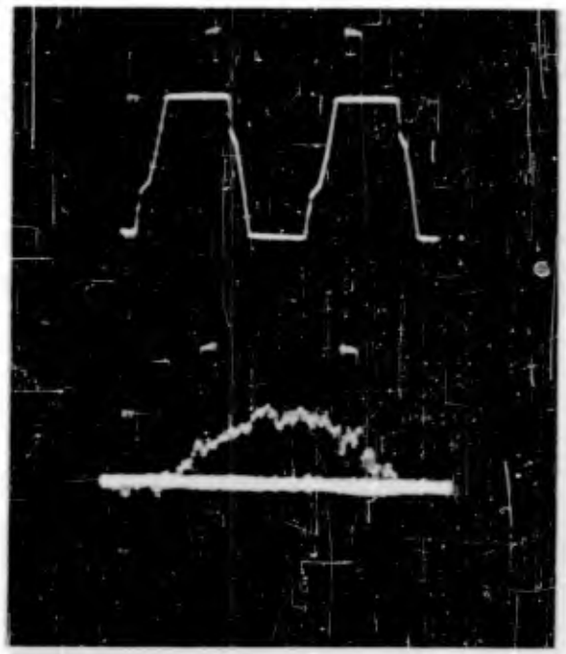

(a)

Upper Trace: Calib. Wave: 60 cps and 40g peak-to-peak
Lower Trace: 1st Pulse of 5" drop

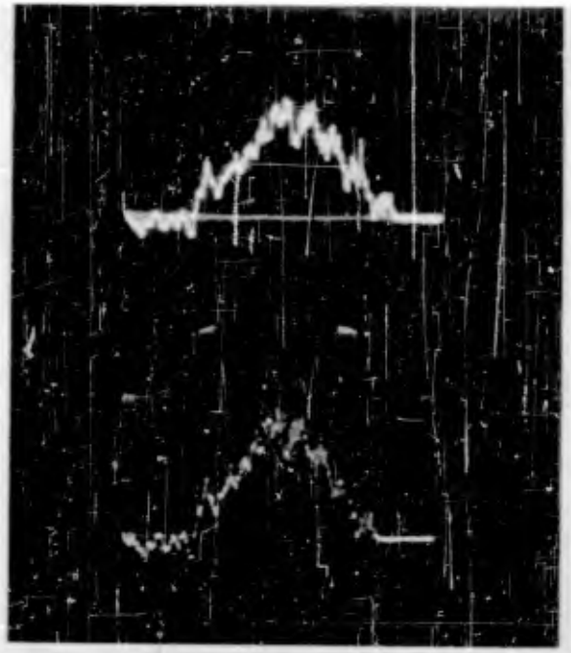

(b)

Upper and Lower Traces: 1st Pulse 10" drop.

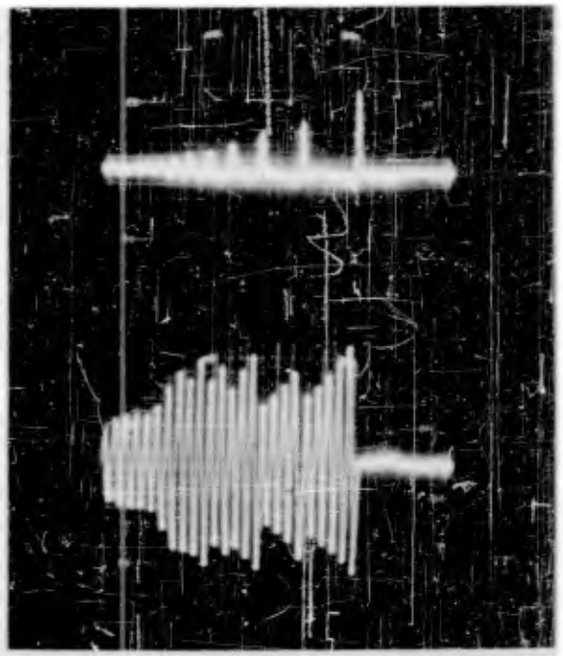

(c)

Upper Trace: Repeated Acceleration Pulses
Lower Trace: Response of 20.4 cps system, Q= 40

Figure 38

Input and Response Acceleration for Repeated Drop Tests of System Having Natural Frequency of 18 cps.

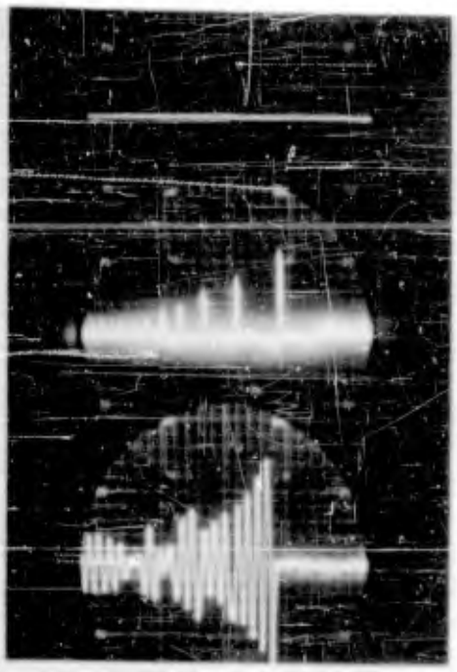

5" Drop - Q = 20
Upper Trace: Input Accel; 24g Max.
Lower Trace: Response Acceleration

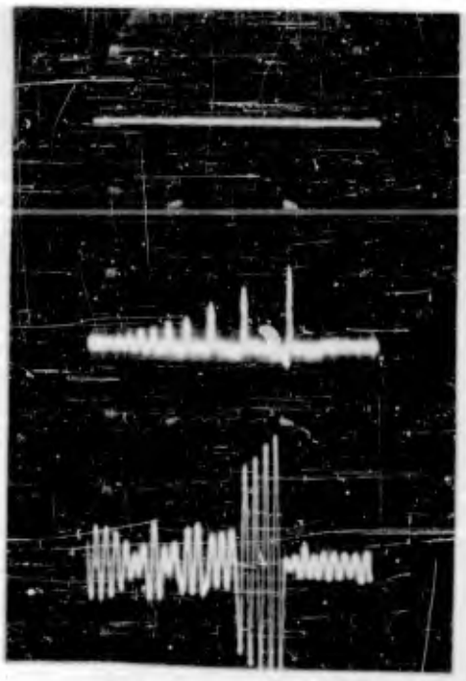

5" Drop - Q = 40
Upper Trace: Input Accel; 24g Max.
Lower Trace: Response Acceleration

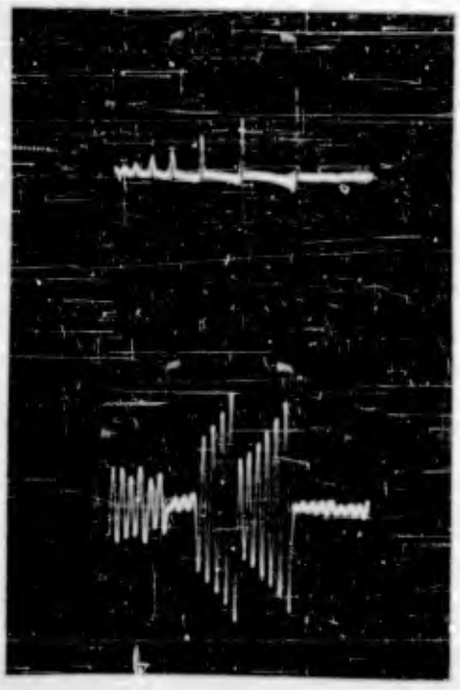

10" Drop - Q = 20
Upper Trace: Input Accel; 28g Max.
Lower Trace: Response Acceleration

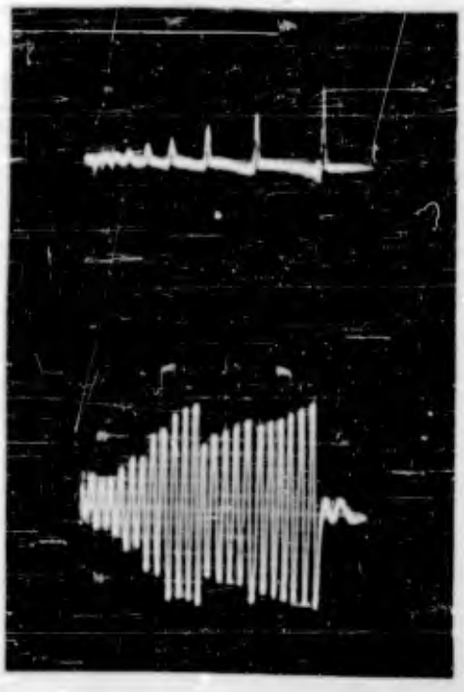

10" Drop - Q = 40
Upper Trace: Input Accel; 28g Max.
Lower Trace: Response Acceleration

TABLE IX

Summary of Stress Reversals During Drop Test - 5 Inch Drop

Q = 20

Number of Stress Reversals	Amplitude Acceleration	Stress/"g"	Stress, psi
1 cycle	30g	@ 2440 psi =	73,300
1 cycle	26g	@ 2440 psi =	63,500
1 cycle	22g	@ 2440 psi =	53,600
2 cycles	16g	@ 2440 psi =	39,000
1 cycle	14g	@ 2440 psi =	34,200

Q = 40

Number of Stress Reversals	Amplitude Acceleration	Stress/"g"	Stress, psi
1 cycle	33g	@ 2440 psi =	80,500
1 cycle	30g	@ 2440 psi =	73,300
1 cycle	28g	@ 2440 psi =	68,400
1 cycle	24g	@ 2440 psi =	58,500
1 cycle	17g	@ 2440 psi =	41,500
1 cycle	16g	@ 2440 psi =	39,000
4 cycles	13g	@ 2440 psi =	31,800

TABLE X

Summary of Stress Reversals During Drop Test - 10 inch Drop

Q = 20

Number of Stress Reversals	Amplitude Accleration	Stress/"g"	Stress, psi
2 cycles	31g	@ 2440 psi =	75,600
2 cycles	25g	@ 2440 psi =	61,000
2 cycles	21g	@ 2440 psi =	51,200
2 cycles	17g	@ 2440 psi =	41,500
1 cycle	14g	@ 2440 psi =	34,200
5 cycles	10g	@ 2440 psi =	24,400

Q = 40

Number of Stress Reversals	Amplitude Acceleration	Stress/"g"	Stress, psi
1 cycle	37g	@ 2440 psi =	90,300
1 cycle	35g	@ 2440 psi =	85,500
2 cycles	30g	@ 2440 psi =	73,300
2 cycles	25g	@ 2440 psi =	61,000
2 cycles	21g	@ 2440 psi =	51,200
1 cycle	19g	@ 2440 psi =	46,400
1 cycle	16g	@ 2440 psi =	39,000
3 cycles	12g	@ 2440 psi =	29,300
3 cycles	10g	@ 2440 psi =	24,400

TABLE XI

Summary of Cycles to Failure at Noted Stresses

Maximum Stress psi	Cycles to Failure	Reciprocal of Cycles to Failure, x 10^4
90,300	2.03×10^4	0.493
85,500	2.17×10^4	0.460
80,500	2.44×10^4	0.410
75,600	3.25×10^4	0.308
73,300	4.30×10^4	0.233
68,400	11.0×10^4	0.091

the number of cycles to failure are also included in Table XI. Taking the average value of $\underline{D}'$ from Tables VII and VIII for the 5 inch and 10 inch drops, respectively, values are computed for the constant $\underline{K}$ as follows for the four different test conditions:

5" Drop - $\underline{Q}$ = 20

$$\underline{K} = 3806\ (1 \times 0.233) \times 10^{-4} = \underline{0.0886}$$

5" Drop - $\underline{Q}$ = 40

$$\underline{K} = 3806\ (1 \times 0.091 + 1 \times 0.233 + 1 \times 0.410\ ) \times 10^{-4} = \underline{0.280}$$

10" Drop - $\underline{Q}$ = 20

$$\underline{K} = 2490\ (1 \times 0.308) \times 10^{-4} = \underline{0.0765}$$

10" Drop - $\underline{Q}$ = 40

$$\underline{K} = 2490\ (1 \times 0.493 + 1 \times 0.460 + 2 \times 0.233) \times 10^{-4} = \underline{0.353}$$

In evaluating the above computation, it must be recognized that the damping capacity of the beam varies as the maximum stress varies. As a consequence, it is not possible to select a single value for $\underline{Q}$ which remains applicable throughout a test wherein the maximum stress fluctuates from cycle to cycle. Reference to Figure 34 indicates, however, that the value of $\underline{Q}$ lies generally between 35 and 45 for the stress levels at which the greatest damage apparently occurs. It is thus concluded that a value $\underline{Q}$ = 40 is more representative for the present investigation. For this value of damping capacity and for the 5 inch and 10 inch drops as computed above, it is noted that the value for the constant $\underline{K}$ is computed as 0.280 and 0.353. This suggests tentatively that a value $\underline{K}$ = 0.3 is the appropriate value to use with Miner's equation, included in this report as equations (24) and (25), when the maximum stress tends to vary in a random manner from cycle to cycle. As pointed out above, Miner initially suggested that $\underline{K}$ = 1, but subsequent investigators have shown that $\underline{K}$ can be substantially greater than or substantially less than unity. Few values of $\underline{K}$ have been as low as 0.3, thus suggesting that the current conditions tend to be unusual, or that the present data are not sufficient to establish a value for $\underline{K}$. It is tentatively concluded on the basis of the limited investigation described above that the Miner theory of cumulative damage in fatigue is applicable to

an analysis of a shock-excited structure, provided an appropriate value can be established for the constant K. It is conceded that the investigation described in the preceding pages would provide a rather tenuous basis upon which to define a value of Miner's constant K. Consequently, in the analysis that follows and the application of Miner's equation, the value of K = 1 will be utilized. It is considered that an extremely worthwhile future investigation would include studies and experimental tests similar to that reported in the preceding pages with the objective being to determine appropriate values for the constant K.

SECTION XI

CONCEPT OF RESPONSE SURFACE TO EVALUATE SHOCK

Adopting the analogy between stress and acceleration (see page 23), the hypothesis is presented that the ability of elastic members to withstand transient vibration may be determined by counting the number of cycles at each acceleration level embodied in the response and applying the theory formulated by Miner. It is convenient now to adopt a procedure for describing the response acceleration of many elements having different natural frequencies, the excitation or input being a single record setting forth acceleration as a function of time. The three parameters which define the response are the natural frequency f_n of the element, the acceleration amplitude $\ddot{y}_o$ embodied in the response, and the number of cycles n at each response acceleration amplitude. These three parameters may be combined to define the response surface illustrated in Figure 39. This surface describes the response of many systems of different natural frequencies to a single input acceleration and should not be confused with the failure surface for steady vibration set forth in Figure 10.

To illustrate the nature of the surface shown in Figure 39, a number of planes are indicated for various elements having discrete natural frequencies f_n', f_n'' and f_n'''. To determine whether failure of one of these elements is likely to occur, the plane is compared with the endurance curve set forth in Figure 31. This requires that the relation between S and $\ddot{y}_o$ be established, as pointed out previously. Applications of Miner's hypothesis to this comparison, in a manner to be hereinafter described, will predict the expected life of each element whose natural frequency is known and for which there is a response surface as illustrated in Figure 39.

An equipment may be considered to consist of an assembly of component structures, each with its own characteristics, and to be defined if the characteristics of the component structures are defined. For purposes of idealizing the equipment, each structure may be assumed to be a single-degree-of-freedom system with linear elasticity and damping. Each system may then be defined in terms of its natural frequency and its damping capacity. The natural frequency is commonly expressed in cycles per second, and the damping capacity may be expressed in terms of a dimensionless damping parameter Q which indicates the maximum transmissibility at resonance during a condition of steady-state vibration.

The three dimensional response surface shown in Figure 39 is better adapted to qualitative than quantitative presentation.

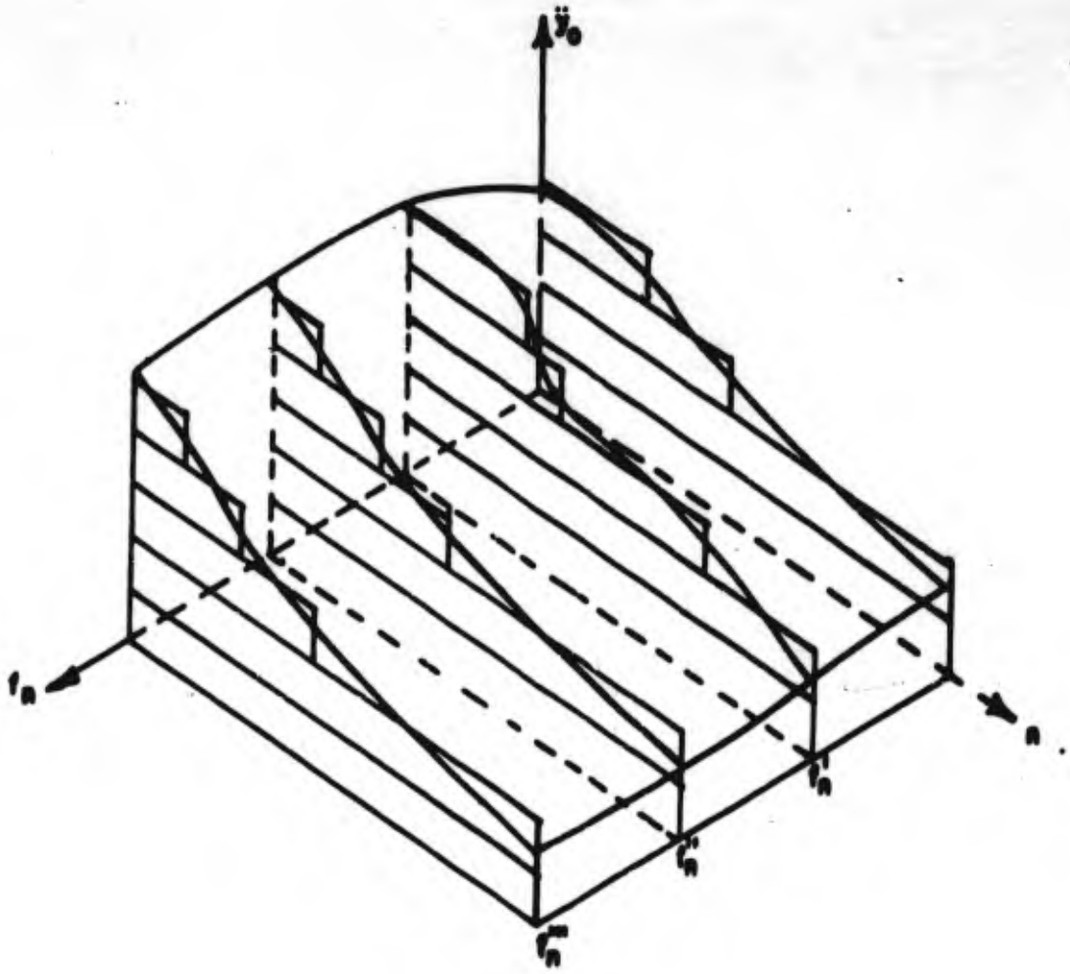

FIGURE 39. TYPICAL RESPONSE SURFACE.

Numerical data can be recorded more conveniently in two dimensional plots of response acceleration amplitude as a function of number of occurrences, one plot being drawn for each discrete value of natural frequency f_n and damping parameter Q. To facilitate the counting of occurrences, it is convenient to establish discrete increments of response acceleration amplitude $\ddot{y}_o$, preferably integral or integral fractional values of the acceleration due to gravity. The results may then be presented numerically in block diagram form, as illustrated in Figure 40 for one particular value of natural frequency and damping parameter. Several block diagrams for different natural frequencies but one damping parameter combine to form the response surface shown in Figure 39. Where different values of the damping parameter Q are involved, a discrete response surface exists for each value of Q.

A number of oscillograms showing the time history of acceleration as measured on aircraft during landing and other shock conditions have been made available to Contractor. Several of these oscillograms have been selected for analysis. The criteria used in selecting the oscillograms were (1) that they embody apparently the most severe conditions among the oscillograms available and (2) that the characteristics of the selected oscillograms be as diverse as possible so that the group selected would represent all possible varieties of shock motions. The selected oscillograms are reproduced as insets to the various Figures in Appendix III. More recent oscillograms have been received which indicate more severe conditions than those referred to in Appendix III. Although the oscillograms of Appendix III are used in the following pages to illustrate the concept of a failure surface, the more recent oscillograms are employed in later sections to define the requirements of a laboratory shock test.

The analysis made on these selected oscillograms includes the determination by electrical analogy of the response acceleration of simple systems having a range of natural frequencies and damping parameters. The results obtained are of the type set forth in Figure 30, wherein the time history of the response acceleration of each system is recorded. The response accelerations are recorded on block diagrams on which response acceleration amplitude $\ddot{y}_o$ is plotted as a function of number of occurrences, as shown in Figure 40 for a typical case. The parameter b in Figure 40 may be an integer or a fraction. Appendix III to this report includes data on the oscillograms selected, together with block diagrams showing response acceleration amplitude as a function of a number of occurrences for each oscillogram. A block diagram is included for each value of natural frequency f_n and damping parameter Q.

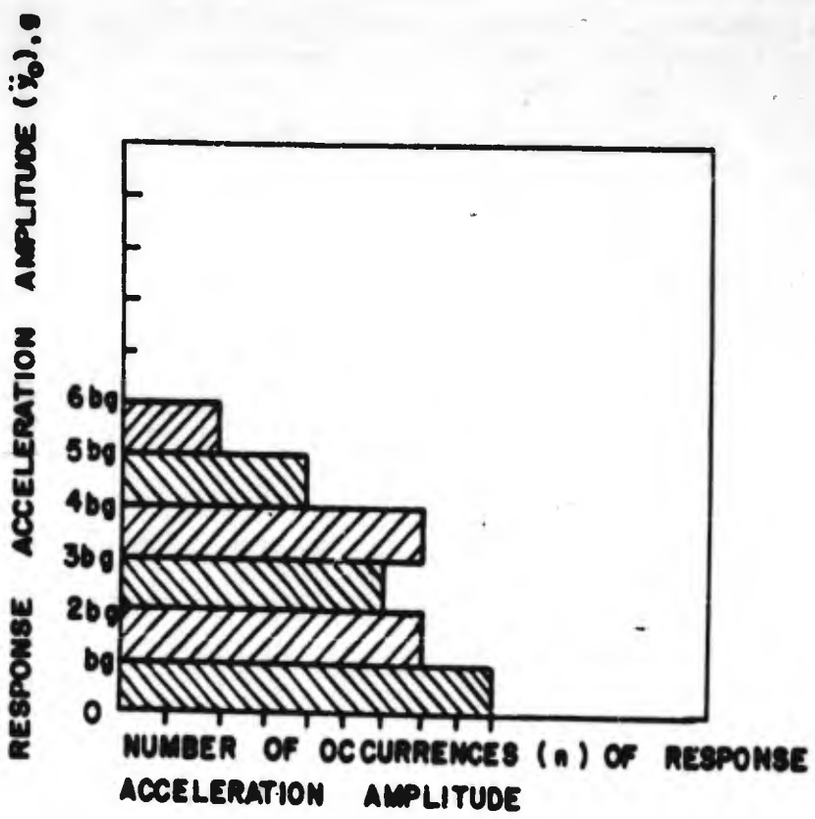

FIGURE 40 TYPICAL BLOCK DIAGRAM SHOWING RESPONSE ACCELERATION AMPLITUDE AS A FUNCTION OF NUMBER OF OCCURRENCES FOR A DISCRETE VALUE OF NATURAL FREQUENCY AND DAMPING PARAMETER.

In equations (24) and (25) representing the Miner theory of cumulative fatigue damage, N is the number of cycles to failure obtained from the conventional stress-cycle curve. For stresses below the endurance limit of the material, N is equal to infinity, and the corresponding term drops out of the equation. The typical stress-cycle curve can be idealized as shown in Figure 41 by introducing the following considerations mentioned previously:

(a) The stress-cycle curve is idealized as a horizontal line for values of N less than 10^3 and greater than 5×10^6, and a straight inclined line between these values of N, when plotted on log-log paper. The ordinate at $N = 5 \times 10^6$ is 38 percent of the ordinate at $N = 10^3$. The basis for this idealization is explained on page 28 in connection with Figure 12.

(b) By analogy between stress in the structure and response acceleration, as discussed on page 99, the dimensions of the ordinate may be changed to response acceleration amplitude. The numerical relation between maximum stress and response acceleration amplitude remains undetermined at this time to be established later.

This report develops the thesis that a shock is defined, not be parameters which are determined by measuring the environment, but rather by the responses of ideal systems to the shock motion defined by these measured parameters. Under this thesis, each shock is defined by a series of response surfaces of the type illustrated in Figure 39, there being one surface for each value of the damping parameter Q. If several shock motions are being compared, the general level of the several surfaces, the value of Q being maintained constant, indicates the relative severity of the respective shock motions. A peak in a response surface at a particular value of natural frequency f_n generally indicates that the shock motion includes a pronounced vibration at a frequency corresponding to the peak in the response surface. Inasmuch as different shock motions generally embody different frequencies, the response surfaces for these shock motions tend to intersect because the peaks occur at different frequencies. In other words, the peaks of one response surface may be aligned vertically with the valleys of another response surface. An envelope of the most severe conditions representative of all shock motions being considered is a resultant response surface drawn through the peaks of the individual response surfaces, all such surfaces being for the same value of damping parameter Q. A resultant response surface is thus obtained for each discrete value of damping parameter Q.

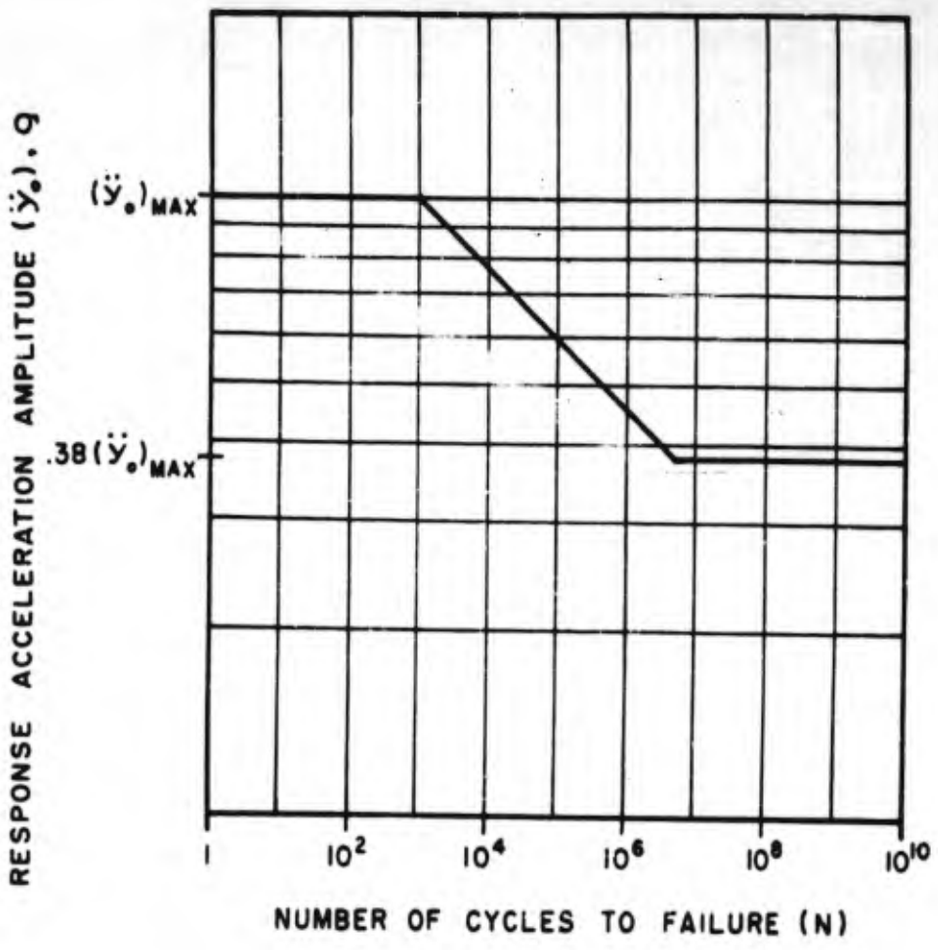

FIGURE 41. IDEALIZED CURVE OF RESPONSE ACCELERATION AMPLITUDE AS A FUNCTION OF NUMBER OF CYCLES TO FAILURE

One of the primary problems in the establishment of a laboratory test to simulate transient environmental conditions is the selection of the most severe environment for use as a basis of simulation. As shown by the block diagrams in Appendix III, certain of the shock motions excite the greatest response at one frequency, while others of the shock motions excite the greatest response at a different frequency. An effective laboratory test must take cognizance of the most severe conditions in general, as defined by the resultant response surface for the series of operating conditions under consideration. This surface may be represented in block diagram form, as shown in Figure 42 for all of the shock motions included in Appendix III. The data in Figure 42 were obtained by first obtaining block diagrams similar to Figure 40 for each value of natural frequency and damping parameter for each of the shock motions being considered. These block diagrams comprise Appendix III. The resultant block diagrams in Figure 42 are plotted by taking the largest number of occurrences from Appendix III for the respective values of natural frequency and damping parameter. The blocks were omitted for small values of $\ddot{y}_o$ because they do not contribute to damage as a result of fatigue.

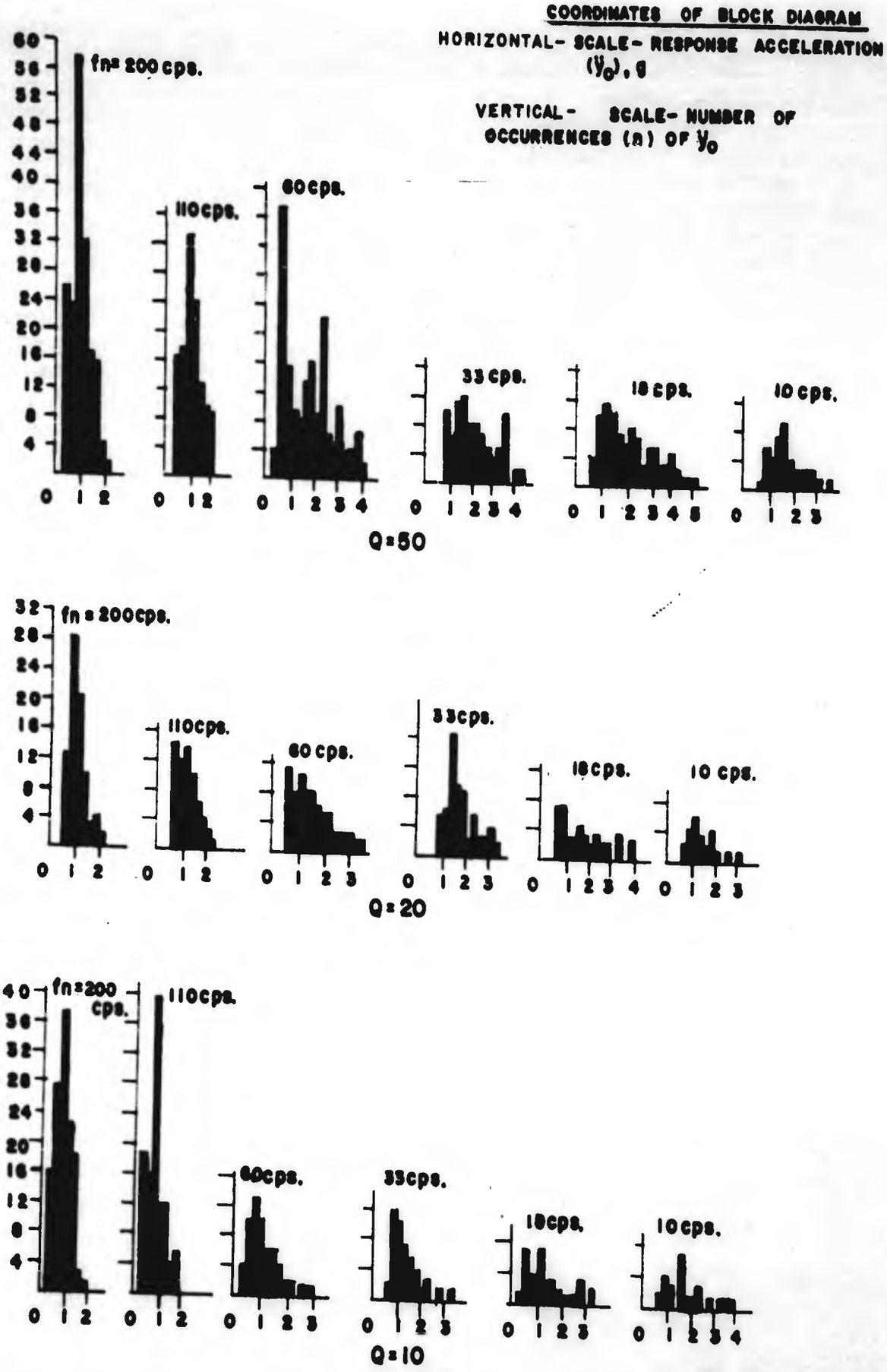

FIGURE 42. RESULTANT BLOCK DIAGRAMS FOR SIX LANDINGS SHOCKS AND SYSTEMS HAVING Q =10,20,50

SECTION XII

REQUIREMENTS FOR A LABORATORY SHOCK TEST

The problem of devising a laboratory shock test to simulate the most severe landing conditions, as defined by the resultant block diagrams in Figure 42, may now be approached. The block diagrams in Figure 42 represent the number of occurrences of response acceleration amplitude Y_o in one landing. An equivalent shock test would have a similar block diagram provided it were desirable to make the number of applications of shock in the laboratory test equal the number of landings experienced by the airplane during its life. In general, this is not a practical requirement inasmuch as the laboratory test should embody fewer applications of shock. Re-examining the Miner hypothesis for cumulative damage in fatigue and assuming that Figure 42 represents a single landing, equations (24) and (25) which refer to cumulative damage in fatigue may be written as follows to define conditions of failure:

$$D\left(\frac{n_1}{N_1} + \frac{n_2}{N_2} + \frac{n_3}{N_3} + \ldots\right) = 1 \qquad (31)$$

where D represents the number of landings in the life of the aircraft and n represents the number of occurrences per landing of each response acceleration amplitude, as indicated in Figure 42. Equation (31) is evaluated for each discrete value of natural frequency and damping ratio. Applying a similar analysis to block diagrams which can be obtained from laboratory records, the same structure may be considered to experience failure during the shock test when

$$D'\left(\frac{n'_1}{N'_1} + \frac{n'_2}{N'_2} + \frac{n'_3}{N'_3} + \ldots\right) = 1 \qquad (32)$$

where D' represents the number of repetitions of the laboratory shock test and values of n' are obtained from block diagrams similar to Figure 42. These block diagrams are obtained by analyzing an oscillogram of acceleration as a function of time as measured on the shock testing machine, using the analog computer to determine the response acceleration amplitudes of simple systems as previously described.

To determine the relation between the resultant response surface for the landing shocks and the response surface for the laboratory shock, it is necessary to establish the relation between the values of N in equation (31) and the corresponding response acceleration amplitude. This was left undetermined when numerical values on the scale of response acceleration

amplitude in Figure 41 were omitted. The required relation is now determined by evaluating equation (31) by a cut-and-try procedure to obtain a numerical value for $(\ddot{Y}_o)$ max in Figure 41.

To evaluate equation (31), it is necessary that numerical values be available for parameters D, n, and N. Values of n and $\ddot{Y}_o$ are known from the resultant block diagrams of Figure 42. The values of N cannot be determined unless numerical values are assigned to the ordinate scale; i.e., unless $(\ddot{Y}_o)$ max is known quantitatively. Numerical values are first assumed for D and for $(\ddot{Y}_o)$ max, thus making it possible to determine N from Figure 41. Using this value of N and the assumed value for D, the left hand side of equation (31) is evaluated numerically. If the result is less than unity, a lower value is assumed for $(\ddot{Y}_o)$ max and the calculation repeated. If the result is greater than unity, a higher value is assumed for $(\ddot{Y}_o)$ max. This process is continued until the left hand side of equation (31) is made equal to unity.

The value assumed for the parameter D depends upon operating conditions. This parameter represents, for example, the number of landings that an aircraft experiences during its life. To investigate the effect that the value of D has upon the result, numerical values of 10,000 and 50,000 respectively, were assumed for D. Equation (31) was then evaluated for each of these assumed values for D, and values of $(\ddot{Y}_o)$ max as a function of frequency were calculated as shown in Figure 43. This result is obtained from the resultant block diagram of Figure 42 for a value of $Q = 20$. It is evident from Figure 43 that the resulting value of $(\ddot{Y}_o)$ max is substantially independent of the value assumed for the parameter D within a reasonable range. In view of this result, all subsequent calculations of this type assume a value $D = 50{,}000$ for the purpose of evaluating equation (31).

The curve of maximum response acceleration amplitude $(\ddot{Y}_o)$ max as a function of frequency, shown in Figure 43 is the intersection of any plane at $n_t = 10^5$ with the minimum acceptable response surface for the shock being analyzed. By definition, $n_t = Dn$. The complete surface is shown in Figure 44. In creating this minimum acceptable response surface, it is assumed that the intersection of the surface with any plane parallel to the $\ddot{Y}_o - f_n$ plane has a shape geometrically similar to Figure 43 but wherein the ordinates are a function of the particular value of n. On the other hand, the intersection of the minimum acceptable response surface with any plane parallel to the $\ddot{Y}_o - n_t$ plane consists of a

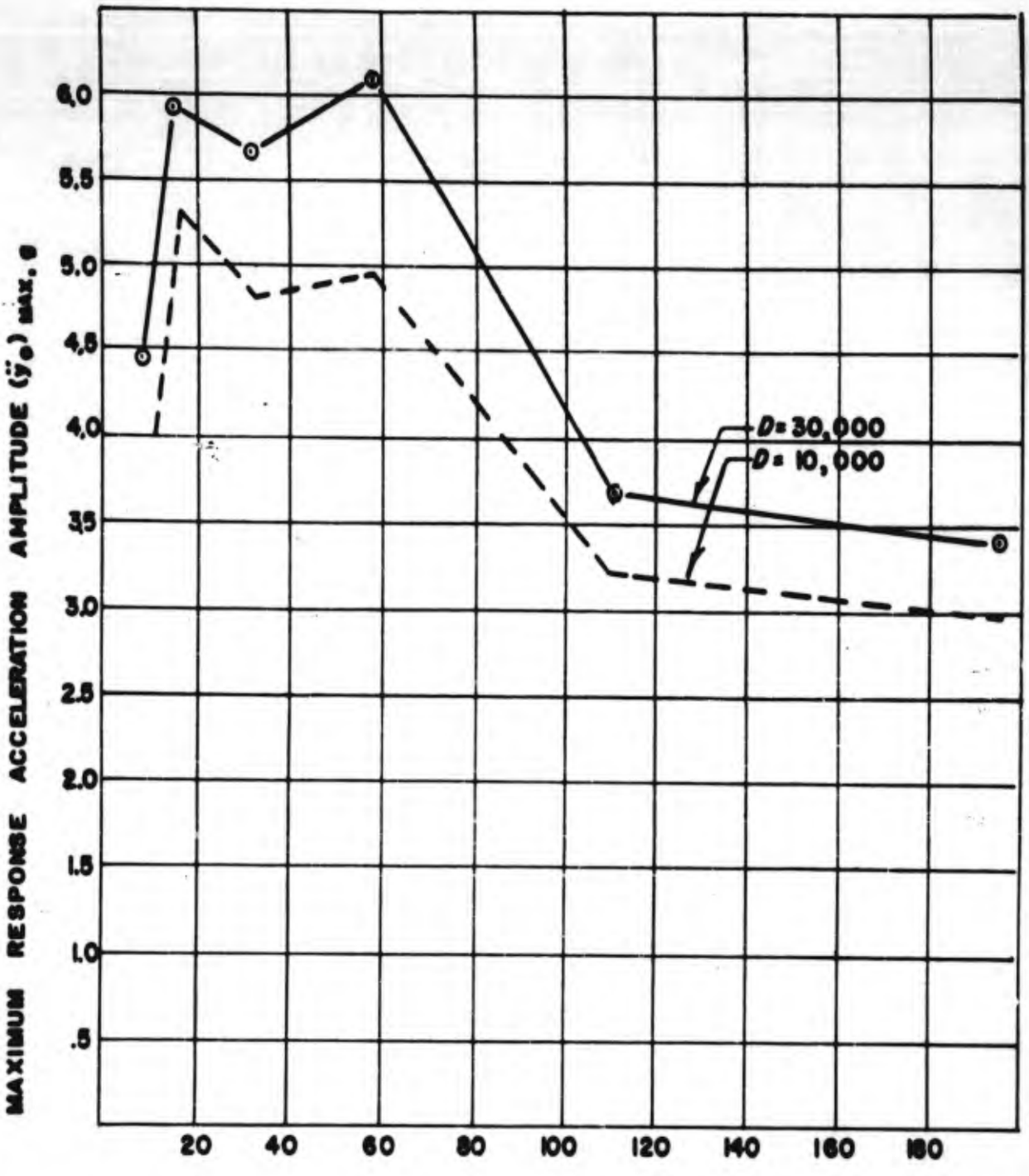

FIGURE 43. MAXIMUM RESPONSE ACCELERATION AMPLITUDE AS A FUNCTION OF NATURAL FREQUENCY FOR ASSUMED VALUES D = 10,000 AND 30,000. DAMPING PARAMETER Q = 20. THESE CURVES ARE INTERSECTION OF MINIMUM ACCEPTABLE RESPONSE SURFACE WITH PLANE $n_f = 10^3$ WHERE $n_f = D$ a.

straight, inclined line extending from $n_t = 10^3$ to $n_t = 5 \times 10^6$ and horizontally extending lines for smaller or larger values of n.

The minimum acceptable response surface illustrated in Figure 44 is very important in the consideration of transient vibration or shock being developed here. This surface may be designated as a surface of required strength for general aircraft use. If an equipment cannot withstand the indicated response acceleration amplitude $\ddot{y}_o$ for the number of cycles n_t set forth in Figure 44, it must be considered unsuitable for service. This condition must be met for any arbitrarily chosen value of n_t, and therefore may be used as a criterion to establish the validity of a laboratory test. A value of n_t, applicable to laboratory testing may be defined as $n_t = D'n'$. In this definition, D' is the number of repetitions of the laboratory test, and n' is obtained from a series of block diagrams similar to Figure 42 but representing an analysis of an oscillogram obtained from the shock testing machine. By assuming a value for a number of test repetitions D', a response surface $n_t - \ddot{y}_o - f_n$ may be superimposed upon the response surface shown in Figure 44. This response surface for laboratory tests will generally involve relatively small values for n_t, and must lie above the surface for the environment shown in Figure 44.

In the preceding discussion, the maximum environment was obtained by inspecting the individual block diagrams, and creating the resultant block diagrams of Figure 42. These resultant block diagrams represent the most severe environment, regardless of the source of shock, and were used to determine the curve of $(\ddot{y}_o)$ max shown in Figure 43. From this, the minimum acceptable response surface shown in Figure 44 was derived. An alternate approach to this problem involves the solution of equation (31) by cut-and-try methods for each individual landing shock, and the ultimate combining of the results to obtain an envelope of maximum values. The results of this analysis for six different landing shocks using $D = 30{,}000$ are shown by the values of $(\ddot{y}_o)$ max set forth on Figures 45 to 47 inclusive, for values of $Q = 10$, 20, and 50, respectively. It is evident from an inspection of these figures that one landing shock may be more severe with respect to systems of a certain natural frequency, while another landing shock may be more severe with respect to systems of other natural frequencies. An envelope encompassing the maximum response acceleration amplitudes at each natural frequency, regardless of landing shock, thus represents the most severe environment to be expected as a result of any landing. These envelopes are drawn in Figure 48 for values $Q = 10$, 20, and 50.

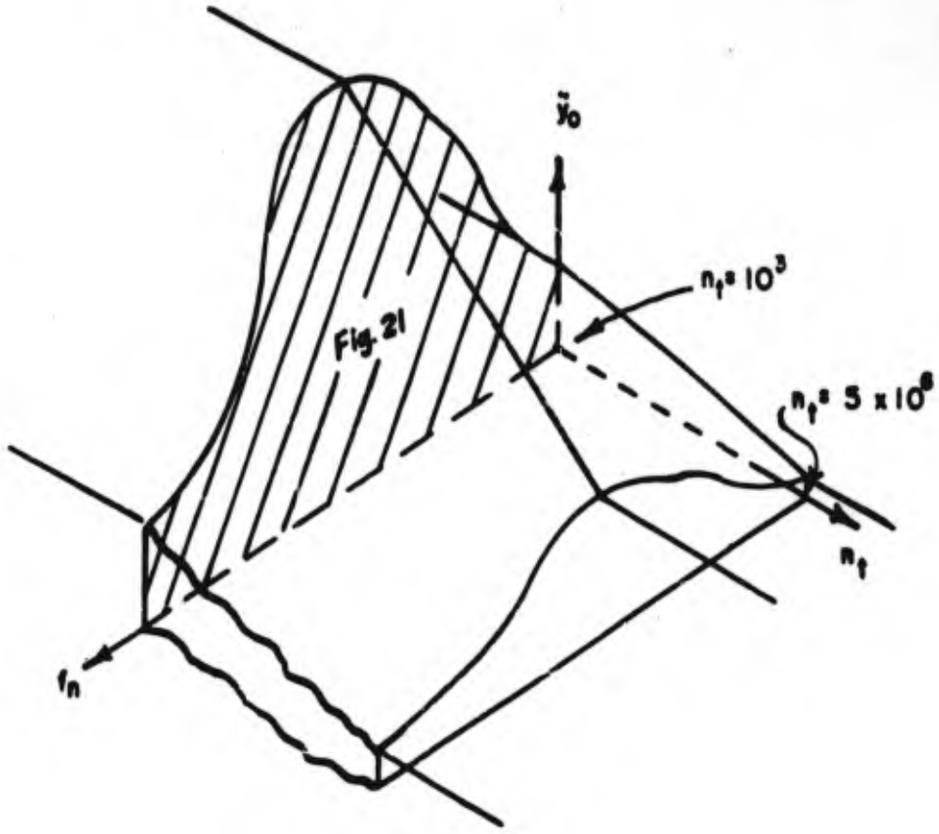

FIGURE 44. ILLUSTRATION OF TYPICAL MINIMUM ACCEPTABLE RESPONSE SURFACE.

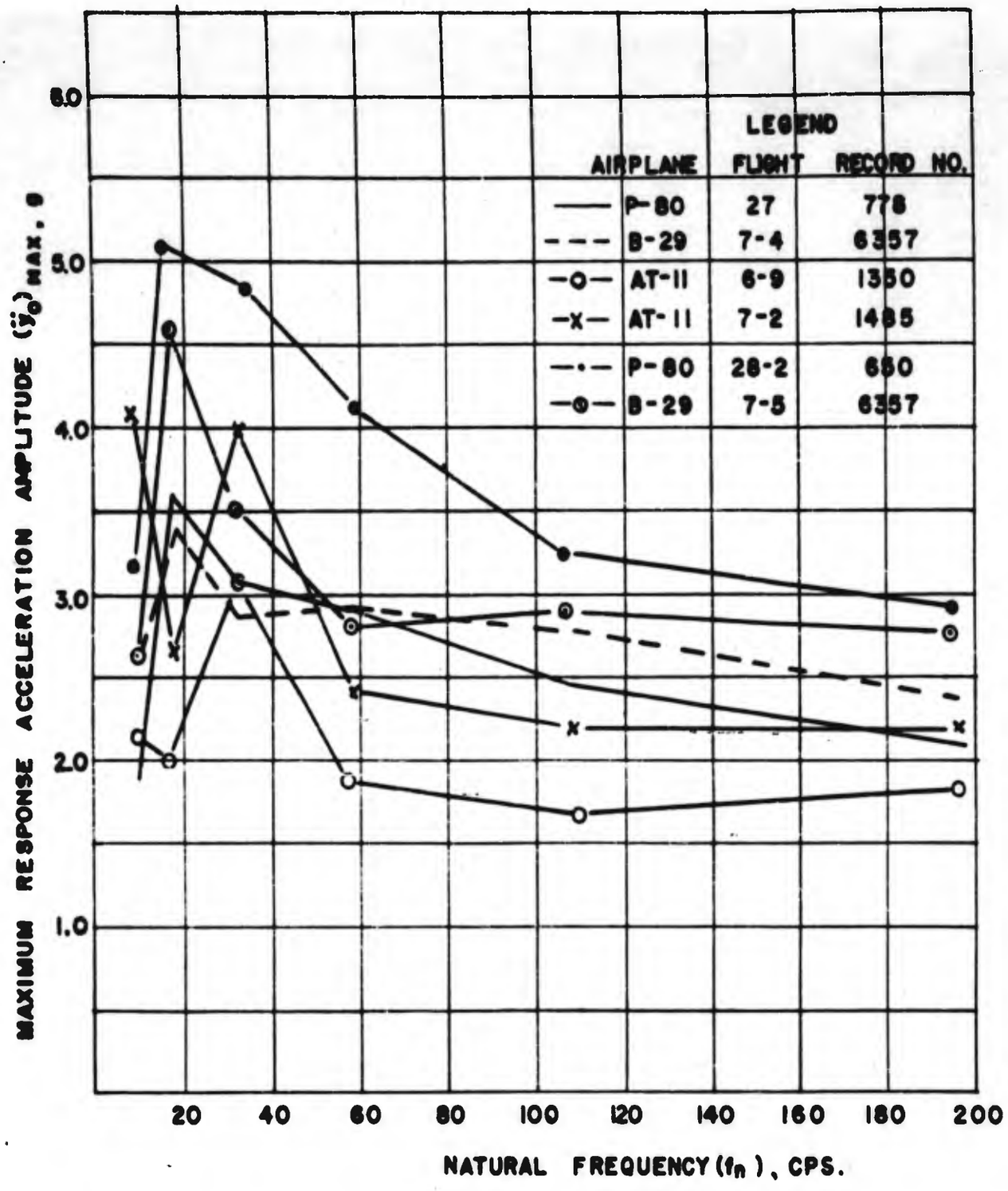

FIGURE 45 CURVES OF MAXIMUM RESPONSE ACCELERATION AMPLITUDE AS A FUNCTION OF NATURAL FREQUENCY FOR INDIVIDUAL LANDING SHOCKS WHEN $Q = 10$ AND $D = 30,000$

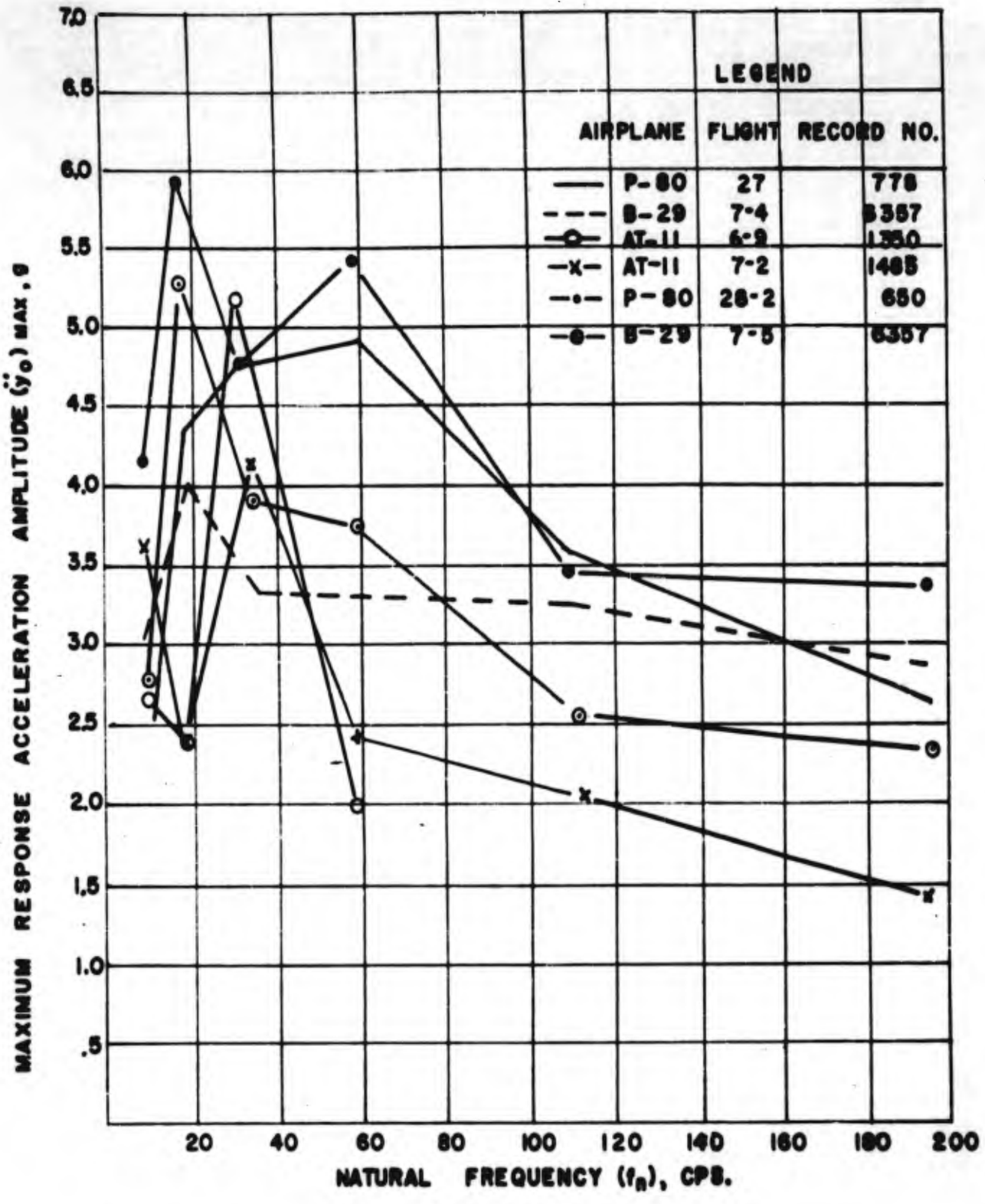

FIGURE 46. CURVES OF MAXIMUM RESPONSE ACCELERATION AMPLITUDE AS A FUNCTION OF NATURAL FREQUENCY FOR INDIVIDUAL LANDING SHOCKS WHEN $Q = 20$ AND $D = 30{,}000$

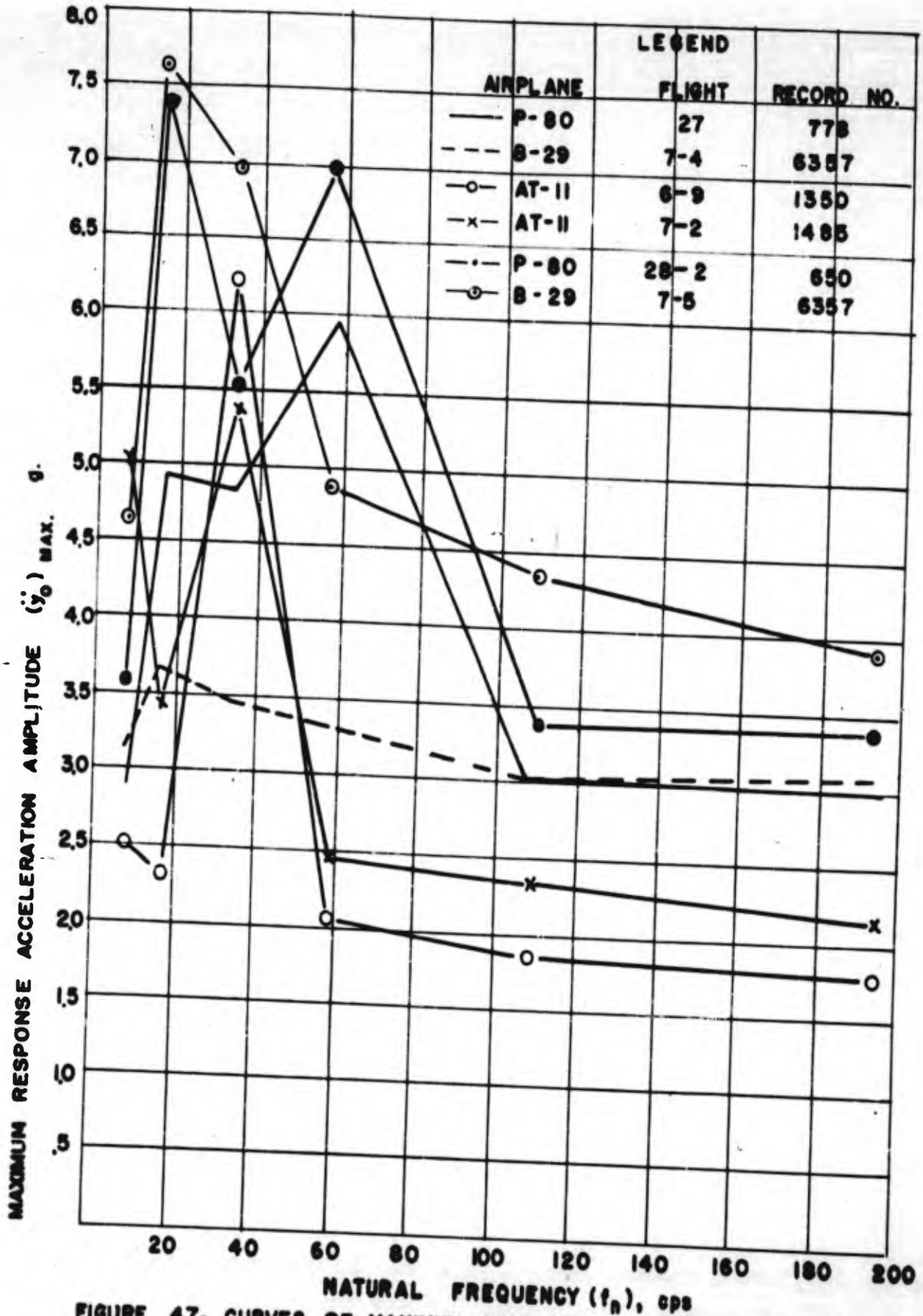

FIGURE 47. CURVES OF MAXIMUM RESPONSE ACCELERATION AS A FUNCTION OF NATURAL FREQUENCY FOR INDIVIDUAL LANDING SHOCKS WHEN $Q = 50$ AND $D = 30{,}000$.

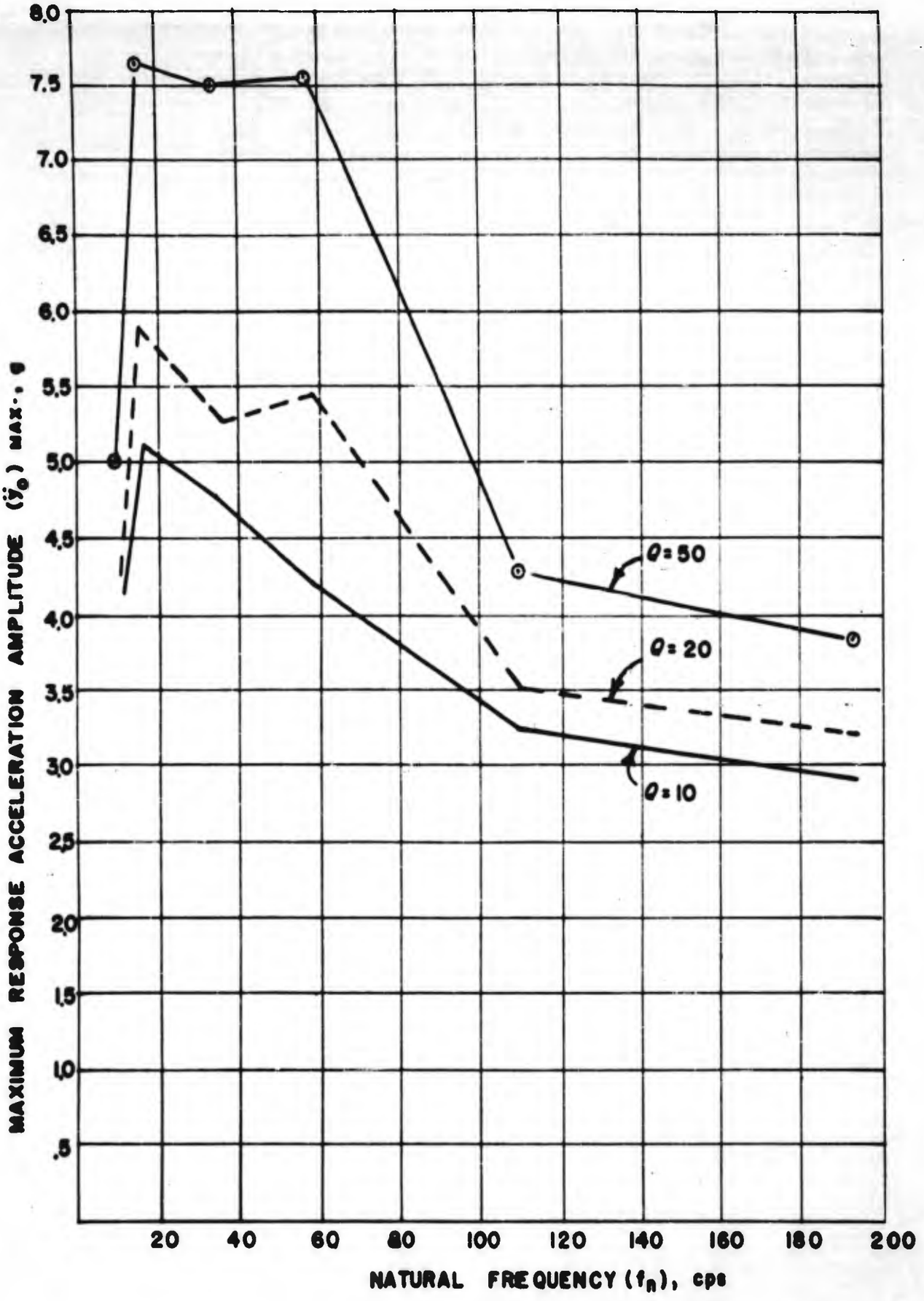

FIGURE 48. ENVELOPES OF CURVES OF ($\ddot{y}_0$) MAXIMUM IN FIGURES 45 TO 47 FOR VALUES Q = 10, 20 AND 50.

A comparison of the maximum response acceleration amplitude $(\ddot{Y}_o)$ max is shown in Figure 49 for the alternate methods of calculation, using the value $Q = 20$ for the damping Parameter. The solid line is reproduced from the curve for $D = 30{,}000$ in Figure 43, and is obtained by evaluating equation (31) directly from the resultant block diagram of Figure 42. The dotted line is the envelope of maximum response acceleration amplitude $(\ddot{Y}_o)$ max when $Q = 20$, for all landings investigated individually as shown in Figure 48. The agreement between the results obtained by these alternate methods is good, and justifies the less laborious procedure which uses the composite block diagram of Figure 42. The curves shown in Figure 49 will be identified here by the designation "cumulative damage criterion" to indicate that they include the effect of cumulative damage from many cycles of smaller stress. This is in contrast to the following analysis which neglects the cumulative effect and considers only the damaging effect of the cycles of stress having the greatest magnitude.

The inclusion of the effects of cumulative damage in the analysis becomes somewhat involved because of the need for evaluating equation (31) by cut-and-try methods. If only the effect of the cycle having greatest stress is considered, the responses may be shown as illustrated in Figures 50 to 52 where the ordinate is the maximum value of response acceleration $\ddot{Y}$ for each natural frequency, independent of number of occurrences. The designation "shock spectra" has received widespread acceptance to describe curves of the type set forth in Figures 50 to 52. Each of Figures 50 to 52 applies to a different value of Q, and each line on a particular figure refers to a different landing shock.

To show a comparison between the shock spectra of Figures 50 to 52 and the curves which consider cumulative damage, the envelope representing the maximum value of response acceleration shown in Figure 51 for $Q = 20$ is reproduced as Curve A in Figure 53. Inasmuch as $D = 30{,}000$ in the preceding calculation, it is assumed now that Curve A represents the maximum value of response acceleration $\ddot{Y}$ that must be endured for 30,000 landings. In the previous calculation, values were calculated for $(\ddot{Y}_o)$ max on the basis that $n_t = 1000$ cycles of stress reversal. On the same basis, a curve corresponding to Curve A but adjusted to 1,000 landings may be derived from Curve A by referring to equation (28) and computing the ratio of accelerations $\ddot{x}_o$ for a ratio of cycles N 30,000 to 1,000. This gives an acceleration ratio of 1.47. The ordinates of Curve A in Figure 53 are now multiplied by 1.47 to obtain Curve B. This curve represents the required response acceleration $\ddot{Y}$ assuming 1000 cycles of stress reversal, and may thus be compared with the results previously obtained

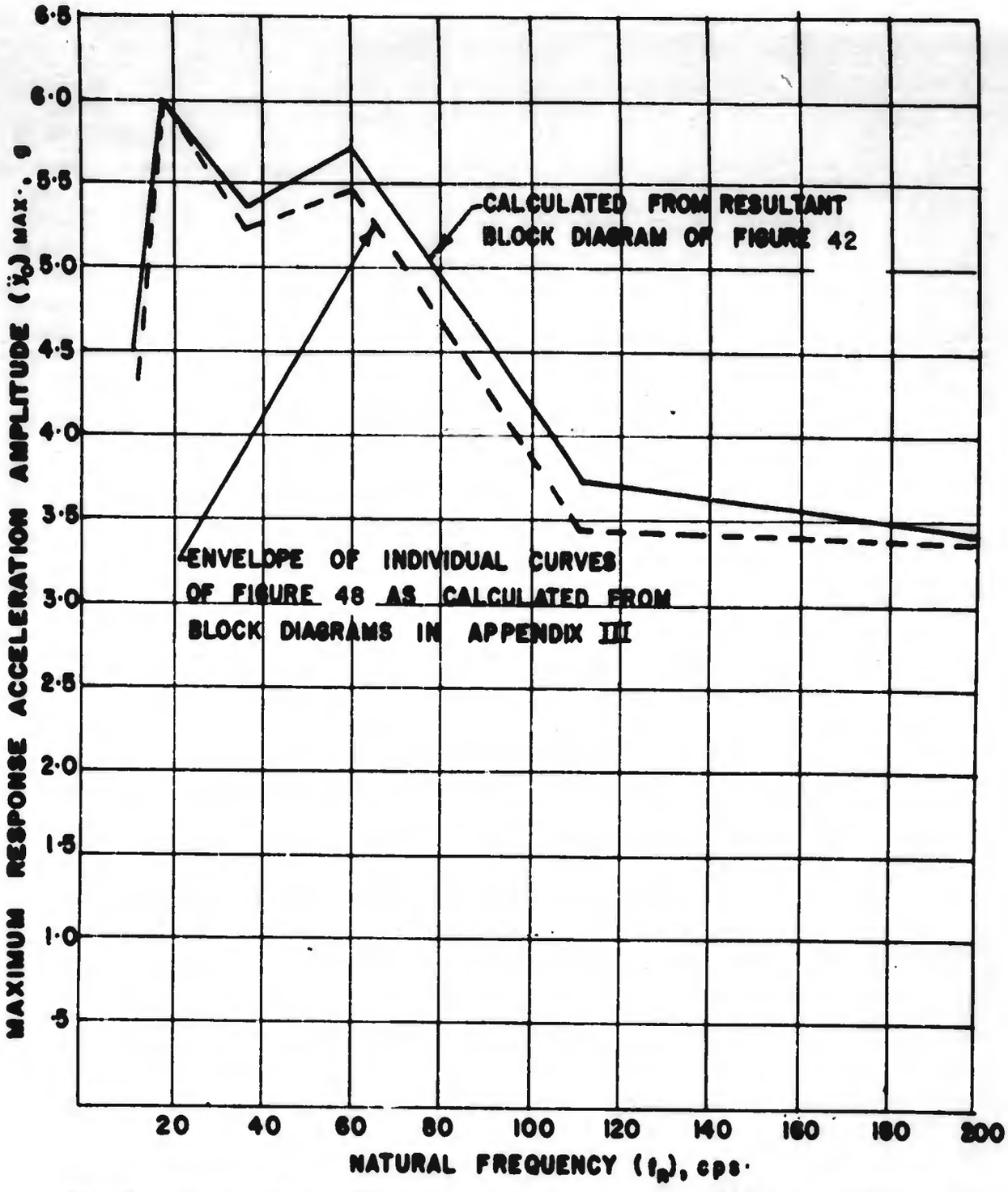

FIGURE 49. MAXIMUM RESPONSE ACCELERATION AMPLITUDE AS A FUNCTION OF NATURAL FREQUENCY FOR $Q = 20$, SHOWING COMPARISON OF RESULTS OBTAINED BY ALTERNATE METHODS OF CALCULATION.

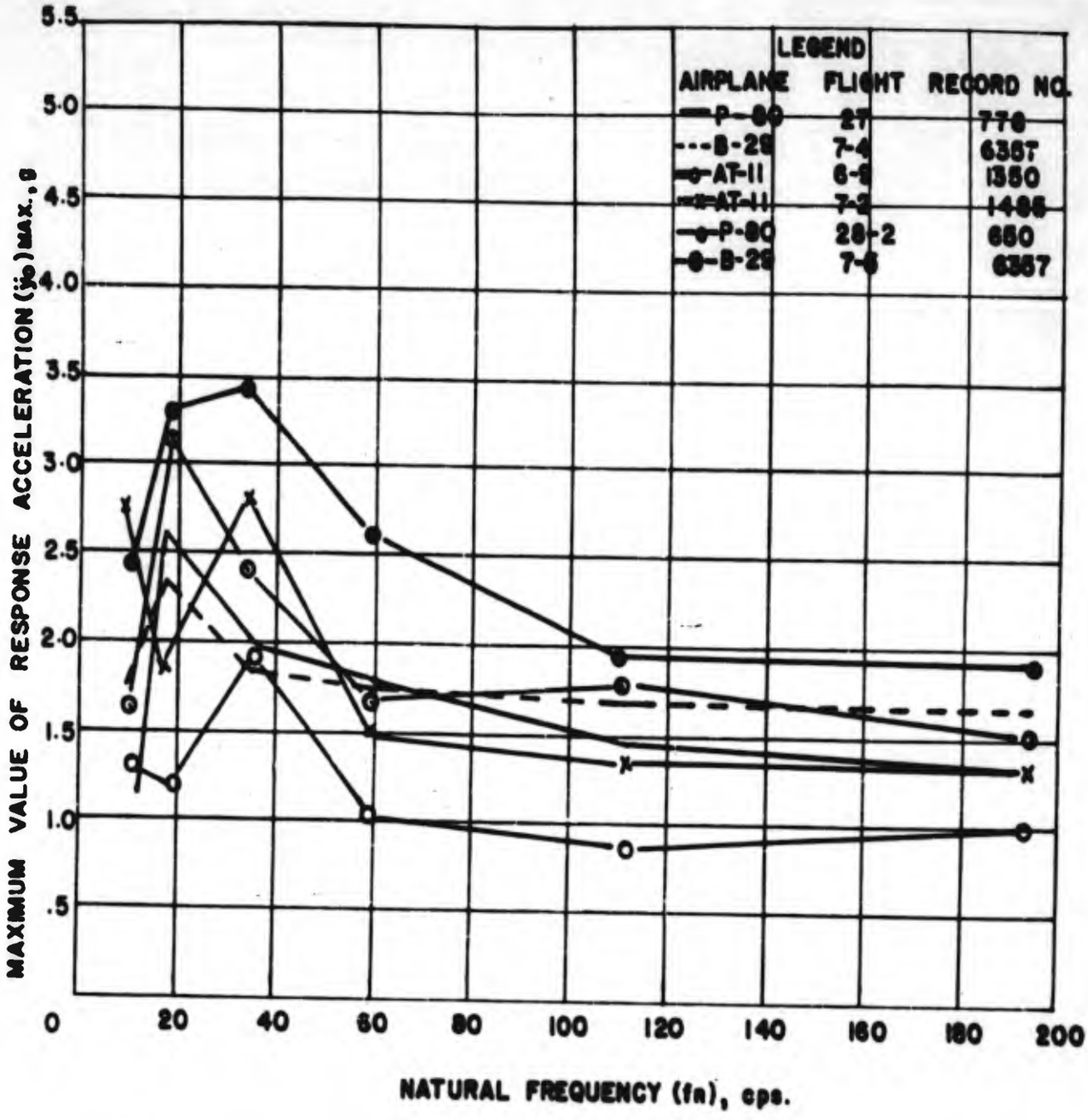

FIGURE 50. SHOCK SPECTRA FOR INDIVIDUAL LANDING RECORDS, $\zeta = .10$.

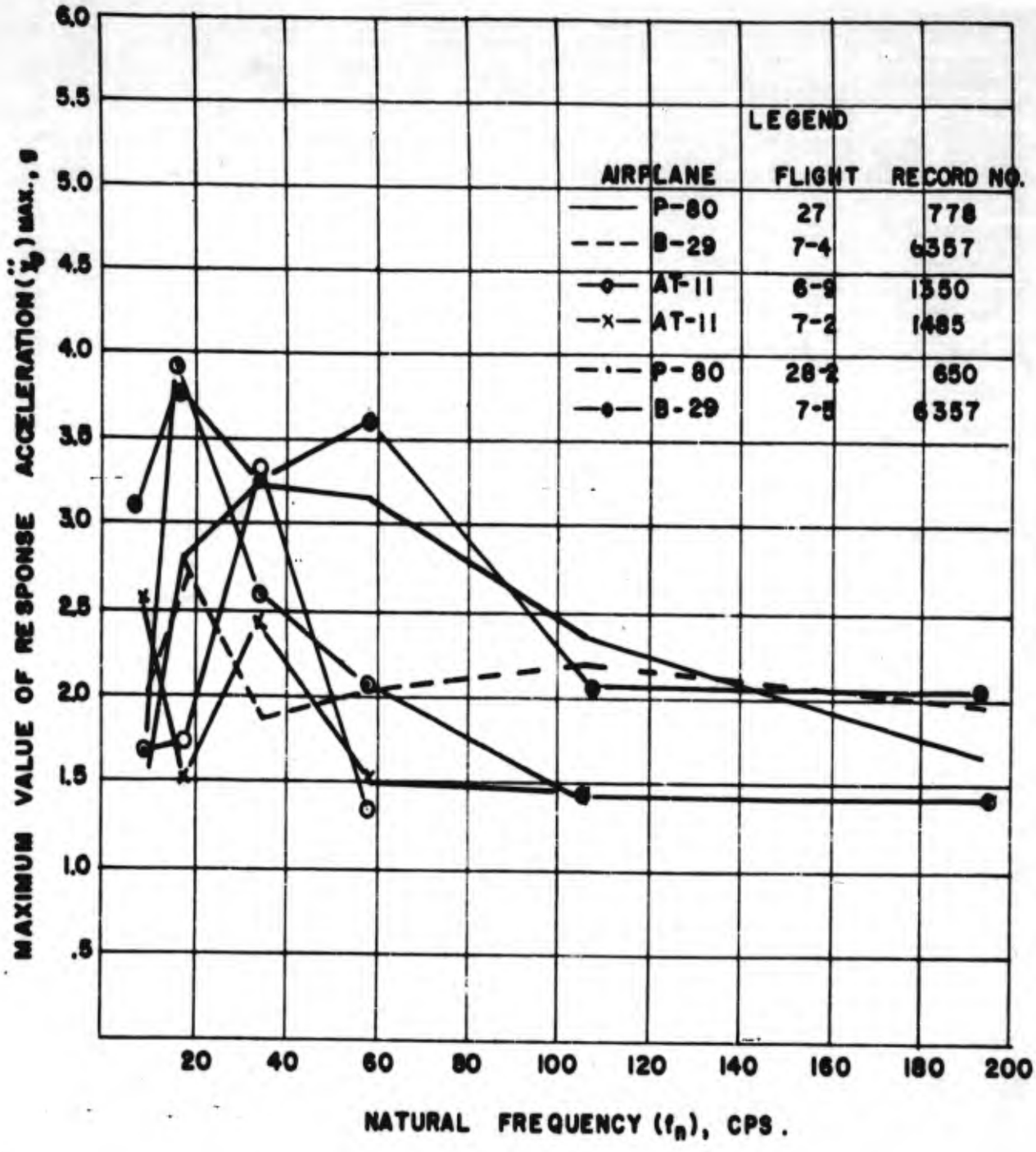

FIGURE 51. SHOCK SPECTRA FOR INDIVIDUAL LANDING RECORDS, $Q = 20$.

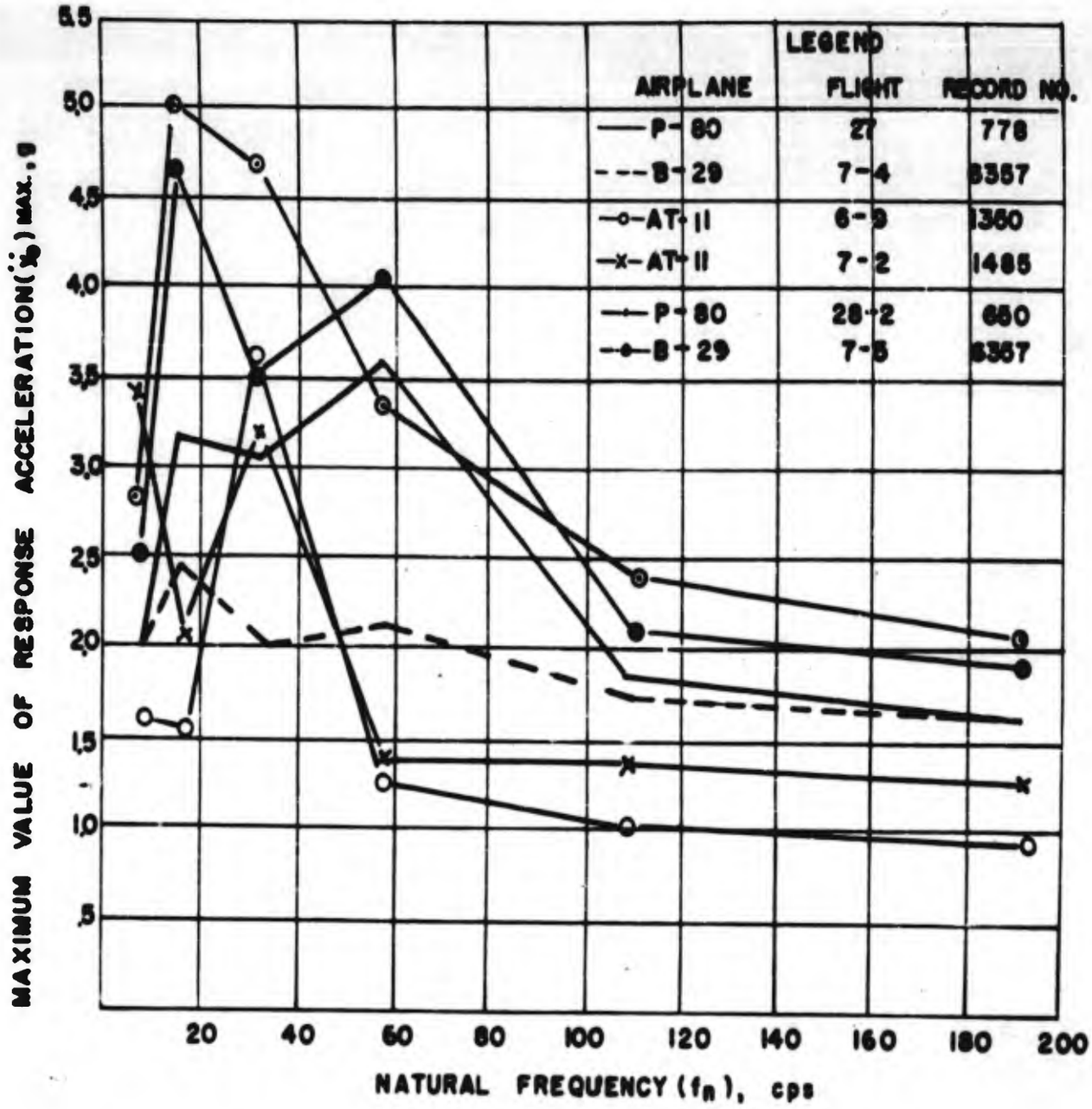

FIGURE 52. SHOCK SPECTRA FOR INDIVIDUAL LANDING RECORDS, Q = 50.

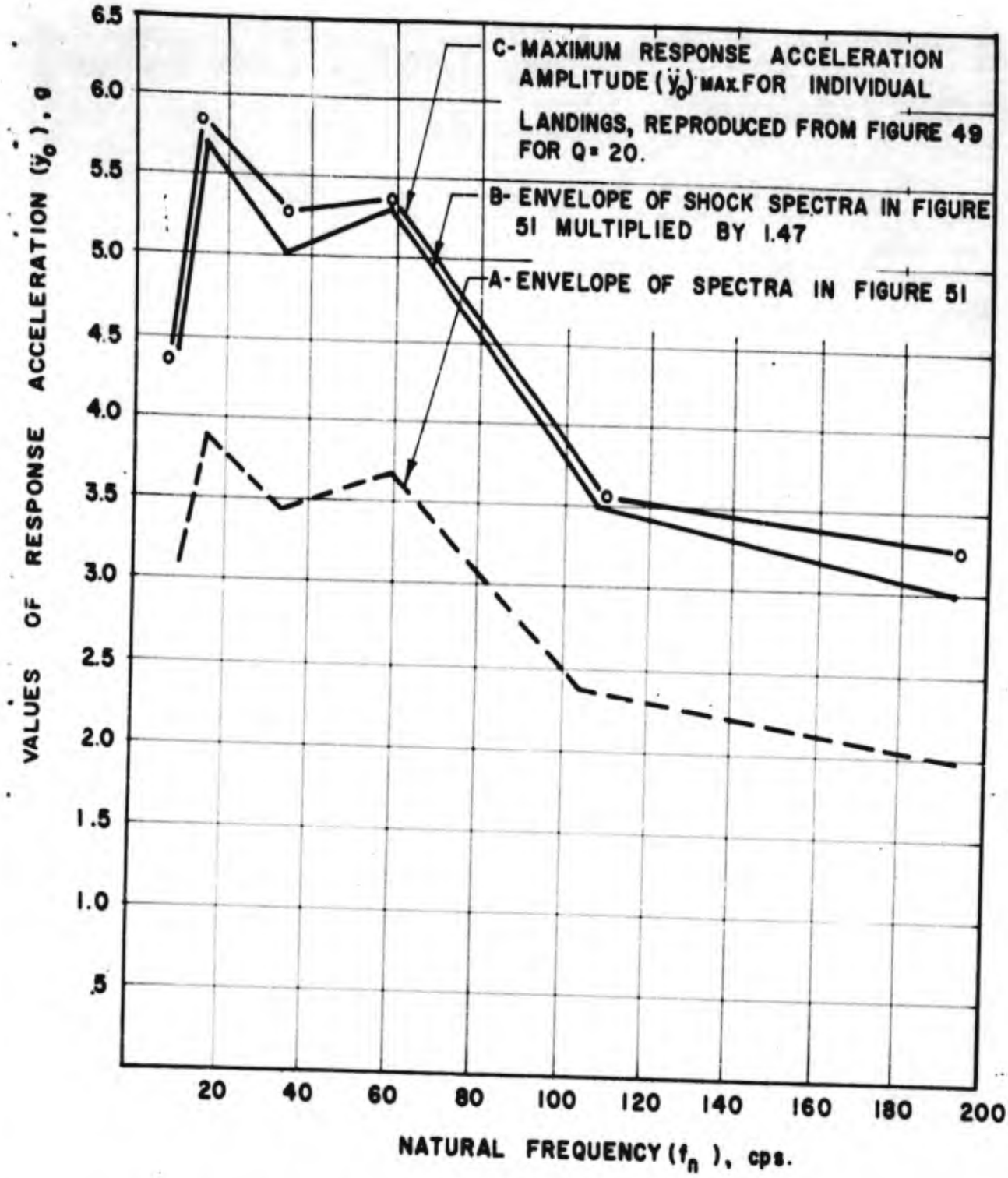

FIGURE 53. COMPARISON OF STRENGTH REQUIREMENTS AS CALCULATED FROM SHOCK SPECTRA AND CUMULATIVE DAMAGE THEORY.

considering the effect of cumulative damage. To facilitate this comparison, the dotted curve on Figure 49 is reproduced as curve C in Figure 53. The extent of the agreement between curves B and C in Figure 53 is an indication of the effect of cumulative damage in evaluating the damaging potential of repeated shocks. The spacing between these curves suggests that the cumulative effect of cycles of lower stress is not appreciable and not so great as to warrant the additional analytical time necessary to make the correction. This should not be construed as a generalization but only a tentative opinion on present conditions. A more complete investigation of this and other problems may lead to a different conclusion.

The minimum acceptable response surface shown in Figure 44 represents the required strength of any equipment which will be subjected to the landing shocks being analyzed here. It may be determined by any convenient analysis, as pointed out in the preceding discussion. Since one of the parameters of the surface is total number of stress reversals experienced by the equipment during its life, it is possible to devise a transformation from actual environment to laboratory conditions. The latter necessarily involves fewer cycles of stress reversal. An analysis based on laboratory testing conditions, however, must yield values of $\ddot{y}_o$ falling above the minimum acceptable response surface for appropriate values of f_n and n_t.

Following the hypothesis formulated by Miner to account for the effect of cumulative damage in fatigue, a shock test is suitable for qualifying equipment to withstand the shock represented by the minimum acceptable response surface shown in Figure 44 if it meets the following requirement:

$$D' \left(\sum \frac{n'}{N} \right) = 1 \qquad (33)$$

where D' represents the number of applications of shock during the test; n' represents the number of occurrences of various maximum values of acceleration response, and N is taken from Figure 41. Equation (33) is patterned after equation (31), and must be applied at each of several natural frequencies. Considerable discernment is necessary in establishing a suitable level for the shock test. It is important that D', the number of applications of shock, not be too great because the test then tends to become laborious. On the other hand, if D' is made too small, the required response acceleration tends to become unduly great and the assumption of linearity for the structure becomes invalid. In other words, referring to Figure 41, the part of the curve for $N < 10^3$ becomes applicable. The need for maintaining D' relatively great perhaps suggests that the shock testing machine should be of an automatically repeating type.

SECTION XIII

DEFINITION OF LANDING SHOCK SPECTRA FOR TESTING PURPOSES

The analysis in the preceding section indicated that, with a suitable correction factor, a shock spectrum could be obtained based upon the maximum envelope values obtained from individual landings which did not differ materially from the shock spectrum obtained when the cumulative damage concept was employed. Based upon the landing shock data available at the time of the analysis, Curve B of Figure 53 would be the shock spectrum selected for use in defining a laboratory shock testing procedure. However, more recent data acquired from the Aircraft Laboratory of the Wright Air Development Center in the form of landing oscillograph records have been analyzed in a manner similar to that employed with the earlier oscillograph records. The results appear as shock spectra, that is, as curves of maximum response acceleration as a function of the natural frequency of the simple system subjected to the landing shock. As in the previous cases of landing shock the records selected represented the most severe impacts for a given series of landing tests on a particular airplane.

These new spectra obtained are for the B-47A bomber, the P2V-5 patrol bomber and the F-84E fighter aircraft. The B-47A and the F-84E aircraft are jet engined powered.

The question has been raised as to whether the landing impacts experienced by jet aircraft are as a rule more severe than those experienced by reciprocating engine aircraft. In order to gain some insight into the question, the landing shock spectrum associated with the P-80A which was the sole jet aircraft in the group of aircraft landing shock spectra plotted in Figure 51, has been removed so that a new individual landing shock spectrum has been formed. This spectrum is shown in Figure 54 and is for reciprocating engined aircraft. An envelope of maximum response points is indicated. The individual landing shock spectra for the P-80, B-47A, and the F-84E have been plotted in Figure 55 and the envelope of maximum response accelerations indicated for these jet engine aircraft. The individual landing shock spectra for the P2V-5 aircraft have also been plotted in Figure 54 and a maximum envelope for these spectra is indicated.

The landing oscillograms which form the basis for determination of all of the shock spectra, with the exception of the P2V-5, were obtained during rather thoroughly instrumented landing tests. In some of the landing tests, the pilots were instructed to make deliberately hard landings, and in others no particular requirement relative to severity of the landing had been established. Consequently some statistical distribution of hard and soft landings was obtained. However, as stated earlier, the landing oscillograms selected for analysis did represent the most severe landings in any given set of landing tests. It is felt that it would be reasonable to assume that the landing shock spectra obtained

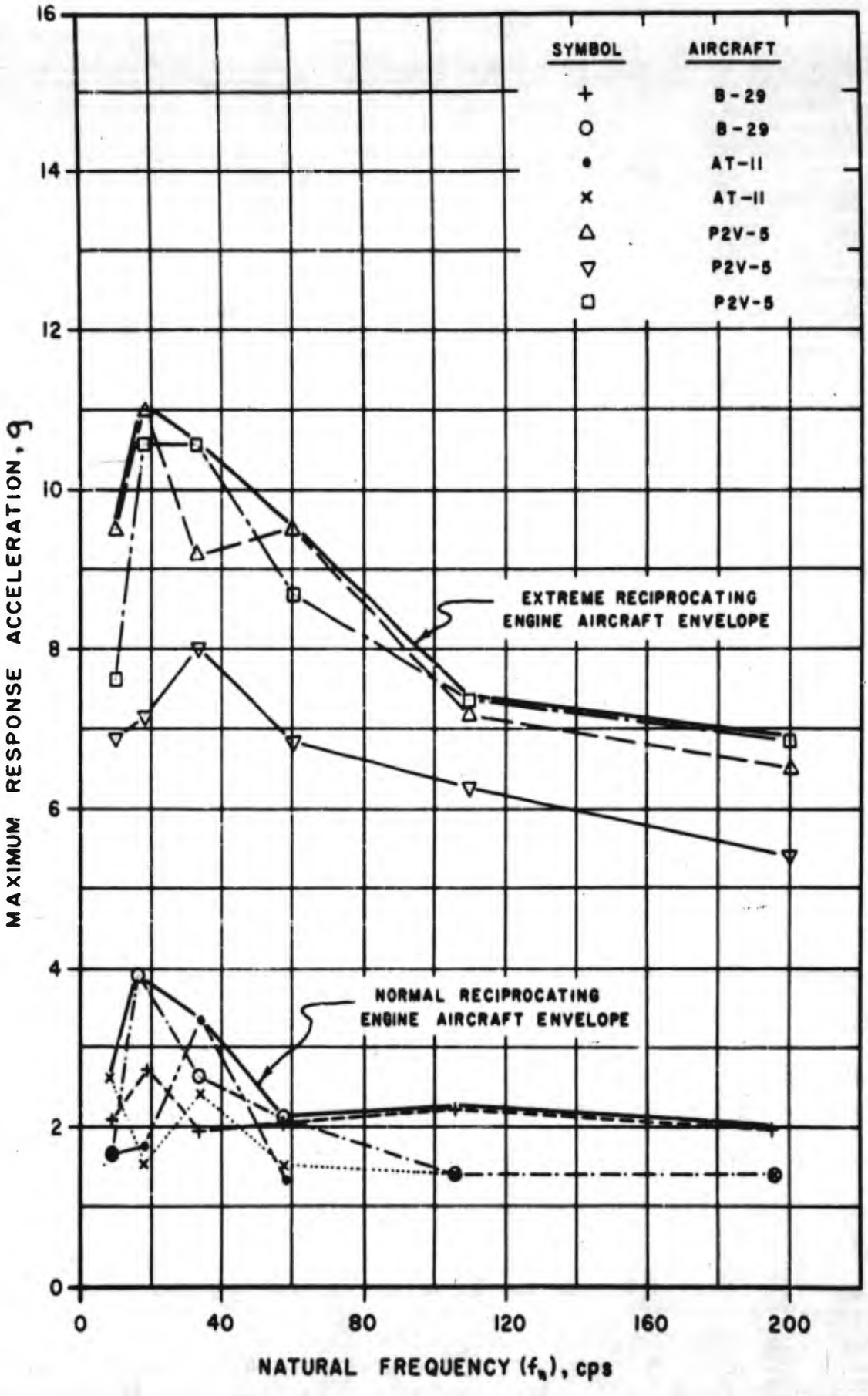

FIGURE 54. SHOCK SPECTRA FOR INDIVIDUAL LANDING RECORDS OF RECIPROCATING ENGINE AIRCRAFT, Q = 20

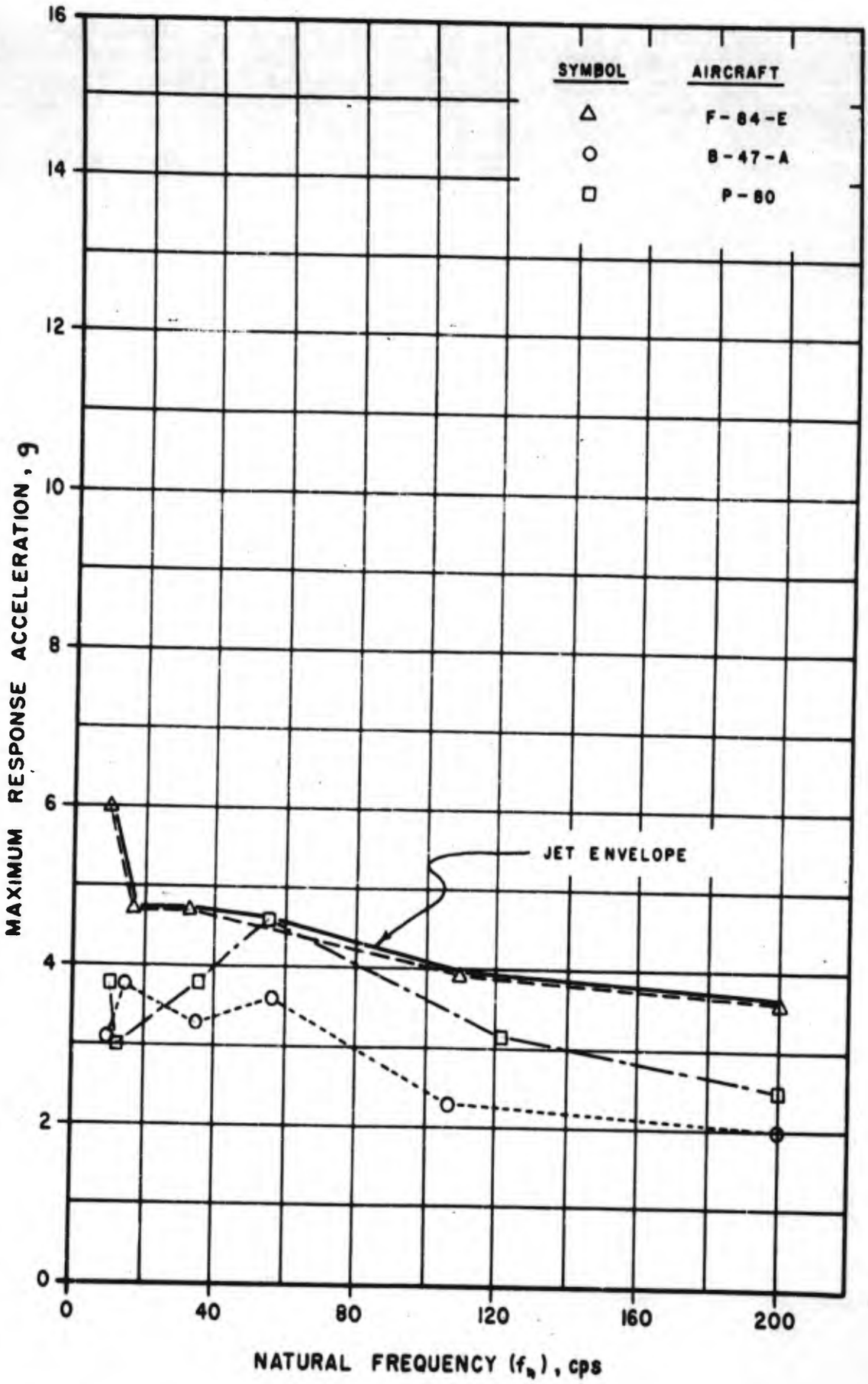

FIGURE 55 SHOCK SPECTRA FOR INDIVIDUAL LANDING RECORDS OF JET AIRCRAFT, Q = 20

approach very closely to the limit of severe impact shock that might be obtained in normal service conditions. Normal service conditions might be roughly defined as those conditions obtained when extremes of weather, piloting skill and aircraft controllability during landing are not experienced. The landing test data obtained for the P2V-5 aircraft do not fall in the normal landing impact category. The landing tests from which the oscillograms were obtained were made under extreme conditions dictated by a requirement for minimum landing distance on unprepared airfields. To achieve successful landings under these conditions, extremely high rates of descent were necessary and the consequent impact severity is shown by the shock spectra presented in Figure 54. It would not be rational to employ P2V-5 shock spectra for any testing procedure which is to be considered representative of normal landings. However, this spectrum will be employed to define a test procedure for an upper limit of landing impact severity.

As a matter of interest, shock spectra have been computed based upon several oscillograms of carrier aircraft landings. The original oscillograph data for the carrier aircraft were obtained from the Carrier Suitability Section of the Naval Air Test Center, Patuxent River, Maryland. Most of the landings were simulated carrier landings and were made on concrete runways using a carrier approach and with arrestment accomplished in a manner similar to that employed on aircraft carriers. The aircraft from which the data was obtained were both jet aircraft and were the F4D-1 and F3H-2N. On an individual landing basis the spectra are shown in Figure 56 and an envelope of maximum response is indicated. It will be noted that these spectra on an individual landing basis represent a considerably more severe level of shock than that experienced by land based aircraft. It was thought advisable to present the information on the Carrier aircraft to indicate the generally greater landing shock severity which should be taken into consideration for equipment that may not only be installed in land based Air Force aircraft but may also be installed in Carrier aircraft. However, these spectra are not considered in the following test procedure development.

In a manner similar to that employed in deriving Curve B of Figure 53 each of the envelopes of the maximum response acceleration on an individual landing basis for the reciprocating engined aircraft (Figure 54), the jet engined aircraft (Figure 55), and the P2V-5 aircraft have been corrected, using the 1.47 factor, to a 1000 landing or stress cycle basis. These maximum response acceleration envelopes for 1000 landings are shown in Figure 57 and are considered to define the service shock spectra. These spectra will be employed in the following section in defining the laboratory shock testing procedures.

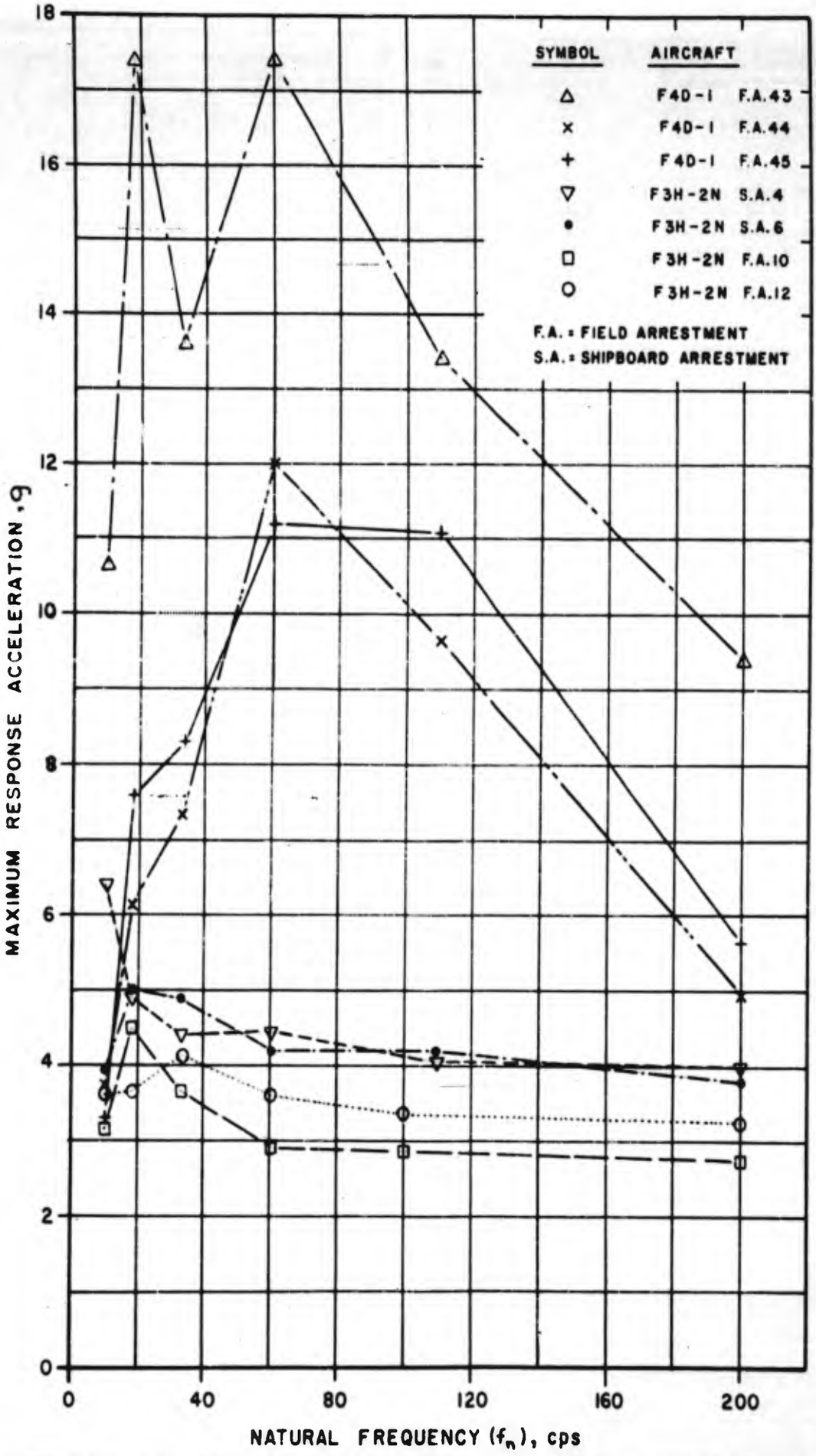

FIGURE 56. SHOCK SPECTRA FOR INDIVIDUAL LANDING RECORDS OF CARRIER AIRCRAFT, Q = 20

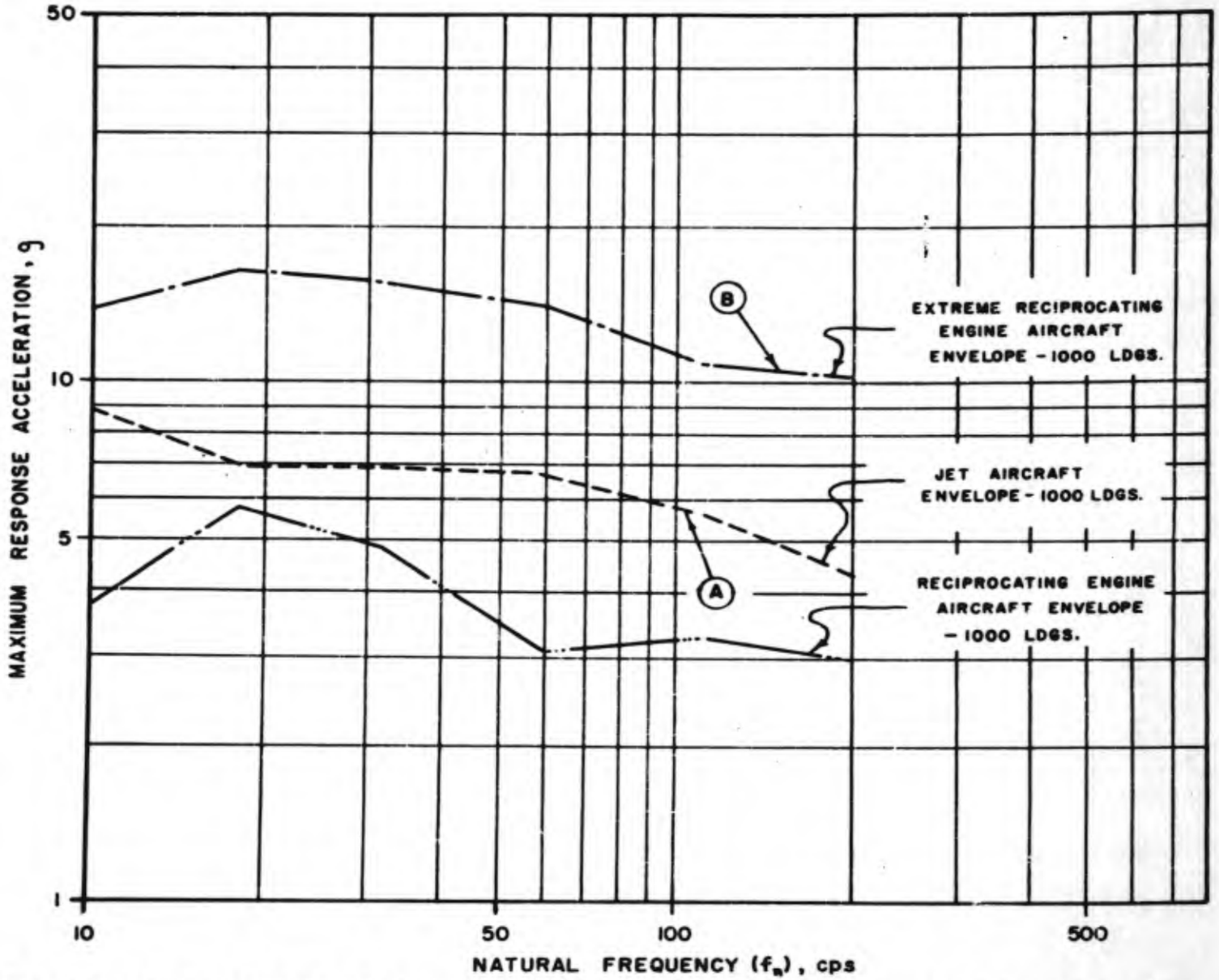

FIGURE 57. ENVELOPE SHOCK SPECTRA FROM FIGURES 54 AND 55, JET AND RECIPROCATING ENGINE AIRCRAFT -1000 LANDINGS, Q = 20

It will be noted that the shock spectra discussed in this section were obtained for a value of Q = 20. This value of the damping capacity sufficient to limit the transmissibility at resonance to 20 has been adopted as a value which is representative from a practical viewpoint and which can form the basis for comparison with the results yielded by other types of analysis.

Referring to Figure 57 and the envelope spectra for the jet and reciprocating engined aircraft it will be noted that the jet engined aircraft envelope spectrum is significantly more severe than that shown for reciprocating engined aircraft. However, this envelope shape and magnitude is generally defined by one landing of an F-84E aircraft. It is believed that to conclude that landing response spectra for jet engined aircraft are generally more severe than the reciprocating engined aircraft would be questionable in view of the limited amount of data considered in this report. It is considered that in the absence of a significant amount of landing acceleration data for jet aircraft that statistical contact velocity measurements will provide a basis upon which to evaluate such a conclusion. Recent programs instigated by the Services are being conducted to collect contact velocity data and this should be available in the near future. Until additional landing acceleration data or contact velocity data become available, it is considered advisable to consider that the response spectra for jet and reciprocating engined aircraft do not differ materially. In selection of a response spectrum for normal service landings to determine spectrum requirements for a testing machine the jet engined aircraft envelope spectrum will be employed as shown in Figure 57.

In Figure 58 a minimum acceptable response surface is depicted which is similar to the minimum acceptable response surface illustrated earlier in Figure 44. However, this response surface (Figure 58) has been constructed directly from the shock spectra for service conditions shown in Figure 57. More specifically, the intersection of the $f_n - \ddot{y}_o$ plane at $n_t = 1000$ is the response spectrum shown in Figure 57 for the jet aircraft (curve A). Starting with this spectrum section as a base the minimum acceptable response surface has been constructed utilizing the idealized endurance curve of response acceleration as shown earlier in Figure 41. The spectrum for the extreme reciprocating engined aircraft service shock of Figure 57, identified as Curve B in Figure 57, has been added to Figure 58 where $n_t = 1$. This portion of Figure 58 will be later utilized in defining a shock test procedure.

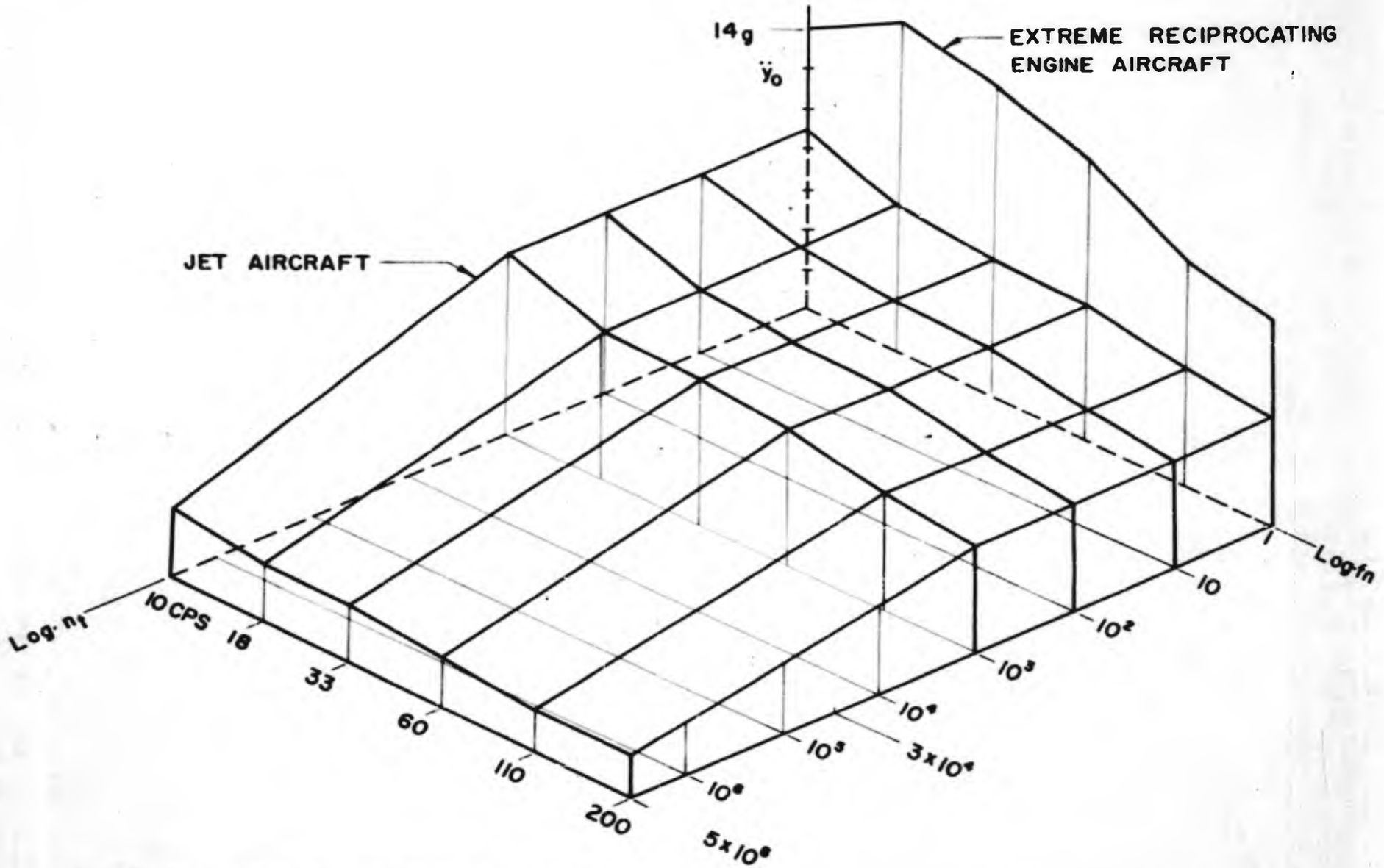

FIGURE 58. MINIMUM ACCEPTABLE RESPONSE SURFACE - Q = 20 BASED ON SHOCK SPECTRA OF FIGURE 57

SECTION XIV

SHOCK TESTING PROCEDURES

Several different types of shock testing machines are in current use for testing equipment intended for airborne service. One of the most commonly used machines is the Type 150-400 VD Variable Duration Shock Testing Machine. The equipment under test is attached to an elevator constrained by suitable guides arranged to move only vertically. To conduct shock tests, the elevator is lifted by a cable arrangement a pre-determined distance by suitable means, and is permitted to fall freely. Downward motion of the elevator is arrested as it falls into a sand box constituting the lower part of the shock testing machine. The bottom of the elevator carries an array of wooden cleats whose arrangement may be varied to change the suddenness of application of the decelerating force. Current specifications often call for shock tests of two different degrees of severity. One of these involves a free fall of approximately four inches, while the other involves a free fall of 13 inches. The time histories of acceleration as measured on the elevator are shown by the oscillograms set forth in Figures 59(A) and (B) respectively.

The oscillograms recorded on magnetic tape shown in Figure 59 have been fed into the analog computer, and shock spectra have been obtained. These shock spectra take into consideration only the maximum response acceleration; they are shown graphically in Figure 59 for both the 4 inch and 13 inch free fall.

To afford a comparison of the shock machine output and the shock experienced during landing as determined from the preceding section, the curves describing the service shock as spectra are reproduced on Figure 60 from Figure 57. It should be noted that these curves include a factor noted in connection with Figure 57 which transforms the magnitude of the response acceleration to a value which is appropriate for 1000 cycles of stress reversal. Current shock testing procedures involves substantially fewer than 1000 cycles of stress reversal. Consequently, the service shock curves in Figure 57 are not strictly comparable with the shock machine spectra because of this disparity in the number of cycles. The curve representing the shock spectra of the landing shocks could not be further transformed by an additional reduction in the number of cycles because of a discontinuity at N = 1000 cycles as indicated in Figure 41. The other alternative involves an increase in the number of applications of shock involved in a representative shock test.

It is apparent from Figure 60 that the spectra from the Type 150-400 VD Shock Machine tend to peak in the region of 80 to 100 cycles per second. The peaks that appear at higher frequencies are the results of structural resonances in the elevator of the shock machine. The significance of these latter peaks cannot be

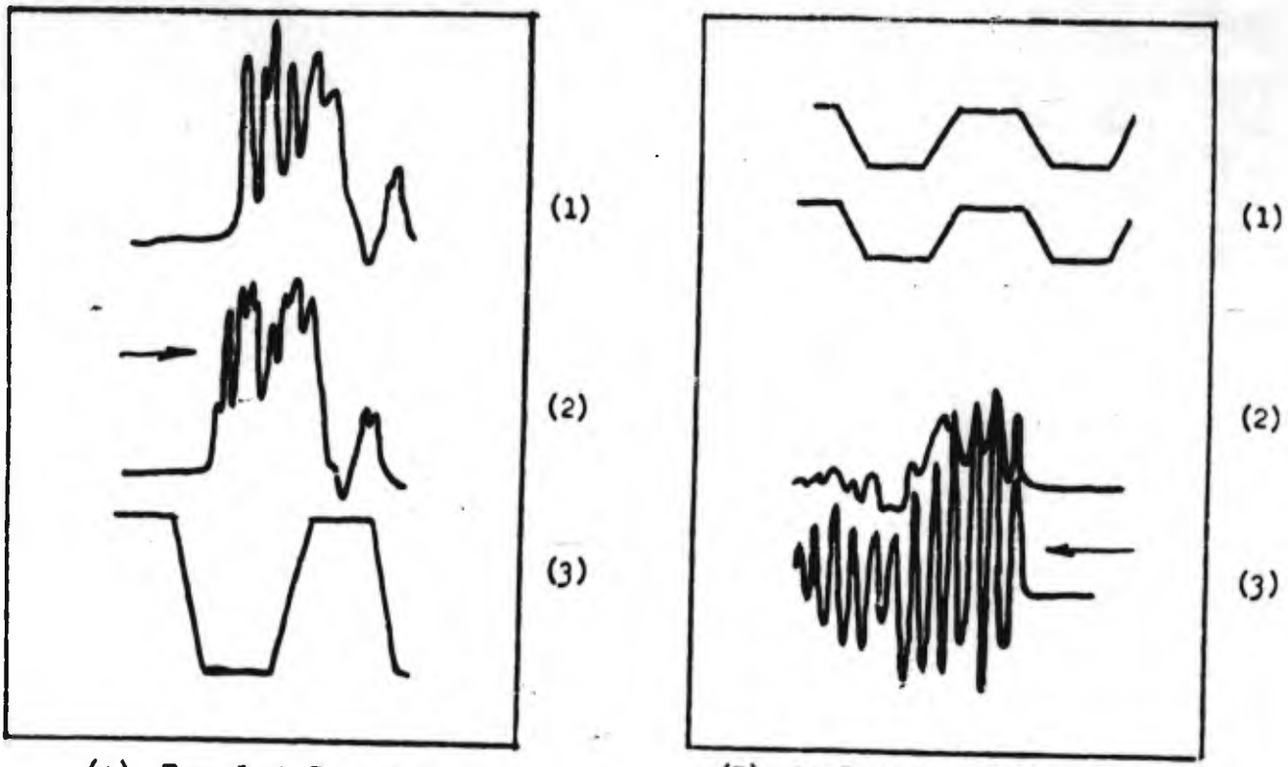

(A) Four Inch Free Fall Time

(1) Acceleration on elevator
(2) Similar to (1)
(3) Calibration trace - 15g (peak-to-peak) and 60 cps

(B) 13 Inch Free Fall Time

(1) Calibration traces - 30g (peak-to-peak) and 60 cps.
(2) Acceleration on elevator
(3) Strain in cantilever beam with natural frequency of 500 cps. mounted on elevator

Figure 59. Oscillograms Showing Performance of 150-400 VD Medium Impact Shock Machine

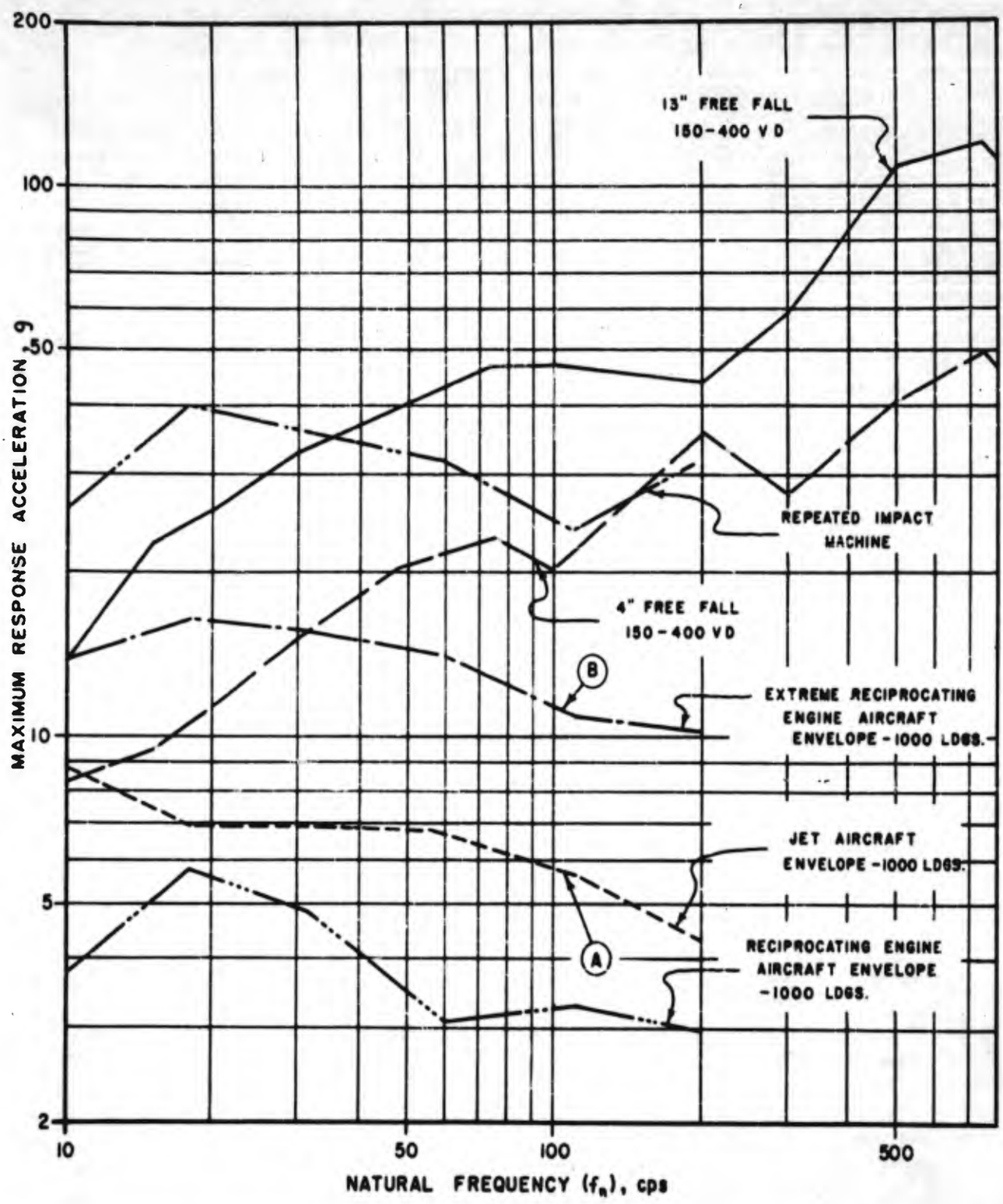

FIGURE 60, COMPARISON OF SHOCK SPECTRA OF SHOCK MACHINES WITH ENVELOPES OF SHOCK SPECTRA FOR AIRCRAFT LANDINGS, Q = 20

compared with similar parts of the landing spectra because the frequency response of the instruments used during field tests of aircraft is somewhat limited and it is believed that the records are not significant at frequencies of the order of 500 to 1000 cycles per second. It is evident, however, that the peaks in the spectra for landing shock conditions tend to occur in the region of ten to twenty cycles per second. This suggests that the type 150-400 VD Shock Machine as currently constructed is not fully representative of the shock experienced by aircraft during landing. The modification which appears to be needed would bring about a change in the frequency at which the maximum amplitude of the spectrum occurs.

The spectrum shown by the dash lines in Figure 60 designated "Repeated Impact", was obtained from a free fall type of shock testing machine in which rubber pads are employed to arrest the downward motion of the table supporting the equipment under test. This machine is automatically operated in that cams are provided to repeatedly lift the table and drop it upon the arresting means. From a very tentative consideration, this machine would appear well suited to the reproduction of landing shock conditions because the maximum amplitude of the shock spectra occurs at frequencies approximately the same as the frequencies of maximum response for the envelopes of the landing shock spectra, and because the machine is adapted to a large number of shock repetitions in a relatively short period of time.

The shock spectrum representing the performance of the shock testing machine at a free fall of 13 inches, as shown by the upper curve in Figure 60, involves values of response acceleration in excess of those indicated by the environmental conditions studied in this analysis. It is understood that the test involving a 13 inch free fall is intended to simulate conditions encountered during minor crashes; it would not be expected, therefore, that oscillograms obtained during normal landings would conform to crash conditions. It is understood by the authors of this report that the level of severity embodied in a 13 inch free fall was established by representatives of the United States Air Force during a study of several airplane crashes. Under these circumstances, and in the absence of numerical test data obtained during crashes, the authors feel that the shock test involving a 13 inch free fall should be reconsidered. It is recommended that every opportunity be used to re-examine the requirements for the more severe shock test with the objectives of determining whether the presently specified test is realistic and whether the test serves its primary function of insuring that equipment does not become a missile within personnel spaces during crash conditions.

SECTION XV

SHOCK MACHINE MODIFICATIONS

At this stage of the investigation, representative shock spectra have been defined for service landings, and it has been shown that the shock spectra obtained with existing shock testing machines of the 150/400VD type do not provide a shock spectrum of the desired shape. One of the requirements of this investigation is that the existing shock machines of the 150/400VD and 20VI type shall be modified to provide for a shock testing procedure that will afford testing conditions more representative of those experienced in actual service use.

The 150VD Shock Testing Machine has been described in an earlier section. The 20VI Machine may be considered to be a small scale version of the 150VD Machine which is limited to an elevator capacity of 20 pounds. The 20VI Machine, however, does employ a cast all-metal elevator and may be adapted for use with wooden blocks and sand or may be used to achieve higher velocity changes with the use of a hardened steel punch attached to the elevator and load blocks. A rigid cross-beam member in the sandbox acts as an anvil when the punch and lead sheet drop method is employed. Comparing these two machines when set up for sandpit dropping the basic difference is that of elevator rigidity which is appreciably higher in the 20VI Machine.

In addition to the requirement for providing the desired shock spectrum, both these machines must be modified to provide for repeated drop testing. The success achieved with the specially fabricated repeating drop test machine described in earlier paragraphs, which basically consisted of a cam lifted elevator which permitted a free fall on rubber blocks, indicated that the existing shock test machines might be readily modified if the elevator were arrested by rubber blocks rather than sand. For both of these machines then, the following design objectives were formulated:

(a) Basic requirement is that the shock spectrum as defined in Figure 57 be achieved in shape and with the intensity of shock regulated by the height of free fall.

(b) Modifications to the existing machines should not extend to the scope of a complete redesign. Existing parts and components are to be used whenever possible. This philosophy dictates use of the existing elevator winch and motor and drum drive.

(c) A means should be devised for repeated raising and releasing the elevator. The use of the existing elevator raising and lowering mechanism would probably provide for not more than five shocks or

five drops per minute. If the drive motor could withstand the duty cycle a faster rate of drop would be desirable.

(d) A means should be provided for counting the number of drops.

(e) Modification should not be so extensive as to preclude changing the machine from a repeated impact tester to a sand pit drop tester. Four hours should be considered a reasonable length of time to accomplish conversion from one type of drop test machine to the other.

The primary modifications to the 150/400VD testing machine consisted of the design of two rather large castings, one designated an anvil which effectively bridged the existing sandbox structure and was provided with a centrally located base for mounting rubber blocks. A second large casting, termed an elevator base, which is attached to the elevator and is also provided with a centrally located boss for attaching rubber blocks. The two castings were designed with the idea of providing as light a structure as practical consistent with the stiffness desired.

A considerable amount of design effort was expended in attempting to utilize a means of raising and lowering the elevator rapidly either by the use of a crank mechanism attached to the end of the existing drum drive or by the use of an over-running clutch installed within the confines of the existing cable drum. Neither of these design approaches would permit ready and quick changeover to the intermittent sandpit drop test configuraion without major changes to the motor and drum drive mechanism. Information received from the manufacturer of the cable and drum drive assembly indicated that continuous operation which would require reversing the drive motor could not be provided with the existing equipment. Replacement of the existing motor drive with a higher rated horsepower drive would permit continuous operation. Inasmuch as the replacement of the existing motor drive would constitute a major modification, additional study of the problem indicated that satisfactory drive performance could be achieved if a time delay relay was provided in the motor reversing circuit to permit operation under a less severe duty cycle. This, of course, would result in a fewer number of drops per minute. A drawing of the revised 150/400VD shock testing machine with the modifications indicated to convert to the repeated drop testing configuration is shown in Figure 61.

The sequence of events for one repeated drop cycle operation is detailed in the following paragraphs:

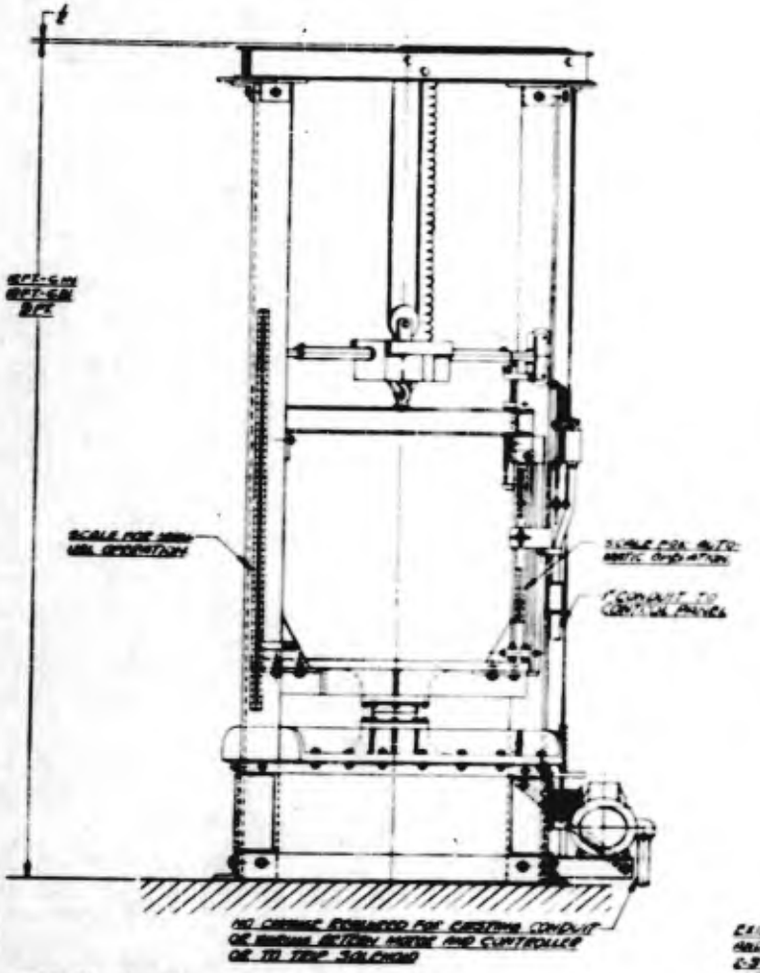

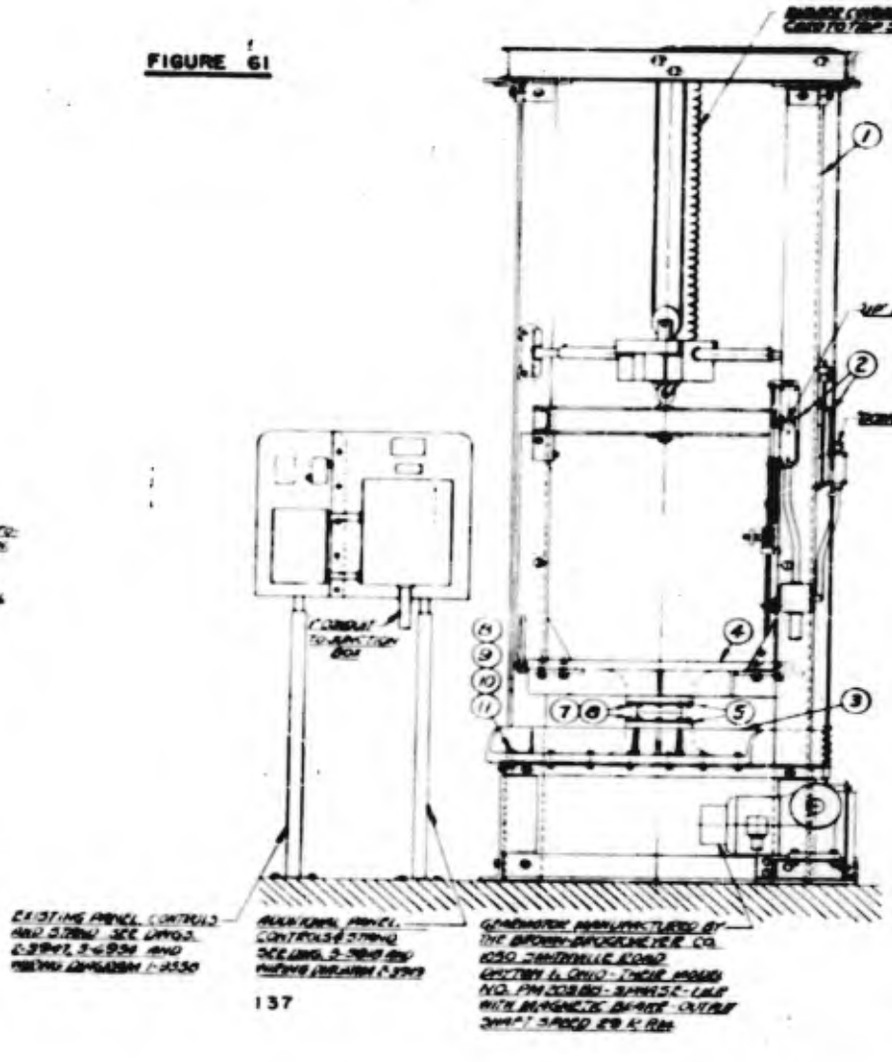

FIGURE 61

1. When the "Cycle Start" button is pressed, the control relay closes and the cycle is set up for automatic operation, but there is no motion either up or down at this time.

2. Pressing the "Jog Up" button initiates upward motion of the motor and elevator instantly with no delay.

3. Pressing the "Jog Down" button initiates downward motion of the motor and elevator instantly with no delay.

4. Assuming the direction selected is "up".

   a. The elevator rises until it comes in contact with the up limit switch.

   b. This switch instantly stops the motor, energizes the trip solenoid, dropping the elevator, and energizes the "up" timer.

   c. After the time delay to which the timer has been set is completed, the trip solenoid is de-energized, the motor reverses and starts the down cycle.

   d. The elevator descends until it contacts the down limit switch.

   e. The down limit switch stops the motor, energizes the solenoid, opening the jaws again, energizes the "down" timer, and operates the Veeder-Root Counter.

   f. After the time delay to which the "down" timer has been set is completed, the trip solenoid is de-energized, closing the jaws, and the motor reverses, raising the elevator.

5. The cycle repeats as above until stopped.

6. Pushing the cycle stop button stops the automatic operation.

Using a 2.2 second time delay relay in the motor reversing circuit to prevent overheating the windings, the machine is capable of approximately nine drops per minute or 540 drops per hour.

In order to convert the repeated drop test machine to a conventional sand pit tester, the anvil and the new elevator table base are removed. The proper block configuration is then attached to the bottom of the elevator table, the sand is raked and leveled, and by utilizing the manual operation "up" and "down" and "trip" buttons, the machine is ready for a sand pit drop test.

In the modified 150 VD and 20 VI machines the elevator is decelerated during each drop by the impact of a circular rubber pad on the elevator with a similar circular rubber pad on the anvil. It was realized that the use of rubber blocks as a decelerating medium rather than sand would provide several rebound impacts during each drop and careful consideration would have to be given to the effect of the successive rebound impacts upon the shock spectrum. An extensive series of tests of different rubber block configurations for both machines were conducted and results of these tests are reported in detail in Appendix IV. Figure 62 presents the shock spectra generated using the selected blocks for the 150 VD and 20 VI machines. The spectrum shown for each machine is that attained from a single drop from a 1 1/2 inch height for a value of Q = 20. In Figure 63 oscillograms are presented which depict the acceleration achieved on the elevator during one drop to illustrate the successive rebound impacts.

Conversion of the 20 VI machine to the repeated drop testing configuration was made somewhat easier in that it was not necessary to design an anvil to support the arresting rubber block. The standard 20 VI machine is provided with a relatively rigid cross member in the sand box which could be simply modified to support the rubber arresting block. An assembly drawing of the modified 20 VI machine is shown in Figure 64.

The sequence of events for one repeated drop cycle operation for the 20 VI machine is similar to that detailed earlier for the 150-400 VD Shock Testing Machine. In order to convert the 20 VI machine to a sand pit drop testing machine, the rubber blocks are removed, one from the elevator and one from the anvil and the wooden block assembly is installed on the elevator. The manual controls are used for sand pit drop testing.

Figures 65 and 66 are photographs depicting the modified 150-400 VD Shock Testing Machine. It will be noted in these photographs that the anvil overhangs the sandbox by approximately 1 inch all around, and that a modification to the left and right main upright members at the attachment to the sandbox is indicated. These modifications were necessary because the Contractor's machine is non standard relative to the sandbox dimensions. The modification components were designed to fit standard 150-400 VD Shock Testing Machines. Figure 67 is a photograph of the modified 20 VI machine. It may be pointed out that in both photographs temporary, rather than permanent wiring as specified in the drawings, was employed for obvious reasons.

FIGURE 62 SHOCK SPECTRA, 20 VI & 150/400 VD MACHINES, SINGLE 1.5" DROP Q=20

20 VI MACHINE

150/400 MACHINE

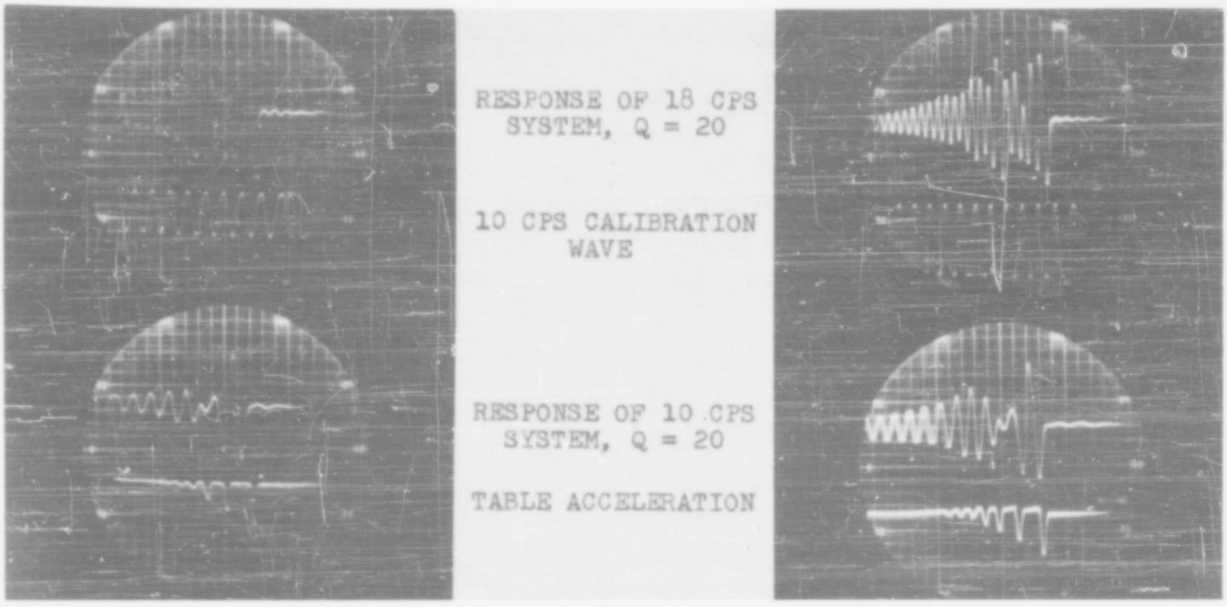

FIGURE 63. TYPICAL OSCILLOGRAMS ILLUSTRATING TABLE ACCELERATION AND RESPONSE OF 10 AND 18 CPS SYSTEMS. MODIFIED 20VI AND 150/400VD MACHINES. 1.5" DROP HEIGHT. BUTYL RUBBER PADS.

FIGURE 64

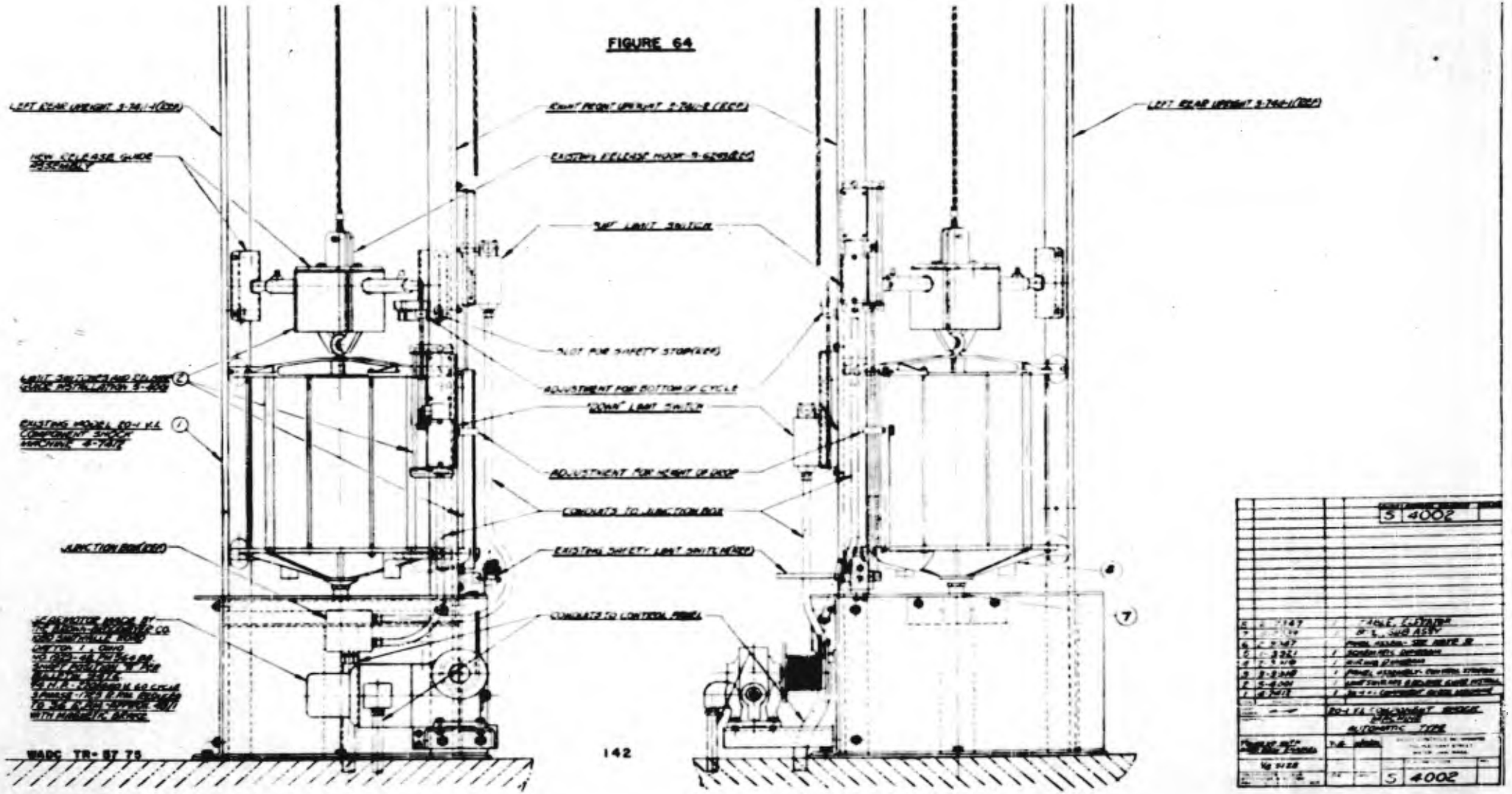

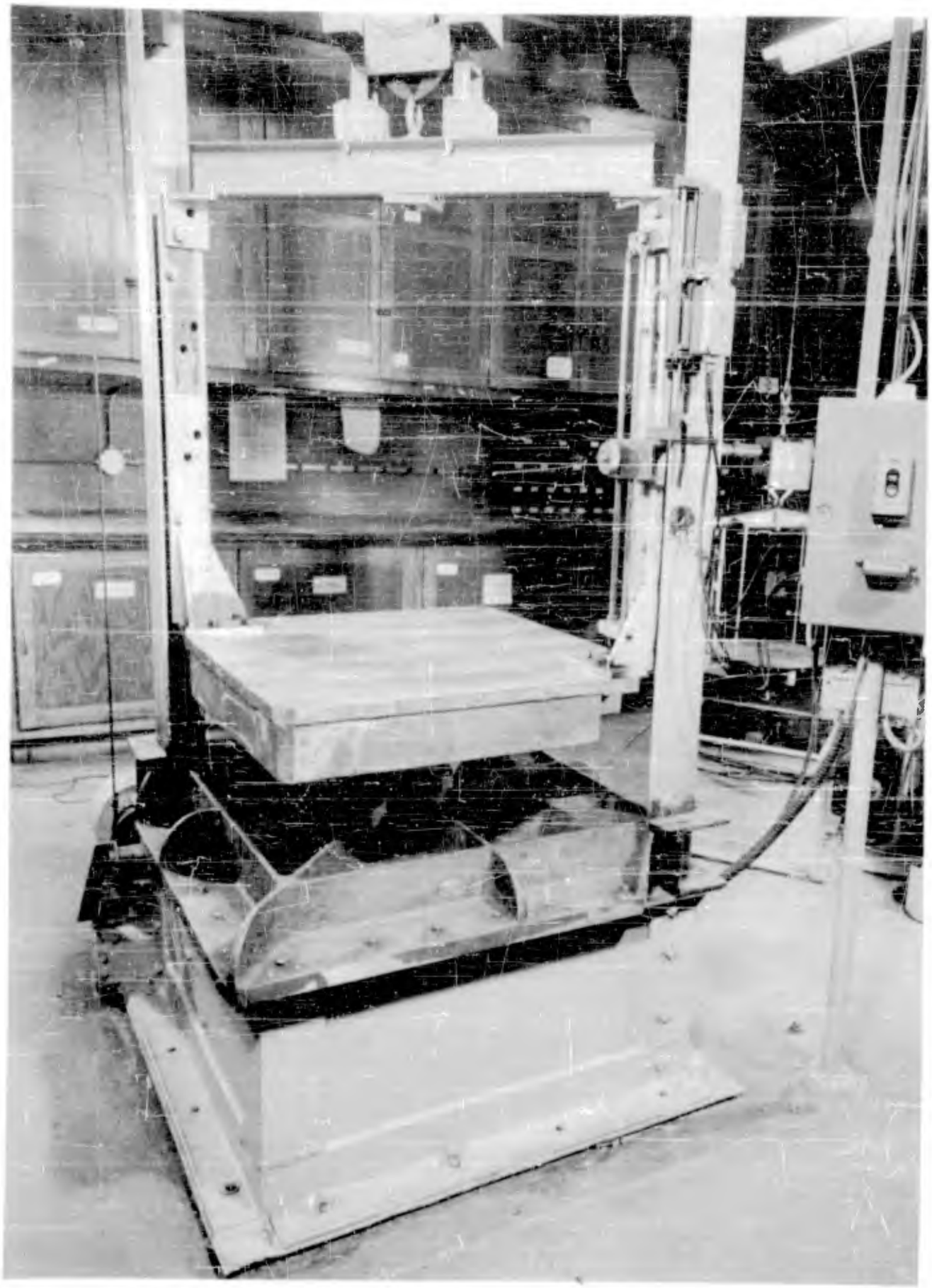

FIGURE 65. 150/400VD SHOCK TESTING MACHINE MODIFIED FOR REPEATED DROP TESTING.

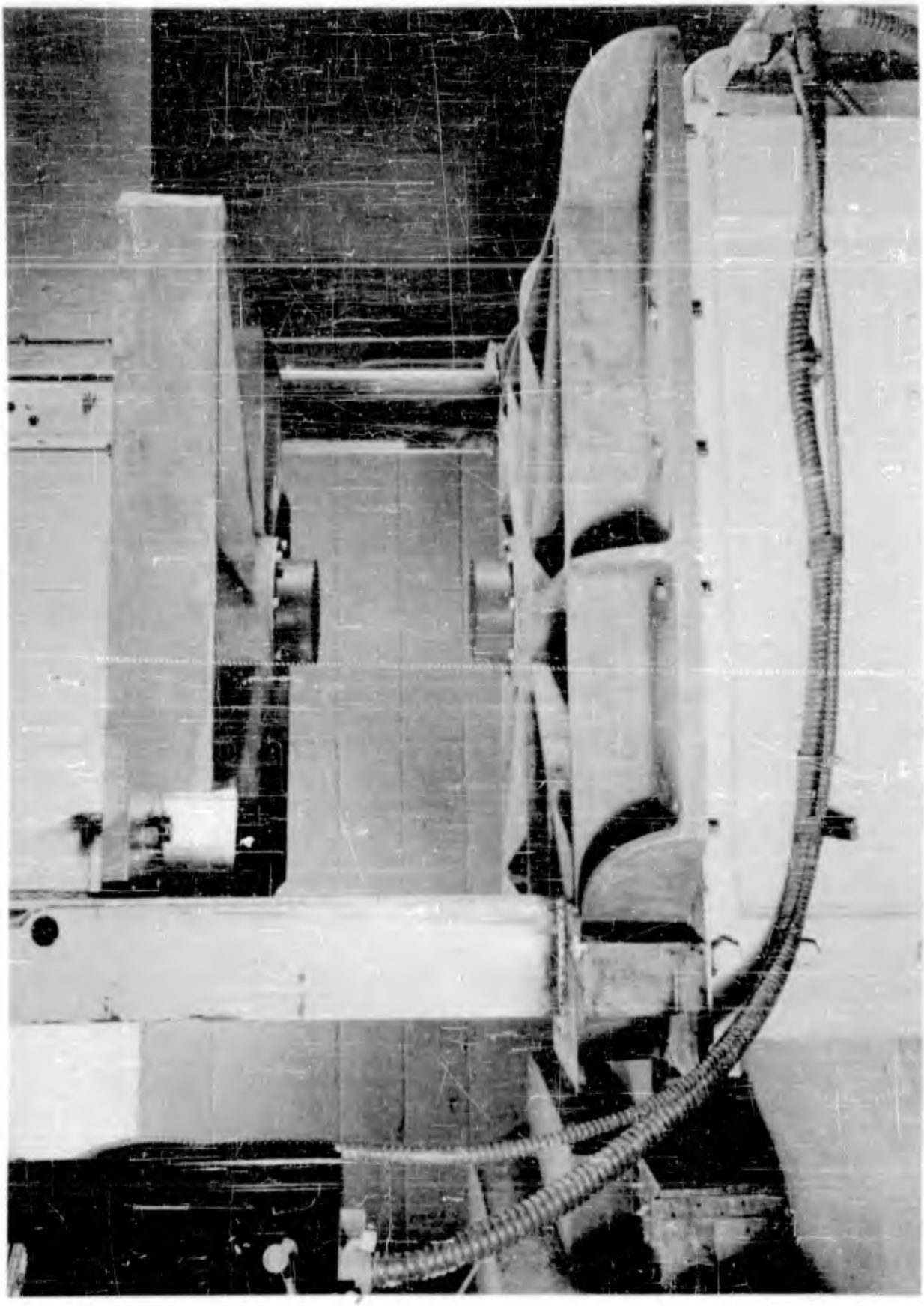

FIGURE 66. 150/400VD SHOCK TESTING MACHINE CLOSE-UP

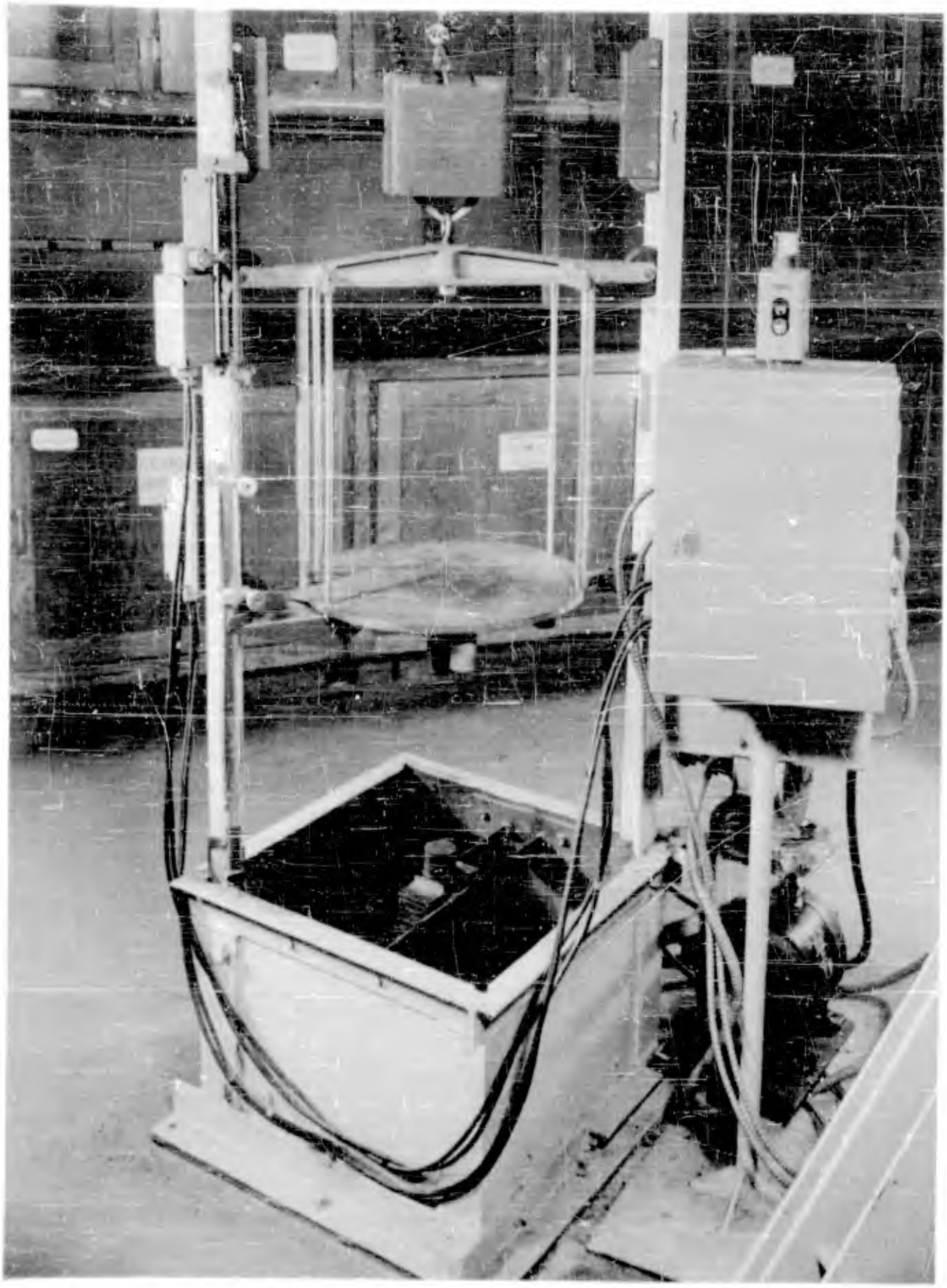

FIGURE 67. 20VI SHOCK TESTING MACHINE MODIFIED FOR REPEATED DROP TESTING

SECTION XVI

SPECIFICATION OF SHOCK TEST

The requirements of this investigation specify that modifications of the existing 150/400VD and 20VI Shock Machines shall be accomplished to provide for a shock test that is representative of the shock environment experienced in service. In accordance with the shock testing philosophy described in an earlier section, that is the concept of a minimum acceptable response surface to evaluate shock, the minimum acceptable response surface presented in Figure 58 will now be utilized in specifying a recommended shock test procedure.

The minimum acceptable response surface shown in Figure 58 represents the required strength of any equipment which will be subjected to the landing shocks analyzed here. Since one of the parameters of the surface is total number of stress reversals experienced by the equipment during its life (n_t), it is possible to devise a transformation from actual environment to laboratory conditions. The latter necessarily involves fewer cycles of stress reversals. An analysis based on laboratory testing conditions however must yield values of $\ddot{y}_o$ falling above the minimum acceptable response surface for appropriate values of f_n and n_t. A shock test is considered suitable for qualifying equipment to withstand the shock represented by the minimum acceptable response surface if it meets the following requirement.

$$D' \left(\sum \frac{n'}{N'} \right) = 1 \qquad (33)$$

where D' represents the number of applications of shock during the test, n' represents number of occurrences of various maximum values of acceleration response and N' is taken from Figure 41. Equation 33 is patterned after equation 31 and must be applied to each of several natural frequencies.

As a result of exploratory testing of the modified shock testing machines utilizing the rubber arresting pads, numerous shock spectra for several drop heights were obtained. From an evaluation of these shock spectra it became apparent that one pad configuration for each machine best approximated the desired spectrum shape and that a suitable drop height to obtain the desired response acceleration would lie between 1 and 2 inches. Practical considerations relative to the duration of the entire shock test procedure indicated that with the dropping rate performance of each machine limited to a maximum drop rate of 540 drops per hour, that a value for the total number of drops, should be somewhere between 100 and 500.

It will be noted that the idealized endurance curve of Figure 41 which defines the relationship between $\ddot{y}_o$ and n_t provides a constant value of $\ddot{y}_o$ maximum for values of n_t less than 1000. In evaluating equation 33 it became apparent

that the defined idealized endurance curve (Figure 41) could not be applied for the values of D' less than 1000. This situation was found to be more prevalent in the calculation of equation 33 for values of f_n greater than 60 cycles. In these instances usually two or three significant response accelerations are obtained and the frequency of occurrence of the given response acceleration is usually unity. The situation is illustrated in the following computation:

From response oscillogram for f_n = 60 cps, Q = 20 and input from 1.5 inch drop:

Response Acceleration	Number of Occurrences	Assumed $\ddot{y}_o$ max. = 8.5	N' from Figure 41 for
$\ddot{y}_o$ - "g"	n'	$\ddot{y}_o/\ddot{y}_o$ max.	$\ddot{y}_o/\ddot{y}_o$ max.
8	1	0.94	1.7×10^3
5	1	0.59	1×10^5

$$D'\left(\sum \frac{n'}{N'}\right) =$$

For D' = 300; $\quad 3 \times 10^2 \left(\frac{1}{1.7 \times 10^3} + \frac{1}{1 \times 10^5}\right) =$

$$3\left(\frac{1}{17} + \frac{1}{1000}\right) = 3(.059 + .001) \neq 1.0$$

Examination indicates that N' cannot be smaller in any case than 1000 and for a D' of 300 or 500 and n' of 1, 2, $D'\left(\sum \frac{n'}{N'}\right)$ cannot reach a value of 1.0.

This appears to be somewhat of an impasse with regard to applying the previously developed philosophy to specification of a laboratory test. It appears that the idealized endurance curve of Figure 41 which assumes that the value of $\ddot{y}_o$ to be constant for values of N less than 1000 cannot be made to apply to drop tests where the **number of drops desired is less than 1000.**

If the idealized endurance curve is modified such that the values of N range from $N = 10^2$ to $N = 5 \times 10^6$ with the $\ddot{y}_o$ ordinate = 1 at $N = 10^2$ and the $\ddot{y}_o$ ordinate = 0.38 at $N = 5 \times 10^6$, and this curve used for the solution of equation 33, a drop test for a number of drops (D') between 100 and 1000 can be specified. A revised idealized endurance curve as described above is shown in Figure 68. From a philosophical

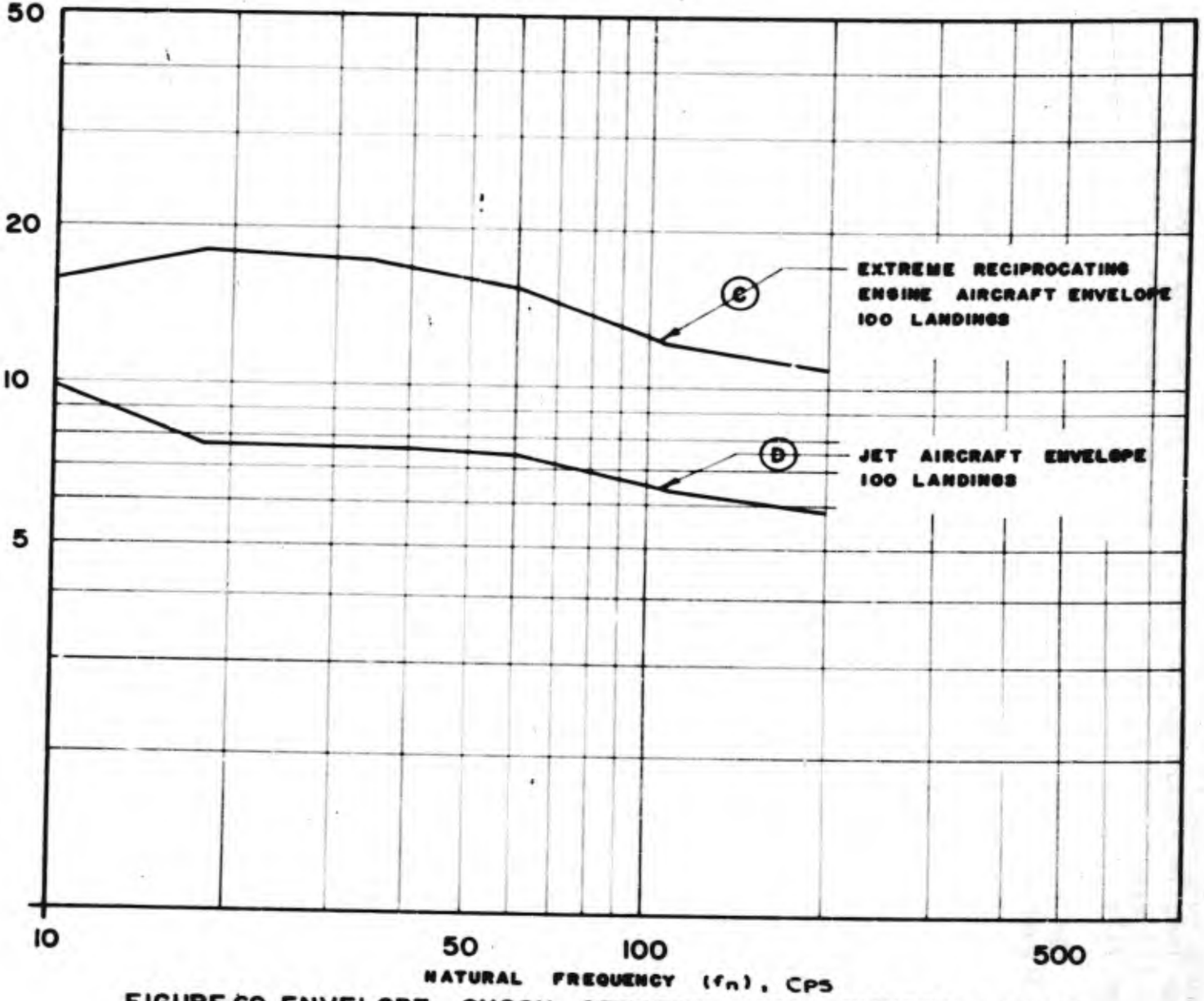

FIGURE 69. ENVELOPE SHOCK SPECTRA FROM FIGURES 54 & 55
100 LANDINGS, Q = 20

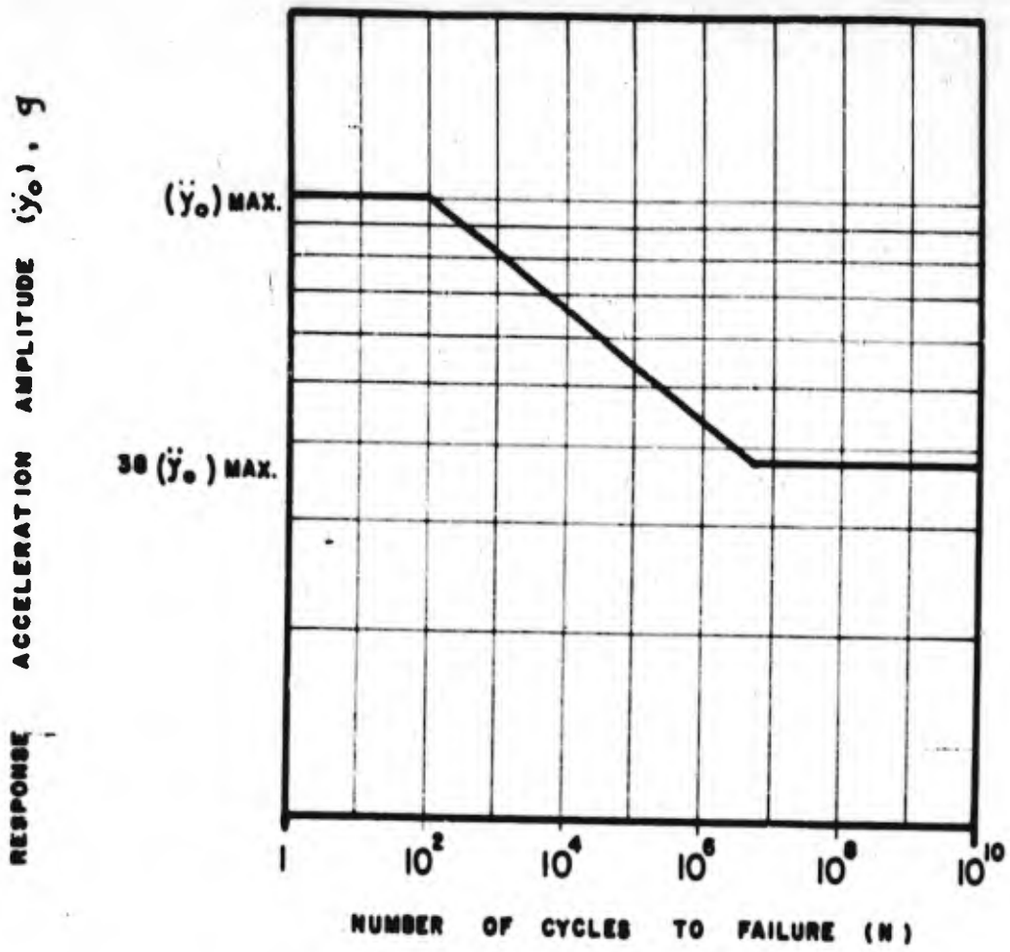

FIGURE 68. REVISED IDEALIZED CURVE OF RESPONSE ACCELERATION AMPLITUDE AS A FUNCTION OF NUMBER OF CYCLES TO FAILURE.

standpoint, the specification of $\ddot{y}_o = 1$ for values of N less than 1000 in Figure 41 was arbitrarily assumed and a value of $N = 100$ might just as rationally have been assumed. (Reference page 31).

The equation of the revised idealized endurance curve shown in Figure 68 is

$$\ddot{y}_o = \frac{N}{10^2}^{-.089} \qquad (33a)$$

As a consequence of this revision to the idealized endurance curve a new minimum acceptable response surface must be constructed. It will be recalled that the previous minimum acceptable response surface was constructed using the spectrum at the value of $n_t = 1000$ as a base. This spectrum in turn had been derived from the envelope shock spectrum for the jet aircraft landings. A factor of 1.47 had been applied to the envelope surface shock spectrum to convert from $n_t = 30{,}000$ to $n_t = 1000$ cycles of stress reversal. In a similar fashion in order to form a base for generating the revised minimum acceptable response surface the shock spectrum for $n_t = 100$ has been derived, the applicable ratio in this case being 1.64. The spectrum for the extreme reciprocating engine aircraft environment has been converted in a similar fashion and again plotted at a value of $n_t = 1$. These revised spectra are shown in Figure 69, curves C and D. The revised minimum acceptable response surface based on these curves is shown in Figure 70.

Oscillograms were obtained with the 20VI Shock Test Machine of the table acceleration for a 1.5 inch drop with the rated table load of 20 pounds. Assuming, as in previous calculations a value of $Q = 20$, response acceleration computations for several values of f_n were made and response block diagrams obtained. Based on the response block diagram, the cumulative damage expression of equation 33 was evaluated for $D' = 300$ drops and the resulting test spectrum is shown in Figure 71. This spectrum lies well above the minimum acceptable response surface at $n_t = 300$.

In the case of the 150/400VD Machine, which has a normally wide (0-400 pounds) table load range, a significant variation in table acceleration and consequent response spectrum is experienced with variation in table load for a constant height of drop. As shown in Figure 62, the greater difference in the spectra appears to be in the zero to 200 pound load range. It would be possible to utilize both the 200 and 400 pound table load acceleration spectra separately in arriving at a test spectra for $D' = 300$ drops; but realizing that all the foregoing spectra have been computed for a nominal value of $Q = 20$, consideration of the table load effect by defining two different drop heights depending on table load seems to be an unjustified refinement at this time. Consequently the table acceleration and response spectrum for the 200 pound table load and 1.5 inch drop height was selected for determination of the shock test response spectrum for $D' = 300$. The resulting test spectrum for $D' = 300$ drops is shown in Figure 71.

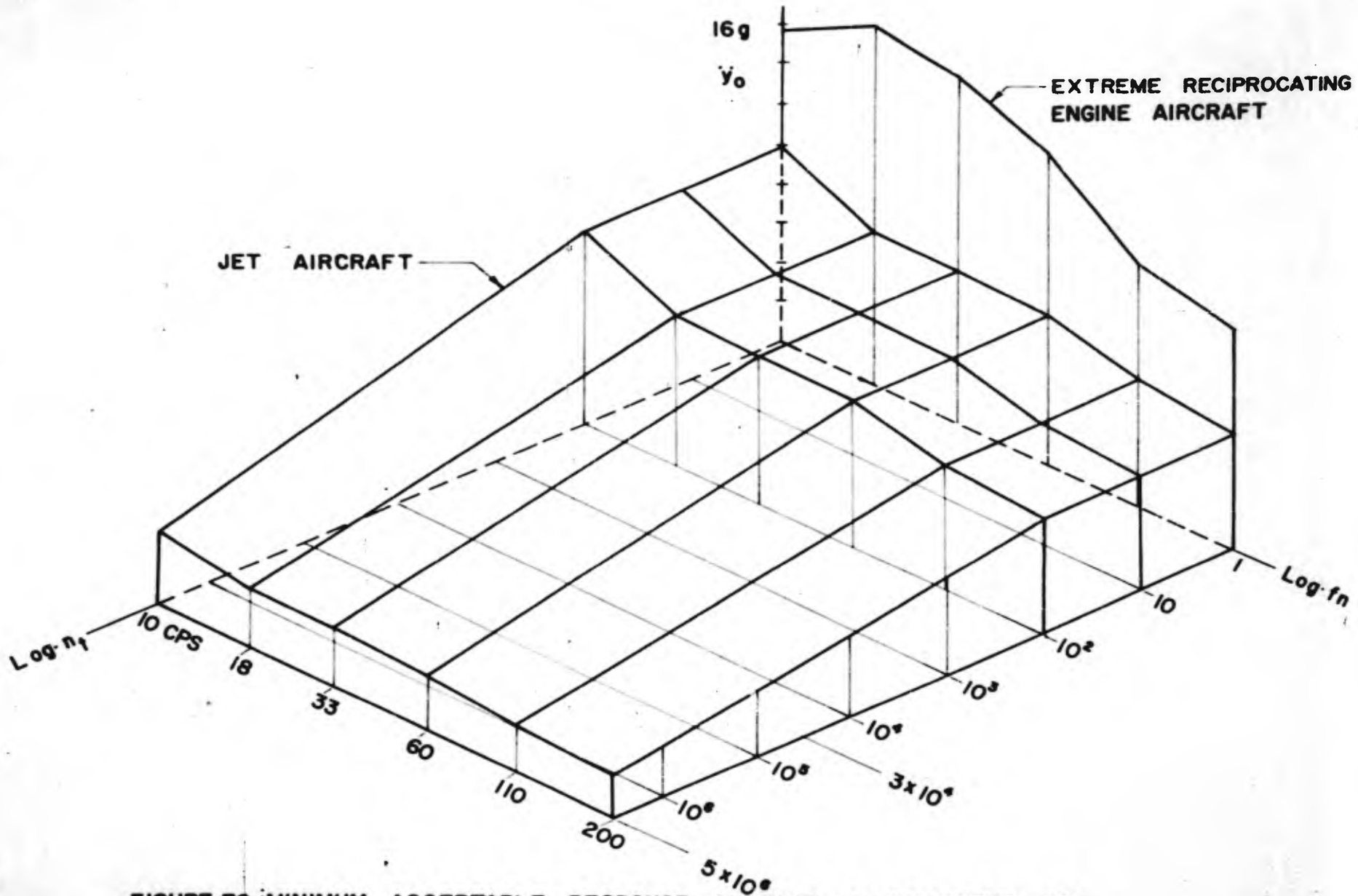

FIGURE 70. MINIMUM ACCEPTABLE RESPONSE SURFACE – Q = 20 BASED ON REVISED SHOCK SPECTRA OF FIGURE 69

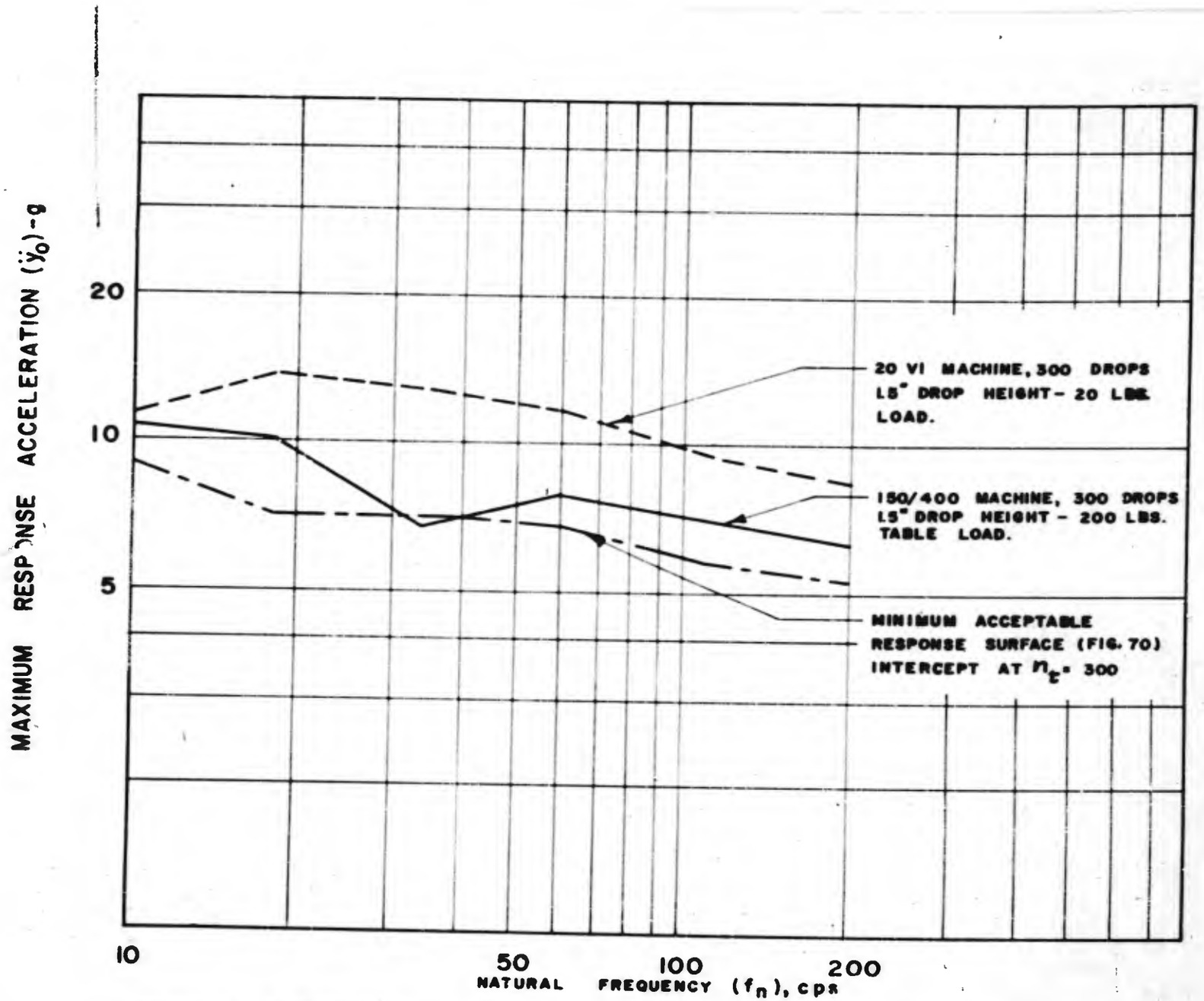

FIGURE 71. COMPARISON OF ENVIRONMENT SHOCK SPECTRA FOR n_t = 300 FROM FIGURE 70 WITH TEST SPECTRA FOR D' = 300

With the exception of one low spot at f_n = 33 cps, this test spectrum for the 150/400VD lies well above the minimum acceptable response surface at n_t = 300.

The response shock spectra obtained for the extreme reciprocating engine aircraft envelope as shown in Curve C of Figure 69 and Figure 70 is considered to represent an upper limit for service landing shock which borders on crash landing severity. It is proposed that this spectrum be utilized to define a drop test which approaches a crash safety type of test after which equipment will be operable. This test would especially apply to components used in aircraft whose mission requires landing on unprepared runways. No structural failure of parts of the components, or tearing loose of the component from the attachment fittings is permitted.

A recommended shock test specification consists of the following:

(a) The component to be tested shall be subjected to 200 drops on the suitable shock testing machine, 20VI or 150/400VD, depending on the weight of the component or equipment. The machines shall have been modified as shown in Barry Drawings S-3812 and S-4002 to provide the desired shock spectra and repeated drop facility. The 300 drops should be applied in turn, in both directions along each of the three principal axes. The following drop heights shall be employed depending on specimen weight:

Specimen Weight Pounds	Machine	Drop Height Inches
0-20	20VI	1.5
0-400	150/400VD	1.5

The test specimen shall not suffer damage or subsequently fail to provide the performance specified in the detail specifications.

(b) Specimens shall be subjected to one drop in each direction along the principal axes from a drop height of 4.5 inches on the applicable modified 20VI or 150/400VD machine. The specimen shall not suffer damage nor subsequently fail to provide the performance specified in the detail specification.

SECTION XVII

OTHER CONSIDERATIONS

Interpretation of Flight Vibration Environmental Data

Data defining the vibration environment in aircraft are usually obtained as a by-product of investigations to determine causes for either structural failures or equipment failures in an aircraft. Accelerometers, velocity pickups, strain gages, or other types of transducers will be installed in the region of concern and the outputs of these instruments will be recorded oscillographically to obtain a time history of the disturbance. Current instrumentation techniques involve tape recorders in place of oscillographic equipment, and this has greatly increased the accuracy and speeded up the analysis of data obtained during such programs. Unfortunately, for purposes of the present investigation, practically all of the data obtained in the past and much of the current data are in the form of oscillograph records on film or paper. Interpretation of these data is not so simple nor is it accomplished quickly. Careful analysis of oscillographically recorded vibration is a laborious procedure and is especially difficult by visual analysis techniques, when the wave form is comprised of a multiplicity of frequencies.

Discussions with various dynamics engineers involved in conducting flight vibration programs indicate two schools of thought with regard to interpretation of flight data. The methods of interpretation depend upon whether the expressed purpose of a particular program is to investigate aircraft structural failures or installed equipment failures. In both cases the flight data represent local responses of the airframe to the various flight condition inputs. Structural failure investigators, however, consider only the maximum value of the airframe response as significant, since this is directly related to maximum stress in the structure and the number of repetitions of this stress will indicate whether fatigue failure is probable. Accurate vibration frequency information is normally of secondary importance here. It is common practice, however, to select two or three predominant cycles of vibration in the vicinity of the maximum value for interpretation into a vibration frequency for data tabulation purposes.

With regard to equipment failures, it is necessary to consider the local airframe responses measured during flight tests, as environmental "inputs" to the equipment installed in the vicinity of these measurements. Since the majority of equipment failures which occur are the result of resonant vibration fatigue conditions, it is of primary concern here to obtain accurate frequency and amplitude information. Hence, in contrast with the "structural" type of data analysis, a second school of opinion exists among dynamics engineers which suggests that all recorded vibration data should be harmonically analyzed to ascertain the

true contribution of the various component frequencies and amplitudes present in a complex vibration wave form. Since the purpose of a laboratory vibration test for electronic equipment is, in effect, to determine the vibration fatigue resistance of such equipment, it is of considerable importance that the test embody the correct amplitudes without improportionate conservatism throughout the frequency range covered by the test.

The importance of accurate amplitude and frequency information can perhaps be best illustrated by considering the resonant responses of the idealized element of an equipment shown in Figure 2, to the two idealized representations of aircraft vibration waveforms shown in Figures 72(c) and 73(c). These waveforms are comprised of two superimposed component frequencies f_1 and f_2 of equal amplitude as shown by (a) and (b) in Figures 72 and 73. In Figure 72, $f_1/f_2 = 2$ and in Figure 73, $f_1/f_2 = 1.11$. A general expression for the idealized aircraft vibration waveforms shown in Figure 72(c) and 73(c) is as follows:

$$X = x_1 \sin 2\pi f_1 t + x_2 \sin (2\pi f_2 t + \theta) \qquad (34)$$

where: X = instantaneous amplitude of complex vibration, inches

x_1 = amplitude corresponding to f_1, inches

x_2 = amplitude corresponding to f_2, inches

f_1 = first frequency component, cps

f_2 = second frequency component, cps

t = time, seconds

θ = initial phase angle between f_1 and f_2, radians

It is perhaps unnecessary to point out here that although displacement amplitudes are indicated in the equations, the ideas are perfectly general and velocity or acceleration amplitudes may be used as well.

The absolute value of the steady-state response of the simple system shown in Figure 2 to each of the component frequencies shown in Figures 72 and 73 may be determined from the following transmissibility expression which appears

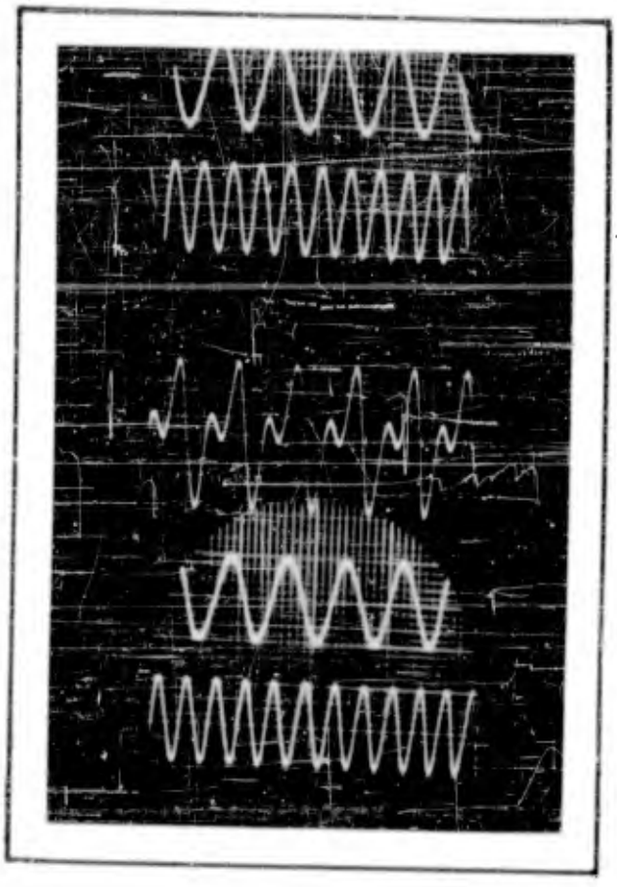

(a)

(b)

(c)

(d)

(e)

(a) Component Frequency f_1

(b) Component Frequency $f_2 = \frac{1}{2}f_1$

(c) Idealized complex wave = $\bar{f}_1 + \bar{f}_2$

(d) Response $x10^{-1}$ for $f_n = f_1$, $Q = 10$

(e) Response $x10^{-1}$ for $f_n = f_2$, $Q = 10$

FIGURE 72. CONSTRUCTION OF IDEALIZED COMPLEX WAVE AND RESONANT RESPONSES TO COMPONENT FREQUENCIES.

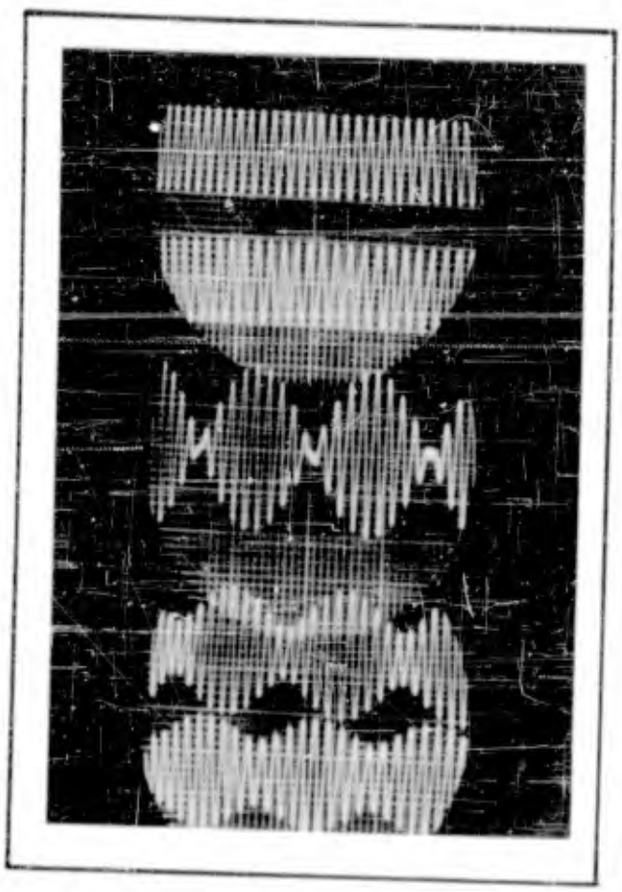

(a)

(b)

(c)

(d)

(e)

(a) Component Frequency f_1

(b) Component Frequency $f_2 = .9\ f_1$

(c) Idealized Complex Wave = $\bar{f}_1 + \bar{f}_2$

(d) Response $x10^{-1}$ for $f_n = f_1$, $Q = 10$

(e) Response $x10^{-1}$ for $f_n = f_2$, $Q = 10$

FIGURE 73. CONSTRUCTION OF IDEALIZED COMPLEX WAVEFORM AND RESONANT RESPONSES TO COMPONENT FREQUENCIES.

frequently in the technical literature:

$$T(f/f_n) = \left|\frac{y}{x}\right| = \sqrt{\frac{1 + \left(2 \frac{f}{f_n} \frac{c}{c_c}\right)^2}{\left(1 - \frac{f^2}{f_n^2}\right)^2 + \left(2 \frac{f}{f_n} \frac{c}{c_c}\right)^2}} \qquad (35)$$

where: $T(f/f_n)$ = transmissibility as a function of frequency ratio, dimensionless

y = response amplitude, inches

f_n = natural frequency, cps

c/c_c = coefficient of critical damping, dimensionless

The phase angle, in radians, between the input and response motions is as follows:

$$\alpha = \arctan \frac{-2 \frac{c}{c_c} \left(\frac{f}{f_n}\right)^3}{\left(1 - \frac{f^2}{f_n^2}\right) + \left(2 \frac{c}{c_c} \frac{f}{f_n}\right)^2} \qquad (36)$$

Equations 35 and 36 are plotted in Figures 74 and 75 respectively for convenient reference.

For a given value of damping, the response of a system with a given natural frequency to each component forcing frequency of a complex wave will be:

$$y_1 = T(f_1/f_n)x_1 \sin(2\pi f_1 t - \alpha_1) \qquad (37)$$

$$y_2 = T(f_2 f_n)x_2 \sin(2\pi f_2 t - \alpha_2 + \theta) \qquad (38)$$

The combined response, Y, is obtained by vector addition of the separate responses to each of the component frequencies.

$$\underline{Y} = y_1 + y_2 \qquad (39)$$

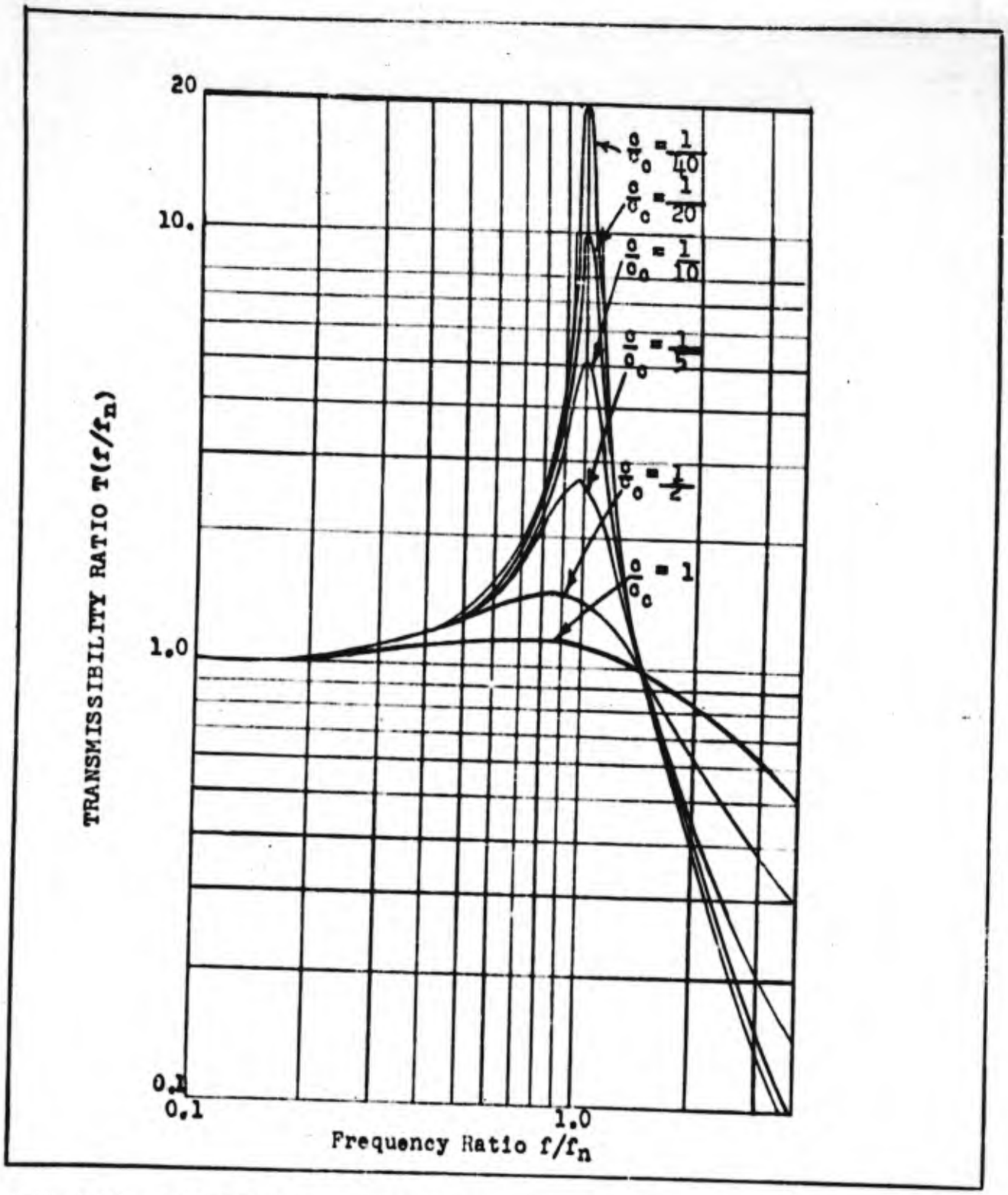

FIGURE 74. TRANSMISSIBILITY RATIO FOR DAMPED SINGLE-DEGREE-OF-FREEDOM SYSTEM

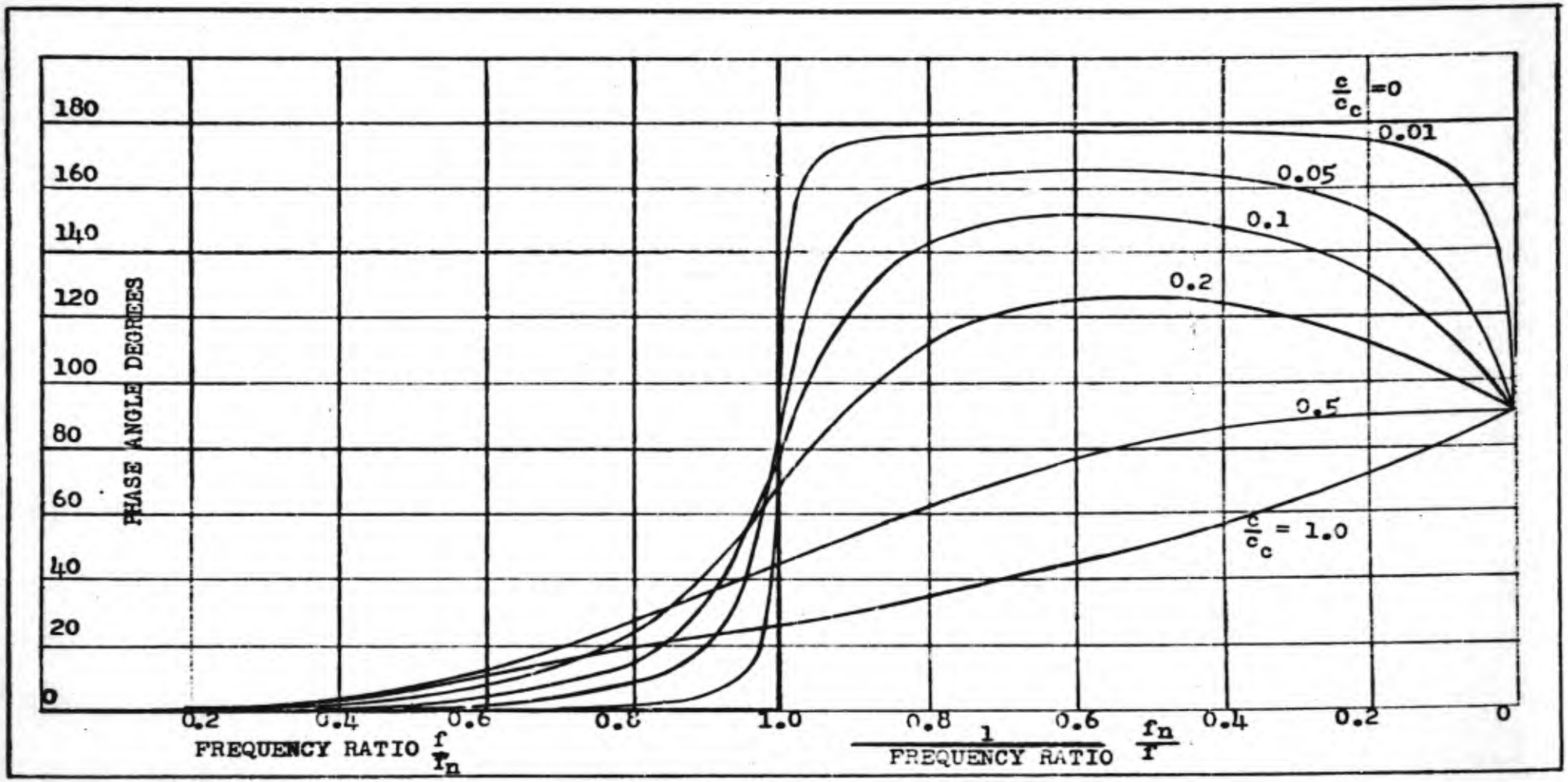

FIGURE 75. PHASE ANGLE BETWEEN APPLIED AND RESPONSE MOTIONS FOR DAMPED SINGLE-DEGREE-OF-FREEDOM SYSTEM

The relationships expressed by equations (34) to (39) are thoroughly documented in the technical literature. See, for example, References 2 and 4 of Appendix V. In order to further illustrate the validity of vectorially adding the separate responses of a simple system to each frequency component of a complex wave, a simple experiment was conducted with the analog computer described in Appendix II. The results of this experiment are summarized in Figures 72 and 73. In these figures, (d) and (e) show the responses of systems with $f_n = f_1$ and $f_n = f_2$ respectively, to the complex input shown in (c). In each case, the damping in the system studies is such that $Q = 10$; i.e., the maximum transmissibility at resonance = 10.

Response to Complex Vibration with $f_1 = 2f_2$

It is of interest to observe in Figure 72 that when the component frequencies in the input complex wave are relatively far apart; i.e., $f_1 = 2f_2$ in this case, the response is a constant amplitude sine wave with no visible distortion. This is due to the relative attenuation of the off-resonant frequency component. It may be seen in Figure 61 that the amplitude of each response is very nearly Q times the amplitude of the resonant frequency component. With the aid of Figures 74 and 75, computations on the responses of systems with $f_n = f_1$ and $f_n = f_2$ respectively have been carried out in Tables XII and XIII to illustrate, by numerical means, what has taken place. Now, in light of the foregoing, consider the amplitude of the complex waveform in Figure 72(c) with regard to visually selecting an amplitude for a vibration test procedure. The complex amplitude in 72(c) is approximately twice the amplitude of the individual frequency components. Hence, if a vibration test were based on this combined or apparent amplitude which would have been tabulated in the "structural" type of analysis described previously, the test would be overly severe by a factor of approximately two times. This illustrates the importance of knowing the method of analysis which has been applied to a recorded waveform when using tabular summaries of data for purposes of establishing a vibration test procedure.

Response to Beat Frequency Vibration

Figures 73 (d) and (e) show the resonant responses of analog systems with $Q = 10$ to the beat frequency input in (c). The input (c) is comprised of equal amplitude components with $f_1 = 1.11\ f_2$, hence the beat amplitude varies alternately

Table XII Numerical Evaluation of $Q = 10$ Response to Complex Vibration with $f_1 = 2f_2$ and $f_n = f_1$.

Frequency Component f	Input Amplitude $\ddot{x}$	Frequency Ratio f/f_n	Transmissibility $T(f/f_n)$	Response Amplitude $\ddot{y}$	Phase Angle α
f_1	1g	1	10	10g	90°
f_2	1g	0.5	1.33	1.33g	01°
				$\Sigma \ddot{y} = 11.33g$	

(when $\ddot{y}_1$ and $\ddot{y}_2$ are in phase)

Table XIII Numerical Evaluation of $Q = 10$ Response to Complex Vibration with $f_1 = 2f_2$ and $f_n = f_2$.

Frequency Component f	Input Amplitude $\ddot{x}$	Frequency Ratio f/f_n	Transmissibility $T(f/f_n)$	Response Amplitude $\ddot{y}$	Phase Angle α
f_1	1g	2	0.34	0.34g	165°
f_2	1g	1	10.0	10.00g	90°
				$\Sigma \ddot{y} = 10.34g$	

(when $\ddot{y}_1$ and $\ddot{y}_2$ are in phase)

between 0 and two times the individual component amplitudes as they phase in and out. The responses for $f_n = f_1$ and $f_n = f_2$ are nearly identical and also vary as a beat. The beat responses vary between 6 and 14 times the individual component amplitudes due to the relatively great amplification of the off-resonant as well as the resonant input frequency components. The computations in Tables XIV and XV illustrate this numerically. Noting that a vibration test of a $Q = 10$ system will produce a steady response of 10 times the input, these results raise the question of whether or not it is unconservative to base tests upon harmonically analyzed amplitudes when the frequency components are close together. The question of whether the best response or the steady-state response is more damaging is beyond the scope of this report. However, it appears likely that application of the accumulative fatigue damage concepts described in earlier sections could establish which condition is most damaging.

Analysis of Acceleration Waveform Produced by Direct Drive Vibration Table

It is generally well known among test engineers that it is extremely difficult to calibrate high natural frequency accelerometers on direct drive type vibration tables. This can be attributed to the fact that as the bearings in the drive mechanism wear, imperceptable displacement waveform variations will be introduced. These minor displacement variations introduce extremely large "hash" variations, superimposed on the fundamental, when the acceleration waveform is observed. In some instances the "hash" almost completely obscures the basic waveform. Figures 76(a), (b) and (c) show portions of a tape recorded accelerometer record obtained from a direct drive vertical vibration table which has been in service for approximately four years. In Figure 76(a) the accelerometer output is filtered to show only the fundamental frequency. Figures 76 (b) and (c) show the same signal without filtering and with slightly different time scales. The vibration table in this particular experiment has a nominal capacity of 100 pounds and in this case is running with a solidly attached load of 60 pounds, at approximately 55 cps and with a total excursion or double amplitude of .060". This setting corresponds with an acceleration (single) amplitude of 9.5g.

In as much as a prime requisite of any testing procedure is to subject specimens to known or controllable conditions, it is a source of concern to observe the high frequency "hash" in Figure 76 during a presumably low frequency sinusoidal vibration test. What will be the effect of this uncontrollable

Table XIV Numerical Evaluation of Q = 10 Response to Beat Frequency Vibration with $f_1 = 1.11f_2$ and $f_n = f_1$.

Frequency Component f	Input Amplitude $\ddot{x}$	Frequency Ratio f/f_n	Transmissibility $T(f/f_n)$	Response Amplitude $\ddot{y}$	Phase Angle α
f_1	1g	1.0	10.00	10.00g	90°
f_2	1g	0.9	4.75	4.75g	20°
				$\ddot{y}_1 + \ddot{y}_2 = 14.75g$	(in phase)
				$\ddot{y}_1 - \ddot{y}_2 = 5.75g$	(out of phase)

Table XV Numerical Evaluation of Q = 10 Response to Beat Frequency Vibration with $f_1 = 1.11f_2$ and $f_n = f_2$.

Frequency Component f	Input Amplitude $\ddot{x}$	Frequency Ratio f/f_n	Transmissibility $T(f/f_n)$	Response Amplitude $\ddot{y}$	Phase Angle α
f_1	1g	1.11	3.92	3.92g	148°
f_2	1g	1.0	10.00	10.00g	90°
				$\ddot{y}_1 + \ddot{y}_2 = 13.92g$	(in phase)
				$\ddot{y}_2 - \ddot{y}_1 = 6.08g$	(out of phase)

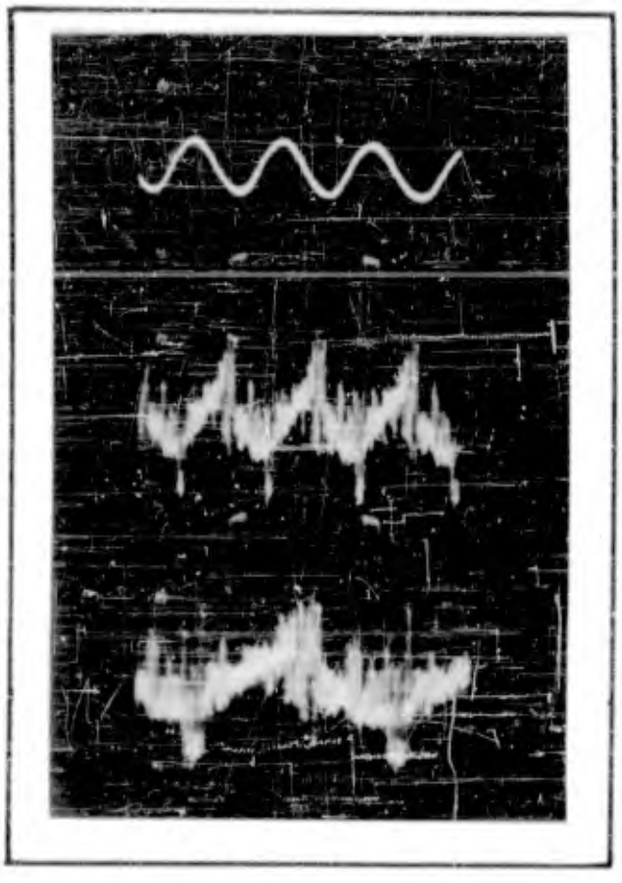

(a) Filtered Accelerometer Signal

(b) Unfiltered Accelerometer Signal

(c) Unfiltered Accelerometer Signal With Expanded Time Axis.

FIGURE 76. TAPE RECORDED ACCELEROMETER RECORD OF DIRECT DRIVE VIBRATION TABLE RUNNING AT 55 cps and .060" DOUBLE AMPLITUDE.

"hash" parameter on complex test specimens comprised of many elements with a variety of natural frequencies? To answer this question the tape record of Figure 76 was first analyzed harmonically to establish its characteristics in detail, and then analyzed by analog computer techniques to determine the nature of equipment responses to this type of input signal. The results of this work are presented in the following paragraphs.

Figure 77 summarizes the results obtained by harmonically analyzing the tape record of Figure 76 with a General Radio type 760-A constant percentage bandwidth analyzer. The bandwidth in cps at the "3db" of the analyzer filter is 2% of the frequency to which the analyzer is tuned, thus permitting relatively fine frequency determination. The readings obtained from the analyzer were extremely steady, which suggests that the frequency components plotted in Figure 77 are steady-state. In order to determine the effect of these components on a system under test, responses of systems resonant with some of the more prominent frequency components in Figure 76 were obtained by analog computer means. Figures 78 and 79 show the responses of systems with Q = 20 and f_n = 165 cps and 330 cps respectively. It can be seen in Figures 78 and 79 that the predominant responses are at the resonant frequencies of the systems although contributions by other frequencies are evident. The 55 cps running speed of the vibration machine is especially prominent. It is perhaps most significant to note in Figures 78 and 79 that the average values of the response amplitudes are approximately Q times the amplitudes indicated by the harmonic analysis of Figure 77. This compares closely with 20 times 3.1g (from Figure 77) or 62g. Numerical analyses similar to Tables XII to XV have been carried out in Tables XVI and XVII for the responses shown in Figures 78 and 79. These computations indicate that the response amplitudes may peak up to maximum enveloping values of 80g and 83g respectively, should all the frequency components fall in phase at any instant.

Vibration theory (Figure 74) indicates a transmissibility ratio of approximately 1, when the natural frequency of a system is several times greater than the applied frequency. Accordingly, if the analyses carried out in the previous paragraphs were not made, it would be anticipated that the response amplitudes in Figures 78 and 79 should be essentially the same as the input, or 9.5g. Inasmuch as the observed responses at high frequencies are several times greater than the input, it must be concluded that direct drive type vibration tables have serious limitations with regard to general testing purposes. For example, it is believed that the direct drive vibration machines can be used quite satisfactorily for testing systems mounted on low natural frequency isolators, because the isolators will attenuate the high frequencies. On the other hand, if the present analysis is typical of direct drive vibration machines in general, such machines should not be used for testing rigidly mounted equipments.

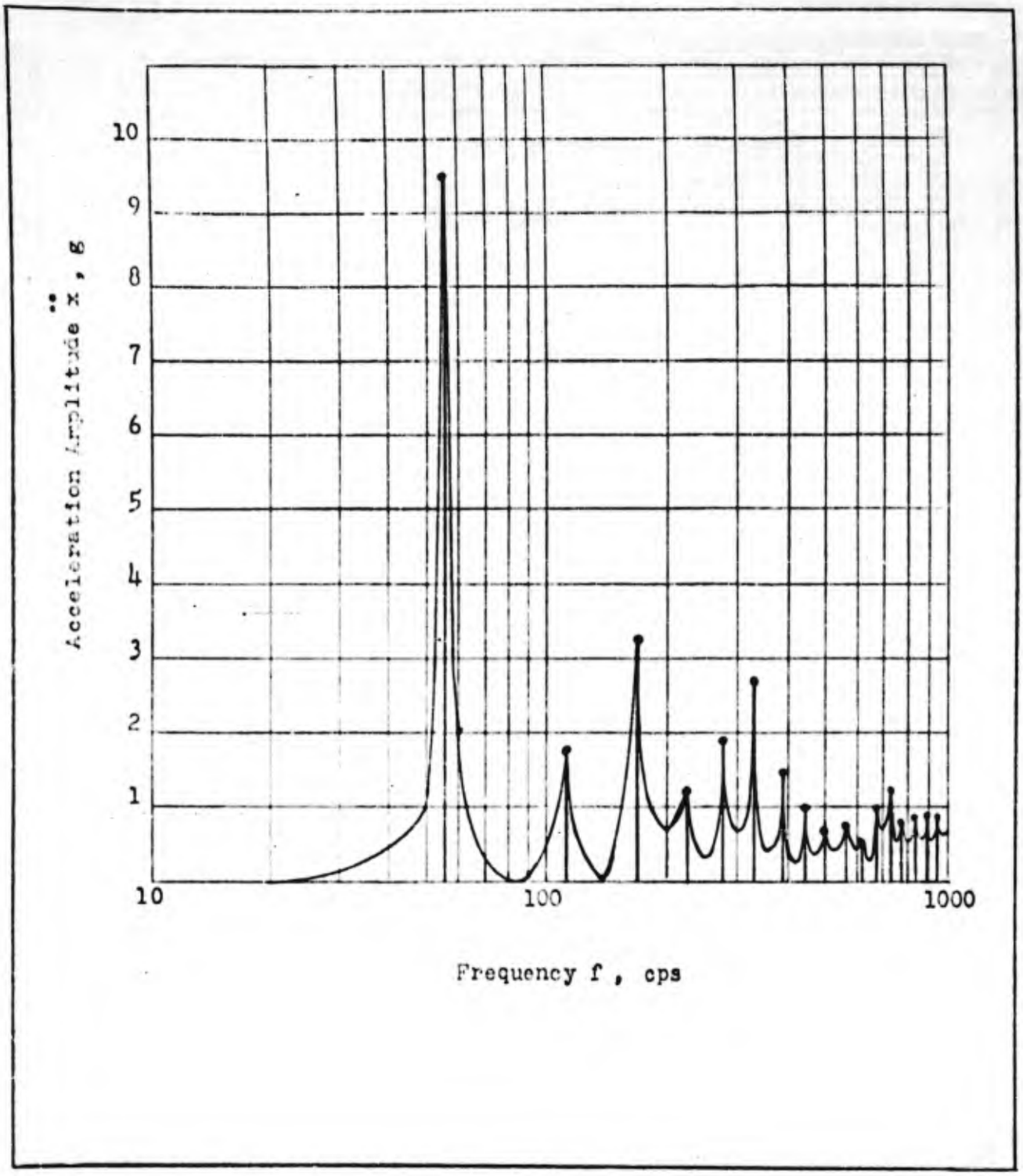

FIGURE 77. HARMONIC ANALYSIS OF DIRECT DRIVE VIBRATION TABLE WAVEFORM IN FIGURE 76

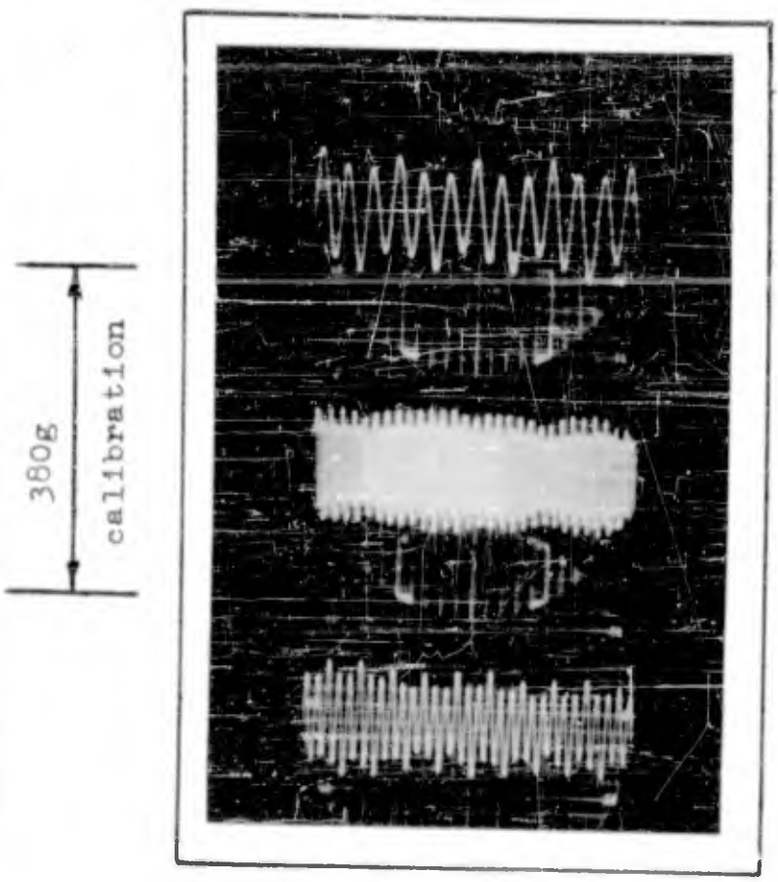

(a) Response

(b) Response, compressed time axis

(c) Response, expanded time axis

FIGURE 78. RESPONSE ACCELERATION OF SYSTEM WITH f_n = 165 cps AND Q = 20 to VIBRATION IN FIGURE 76.

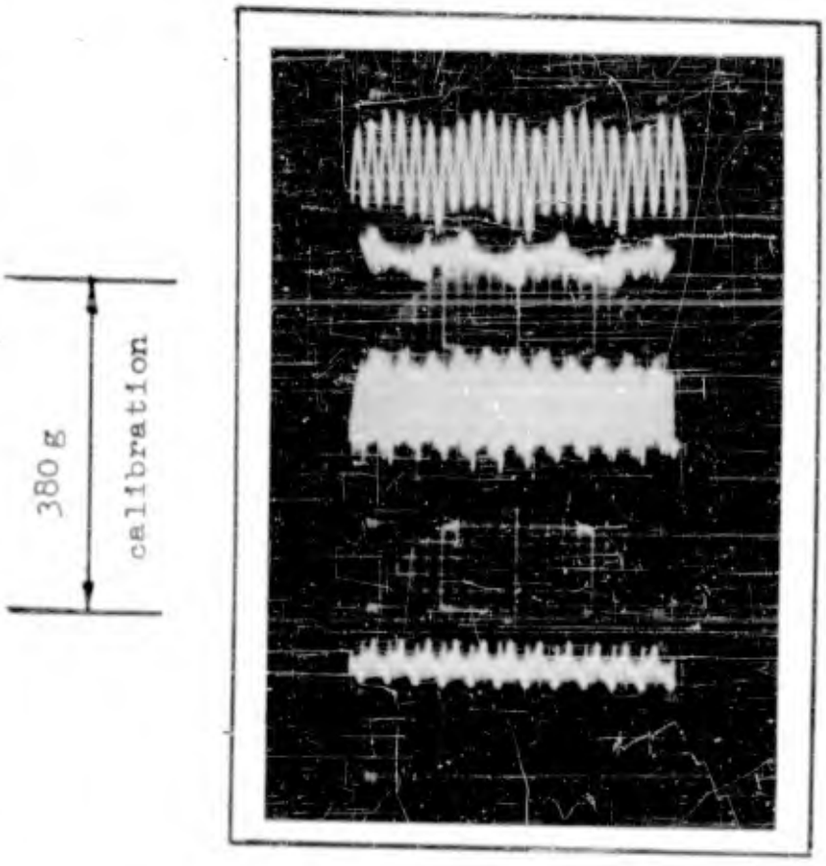

(a) Response
(b) Input
(c) Response, compressed time axis
(d) Input, compressed time axis

FIGURE 79. RESPONSE ACCELERATION OF SYSTEM WITH f_n = 330 cps and Q = 20 TO VIBRATION IN FIGURE 76.

Table XVI Numerical Evaluation of Response of $Q = 20$ $f_n = 165$ cps System to Direct Drive Vibration Table Waveform Based upon Harmonic Analysis in Figure 76.

Frequency Component f	Input Amplitude $\ddot{x}$	Frequency Ratio f/f_n	Transmissibility $T(f/f_n)$	Response Amplitude $\ddot{y}$	Phase Angle α
55 cps	9.5g	1/3	1.15	10.9g	0°
110 cps	1.7g	2/3	1.8	3.1g	0°
165 cps	3.1g	1	20.0	62.0g	90°
220 cps	1.2g	1 1/3	1.3	1.6g	177°
275 cps	1.9g	1 2/3	0.5	0.9g	177°
330 cps	2.7g	2	0.35	0.9g	177°
385 cps	1.4g	2 1/3	0.23	0.3g	

$\sum \ddot{y}$ = 79.7g (when in phase)

Table XVII Numerical Evaluation of Response of $Q = 20$, $f_n = 330$ cps System to Direct Drive Vibration Table Waveform Based upon Harmonic Analysis in Figure 76.

Frequency Component f	Input Amplitude $\ddot{x}$	Frequency Ratio f/f_n	Transmissibility $T(f/f_n)$	Response Amplitude $\ddot{y}$	Phase Angle α
55 cps	9.5g	1/6	1.0	9.5g	0°
110 cps	1.7g	1/3	1.15	1.9g	0°
165 cps	3.1g	1/2	1.36	4.2g	0°
220 cps	1.2g	2/3	1.8	2.2g	0°
275 cps	1.9g	5/6	3.0	5.7g	2°
330 cps	2.7g	1	20.0	54.0g	90°
385 cps	1.4g	1 1/6	3.0	4.2g	176°
440 cps	1.0g	1 1/3	1.2	1.2g	177°

$\sum \ddot{y}$ =82.9g (when in phase)

Transportation and Handling Shock and Vibration

A review of the available data and literature on the nature of the vibration and shock experienced in common carriers indicates that not until relatively recently have field measurements been made of this environment that would be useful in defining vibration environment terms of frequency and amplitude or shock environment in terms of shock spectra or acceleration versus time histories. It is considered that although the vibration and shock environmental data obtained for aircraft have limitations as described in earlier pages, and although aircraft shock data is relatively limited, the information available on shock and vibration environments in aircraft is generally more complete than that available today for the common carrier. It is considered, however, that the conditions of shock and vibration that may be experienced in railroad cars during the humping operation and in trucks in transit over rough highways may be as severe and in some cases substantially more severe than the aircraft shock and vibration environment.

Early attempts in defining the shock and vibration environment in common carriers utilized instrumentation that was limited in frequency range and of somewhat questionable accuracy. In more recent investigations, instrumentation similar to that used in determination of aircraft shock and vibration environment has been used, and it is believed that it is only a question of time when enough statistically significant data will be obtained to permit an investigation similar to the work in this report.

The considerable damage to lading experienced during World War II has precipitated several studies on improvements in packaging methods for road, rail, air and over water shipments. Several investigators have surveyed literature available on common carrier transportation vibration, and shock. See References 116, 117, 118, and 119.

In attempting to establish vibration and shock testing procedures representative of the service environment experienced by electronic components, it is realized that transportation in handling shock and vibration environments should be considered. However, the investigation presented in this report was primarily based upon a collection of vibration data as reported in Reference 65 and the major effort of this investigation was concerned with collection of additional vibration data to bring the environment definition up to date and the collection of as much shock data consistent with the specified period of investigation. Unfortunately, no comparable comprehensive collection of information on ground transportation handling shock and vibration exists at this time to permit a development of testing procedures in a manner analogous to those developed in this report.

The term "ground handling shock" is sometimes used to designate the type of shock experienced by equipment as a result of handling during servicing, installation, and rearrangement in aircraft in common carriers during practical use. It is understood that equipment is sometimes set down on a hard bench or on the floor, or upon a table of an aircraft or common carrier where vibration is normally present. Under these types of handling, isolators often are not present to afford protection to the equipment. While it is conceded that the shock experienced during such handling is of importance, it did not appear possible to include a consideration of these conditions in this analysis for at least two reasons as follows:

(a) This analysis is based primarily upon numerical data represented of service conditions. At the present time enough statistically significant numerical data that would serve to define representative ground handling conditions does not exist.

(b) The avoidance of damage during ground handling conditions should be controllable at least to some degree by proper education of ground handling personnel. Certainly the handling of ammunitions and explosive materials, even under combat conditions, is controlled by the mere nature of the penalty that will be incurred if the material is handled roughly. Improved packaging methods, and considerable effort is being devoted to this problem currently, will go a long way towards reducing damaged incurred during handling. However, a further reduction in damage may be obtained through the proper education of ground handling personnel and damage alleviating techniques.

Use of Isolators

The analysis used in this investigation for both steady-state and transient conditions is based upon the assumption that the equipments being investigated can be idealized as single-degree-of-freedom systems. This is indicated in Figure 1, and the discussion pertaining thereto. Although the natural frequencies of structures in higher modes of vibration are of appreciable significance, it is felt that considerable insight into the strength of equipment subjected to vibration and shock can be achieved by considering the equipments and components thereof as simple systems. When such equipments are supported by isolators, an additional factor is introduced. Considering the equipment to be comprised of concentrated masses and massless springs, the equipment on isolators must be considered as at least a two-degree-of-freedom system. One of the degrees of freedom is associated with the entire equipment on isolators, while the other degree-of-freedom pertains to the individual components with reference to the chassis of the equipment. A doubt may arise concerning the validity of the results obtained on the basis of the single-degree-of-freedom concept. This question can best be answered by considering the steady-state and transient conditions independently.

The laboratory tests which simulate the conditions of steady-state vibration in aircraft are true simulated tests in the sense that the laboratory tests reproduce both the frequency and amplitude of the environment with such modifications as required to compensate for the relatively short duration of the laboratory tests. Isolators are frequency-sensitive elements, with the result that all amplitudes in a system retain their proportionallyy at a given frequency. In other words, the responses of components of the equipment have a certain relation to the environment independent of the vibration amplitude embodied in the environment. The use of isolators, therefore, does not influence the selection of the exaggeration factor employed to select an amplitude for the vibration test which simulates the steady-state aspect of the environment. The analysis which establishes the test for steady-state conditions thus remains rigorous, with or without the use of isolators to support the equipment during tests.

In the transient vibration or shock aspect of the problem, the laboratory test is not a direct simulation in the sense that frequencies and amplitudes are reproduced. The laboratory test is considered to simulate the environment if the responses of a wide range of equivalent systems are equivalent. Under these circumstances, it is probable but not essential that a large response in a system of a particular natural frequency will be the result of vibration present in the environment at this frequency. Inasmuch as isolators are frequency-responsive elements,

they thus tend to function during laboratory testing in a manner similar to that in which they function during actual service. A discrepancy in this reasoning may arise as a result of non-linearity in the isolators, particularly if the non-linearity is severe as in the case of hard bottoming. This introduces a degree of doubt regarding the validity of the test if isolators are used during the simulation of transient vibration or shock.

The above discussion indicates that the use of isolators during steady-state vibration does not invalidate the laboratory test. With regard to the shock tests used to simulate transient conditions, there is a point of doubt introduced primarily by the non-linearity of isolators. It is believed, however, that the conditions will be made more nearly representative of actual conditions by employing isolators than by eliminating them. As a consequence, it is recommended that any equipment mounted upon isolators in actual service installations be similarly mounted during laboratory tests.

SECTION XVIII

CONCLUSIONS

The desired end result of the analysis reported here is a testing procedure for laboratory use, of established validity for certifying that electronic and accessory equipment is qualified to withstand the vibration and shock encountered in aircraft service. Inasmuch as the present program does not include within its scope the actual measurement of vibration and shock in aircraft, reliance must be placed on the use of existing measured data. Unfortunately, the data made available to the Contractor are incomplete in many instances, are of doubtful validity in other instances, and often are not presented in a form that is useful in the type of analysis carried out here. For these reasons, the conclusions set forth here must be regarded as tentative, pending the opportunity to remove the inadequacies in the data.

Although vibration and shock are often referred to as a type of environment, they are basically different phenomena. The former is steady-state in nature, while the latter is transient. Consequently, they require different methods of analysis, the results are presented in different forms, and different testing methods are required. They are considered separately throughout the report, and the conclusions are presented separately.

A recapitulation of the state of knowledge of vibration and shock environment indicates the following:

(a) It is understood that the vibration level experienced in helicopters is relatively severe with predominant vibratory frequencies in the low frequency range. A very limited amount of information on the environment in this type of aircraft is available and is not considered a firm enough basis upon which to define a vibration test specifically tailored for equipment that is to be installed in helicopters.

(b) As indicated in the report, useful data on aircraft landing accelerations is relatively scarce. Information on the vibration and shock experienced during aircraft ground handling conditions which include engine run up, straight taxi runs, and turning conditions is scarce. These ground maneuvering conditions apply significant loading to electronic equipment and it appears that the accelerations experienced during ground maneuvers would generally be transient in nature.

(c) The information presented in the report on steady-state vibration undoubtedly contains some acceleration data which results from the response of the aircraft to atmospheric turbulence or to discrete gusts. However, without access to the original recordings from which the data in Reference (65) were obtained, determination of the classification of these phenomena is impossible. Present investigators are treating, for purposes of airplane structural design, the response of the aircraft structure as being generated by a normally distributed random gust input. It is believed that further investigation of the contributions of randomly occurring gusts to the acceleration response of the airplane is warranted.

(d) Equipments located in the vicinity of either fixed or moveable aircraft armament (machine guns) are subjected to extremely high accelerations which are pseudo-laboratory vibratory in character. The environment generated by gun firing is not only a function of the firing rate of the gun, but also is a function of the flexibility of the attachment of the gun or guns to the primary structure. The problem of determining the reaction of gun firing especially in multiple gun firing installations is quite complex. This area appears worthy of further investigation.

(e) Until relatively recently the problem of defining the environment associated with the flight of aircraft through the transonic speed regime existed only in relatively rare instances. However, with the advent of higher speed aircraft such that transonic flight has become almost routine, the question has been raised as to whether the aerodynamic disturbances may not generate a new environmental area. This area should be explored to determine whether or not the vibration or shock associated with transonic flight is significant with regard to its effect on electronic components and equipments.

(f) It is believed that the collection of environmental data on transportation and handling shock should be further accelerated, especially in the ground handling area. The trend toward the use of improved instrumentation in this field is encouraging, and because of the very nature of this environment the statistical approach employed in the past should be further exploited.

(g) Vibration data obtained for the jet bomber aircraft indicates significant vibration at frequencies that in the past were not recorded, possibly due to limitations in the then existing instrumentation. Measurements of vibration environment in jet aircraft should make use of higher frequency instrumentation.

It is generally conceded that vibration tests should cover the frequency range between the lowest and highest vibration frequency encountered in the actual environment. The range of frequencies may be covered by continuously changing the test frequency in a pattern leading from minimum to maximum and back to minimum. As an alternative, the vibration test may be conducted at discrete frequencies separated by predetermined frequency intervals. For reasons which are set forth in the body of this report, it is concluded that the sweep frequency method is preferable. Recommendations with regard to the vibration test are as follows:

(a) It should be required that equipment installed in reciprocating engined and jet fighter aircraft operate properly while vibrating at any frequency between 5 and 50 cps with a displacement amplitude of 0.030" peak to peak, and at any frequency between 50 and 500 cps with an acceleration amplitude of $\pm$4g. These values represent the Contractor's estimate of expected maximum environment for the subject aircraft. This test is only to insure that the equipment will remain operative when subjected to the actual environment.

(b) The equipment should be required to withstand without failure when installed in reciprocating engined and jet fighter aircraft, vibration at a displacement amplitude of 0.070" peak to peak at all frequencies between 5 and 50 cps, and an acceleration amplitude of $\pm$9.5g at all frequencies between 50 and 500 cps. This test is to be continued for a period of approximately four hours in each of three directions, and involves a rate of change of frequency as set forth in Figure 25 of this report. This is the accelerated vibration test for reciprocating engined and jet fighter aircraft. It is not contemplated that the equipment be required to operate properly during this test, but that it should be operative at the conclusion of the test and it should not sustain damage during the test.

The recommended vibration tests for jet bomber aircraft equipment and components are as follows.

(c) A scanning test at a displacement amplitude of 0.030" peak to peak throughout a frequency range of 5 to 50 cps for a period of 210 minutes, and an acceleration amplitude of 4g throughout the frequency of 50 to 225 cps for a period of 16.9 minutes, a vibration amplitude of 0.0015" throughout the frequency range from 225 to 350 cps for a period of two minutes, and a constant 10g acceleration amplitude from 350 to 1000 cps for a period of 2.50 minutes. This is a sweep frequency test in which the test frequency is continuously varied with any of the rates setforth in Figure 25. This test is intended not to investigate the structural integrity of the equipment, but only to determine that it operates satisfactorly. This vibration test is considered to simulate the expected maximum environment.

(d) Vibration at a displacement amplitude .070" peak to peak throughout a frequency range of 5 to 50 cps for an elapsed time of 210 minutes, vibration at an acceleration amplitude of 9.5g throughout the frequency range of 50 to 225 cps for an elapsed time of 16.9 minutes, vibration at a displacement amplitude of .0036" peak to peak throughout a frequency range of 225 to 350 cps for a period of two minutes, vibration at an acceleration amplitude of 23.7g throughout the frequency range of 350 to 1000 cps for a period of 2.49 minutes. This is a sweep frequency test and any of the rates of change of test frequency as setforth in Figure 25 may be applied. This test is to be continued for a period of approximately four hours in each of three directions. This test is to investigate structural strength. Equipment should not be required to function during this test but should remain undamaged and fully operative at the conclusion of the test.

Transient vibration or shock cannot be defined in terms of frequency and amplitude. Consequently, the preceding type of analysis is inapplicable to a consideration of transient conditions. A time history of the transient environment is required. A group of oscillograms giving the time history of acceleration experienced during landing of aircraft was made available to the Contractor. From this group of records, certain records were selected for analysis. Insofar as could be determined prior to analysis, these records were selected on the basis that they should be the most severe of the group, and represent a diversity of characteristics so that the result would be representative of a range of transient conditions.

As a result of the analysis completed at this time, however, certain tentative opinions may be expressed regarding the shock test:

(a) The analysis does not indicate a level of shock as great as that embodied in the conventional laboratory test involving a height of drop of 13 inches, often referred to as a test with a maximum acceleration of 30g and a duration of 0.011 second. This conclusion apparently is justified, inasmuch as the 13 inch shock test is considered to be representative of crash conditions, and the records available to the Contractor do not include crash conditions.

(b) Current shock testing specifications also call for a shock test involving a free fall of 4 inches, often referred to as a test with a maximum acceleration of 15g and a duration of 0.011 second. This is considered to be representative of severe operating conditions. The analysis carried out here indicates that the shock test should be modified to include a substantially greater number of applications of shock, at a somewhat lower severity.

A recommended shock test specification consists of the following:

(a) The component to be tested shall be subjected to 200 drops on the suitable shock testing machine, 20VI or 150/400VD, depending on the weight of the component or equipment. The machines shall have been modified as shown in Barry Drawings S-3812 and S-4002 to provide the desired shock spectra and repeated drop facility. The 300 drops should be applied in turn, in both directions along each of the three principal axes. The following drop heights shall be employed depending on specimen weight:

Specimen Weight Pounds	Machine	Drop Height Inches
0-20	20VI	1.5
0-400	150/400VD	1.5

The test specimen shall not suffer damage or subsequently fail to provide the performance specified in the detail specifications.

(b) Specimens shall be subjected to one drop in each direction along the principal axes from a drop height of 4.5 inches on the applicable modified 20VI or 150/400VD machine. The specimen shall not suffer damage nor subsequently fail to provide the performance specified in the detail specification.

The analysis of steady-state vibration included in this report is predicated primarily upon the data set-forth in Reference 65. As explained in a preceding paragraph, an attempt was made to re-evaluate the data with the objective of eliminating non-representative portions thereof. This re-evaluation was of a cursory nature, however, because it was not included within the scope of the project as initially established, and resources were not available to make a comprehensive re-examination. The authors remain somewhat dissatisfied with the result, and suggest a comprehensive re-evaluation of steady-state vibration conditions to include the following:

(a) It should be determined by examining representative portions of the original records that the reported amplutudes and frequencies are sufficiently periodic to make a tabular presentation significant. There is reason to suspect that certain data in Reference 65 which appear to indicate steady-state conditions actually refer to transient conditions.

(b) Where amplitudes and frequencies are reported in numerical terms, it should be a requirement of such a presentation that a harmonic analysis of the original oscillogram has been made. Attempts to determine amplitude and frequency of a complex record by inspection may be misleading unless care is exercised.

(c) Much of the data set forth in Reference 65 refer to measurements made at locations within the aircraft not representative of positions for installation of electronic or accessory equipment. Many points were eliminated from the tabular data in Reference 65 by noting the location of the measurement. It is questionable that a mere replot of the tabular data is justified without at the same time examining such data to determine that they represent steady-state conditions, and that the amplitudes refer only to harmonic, steady-state components of the vibration.

(d) Although the flight conditions are not well documented in Reference 65, there is evidence that they represent, in some cases, unusual tactical flight conditions as well as a multiplicity of measurements made in the interests of correcting specific difficulties on particular aircraft. When such circumstances contribute a substantial portion of the data, incorrect conclusions can be drawn concerning the probability of a particular vibration level being encountered in flight.

(e) The vibration data set forth in Reference (65) should be supplemented by vibration data obtained from new aircraft. It is recommended also that data obtained from experimental models be eliminated so that the mass of data tends to indicate probability of occurrence of vibration in existing types of aircraft.

The analysis used in this report is based to a considerable extent upon the strength of materials subjected to repeated cycles of stress. The technical literature abounds with the results of endurance testing of materials, and the results are presented in the form of conventional stress-cycle curves. Ideally, the analysis should be based upon the results of vibration tests in which duplicate equipments are vibrated at various levels of vibration severity, and the number of cycles to failure noted for each severity. Contractor made numerous written and oral inquiries attempting to locate results of vibration tests of this type. It was discouraging to find that only a negligible quantity of test results of this nature are available. It seems evident that such tests must ultimately be conducted to serve as a basic for the formulation of procedures for laboratory testing. A program directed toward obtaining such test results should be encouraged if analyses of the type set forth in this report are to acquire greater validity.

However, until vibration test data for duplicate equipments which are vibrated at various levels of vibration severity can be obtained, further development of the philosophy employed in this report must be related to the S-N investigations for materials. One current investigation which relates to the effect of the sequencing of the load or stress levels on the cumulative damage is currently nearing completion, and the findings from this investigation may be applicable to the philosophy developed from cumulative damage considerations for shock testing. Further effort should be expended in determining or validating the relationship expressed in equation (18) for the relation between stress and acceleration. Further work in determining the value of Miner's constant (K) similar to that conducted by the Contractor for an idealized system will assist in validating or revising some of the assumptions made in the development of a shock test procedure.

A more comprehensive analysis of records is needed, preferably to include a statistical study to determine the probability of occurrence of shock of various levels of severity. This report includes an analysis of a number of landing shocks selected at random from among the oscillograms available. The records were selected on the basis that they appear to be among the most severe insofar as could be estimated from the records themselves, and that they represent a diversity of conditions and aircraft. A composite envelope was drawn representing the most severe aspects of the group of landing shocks being analyzed. The assumption that this composite

envelope would be experienced or duplicated a given number of times in the life of the aircraft appears to be the only logical assumption in the absence of statistical data indicating the probable occurrences of various levels of shock severity.

It is pointed out in this report that a transient vibration or shock can best be evaluated by determining the response of systems subjected to such vibration or shock. This can be done quite readily for single-degree-of-freedom systems having natural frequencies and damping parameters within representative ranges. Many actual equipments involve not single-degree-of-freedom systems but multi-degree-of-freedom systems; non-linear elasticity often exists in place of the assumed linear elasticity. No attempt was made in this analysis to investigate the effect of either added degrees of freedom or non-linearity. While it is believed by the authors that a damped, linear single-degree-of-freedom system may serve as a fairly satisfactory criterion for comparing environmental conditions with laboratory test conditions, it seems evident that future investigations should include the effects of non-linearity and additional degrees of freedom if the method of analysis is to be refined.

This report includes data on the response acceleration which serves to define environmental conditions arising from shock or transient vibration. Methods of using such response data to formulate a requirement for laboratory testing are explained. A brief analysis of current shock testing machines is included and the modifications necessary to two existing types of shock testing machines are described to permit use of these machines in simulating an equivalent amount of damage be repeated drop testing based upon a defined service shock spectrum.

A program should be established to validate the conclusions reached here on the basis of hypothesis and idealization. Such validation can be obtained only by comparing the results of laboratory tests of equipment with the experience gained by operation of such equipment in actual flight environments. It is recommended that a system be established for comparing these experiences. Failure of any equipment, with as much detail on failed components as possible, should be reported to a central agency whenever the failure appears to be the result of vibration or shock. If similar failures are not noted as a result of laboratory testing, there would be an indication that the tests are not effective in simulating the environmental conditions encountered in flight. This would then call for a re-evaluation of laboratory testing conditions. It is recommended that such a data collection procedure be instituted immediately, and that the system include means to compare the results of laboratory testing with actual experience in flight environments.

The ability of equipment to withstand transient environmental conditions is a function not only of the environment but also of the strength of the equipment. A particular equipment may be constructed with relatively great strength and, at the same time be particularly vulnerable to a given environment if the environment includes vibration at frequencies which correspond to the natural frequencies of critical components of the equipment. On the other hand, another equipment with much lower inherent strength may be able to better withstand the same environment because this coincidence of frequencies does not exist. Conclusions reached in this analysis are based upon an idealization of an equipment as a single-degree-of-freedom system. This type of idealization undoubtedly overlooks many important factors which can be included only be extending the analysis to include various types of multi-degree-of-freedom systems. This would make it possible to include the effect of relatively heavy components overlooked in the current analysis, and to better evaluate the effect of isolators. This latter evaluation would be particularly effective if it could include non-linearity in the characteristics of isolators.

APPENDIX I

EVALUATION OF LONGITUDINAL AND CROSS SECTIONAL STRESS DISTRIBUTION FACTORS CONTRIBUTING TO RESONANT RESPONSE

1. Longitudinal stress distribution factor $\underline{K}_s$ for vibrating cantilever beam with distributed mass.

Reference 22 of Appendix V gives the following general expression for $\underline{K}_s$:

$$\underline{K}_s = \frac{\int_o^L (Sa/Sm)^2 \, da}{\int_o^L (Sa/Sm)^n \, da} \qquad (I\text{-}1)$$

Assuming $\underline{n} = 3$ and a longitudinally varying stress such that:

$$S_a = S_m \sin\left(\frac{\pi a}{2L}\right) \qquad (I\text{-}2)$$

then

$$K_s = \frac{\int_o^L \sin^2\left(\frac{\pi a}{2L}\right) da}{\int_o^L \sin^3\left(\frac{\pi a}{2L}\right) da} = \frac{L/2}{4L/3\pi} = \frac{3\pi}{8} \qquad (I\text{-}3)$$

2. Longitudinal stress distribution factor $\underline{K}_s$ for vibrating cantilever beam with concentrated end load.

If the load on the end of the beam is large with respect to the weight of the beam, then the longitudinal stress distribution in the beam may be considered as:

$$S_a = S_m \left(\frac{a}{L}\right) \qquad (I\text{-}4)$$

and

$$K_s = \frac{\int_o^L \left(\frac{a}{L}\right)^2 da}{\int_o^L \left(\frac{a}{L}\right)^3 da} = \frac{L/3}{L/4} = \frac{4}{3} \qquad (I\text{-}5)$$

3. Cross sectional shape stress distribution factor $\underline{K}_c$ for rectangular section.

Reference 22 of Appendix V gives the following general expression for $\underline{K}_c$:

$$K_c = \frac{I \, t_o^{n-2}}{\int_{-t_o}^{t_o} bt^n \, dt} \qquad (I\text{-}6)$$

Solving (I-6) $$K_c = \frac{(n + 1)\ I\ t_o^{n-2}}{2\ bt_o^{n+1}} \qquad (I-7)$$

Substituting for a rectangular cross section $I = \frac{b(2t_o)^3}{12}$

we obtain:

$$K_c = \frac{n + 1}{3} \qquad (I-8)$$

then for $n = 3$

$$K_c = \frac{4}{3} \qquad (I-9)$$

4. Cross sectional shape stress distribution factor K_c for circular section.

Equation (I-6) may be expressed in polar coordinates as:

$$K_c = \frac{I\ t_o^{n-2}}{4\int_o^{t_o}\int_o^{\pi/2} t^{n+1}\sin^n\theta d\theta dt} \qquad (I-10)$$

Solving (I-10) $$K_c = \frac{n + 2}{4t_o^{n+2}} \cdot \frac{It_o^{n-2}}{\int_o^{\pi/2}\sin^n\theta d\theta} \qquad (I-11)$$

Substituting for a circular section $I = \frac{\pi t_o^4}{4}$ we obtain:

$$K_c = \frac{0.196\ (n + 2)}{\int_o^{\pi/2}\sin^n\theta d\theta} \qquad (I-12)$$

then, for $n = 3$

$$K_c = \frac{(0.196)\ (5)}{\int_o^{\pi/2}\sin^3\theta d\theta} = \frac{(0.196)\ (5)}{2/3} = 1.47 \qquad (I-13)$$

APPENDIX II

ANALOG COMPUTER

Where transient vibration or shock is included in the environment, a definition of the environment may be obtained by recording the time history of displacement, velocity or acceleration. In the analysis carried out in this report, the environment is defined in terms of acceleration as shown by the acceleration-time curves set forth as insets to the Figures of Appendix III. As explained in Section 9 of this report, the severity of the environment is evaluated by determining the acceleration response of single-degree-of-freedom systems having various natural frequencies and various degrees of damping. This Appendix describes the analog methods used to obtain the responses.

The system being investigated is shown by the schematic diagram in Figure 80 where x indicates the displacement of the airframe structure and y indicates the displacement of any equipment component attached to the airframe. The mass m, stiffness k, and damping coefficient c define the physical characteristics of the component whose response is to be determined. The differential equation of motion of the mass m is written as follows:

$$m\ddot{y} = c(\dot{x}-\dot{y}) + k(x-y) \qquad \text{(II-I)}$$

Letting the relative motion of y with respect to x be represented by a new variable $\delta = x - y$, equation II-I may be rewritten as follows:

$$m(\ddot{x}-\ddot{\delta}) = c\dot{\delta} + k\delta \qquad \text{(II-2)}$$

This equation may be written:

$$m\ddot{y} = c\dot{\delta} + k\delta \qquad \text{(II-3)}$$

Collecting all terms containing δ in equation II-2 on the right hand side of the equation:

$$m\ddot{x} = m\ddot{\delta} + c\dot{\delta} + k\delta \qquad \text{(II-4)}$$

Equation (II-4) may be expressed in block diagram form as shown in Figure 81 . In this Figure, the blocks indicated by J perform the operation of integration, those indicated

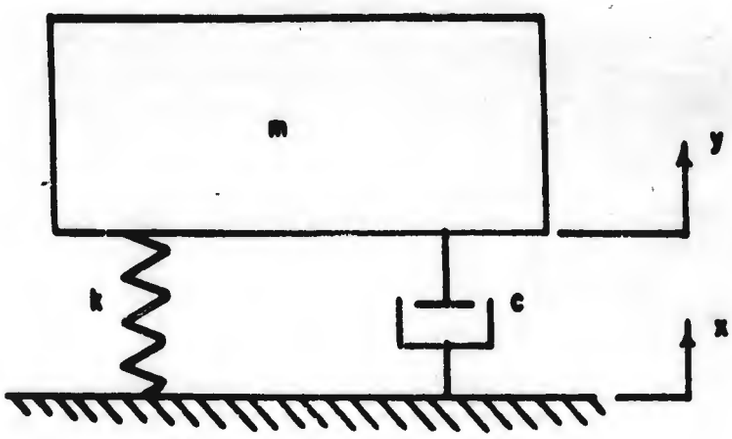

FIGURE 80. DAMPED, SINGLE-DEGREE-OF-FREEDOM SYSTEM WHOSE RESPONSE IS DETERMINED ON ANALOG COMPUTER.

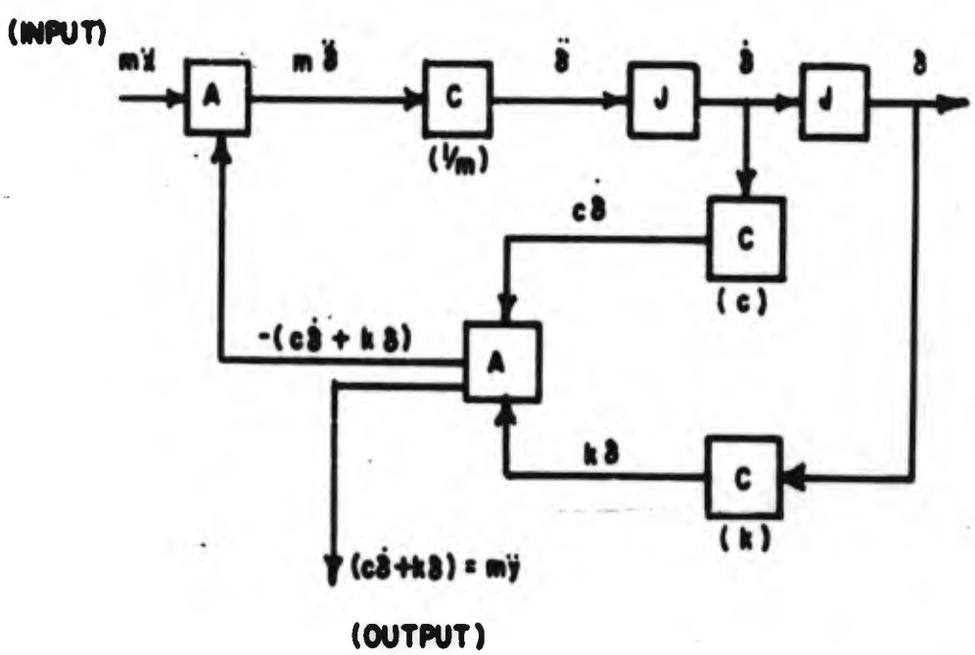

FIGURE 81. OPERATIONAL BLOCK DIAGRAM FOR EQUATION (II-4).

by C perform the operation of multiplication by a constant wherein the constant is given in parentheses below the block, and those indicated by A perform the operation of addition of several quantities. All operations take place in the direction indicated by the arrows. The environment is defined by $\ddot{x}$ which is, in effect, multiplied by the coefficient m to obtain the input $m\ddot{x}$ to the analog computer. The output is $m\ddot{y}$, in accordance with equation (II-3). This is converted to the desired response acceleration $\ddot{y}$ by dividing, in effect, by the constant m used initially to convert $\ddot{x}$ to $m\ddot{x}$.

The electrical analogy method consists of employing electrical quantities corresponding to the variable terms in equation (II-4), and performing the indicated integration, in the order indicated by the block diagram of Figure 81. Equipment for performing these operations electrically is available commercially from several sources. The project described in this report does not justify the cost of analog computer components of relatively great accuracy, because the acceleration records which define the environments in aircraft are generally not precise. Taking these limitations into consideration, an analog computer suitable for this investigation has been assembled from components manufactured by George A. Philbrick Researches, Inc. of Boston. Each component represented by one of the blocks in Figure 81 is self-contained; it embodies a housing and convenient output and input terminals together with a dial for adjusting the characteristics of the component. These components, together with the necessary power supply, rack and attaching cables, are assembled together as shown at the right hand side of the photograph constituting Figure 82.

The input to the computer is a voltage proportional to $\ddot{x}$ which varies with time in an irregular manner. It was necessary to construct a special function generator to generate a voltage proportional to the ordinate on the acceleration-time diagrams shown as insets to the Figures in Appendix I. A special function generator suitable for this purpose was designed and constructed by Professor James R. Keswick of the Mechanical Engineering Department of the Massachusetts Institute of Technology. This function generator is shown with its cover elevated on the wheeled table at the center of the photograph in Figure 82.

A schematic view of the function generator is shown in Figure 83. It is comprised basically of an oscilloscope, a transparent drum mounted on a turn table, and a photo multiplier tube. The record which is being studied must be traced with a heavy dark line on transparent material and then attached to the transparent drum. The record is rotated in front of the oscilloscope screen, and the photo multiplier tube causes the beam of the cathode ray tube to follow the dark line of the record as it is rotated in front

FIGURE 82. PHOTOGRAPH SHOWING ANALOG COMPUTER AND FUNCTION GENERATOR

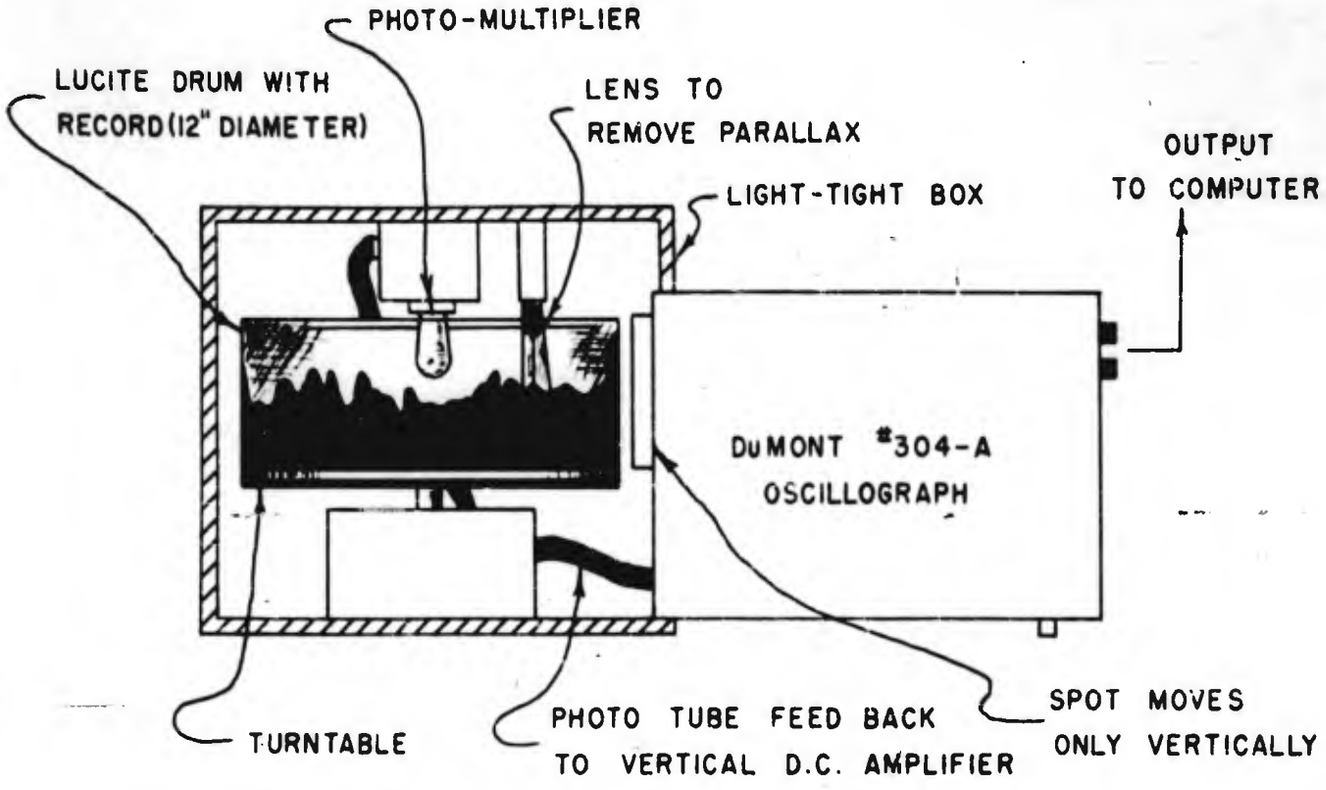

FIGURE 83. SCHEMATIC VIEW OF FUNCTION GENERATOR

of the tube. This occurs because the beam has a constant upward potential; when it stays above the dark line, the photo multiplier tube feeds a voltage back into the vertical DC amplifier of the oscilloscope and drives the beam down behind the dark line. Consequently, the beam of the oscilloscope rides below the edge of the dark line of the record, and the varying voltage necessary to hold the beam on the dark line can be picked off the plate terminals at the back of the oscilloscope.

The circumference of the transparent drum is approximately 36 inches. The function generator thus accommodates any random record of this length and converts it into a steady-state function because it repeats itself at each revolution of the drum. The voltage which is picked off the plate terminals of the oscilloscope thus represents this steady-state function; it can be viewed on another oscilloscope or used as the input to the analog computer. In the work reported herein, a Dumont Type 322 Dual Beam Oscillograph is used with the function generator and analog computer so that both the input to and the output from the analog computer can be observed simultaneously.

An investigation was carried out to establish the equivalence of the response of a system as determined by the function generator and analog computer to the actual response of a mechanical structure subjected to a shock motion. This was done to gain confidence in the accuracy and validity of the analog computer and function generator. The mechanical structures used for this investigation were five cantilever beams, ranging in natural frequency from 30 to 500 cps. The beams were subjected to the shock motion produced by the Type 150 VD Shock Machine, and the strain in each beam was measured by a SR-4 strain gage feeding through a carrier type amplifier and detector into the channel of a Dumont Type 322 Dual Beam Oscillograph. The outputs of the strain gages were recorded photographically. Simultaneously with the measurement of strain in each cantilever beam, the time history of the acceleration on the elevator of the shock machine were recorded by a Calidyne accelerometer having a natural frequency of 1050 cps placed adjacent to the beam.

A typical record obtained from the tests of the cantilever beams is shown in figure 84 (a). The 60 cps calibration traces at the upper part of the record each have an amplitude of 30g peak-to-peak. The next trace is the accelerometer output and the bottom most trace is the strain of a cantilever beam having a natural frequency of 493 cps. The accelerometer record was enlarged four times by photographic means, traced on acetate, and attached to the transparent drum of the function generator. The analog computer was set to compute the response of a system having a natural

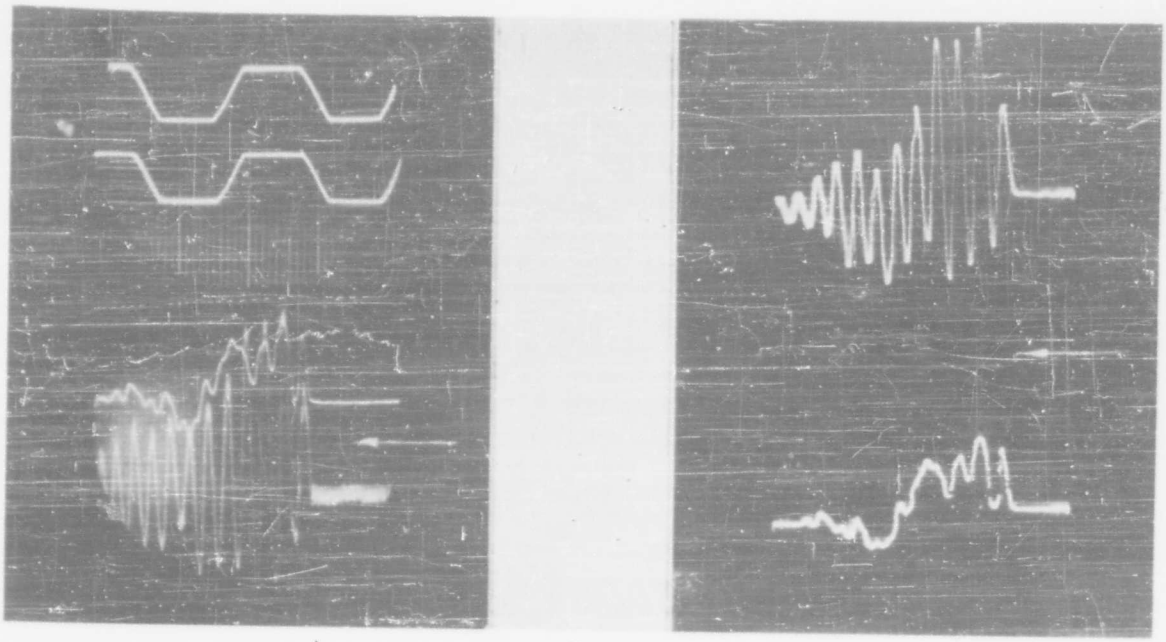

(a)

(1) Calibration trace - 60 cps. and 30g peak-to-peak.
(2) Same as (1).
(3) Acceleration measured on Table of Type 150-400 VD Shock Machine.
(4) Strain in cantilever beam mounted on Table - Natural frequency = 493 cps.

(b)

(1) Response of analog circuit with natural frequency of 493 cps. to trace (2).
(2) Trace (a) 3 as reproduced by function generator.

Figure 84. Comparison of response of analog circuits to actual physical response.

frequency of 493 cps the accelerometer record as reproduced by the function generator. Figure 84(b) shows the results of this work. The response as determined by the analog computer is shown as the upper trace in Figure 84(b) and the reproduction of the accelerometer record by the function generator is shown as the lower trace. Comparison of Figures 84(a) and 84(b) shows excellent correlation between the experimentally obtained response of the beam system and the results obtained from the analog computer. The slight wavering of the lower trace in Figure 84(b) is attributed to a bad contact in the time generating potentiometer of the function generator. This has since been corrected.

It was noted that systems with small degrees of damping could not be studied accurately on the analog computer because oscillations were present from the solution generated at the immediately preceding revolution of the drum of the function generator. This introduced a slight error because these oscillations were superimposed upon the solution generated at each subsequent revolution of the drum. The function generator has been reworked to incorporate a "clamping device" which automatically zeros the computer after each complete revolution of the record drum.

The analog computer described in this Appendix has received extensive use in the investigation and evaluation of environmental conditions defined by transient records. Approximately 350 response accelerations have been determined, representing the responses of systems having various natural frequencies and damping constants to the landing shocks recorded in various aircraft. The analog computer and the accompanying function generator have been found reliable and convenient to operate. For the purposes of this study, the analog computer is considered to be practical in evaluating transient conditions.

APPENDIX III

BLOCK DIAGRAMS OF RESPONSE ACCELERATION

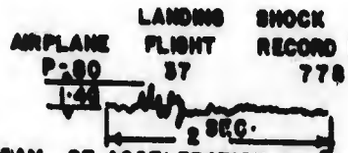

OSCILLOGRAM OF ACCELERATION AS A FUNCTION OF TIME MEASURED ON AIRCRAFT DURING LANDING (INPUT TO ANALOG COMPUTER).

COORDINATES FOR BLOCK DIAGRAMS

HORIZONTAL-RESPONSE ACCELERATION, g.

VERTICAL - NUMBER OF OCCURRENCES AT EACH ACCELERATION LEVEL.

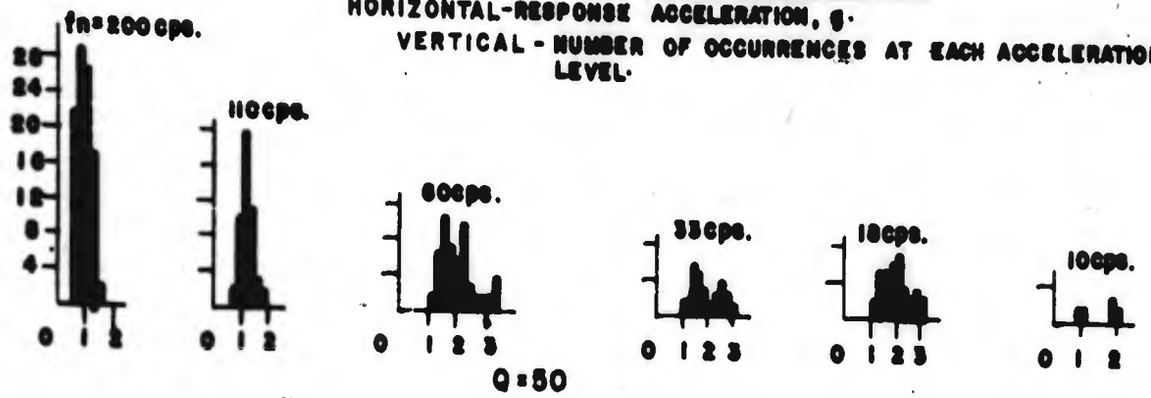

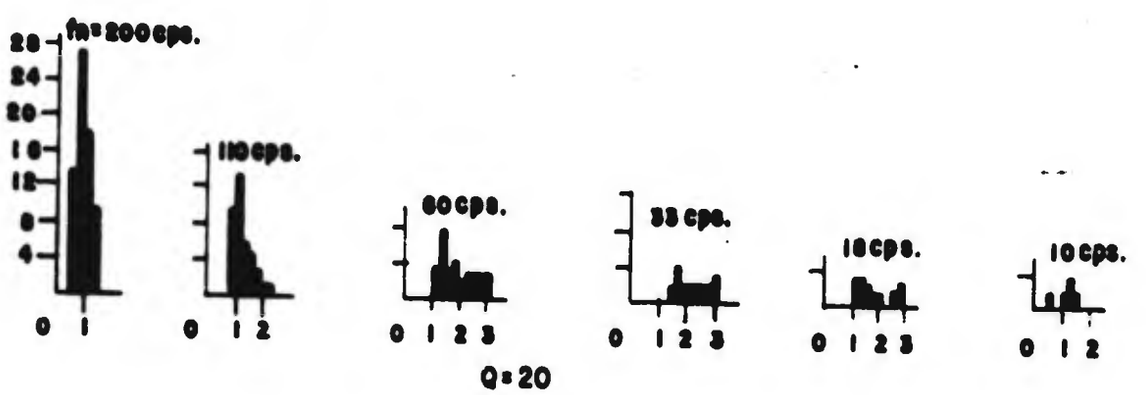

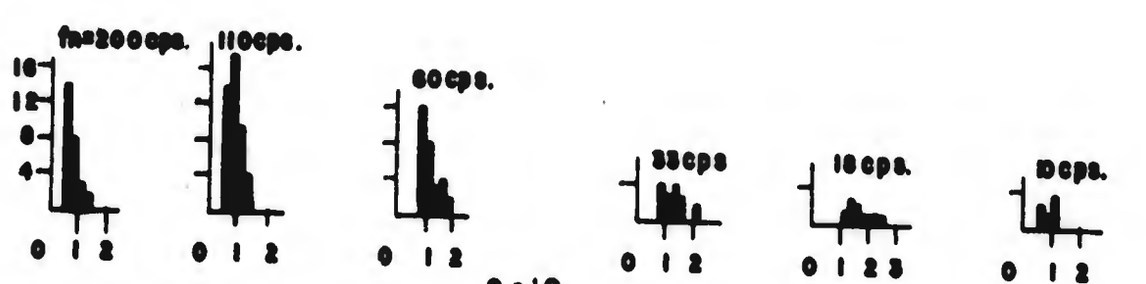

FIGURE 85. BLOCK DIAGRAMS OF RESPONSE ACCELERATION AS A FUNCTION OF NUMBER OF OCCURRENCES FOR SYSTEMS HAVING Q=10, 20, & 50, SUBJECTED TO P-80 LANDING SHOCK.

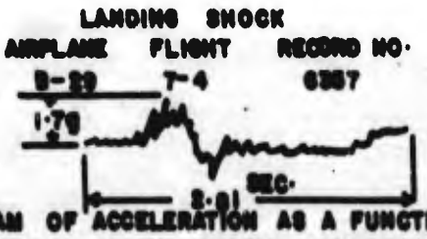

OSCILLOGRAM OF ACCELERATION AS A FUNCTION OF TIME MEASURED ON AIRCRAFT DURING LANDING (INPUT TO ANALOG COMPUTER).

COORDINATES FOR BLOCK DIAGRAM

HORIZONTAL - SCALE - RESPONSE ACCELERATION, g.
VERTICAL - SCALE - NUMBER OF OCCURRENCES AT EACH ACCELERATION LEVEL.

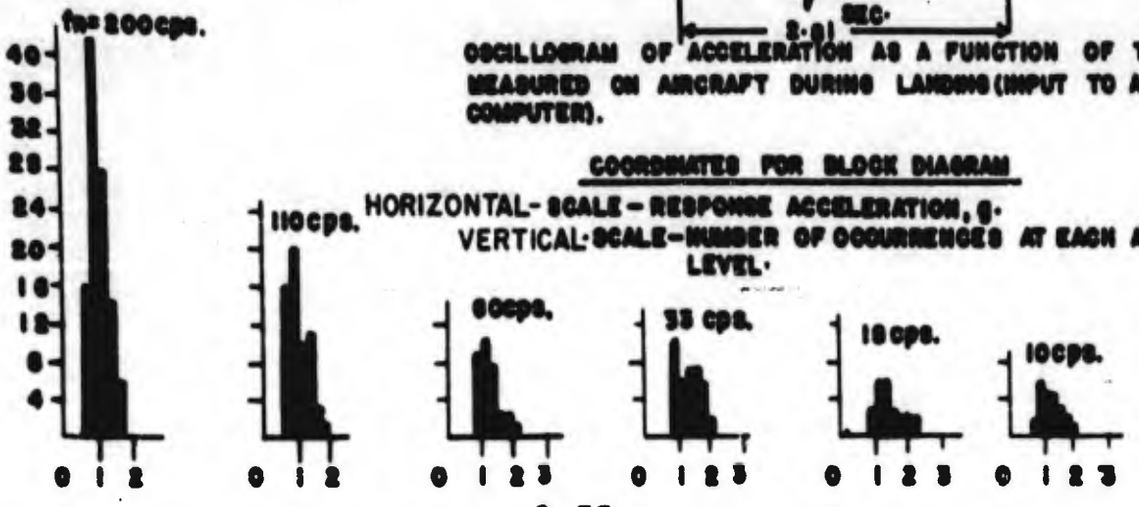

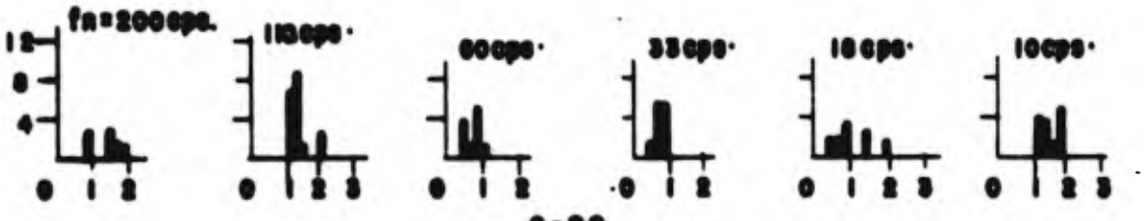

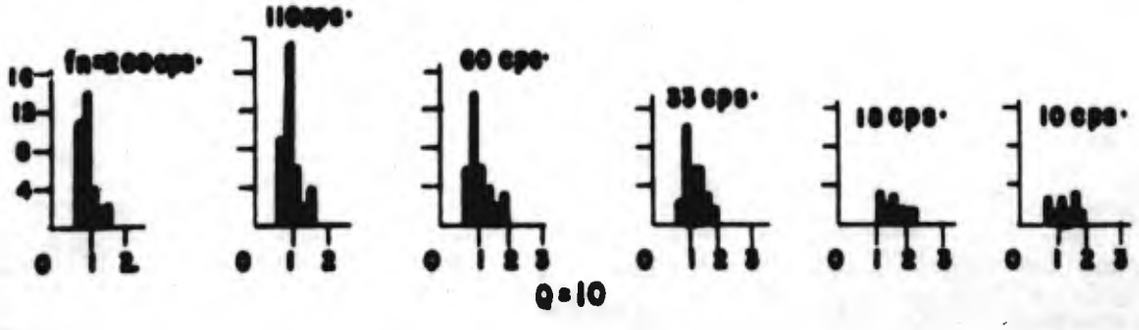

FIGURE 86. BLOCK DIAGRAMS OF RESPONSE ACCELERATION AS A FUNCTION OF OCCURRENCES FOR SYSTEMS HAVING Q = 10, 20, 50, SUBJECTED TO B-29 LANDING SHOCK.

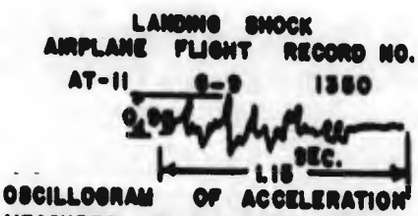

OSCILLOGRAM OF ACCELERATION AS A FUNCTION OF TIME MEASURED ON AIRCRAFT DURING LANDING (INPUT TO ANALOG COMPUTER)

COORDINATES FOR BLOCK DIAGRAMS.

HORIZONTAL - RESPONSE ACCELERATION, g.

VERTICAL - NUMBER OF OCCURRENCES AT EACH ACCELERATION LEVEL.

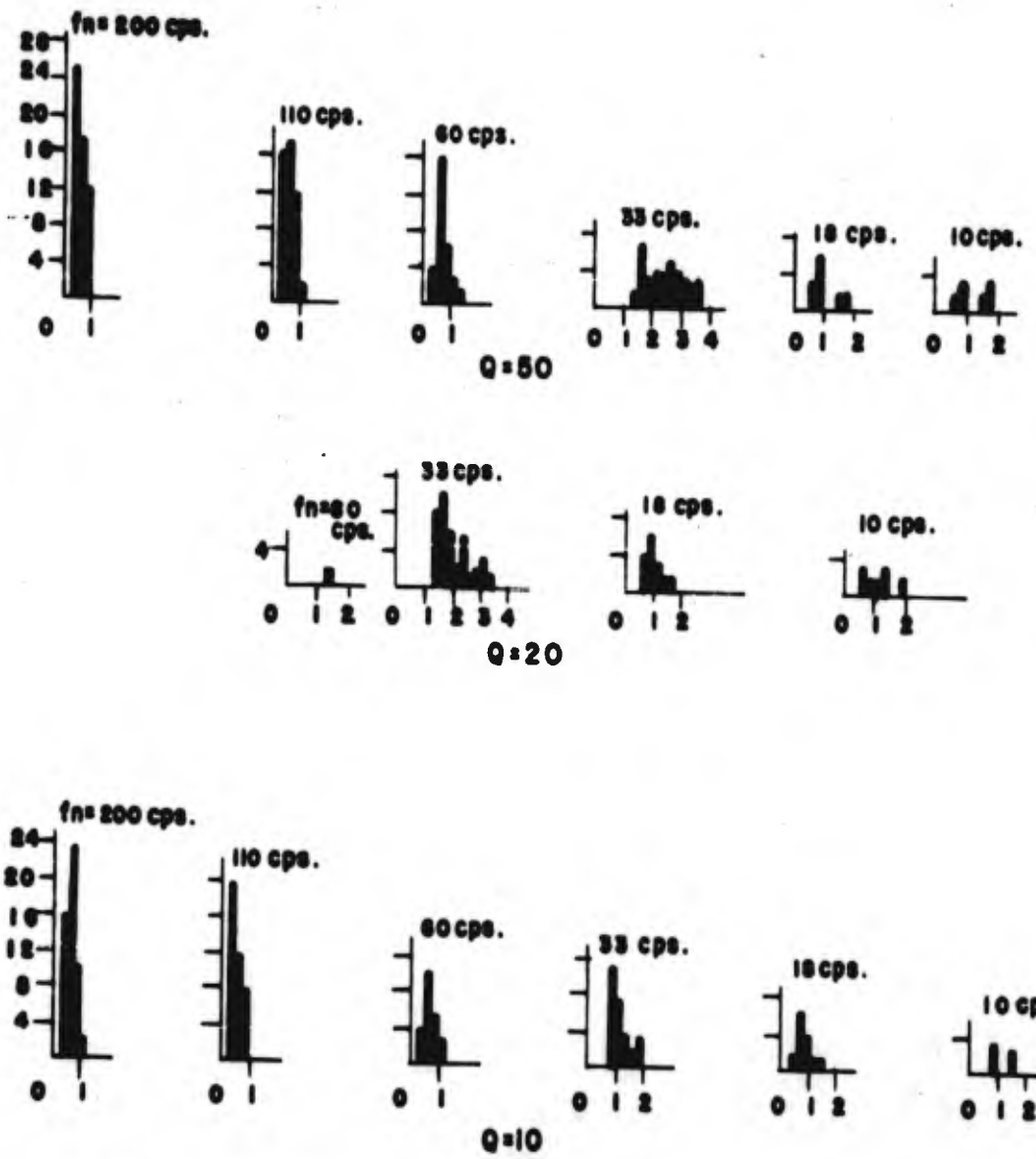

FIGURE 87. BLOCK DIAGRAMS OF RESPONSE ACCELERATION AS A FUNCTION OF NUMBER OF OCCURRENCES FOR SYSTEMS HAVING Q=10,20,& 50, SUBJECTED TO AT-11 LANDING SHOCK.

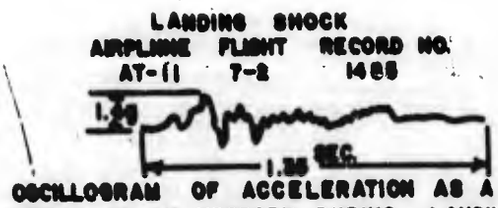

OSCILLOGRAM OF ACCELERATION AS A FUNCTION OF TIME MEASURED ON AIRCRAFT DURING LANDING (INPUT TO ANALOG COMPUTER)

COORDINATES FOR BLOCK DIAGRAMS

HORIZONTAL - RESPONSE ACCELERATION, g.

VERTICAL - NUMBER OF OCCURRENCES AT EACH ACCELERATION LEVEL.

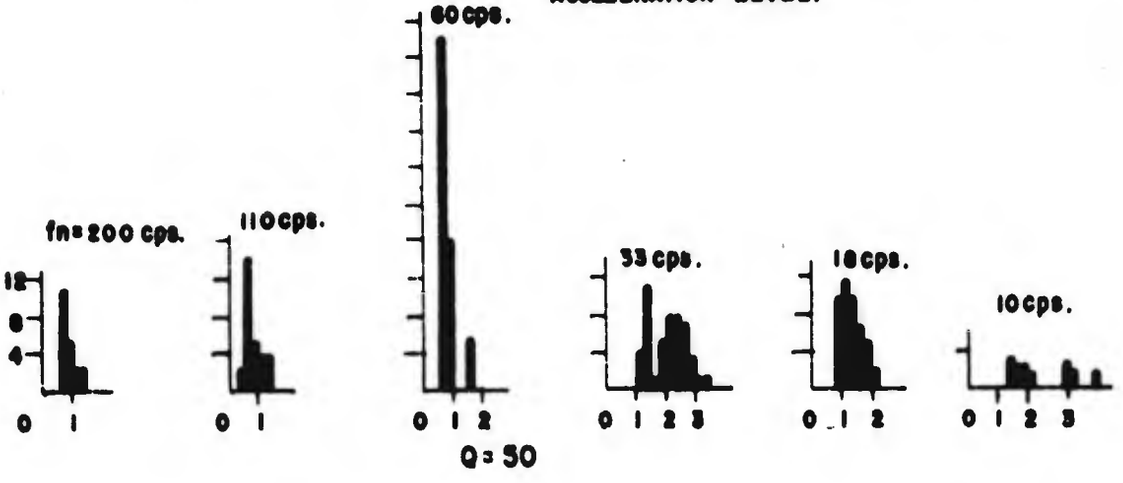

FIGURE 88. BLOCK DIAGRAMS OF RESPONSE ACCELERATION AS A FUNCTION OF NUMBER OF OCCURRENCES FOR SYSTEMS HAVING Q=10,20, 50, SUBJECTED TO AT-11 LANDING SHOCK.

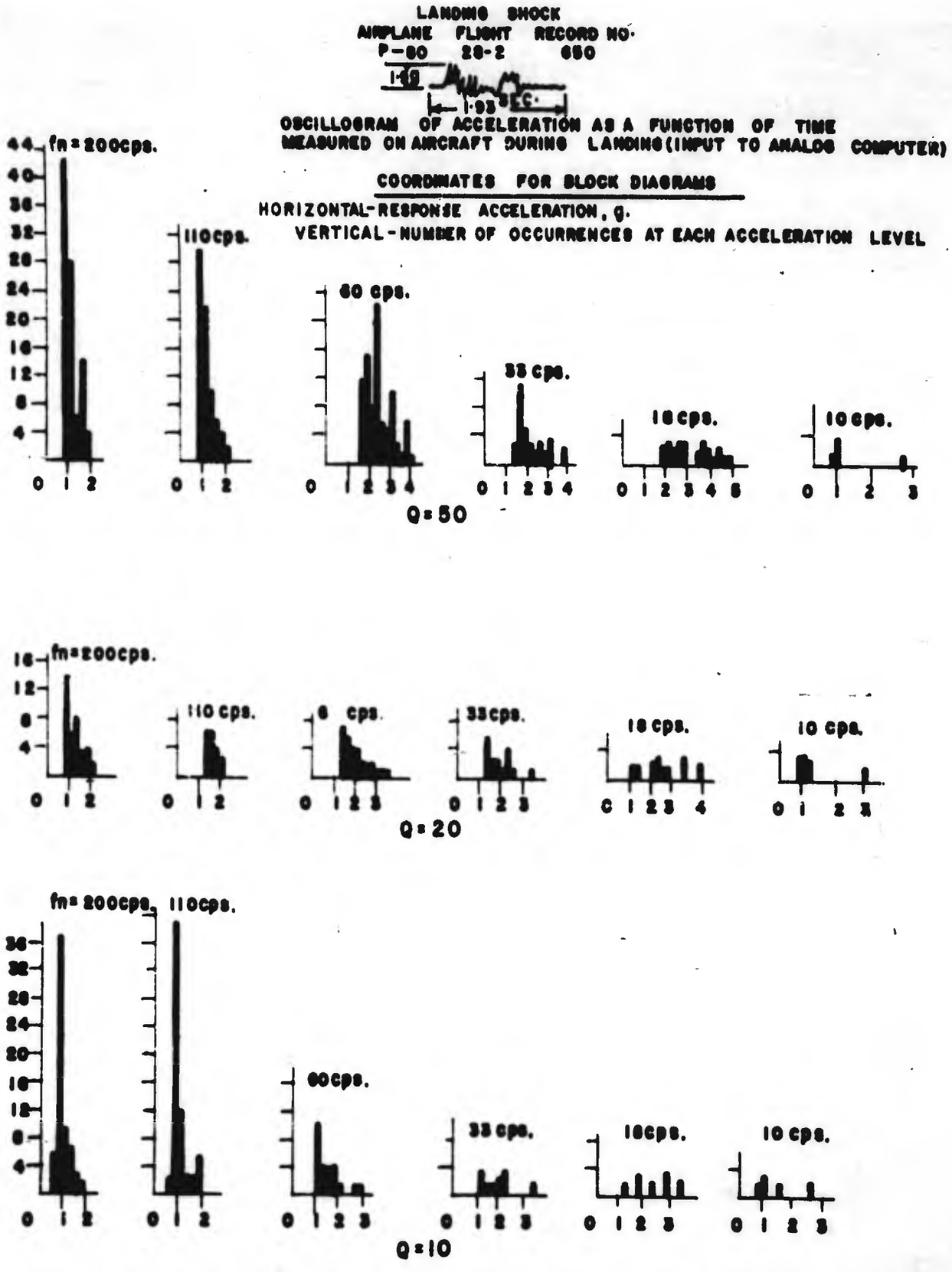

FIGURE 89. BLOCK DIAGRAMS OF RESPONSE ACCELERATION AS A FUNCTION OF NUMBER OF OCCURRENCES FOR SYSTEMS HAVING Q=10, 20, & 50, SUBJECTED TO P-80 LANDING SHOCK.

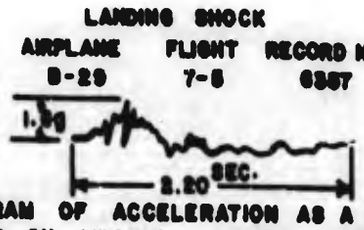

OSCILLOGRAM OF ACCELERATION AS A FUNCTION OF TIME MEASURED ON AIRCRAFT DURING LANDING (INPUT TO ANALOG COMPUTER).

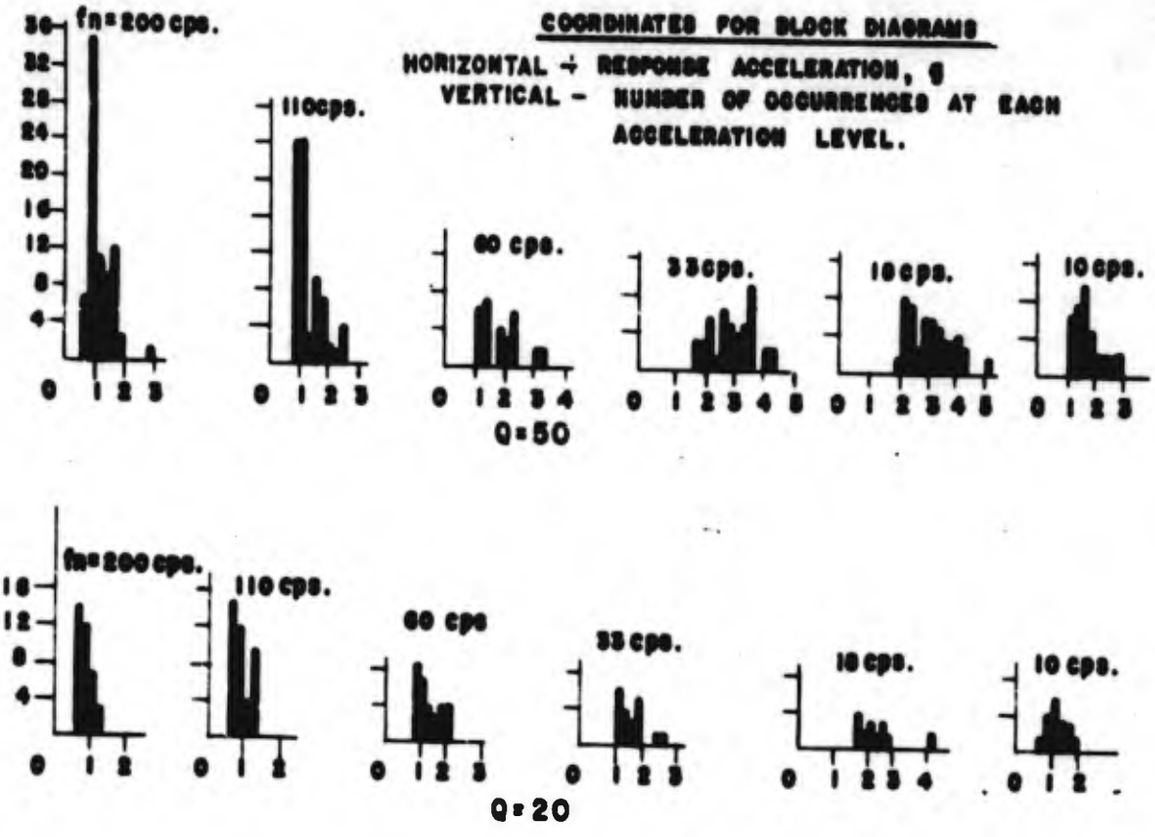

FIGURE 90. BLOCK DIAGRAMS OF RESPONSE ACCELERATION AS A FUNCTION OF NUMBER OF OCCURRENCES FOR SYSTEMS HAVING Q=10, 20, 50, SUBJECTED TO B-29 LANDING SHOCK.

APPENDIX IV

SELECTION OF ARRESTING PADS FOR SHOCK MACHINES

In contrast to the more mechanical design problems associated with conversion of the existing 20VI and 150/400VD Shock Machines to repeated impact or automatic operation, the problem of selecting a suitable arresting means for the elevator was approached from an experimental standpoint. Past experience with a cam operated repeated impact testing machine which employed rubber blocks for arresting the elevator indicated that the rubber block arresting means would probably be best suited for converting the existing shock machines.

Consequently, the approach employed consisted of designing a family of rubber pads suitable for each machine which varied in geometric shape and stiffness. In the case of each machine a pair of rubber pads are employed, one attached to the elevator and one attached to the anvil. In Figure 91 the geometric, material and durometer characteristics of each of the pads tested are described. As shown in Figure 91 all the pads were cylindrical in shape with the base or attaching ends of each pad bonded to a circular steel plate suitable for attachment to the elevator or anvil of the particular shock test machine.

The table acceleration during each shock test was measured employing a Calidyne Model 18B Accelerometer which had a natural frequency of 475 cycles per second. The accelerometer output was recorded on a dual beam oscilloscope employing a Polaroid Land Oscilloscope Camera.

Typical acceleration time histories of the elevator acceleration are shown in Figure 92. One set of photographs in this figure shows the shape of the first pulse experienced for a two (2) inch drop height employing the 20VI machine and pad number 1281-1.6 and the 150/400VD machine and pad number 1469. Both pads were made of natural rubber. The second set of photographs in Figure 92 shows the acceleration time history for the same drop condition but depicts the successive rebound impacts. It will be noted that at least ten (10) significant successive rebound accelerations are experienced before the elevator comes to rest. It may also be noted that the first pulse is relatively clean and is approximately sinusoidal in shape.

Response spectra were obtained for the various rubber pad configurations and for various drop heights for both the 20VI and the 150/400VD machines. These response spectra, each for a single drop, are shown in Figures 93 and 94. Upon examination of these figures it will be noted that the spectra are relatively flat in the region of 100-200 cycles per second, and that in all cases except one the maximum response acceleration

20 VI MACHINE PADS

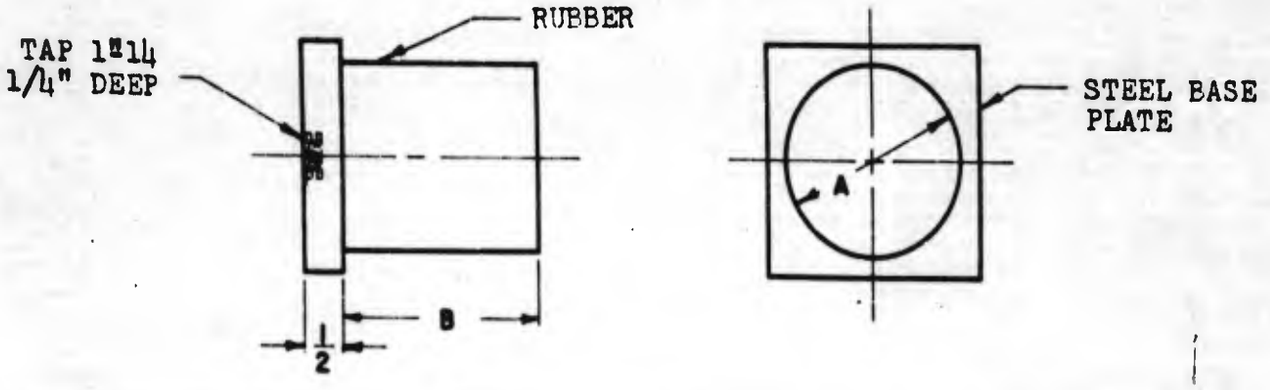

PAD NO.	DIMENSIONS		COMPOSITION	DUROMETER
	"A"	"B"		
1282	3.62	2.52	NATURAL	35
1281-75	2.13	0.75	NATURAL	55
1281-1.6	2.13	1.63	NATURAL	55
1281-1.6BU	2.13	1.63	BUTYL	55

150/400 VD MACHINE PADS

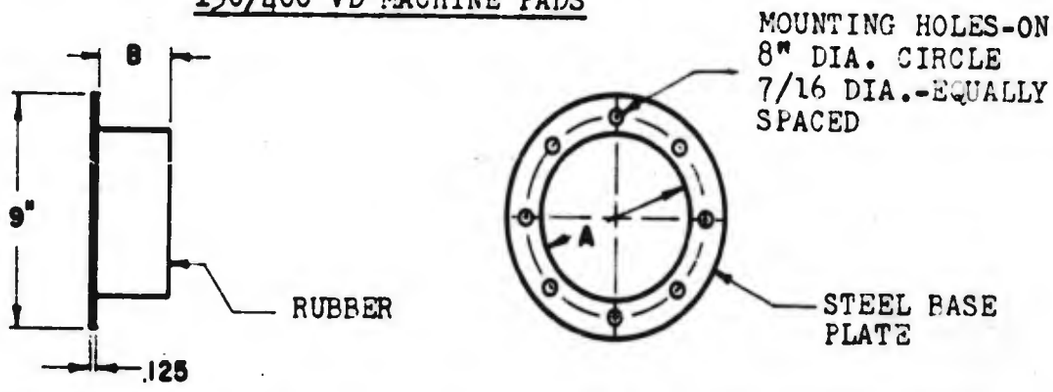

PAD NO.	DIMENSIONS		COMPOSITION	DUROMETER
	"A"	"B"		
1468	7.1	1.7	NATURAL	50
1469	6.4	2.4	NATURAL	55
1470	6.0	1.2	NATURAL	55
1471	5.1	0.80	NATURAL	65
1472	4.9	1.3	NATURAL	65
1469BU	6.4	2.4	BUTYL	55

FIGURE 91. CONFIGURATION OF ARRESTING PADS TESTED

20 VI MACHINE

150/400 VD MACHINE

15g Double Amplitude
60 cps

First Impact Pulse

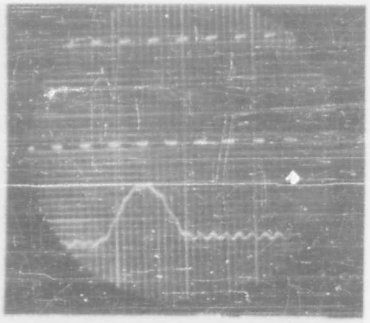

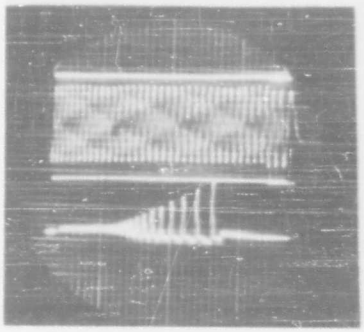

15g Double Amplitude
10 cps

Complete Impact

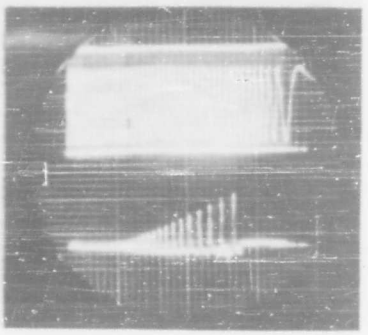

FIGURE 92. TYPICAL TABLE ACCELERATION CHARACTERISTICS WITH RUBBER PAD ARRESTMENT - 20 VI AND 150/400 VD MACHINE

occurs between 10 and 20 cycles per second. It should also be noted that the response spectra have been plotted on linear graph paper rather than logarithmic. Inasmuch as selection of the proper pad for each shock test machine should be based on achieving a spectrum shape generally similar to that derived for the service shock conditions, it is apparent that the spectra achieved with all the natural rubber pads provide undesirably large response acceleration values in the 10 to 60 cps natural frequency range.

Although there was not too much choice between the spectra provided by pad number 1468 and 1469, pad number 1469 was selected as the most desirable of the natural rubber lot and a similar pad with the same geometric and durometer characteristics was molded up of butyl rubber. Butyl rubber has somewhat different elastic and internal damping properties than natural rubber. A comparison of the response spectra achieved with the number 1281-1.6 butyl rubber pad on the 20VI machine and the 1469 butyl rubber pad on the 150/400 machine with the same pads of natural rubber is shown in Figures 95 and 96. It will be noted that the butyl rubber pad response spectra have a pronounced decrease in response acceleration below 60 cycles when compared to the response accelerations for the natural rubber pads for the same dropping height. The single drop response spectra obtained on each of the two machines are quite similar in shape although it will be noted that for the same height of drop the 20VI spectrum is appreciably higher in acceleration level. (Reference Figure 62). It will also be noted that the response spectra achieved with the butyl rubber pads for each machine when compared with the service shock spectra are quite similar in general shape.

In Figure 97 the complete series of response oscillograms are shown for the selected butyl rubber pad for the 20VI machine. In addition to providing a flatter response spectrum it will be noted that significantly fewer rebound impacts are experienced on the table with the butyl rubber pad and the table response accelerations for each succeeding impact decay much more rapidly than those generated with natural rubber pads. A further consequence of the use of butyl rubber pads is that significantly fewer cycles of stress reversal at each natural frequency are afforded by the butyl rubber arresting pads.

The response spectra shown in Figure 62 and the resulting response spectra computed for 300 drops in each machine for a 1 1/2 inch drop height as shown in Figure 71 previously are based upon a table load of 20 pounds for the 20VI machine and 200 pounds for the 150/400 machine. In the case of the 150/400 machine the effect of table load variations upon the maximum acceleration values which determine the shock spectrum for a given drop height is quite appreciable. In Figure 99 the effect of table load on the response spectra

for 200 and 400 pound table loads for drop heights of 1.5 and 3.5 inches is depicted. Because of this variation the drop test procedure recommended for the 150/400 machine has been based on a table load of 200 pounds. It was first considered that compensation for the effect of the table load in the 200-400 pound region might be effected by specifying a greater dropping height. However, consideration of the effect of variations in Q on the response and test spectra would make such a refinement in the test specification questionable and irrational.

This situation does not exist with the 20VI machine and the recommended shock test procedure applies for table loads of 0 to 20 pounds.

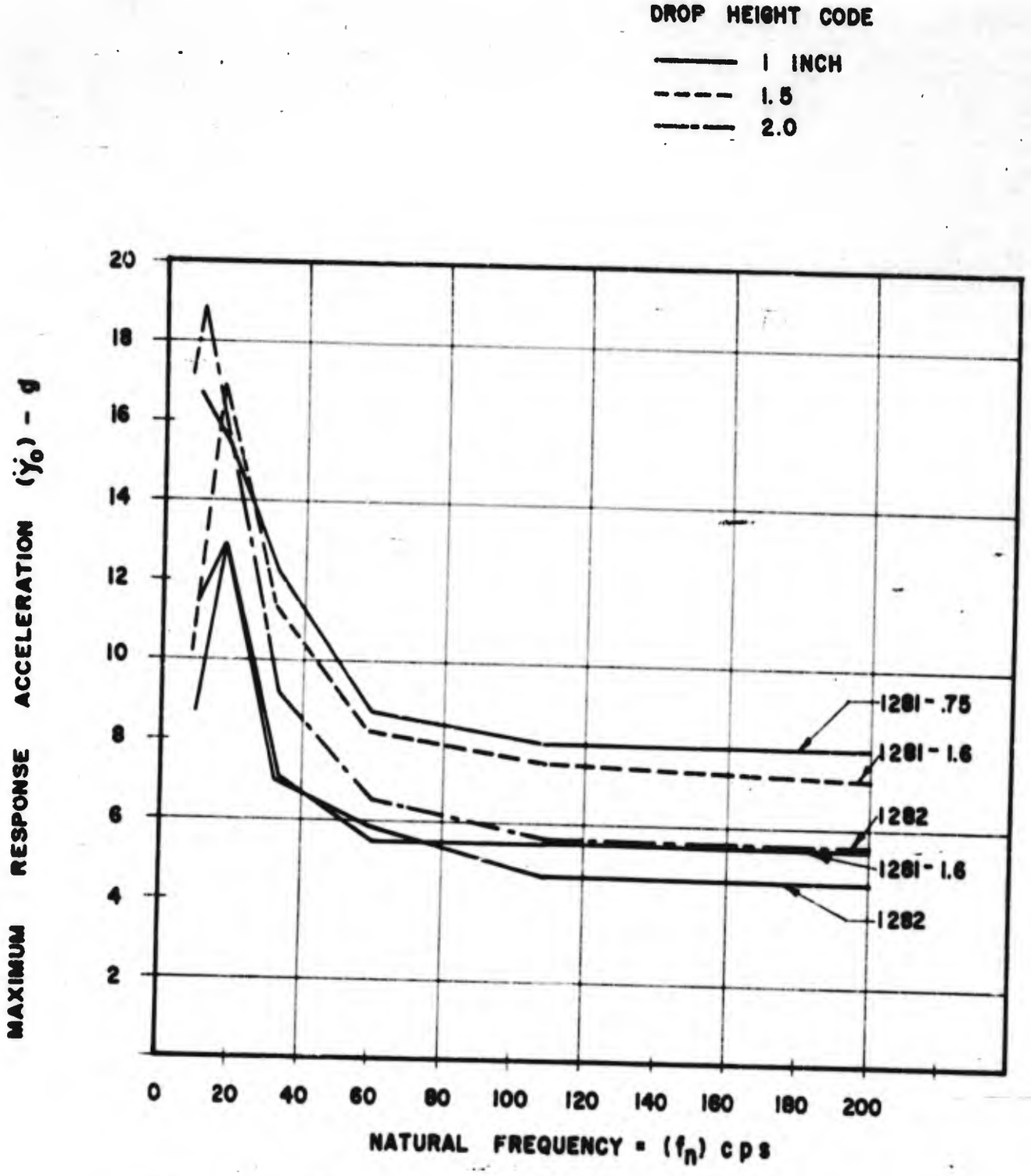

FIGURE 93. RESPONSE SPECTRA- 20 VI MACHINE FOR VARIOUS NATURAL RUBBER PAD CONFIGURATIONS AND DROP HEIGHTS - Q = 20 20 LBS. TABLE LOAD.

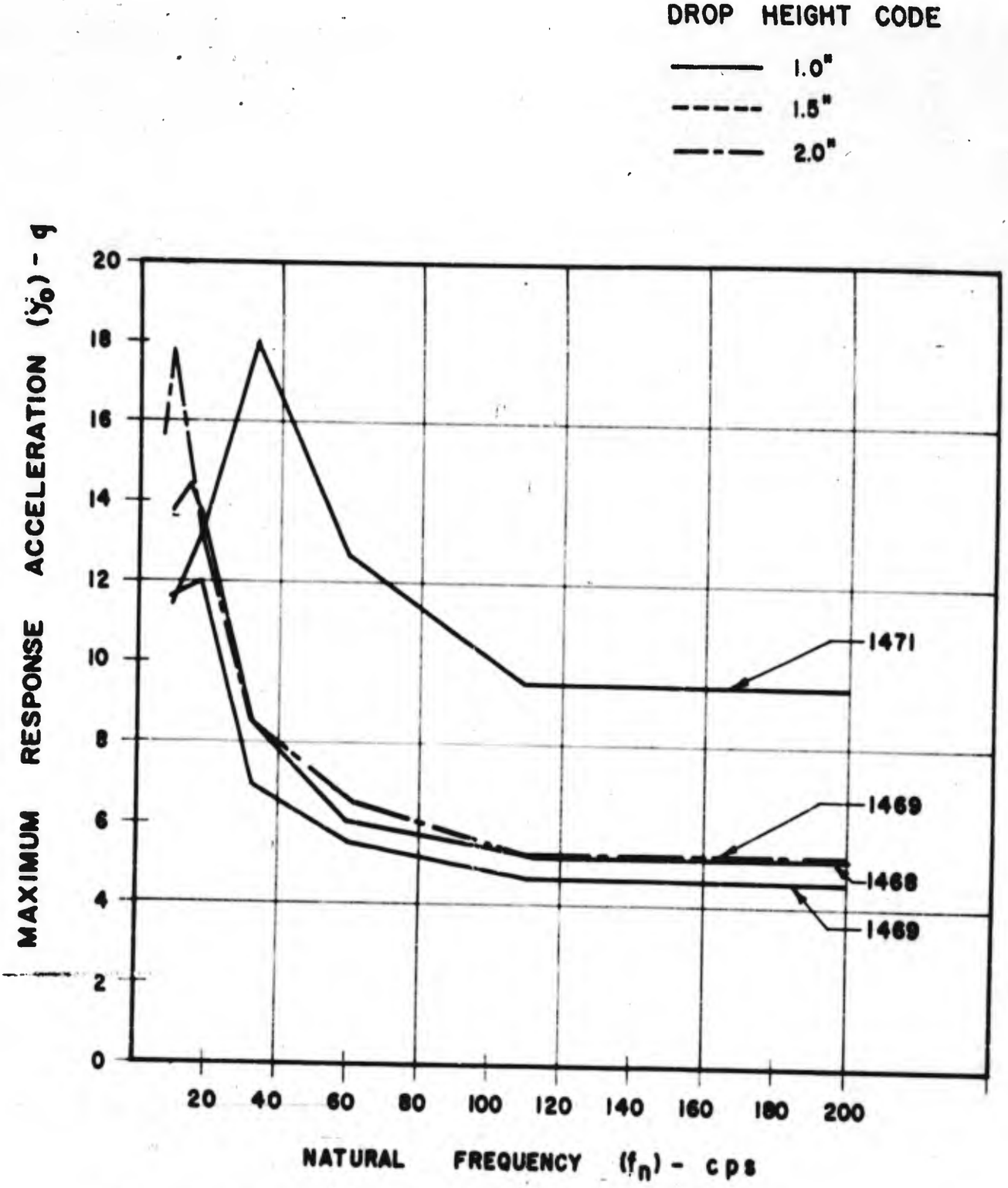

FIGURE 94. RESPONSE SPECTRA - 150/400 MACHINE FOR VARIOUS NATURAL RUBBER PAD CONFIGURATIONS AND DROP HEIGHTS. Q = 20. NO TABLE LOAD.

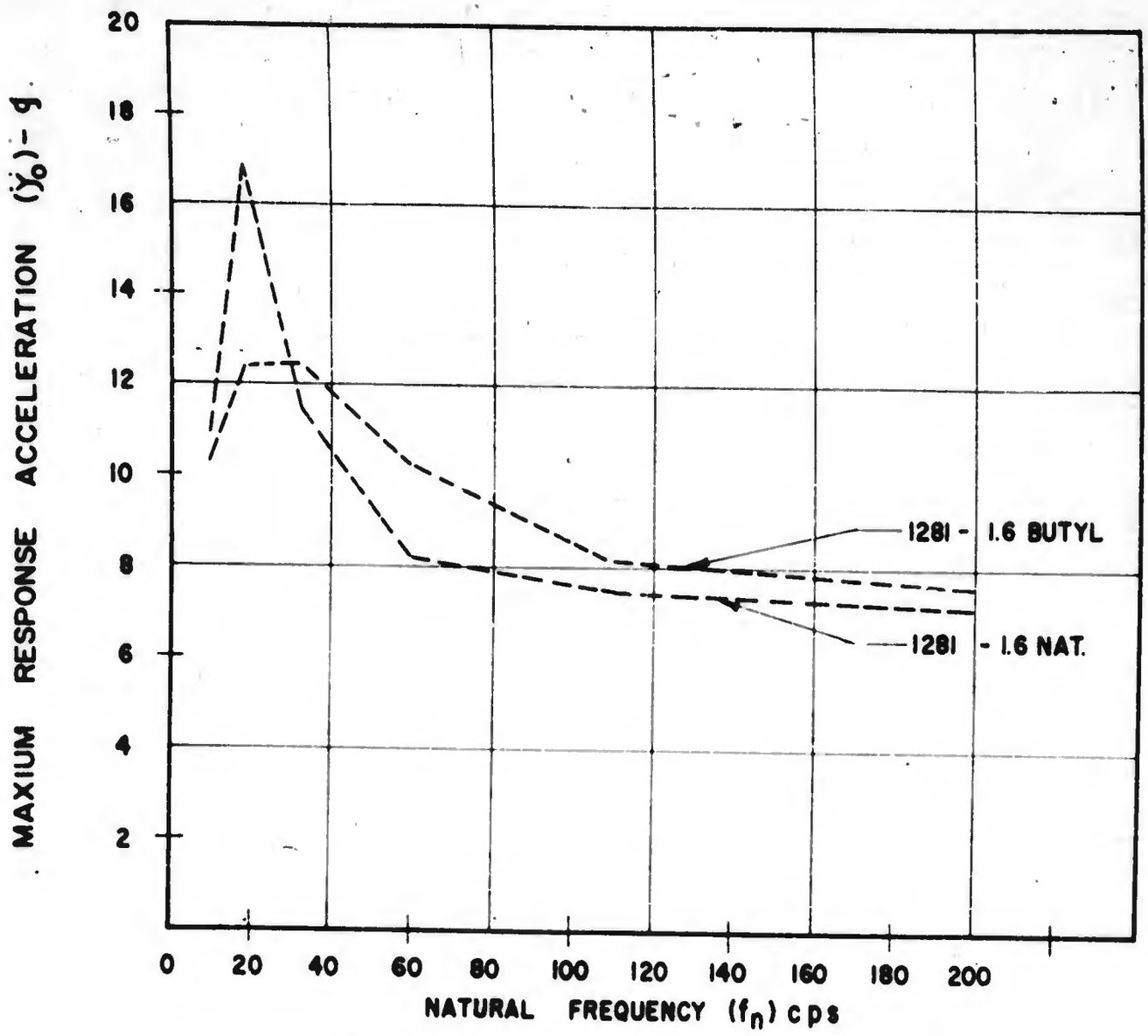

FIGURE 95. COMPARISON OF RESPONSE SPECTRA OBTAINED WITH BUTYL & NATURAL RUBBER PADS OF SAME CONFIGURATION - 20 VI MACHINE 1.5" DROP. 20 LBS. TABLE LOAD.

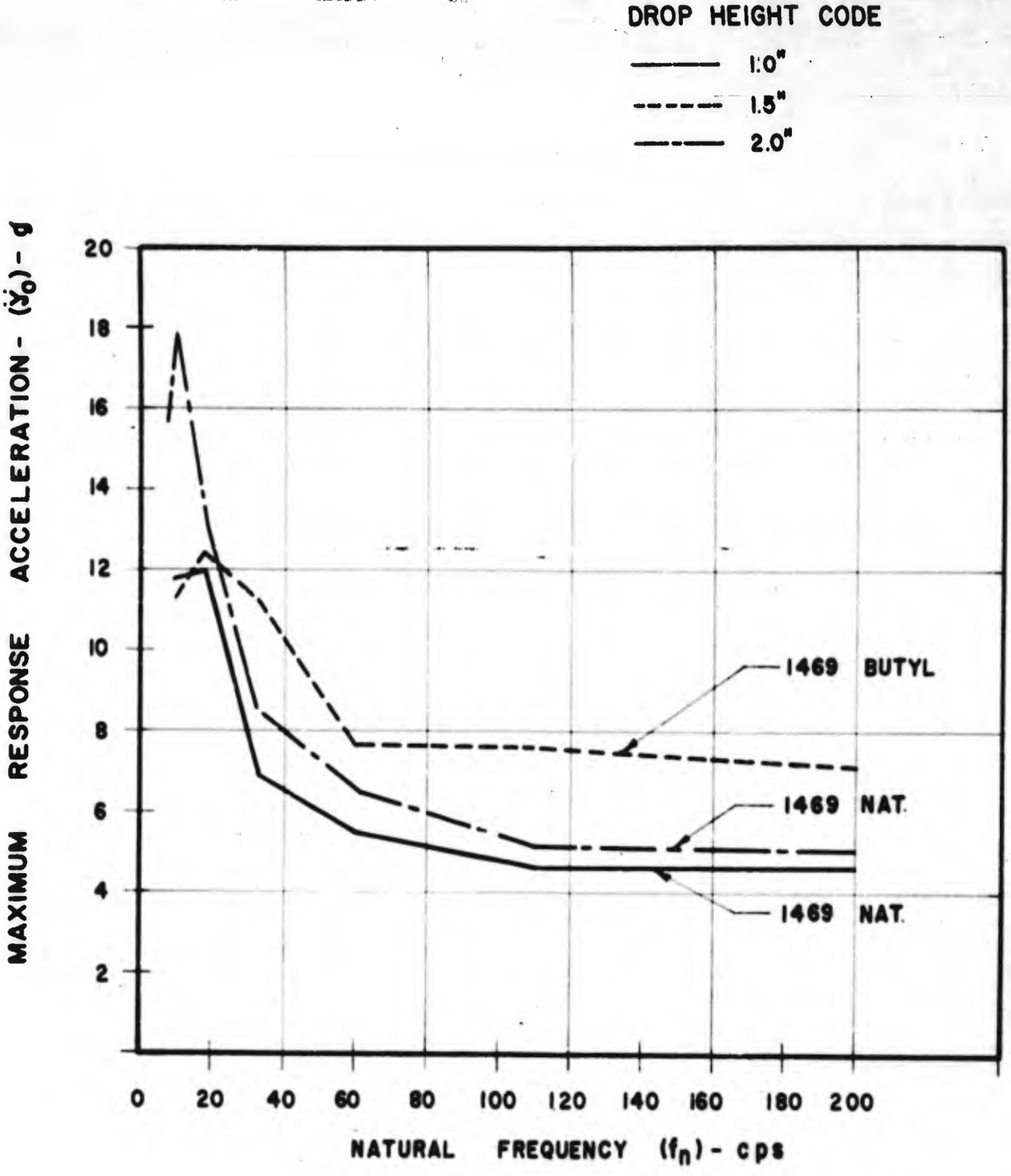

FIGURE 96. COMPARISON OF RESPONSE SPECTRA OBTAINED WITH NATURAL & BUTYL RUBBER PADS OF SAME CONFIGURATION - 150/400 MACHINE - NO TABLE LOAD - Q = 20

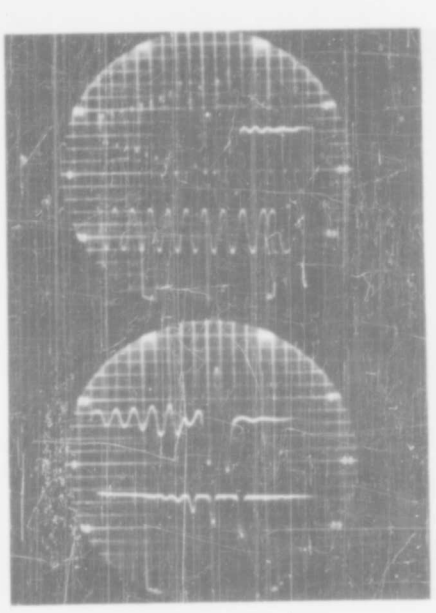

(1) RESPONSE OF 18CPS SYSTEM (TOP)
(2) 10CPS SINE WAVE
(3) RESPONSE OF 10CPS SYSTEM
(4) TABLE ACCELERATION (BOTTOM)

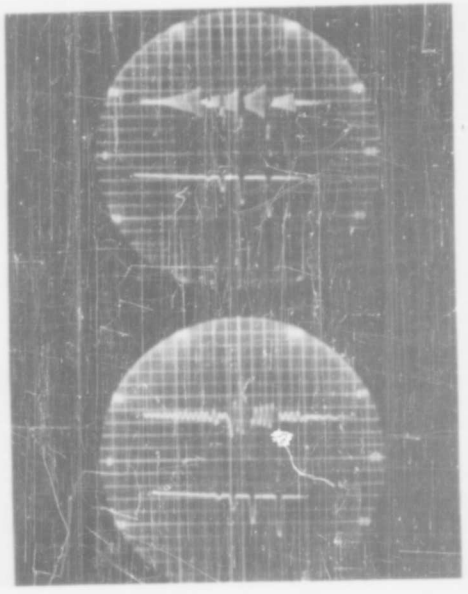

(1) RESPONSE OF 60CPS SYSTEM (TOP)
(2) TABLE ACCELERATION
(3) RESPONSE OF 33CPS SYSTEM
(4) TABLE ACCELERATION (BOTTOM)

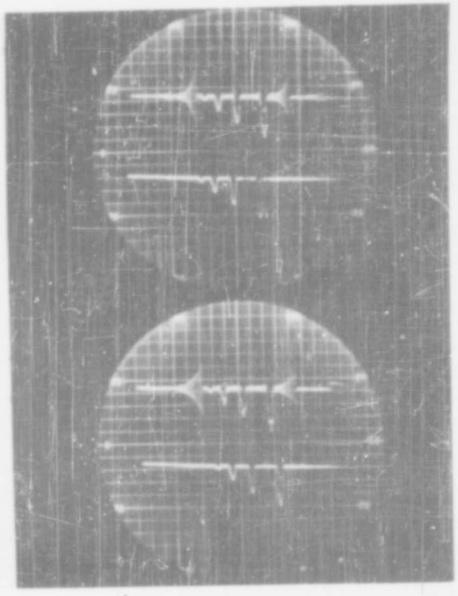

(1) RESPONSE OF 200CPS SYSTEM (TOP)
(2) TABLE ACCELERATION
(3) RESPONSE OF 110CPS SYSTEM
(4) TABLE ACCELERATION (BOTTOM)

FIGURE 97. TYPICAL RESPONSE OSCILLOGRAMS - 20 VI MACHINE - SINGLE 1.5" DROP
BUTYL RUBBER PAD 1281-1.6BU. 20 POUNDS TABLE LOAD. Q = 20

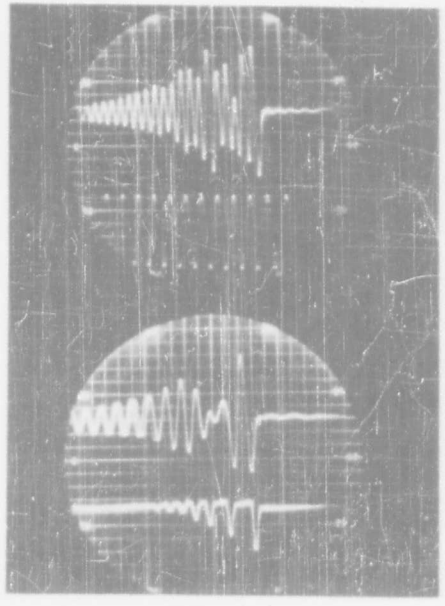

(1) RESPONSE OF 18CPS SYSTEM (TOP)
(2) 10 CPS SINE WAVE
(3) RESPONSE OF 10 CPS SYSTEM
(4) TABLE ACCELERATION (BOTTOM)

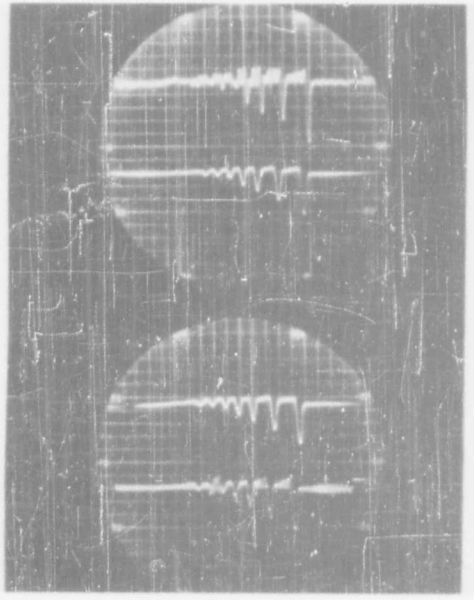

(1) RESPONSE OF 30CPS SYSTEM (TOP)
(2) TABLE ACCELERATION
(3) TABLE ACCELERATION
(4) RESPONSE OF 60 CPS SYSTEM (BOTTOM)

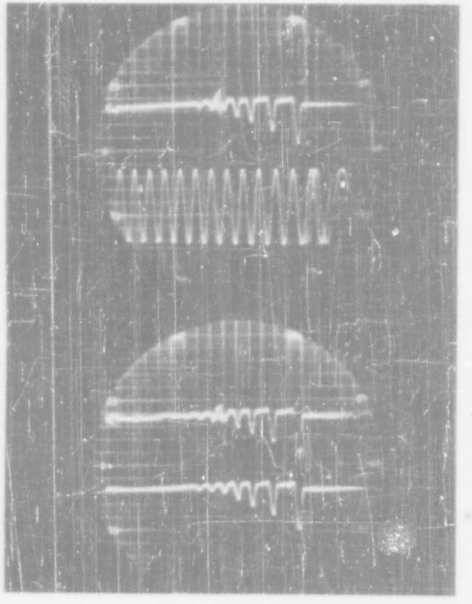

(1) TABLE ACCELERATION (TOP)
(2) 10 CPS SINE WAVE
(3) RESPONSE OF 110 CPS SYSTEM
(4) RESPONSE OF 200 CPS SYSTEM (BOTTOM)

FIGURE 98. TYPICAL RESPONSE OSCILLOGRAMS - 150/400 VD MACHINE - SINGLE 1.5" DROP BUTYL RUBBER PAD 1469BU. ZERO TABLE LOAD. Q = 20

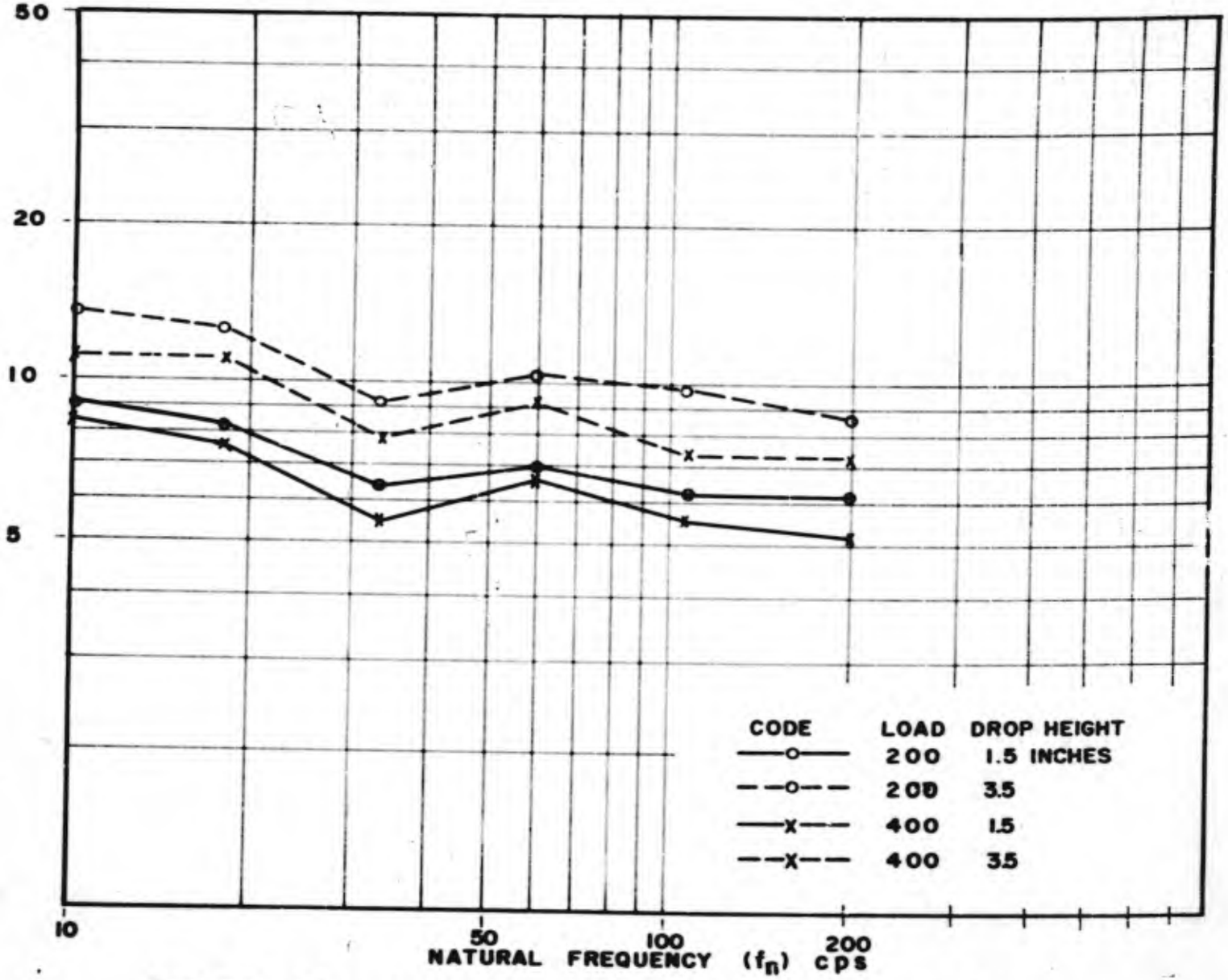

FIGURE 99. 150/400 MACHINE- VARIATION IN RESPONSE SPECTRA- SINGLE DROP WITH TABLE LOAD. BUTYL RUBBER PAD 1469 Q=20

APPENDIX V

BIBLIOGRAPHY

1. Battelle Memorial Institute Staff, "The Fatigue of Metals and Structures", Navaer - 00-25-534, 1954.

2. Battelle Memorial Institute Staff, "Prevention of Fatigue of Metals", John Wiley and Sons, Inc., New York, 1941.

3. Crede, C. E., "Vibration and Shock Isolation", John Wiley and Sons, Inc., New York, 1951, p.33.

4. Fry, T. C., "Probability and Its Engineering Uses", D. Van Nostrand Co., New York, 1928.

5. Manley, R. G., "Fundamentals of Vibration Study", John Wiley and Sons, Inc., New York, 1943.

6. Manley, R. G., "Waveform Analysis", John Wiley and Sons, Inc., New York, 1946.

7. "Mechanical Properties of Metals and Alloys", National Bureau of Standards, Circular C-447, December, 1943.

8. Murray, W. M., "Fatigue and Fracture of Metals - A Symposium", Technology Press of M.I.T. and John Wiley and Sons, Inc., New York, 1952.

9. Den Hartog, J. P., "Mechanical Vibrations", McGraw Hill Book Company, Inc., New York, 1940.

10. Bennett, G. S., "On Multiple Excitation of an Elastic System", J. Acoustical Society of America, Vol. 23, No.2, March 1951.

11. Bennett, R. R. and McCann, G. D., Jr., "Vibration of Multifrequency Systems During Acceleration Through Critical Speeds", ASME Paper 49-APM-10.

12. Biot, M. A., "Analytical and Experimental Methods in Engineering Seismology", Trans. ASCE, Vol. 108, 1943, p. 365.

13. Biot, M. A., "A Mechanical Analyzer for the Prediction of Earthquake Stresses", Bulletin of the Seismological Society of America. (1940)

14. Bisplinghoff, R. L., Pian, T. H. H., & Levy, L. I., "A Mechanical Analyzer for Computing Transient Stresses in Airplane Structures"., J. App. Mech., Vol. 17, No. 3., Sept. 1950, p.310.

15. Cochardt, A. W., "A Method for Determining the Internal Damping of Machine Members", ASME Paper No. 53-A-44.

16. Conrad, R. W. & Vigness, I., "Calibration of Accelerometers by Impact Techniques", Instr. Soc. of America, Paper No. 53-11-3.

17. Den Hartog, J. P., "The Use of Models in Vibration Research", Trans. ASME Paper No. APM-54-14.

18. Evaldson, R. L., Ayre, R. S., & Jacobsen, L. S., "Response of an Elastically Non-Linear System to Transient Disturbances", J. Frank. Inst., Vol. VI, No. II, (1947)

19. Frankland, J. M., "Effects of Impact on Simple Elastic Structures", Proc. SESA, Vol. VI, No. II. (1947)

20. Hsia, Wei-Su, "A Graphical Analysis for Non-Linear Systems", Proc. Inst. E. E., Vol. 99 Part II, No. 68, April, 1952.

21. Housner, G. W., "Characteristics of Strong-Motion Earthquakes", Bul. Seis. Soc. of Am., Vol. 37, No. 1, Jan. 1947.

22. Lazan, B. J., "Effect of Damping Constants and Stress Distribution on the Resonance Response of Members", ASME Paper No. 52-A-8.

23. Lazan, B. J., "Some Mechanical Properties of Plastics and Metals Under Sustained Vibrations", Trans. ASME, February, 1953.

24. Levy, S., & Kroll, W. D., "Response of Accelerometers to Transient Accelerations", Journal of Research, National Bureau of Standards, Vol. 45, No. 4, October 1950. (Research Paper No. 2138).

25. Lewis, F. M., "Vibration During Acceleration Through a Critical Speed", Trans. ASME, 1932, p.253-61.

26. McCann, G. D. & MacNeal, R. H., "Beam-Vibration Analysis with the Electric Analog Computer", ASME, Paper No. 49-SA-3.

27. Meuser, R. R. & Weibel, E. E., "Vibration of a Non-linear System During Acceleration Through Resonance", ASME, Paper No. 47-A-53.

28. Miles, J. W., "Structural Fatigue under Random Loading", Journal of Aeronautical Sciences, November 1954.

29. Mindlin, R. D., Stubner, F. W., & Cooper, H. L., "Response of Damped Elastic Systems to Transient Disturbances", Proc. Soc. Exp. Stress Anal., Vol. V, No. II. (1947)

30. Miner, M. A., "Cumulative Damage in Fatigue", Jour. App. Mech., Vol. 13, No. 3, Sept. 1945, p. A-159.

31. Moore, H. F. and Jasper, T. M., "An Investigation of the Fatigue of Metals", Bull. 152, Eng. Expt. Sta., University of Illinois, 1925.

32. Pardue, T. E., Melchor, J. L., and Good, W. B., "Energy Losses and Fracture of Some Metals Resulting from a Small Number of Cycles of Strain", Proc. SESA, Vol. VII, No. II.

33. Ramberg, W. & McPherson, A. E., "Experimental Verification of Theory of Landing Impact", BU. Stds. Paper RP 1936, Vol. 41, Nov. 1948.

34. Richart, F. E., Jr., and Newmark, N. M., "An Hypothesis for the Determination of Cumulative Damage in Fatigue", Proc. ASTM. Vol. 48, 1948.

35. Robertson, J. M., and Yorgiadis, A. J., "Internal Friction in Engineering Materials", Jour. App. Mech., ASME, 1946.

36. Roberson, R. E., "Vibrations of a Clamped Circular Plate Carrying Concentrated Mass", J. App. Mech., Dec. 1951.

37. Scanlan, R. H., "An Analytical Study of the Landing Shock Effect on an Elastic Airplane", Jour. Aero. Sci., Vol. 15, No. 5, May 1948.

38. Shapiro, A. and Hudson, D. E., "The Measurement of Acceleration Pulses with the Multifrequency Reed Gage", ASME Paper 53-SA-8.

39. Shou-Ngo Tu, "Dynamic Loads in Airplane Structures During Landing", J. Aero. Sci., VI 3 n7, July 1946, p.581.

40. Sinclair, G. M., and Dolan, T. J., "Effect of Stress Amplitude of Statistical Variability in Fatigue Life of u55-T6 Aluminum Alloy", ASME Paper No. 52-A-82.

41. Smith, A. D. N., "An Electronic Instrument for the Measurement of the Dampong Capacity of Materials", J. Sci. Instr., Vol. 28, 1951.

42. "Some Simple Electrical Analogies", Product Engineering, July 1947, pp. 126-130.

43. Soroka, W. W., "Experimental Aids in Engineering Design Analysis", Mech. Eng., Vol. 71, No. 10, Oct. 1949.

44. Soroka, W. W., "Mechanical and Electrical Analogues For Vibration Isolation Problems", Prod. Eng., February, 1950.

45. Starkey, W. L., & Marco, S. M., "A Concept of Fatigue Damage", ASME Paper No. 53-A-143.

46. Weibull, W., "Statistical Design of Fatigue Experiments", J. App. Mech., March 1952, Vol. 1, p. 109.

47. Weisman, M. M., & Kaplan, M. M., "The Fatigue Strength of Steel Through the Range from One-half to 30,000 Cycles of Stress", Proc. ASTM, 1950.

48. Wilbur, J. B., "The Action of Impulsive Loads on Elastic Structures", Boston Soc. of Civil Eng., July 1946.

49. Woodson, J. B., "The Dynamic Response of a Simple Elastic System to Antisymmetric Forcing Function Characteristic of Airplanes in Unsymmetric Landing Impact", ASME Paper No. 48-A-16.

50. "Aeronautical Structures Laboratory Report on Repeat-Load Tests of Model AD Wing Outer Panels", Naval Air Experimental Station, Naval Air Material Center, Philadelphia, Report No. ASL NAM DE-247, January 6, 1953.

51. "Aircraft Radio Equipment Airworthiness," Civil Aeronautics Manual 16, Department of Commerce, Civil Aeronautics Administration, Washington, February 13, 1941.

52. Alford, J. L., Housner, G. W., and Martel, R. R., "Spectrum Analyses of Strong-Motion Earthquakes", Earthquake Research Laboratory, California Inst. of Tech., First Tech. Report under Contract N6Onr-244, August 1951.

53. Carnahan, K. R., "Interim Engineering Report on Investigation of Vibration and Shock Requirements for Airborne Electronic Equipment", Curtiss-Wright Corp. Report No. 120X-4, May 27, 1950, AF 33(038)-7379.

54. "A Collection of Considerations Towards a Rational Mechanical Engineering Practice for Communication Equipment", Signal Corps Engineering Laboratories, Bradley Beach, New Jersey, October 3, 1947.

55. "Cooperative Freight Truck and Snubber Research Program and Related Freight Car Research Programs", Summary Report of Road Tests, Association of American Railroads, Operations and Maintenance Department, Mechanical Division, Report No. f3800, June 30, 1951.

56. Crim, A. D., and Hazen, M. E., "Normal Accelerations and Operating Conditions Encountered by a Helicopter in Air-Mail Operations", NACA Technical Note 2714, June 1952.

57. Cross, W. H., and McWhirter, M., "Railroad Switching Shock", Association of American Railroads, Operations and Maintenance Department.

58. Davidson, S. and Adams, E. J., "A Theoretical Study of the Multifrequency Reed Gage for Measuring Shock Motion", The David Taylor Model Basin, U. S. Navy Report 613, July 1949.

59. "The Destructive Effects of Vibrations and Shocks", Navy Department, Bureau of Ships, NavShips 900,036, April 1944.

60. "Differential Analyzer", Signal Corps Engineering Laboratories, Fort Monmouth, New Jersey, February 28, 1952, Information Bulletin No. 1.

61. "Digital and Analog Computers and Computing Methods", Symposium at the 18th Applied Mechanics Division Conference of the ASME held at The University of Minnesota, June 18-20, 1953.

62. "Evaluation of Mechanical Design Level of Electronic Equipment Leading to Vibration and Shock Criteria", Armour Research Foundation, Project No. K044-1, Report No. 14, September 25, 1953.

63. "Evaluation of Mechanical Design Level of Electronic Equipment Leading to Vibration and Shock Criteria", Armour Research Foundation, Project No. K044-1, Report No. 19, January 27, 1954.

64. "Evaluation of Mechanical Design Level of Electronic Equipment Leading to Vibration and Shock Criteria", Armour Research Foundation, Project No. K044, Report No. 26, August 4, 1954.

65. "Final Engineering Report on Investigation of Vibration and Shock Requirements for Airborne Electronic Equipment", North American Aviation, Inc., Report No. 120X-7, March 30, 1951, Contract No. AF 33(038)-7379.

66. Firmage, D. A., "Transportation Shock and Vibration Studies", Engineering and Industrial Experiment Station, University of Florida, Final Report under Contract No. DA 44-009 eng-460, February 25, 1952.

67. Fischer, E. G., "Preliminary Report on the Mathematical Analysis of the Shock Problem," Research Report No. SR-136 from Westinghouse Research Laboratories.

68. Floor Ir. W. K. G., "Reliability of the Drop Weight Reduction Method for Simulating Wing Life Effect in Landing Gear Drop Tests", National Aeronautical Research Institute, Amsterdam, Rpt. S.340, July 30, 1948.

69. Gee, J. M., Guttwein, G. K., and Priebe, F. K., "Evaluation of the Behavior of Electronic Equipment During Vehicular Transportation", Engineering Report No. E-1098, Signal Corps Engineering Laboratories, Fort Monmouth, New Jersey, August 25, 1952.

70. Gee, J. M., Guttwein, G. K., and Priebe, F. K., "Investigation of Shock and Vibration Encountered During Railroad Switching Operation", Engineering Report No. E-1093, Signal Corps Engineering Laboratories Fort Monmouth, New Jersey, June 3, 1952.

71. Geiger, P. H., "Vibration Damping", University of Michigan, Office of Naval Research, Contract No. N6 onr-[illegible]211, October 1, 1950

72. Goldberg, B. and Pardue, T. E., "Resistance of Materials to Mechanical Shock", Naval Research Laboratory, Report 3828, July 13, 1951.

73. Hendrickson, A. C., "Slopeline-Graphical Solutions of Ordinary Non-linear Differential Equations with Engineering Applications", M.I.T. Thesis, E. E. Dept., 1952.

74. Hoffer, E. S., "An Electronic Method of Approximating the Frequency Spectra of Transient Functions", Naval Research Laboratory, Washington, D. C., Report F-3406, January 27, 1949.

75. Howard, D. M., and Smith, F. C., "Fatigue and Static Tests of Flush-Riveted Joints", NACA, Technical Note 2709, June 1952.

76. Hudson, D. E., Alford, J. L., and Housner, G. W., "Response of a Structure to an Explosive-Generated Ground Shock", California Institute of Technology, Earthquake Research Laboratory, A Report on research conducted under contract with the Office of Naval Research Contract N6 Onr-244, September 1952, Third Technical Report.

77. Hudson, G. E., "A Method of Estimating Equivalent Static Loads in Simple Elastic Structures", David W. Taylor Model Basin, U.S. Navy Report 507, June 1943.

78. "Interim Engineering Report of Investigation of Vibration and Shock Requirements for Airborne Electronic Equipment", North American Aviation, Inc., Report No. 120X-6, January 7, 1951, Contract AF 33(038)-7379.

79. Jacobson, J. M., and Nietsch, H. E., "An Approach to the Analysis of Landing Test Data for Use in Fatigue Calculations", Glenn L. Martin Company, Presented at SESA Detroit, Mich., May 19, 1949.

80. Kennard, D. C., Jr., "Measured Aircraft Vibration as a Guide to Laboratory Testing", AF Technical Report No. 6429, May 1951.

81. Kennard, D. C., Jr., and McIntosh, V. C., "Theory and Practice in Measuring Resonant Frequencies of Aircraft Generators and Alternators", USAF Technical Report No. 6125, August 1950.

82. Laverne, M. E., and Boksenbom, A. S., "Frequency Response of Linear Systems From Transient Data", National Advisory Committee for Aeronautics, Report 977, 1950.

83. Lazan, B., Gannett, A., Kirmser, P., Klumpp, J., and Brown, J., "Dynamic Testing of Materials and Structures with a New Resonance-Vibration Exciter and Controller", Wright Field, Technical Report 52-252, December 1952.

84. Lee, Norman E., "Mechanical Engineering as Applied to Military Electronic Equipment", Technical Memorandum No. M-1177, Signal Corps Engineering Laboratories, Forth Monmouth, New Jersey, June 22, 1949.

85. Levenson, M., and Sussholz, B., "The Response of a System with a Single Degree of Freedom to a Blast Load", The David W. Taylor Model Basin, U. S. Navy Report 572, December 1947.

86. "Lockheed P-90A Airplane - Flight Vibration Characteristics of Jettisonable, Wing-Tip Fuel Tanks", Army Air Forces Air Technical Service Command, Wright Field, Memorandum Report No. MCREXA5-524-5, April 16, 1948.

87. McGolddrick, R. T., "Shock and Vibration Instrumentation for Ships", Symposium on Shock & Vibration Instrumentation at the 17th Applied Mechanics Division Conference held at Penn. State College, State College, Pa., June 19-21, 1952

88. Muller, J. T., "Transients in Mechanical Systems", American Telephone and Telegraph Company, New York.

89. Powell, H. R., "Drop-Table Type Shock Tester", Boston University Upper Atmosphere Research Laboratory, Technical Note No. 9, August 15, 1950.

90. "Prediction of Electronic Failure", National Bureau of Standards Technical News Bulletin, Vol. 36, No. 12, December 1952.

91. Press, H., "An Approach to the Prediction of the Frequency Distribution of Gust Loads on Airplanes in Normal Operations", NACA Technical Note 2660, April 1952.

92. Press, H. and McDougal, Robert L., "The Gust and Gust-Load Experience of a Twin-Engine Low-Altitude Transport Airplane in Operation on a Northern Transcontinental Route", NACA Technical Note 2663, April 1952.

93. "Repeat-Load Tests of Model F8F Airplane Wings", Aeronautical Structures Laboratory, Naval Air Experimental Station, Naval Air Material Center Philadelphia, Report No. ASL NAM DE-281, Nov.20,1952.

94. "Republic F-84 Airplane Vibration Measurements on General Electric J-35 Engine Installations", Aircraft Laboratory, Wright Field, Memorandum No. MCREXA5-4554-2-1, October 1, 1948.

95. "Resilient Mountings for Reciprocating and Rotating Machinery", Illinois Institute of Technology, Engineering Report No. 2, Cont. N7-onr-32904, June, 1950.

96. "Response of a Yielding Vibratory System of Transient Forcing Functions (I)", Vibration Research Laboratory School of Engineering, Stanford University, Structural Dynamics Technical Report No. 11, Navy Contract N6-ORl, 154, Task Order I.

97. "Response of a Yielding Vibratory System to Transient Forcing Functions (II)", Vibration Research Laboratory, School of Engineering, Stanford University, Structural Dynamics Technical Report No. 14, Navy Contract N6-ORl 153, Task Order 1.

98. "Report of Test on Mechanical and Electrical Effects of Vibration on Tube Type 6AR6", The University of Dayton, Task 196, May 1954.

99. Sinclair, G. M., And Dolan, T. J., "Use of a Recrystallization Method to Study the Nature of Damage in Fatigue of Metals", Research Project of the Department of Theoretical and Applied Mechanics, Engineering Experiment Station, Univ. of Illinois, Technical Report No. 21, Feb. 1951.

100. Steiner, R., and Persh, D. A., "Normal Acceleration and Associated Operating Conditions on Four Types of Commercial Transport Airplanes from VGH Data Available as of September 1951", NACA Research Memorandum L52A28, May 19, 1952.

101. Trotter, W.D., "Flight Vibration and Acceleration Measurements", Prepared by Boeing Airplane Company, January 29, 1952.

102. Trotter, W. D., Nute, C. H., and Merritt, J. E., "Structural and Equipment Vibration Measurements", Prepared by Boeing Airplane Company, October 3, 1952.

103. "Vibration Characteristics Measured at Compass Transmitter Location in North American Type F-86-A5 Airplane", Wright Air Development Center, Technical Memorandum Report WCLE-52-7, January 16, 1953.

104. "Vibration Recording and Analysis Used in the Association of American Railroads Test Train, Clinton, Illinois", Signal Corps Engineering Laboratories, Technical Memorandum N. M-1321, October 20, 1950.

105. Vigness, I., "Measurements of Mechanical Shock by Peak-Reading Instruments," Naval Research Laboratory, Report No. 3818, May 25, 1951.

106. Wagenseil, W., "The Destructive Effects of Vibration and Shocks", Bureau of Ships, NavShips 900,036, April, 1944.

107. Wagenseil, W., "Memorandum Concerning the Mounting of Electrical Equipment Used by Armed Forces on Shock Mounts", Bell Telephone Labs, August 21, 1943.

108. Walker, W. G., and Schumacher, P. W. J., "An Analysis of the Normal Accelerations and Airspeeds of a Two-Engine Type of Transport Airplane in Commercial Operations on Routes in the Central United States - From 1948 to 1950", NACA Tech. Note 2735, July 1952.

109. Walker, W. G., and Steiner, R., "Summary of Acceleration and Airspeed Data from Commercial Transport Airplanes During the Period from 1933 to 1945", NACA Technical Note 2625, February 1952.

110. Walsh, J. P., and Blake, R. E., "The Equivalent Static Accelerations of Shock Motions", Naval Research Laboratory, Report No. F-3302, June 21, 1948.

111. Weaver, P. R., and Hoeschele, D. F., "A Vibration Simulator for Bureau of Aeronautics for Department of the Navy", National Bureau of Standards Report No. 2582, June 1953.

112. Welch, W. P., "Impact Considerations in Design", Scientific Paper No. 1337 from Westinghouse Research Laboratories, November 17, 1947.

113. Welch, W. P., "Mechanical Shock on Naval Vessels", NavShips 250-660-26, Bureau of Ships, Washington, D. C., March 1, 1946.

114. Wilts, C. H., and McCann, G. D., "New Electric Analog Computers and Their Application to Aircraft Design Problems", California Institute of Technology.

115. Wrisley, D. L., and Knowles, W. S., "Investigation of Fasteners for Mounting Electronic Components", The Calidyne Company, Contract No. DA-30-039 Sc-5545, April 15, 1951 - August 15, 1952, U. S. Army Signal Corps, Engineering Laboratories, Fort Monmouth, N. J.

116. Firmage, D. A., "Transportation Shock and Vibration Studies", Final Report. Project No. 8-91-06-002 Engineer Research and Development Laboratories, Fort Belvoir, Va., and Modification No. 1 to above Report dated February 25, 1952.

117. Booz, Allen, and Hamilton, "Acceleration, Shock and Vibration Criteria for Aircraft and Airborne Equipment", Wright Air Development Center Technical Report 55-99 (Confidential) June 1955

118. Department of Defense - "Shock and Vibration Bulletin", Numbers 15, 16, 21. (Confidential)

119. Department of Defense, Office of Asst. Secretary of Defense, Research and Development - "Fundamentals of Guided Missile Packaging - Shock and Vibration Design Factors", July 1955.

120. Air Materiel Command - Memorandum Report - Aircraft Laboratory - MCREXA-5-113-4-1, "Lockheed F-80A Airplane-Vibration due to Firing of Fixed M-3 Guns", May 1949.

121. Wright Air Development Center Technical Note 55-790, "Flight Vibration Survey F-86D Aircraft-Serial 5-464" October 1955.

122. Wright Air Development Center Memorandum Report WCLE-53-221, "F-89A Airplane - Flight Vibration Survey, - Starter, Generator, and Engine", November 1953.

123. Northrop Aircraft, Incorporated - Monthly Progress Report No. FTS-16-10, "F-89D Airplane - Radome Vibration in Flight and Landing", March 1955

124. Bureau of Aeronautics Report, "Vibration Survey of XF6U-1, During Muroc Flight", January 1948.

125. Naval Air Test Center Report, "Vibration Survey of the Electronics Compartment in an F-9F-5 Airp

126. Boeing Airplane Company, Report T-28270 - "B-47 Flight Vibration and Acceleration Measurements".

127. Wright Air Development Center Technical Note 55- "Flight Vibration Survey - Instrument Panel B-4 Airplane", September 1955.

128. Boeing Airplane Company Report T-29393-YB-52, Airplane, "Structural and Equipment Vibration Measurements", October 1952 and February 1955.

UNCLASSIFIED